UCRL-LR-139215
Thesis

Development of Trivalent Ytterbium Doped Fluorapatites for Diode-Pumped Laser Applications

Andrew J. Bayramian

Ph.D Dissertation

June 21, 2000

U.S. Department of Energy
Lawrence Livermore National Laboratory

DISCLAIMER

Work performed under the auspices of the U. S. Department of Energy by the University of California Lawrence Livermore National Laboratory under Contract W-7405-Eng-48.

Development of Trivalent Ytterbium Doped
Fluorapatites for Diode-Pumped Laser Applications

BY

ANDREW JAMES BAYRAMIAN
B.S. (Montana State University) 1995
M.S. (University of California, Davis) 1998

THESIS

Submitted in partial satisfaction of the requirements for the degree of

DOCTOR OF PHILOSOPHY

in

Applied Science

in the

OFFICE OF GRADUATE STUDIES

of the

UNIVERSITY OF CALIFORNIA

DAVIS

Approved:

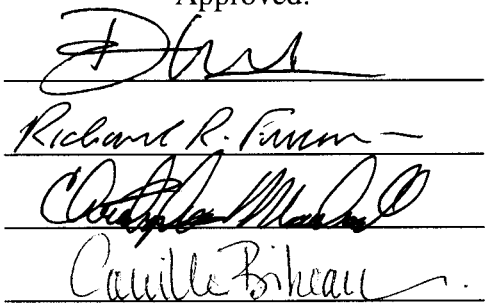

Committee in Charge

2000

ACKNOWLEDGEMENTS

I would like to thank my advisors Denise Krol, Ray Beach, Camille Bibeau, Chris Ebbers, Christopher Marshall, Steve Payne, and Kathleen Schaffers for each lending me their unique outlook on problem solving and communication of results. I think all of my publications, including this thesis have benefited remarkably from this diverse viewpoint. I'd like to especially thank Kathleen Schaffers, John Tassano, Phil Waide, Peter Thelin, and Ron Vallene, for growing and preparing fluorapatite samples for me to use in this thesis. I would like to thank Brian Kolner, Denise Krol, and Richard Freeman for the upper division graduate classes they taught and the outlook on science and performing science that was communicated to me. As a scientist I have benefited and will continue to benefit from their advice. I'd like to thank Keith Kanz, Larry Smith, Joel Speth, John Tassano, Everett Utterback, and Gary Wilke for their help in making lab equipment function properly and for the many priceless rules of thumb when working in the lab. At special facilities like the Optical Sciences Lab, I'd like to thank Dave Milam and Walter Sell for their time and use of their facilities. I'd also like to thank William Eickelburg for use of his high precision interferometer. A special thanks to Terry Duewer for mass spectral analysis done on several of my ytterbium doped samples. Thanks is offered to Mark Henesian, John Murray, and Dave Eimerl for many useful discussions concerning Raman generation and gain. I'd like to thank my fellow graduate students: John Adams, Mike Nostrand, and Falgun Patel for their assistance in the lab and many useful discussions about physics and modeling physics. I would like to thank my undergraduate thesis advisor, John Carlsten, for his love of physics and for nurturing that same love and talent in me. I would like to thank Ralph Johnson, then Dept head of the University

Honors Program, for his support and advise on my future career and the utility of multidisciplinary research. I would like to thank my junior high life sciences teacher, Mrs. Stover, who got me started as a scientist. I'd like to thank my family and friends for their support – money, time, and moral, of my interest in science. I'd like to thank my wife Laurie for putting up with my long hours, my stressed out condition, and the many scientific discussions (however dry). Finally, I'd like to thank God for giving me the talent and peace of mind to perform all of this work, which is hopefully the correct path he wants me to follow.

I'd like to acknowledge the National Science Foundation Graduate Fellowship, the John and Fannie Hertz Foundation Fellowship, and the Lawrence Livermore National Laboratory Student-Employee program for their financial support of my graduate education and doctoral research. This work was performed under the auspices of the Basic Energy Sciences Program within the U.S. Department of Energy by Lawrence Livermore National Laboratory under contract No. W-7405-Eng-48.

TABLE OF CONTENTS

ABSTRACT:

One of the major motivators of this work is the Mercury Project, which is a 1 kW scalable diode-pumped solid-state laser system under development at Lawrence Livermore National Laboratory (LLNL). Major goals include 100 J pulses, 10% wallplug efficiency, 10 Hz repetition rate, and a 5 times diffraction limited beam. To achieve these goals the Mercury laser incorporates ytterbium doped $Sr_5(PO_4)_3F$ (S-FAP) as the amplifier gain medium. The primary focus of this thesis is a full understanding of the properties of this material which are necessary for proper design and modeling of the system.

Ytterbium doped fluorapatites, which were previously investigated at LLNL, were found to be ideal candidate materials for a high power amplifier systems providing high absorption and emission cross sections, long radiative lifetimes, and high efficiency. A family of barium substituted S-FAP crystals were grown in an effort to modify the pump and emission bandwidths for application to broadband diode pumping and short pulse generation. Crystals of $Yb^{3+}:Sr_{5-x}Ba_x(PO_4)_3F$ where $x < 1$ showed homogeneous lines offering 8.4 nm (1.8 times enhancement) of absorption bandwidth and 6.9 nm (1.4 times enhancement) of emission bandwidth. The gain saturation fluence of Yb:S-FAP was measured to be 3.2 J/cm^2 using a pump-probe experiment where the probe laser was a high intensity Q-switched master oscillator power amplifier system. The extraction data was successfully fit to a homogeneous extraction model.

The crystal quality of Czochralski grown Yb:S-FAP crystals, which have been plagued by many defects such as cracking, cloudiness, bubble core, slip dislocations, and anomalous absorption, was investigated interferometrically and quantified by means of

Power Spectral Density (PSD) plots. The very best crystals grown to date were found to have adequate crystal quality for use in the Mercury laser system. In addition to phase distortions which are fixed by material growth, thermal loading of the S-FAP media also leads to distortions due to thermal expansion, α, temperature dependent refractive index, $\partial n/\partial T$, and stress optic effects. The stress optic coefficients necessary for modeling thermal distortions in Yb:S-FAP slab amplifiers were measured giving $q_{33} = 0.308 \times 10^{-12}$ Pa^{-1}, and $q_{31} = 0.936 \times 10^{-12}$ Pa^{-1}.

Nonlinear optical losses due to high intensity laser interaction with S-FAP were evaluated including Stimulated Raman Scattering (SRS) and Stimulated Brillouin Scattering. The SRS gain coefficient was measured to be 1.3 cm/GW. The SRS losses in the Mercury amplifier system were successfully modeled and shown to be an issue for high-energy short pulse operation. Countermeasures including the addition of bandwidth to the extraction beam and wedging of amplifier surfaces would allow operation of the Mercury laser at 100 J and 2 ns output below SRS threshold. A simple model of SBS losses in the Mercury laser system shows SBS will also be a problem, however suppression is possible with the introduction of moderate bandwidth (relative to the SRS case).

Finally, a Q-switched Yb:S-FAP oscillator was developed which operates three-level at 985 nm with a 21% slope efficiency. Frequency conversion of the 985 nm light to the 2^{nd} harmonic at 492.5 nm was achieved with a 31% conversion efficiency. A diode pumped, doubled Yb:S-FAP laser at 492.5 nm would make a compact efficient blue laser source.

Chapter 1. INTRODUCTION

I. The Ytterbium Ion

The trivalent ytterbium ion[1-5] is attractive as a laser ion due to its simple electronic structure, long radiative lifetimes, and high quantum efficiency. The electronic structure of trivalent ytterbium can be derived from the outer orbital configuration of $4f^{13}$, or 1 unpaired electron in the 4f shell. This gives rise to only two energy levels in the free ion, since $J = L + S = 3 \pm ½$, with Russell-Saunders notation $^2F_{7/2}$ and $^2F_{5/2}$. Since the 4f shell is more than half filled, Hund's rules dictate that the $^2F_{7/2}$ level will be the lower level (ground state) and the $^2F_{5/2}$ level the upper one. Quantum mechanics gives 2J + 1 possible states for each of these levels, but since the number of electrons is odd (13 in the f orbital), Kramer's degeneracy states that there must be at least a two-fold degeneracy of these states. Therefore, the $^2F_{5/2}$ will split into three levels, and the $^2F_{7/2}$ into four levels. When Yb^{3+} is doped into a crystalline or glass host medium, these levels are Stark split forming excited and ground state manifolds of three and four levels respectively (Fig. 1). The long radiative lifetimes of ytterbium doped materials make it possible to excite these materials to inversion at lower intensities, since there is a longer integration time. The quantum defect is defined as $\eta_q = \nu_{laser}/\nu_{pump}$, where ν_{pump} is the pump frequency, and ν_{laser} is the laser frequency. Since the Yb^{3+} ion has only two electronic levels, even the worst case quantum defect is only the deficit incurred from the combined widths of the excited and ground state manifolds (usually > 70%). Of course the great quantum efficiencies aren't without fault: a high quantum efficiency necessarily implies closely space pump and emission lines which in turn leads to three-level or quasi-three level operation. By contrast, trivalent neodymium, a well known laser ion, has a complex

electronic structure, shorter radiative lifetime, and lower quantum efficiency at the one-micron transition when compared to ytterbium, as well as excited state absorption and multiphoton absorption at higher pump intensities. Due to shorter lifetime, which is generally less than half of the ytterbium lifetime, higher intensity pump sources are required to store the same amount of energy. The lower quantum efficiency directly effects the wallplug efficiency of high power lasers and amplifiers, although this is partly offset by the low pump threshold of true four-level operation. Thus, for applications where low brightness pump sources, such as diode lasers, are employed, ytterbium's electronic properties are advantageous. The proper choice of a host medium for the ytterbium ion, such that is has high absorption and emission cross sections, can further enhance the utility of ytterbium as an efficient laser ion.

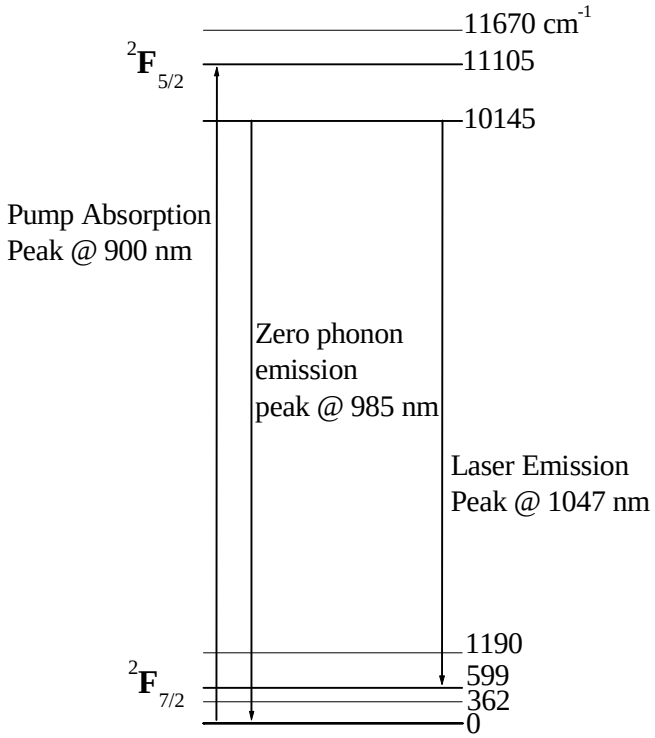

Fig. 1. Energy level diagram for Yb^{3+}:S-FAP (typical for Yb^{3+} doped materials)

II. The Apatite Crystal Host

The apatite family of crystalline materials includes a large class of minerals and synthetic compounds crystallizing in a few different, but related, hexagonal and pseudo-hexagonal structures. These compounds are represented by the chemical formula $A_{10}(MO_4)_6X_2$. The A cation can be a divalent or trivalent ion (with charge compensation), but is often an alkaline earth or a RE ion. The ten A ions occupy two different crystallographic sites: four of the ions occupy a nine coordinate oxygen polyhedron, with trigonal point symmetry[6] (identified as A_I), and six ions occupy a seven coordinate polyhedron containing 6 oxygen and 1 fluorine ion with monoclinic symmetry (identified as A_{II}). The M cation, which generally has tetrahedral symmetry (although planar ions are possible[7,8], such as BO_3^{3-}), is generally from the group 4 and 5 elements on the periodic table, as well as transition metal ions capable of tetrahedral symmetry (i.e. Si, Ge, P, As, V). The X anion is usually a halide, hydroxide, oxide, or sulfide ion.

Apatite, $Ca_5(PO_4)_3(OH, Cl, F)$, is the most abundant of the phosphate materials in the earth's crust[9] and is the building block for a wide variety of biological, chemical, and optical systems. Fluorapatite is the basis of tooth enamel and one of the structural components of bone. Apatites have been studied and used for the dating of rocks, archaeological artifacts, and fossils[10,11], fission track detection[12], surface failure of materials[13], the elastic properties of bone and tooth enamel[14], acousto-optic devices[15,16], for the production of phosphorus containing mineral fertilizers[17], and as an ore source for rare earth (RE) elements[6]. A wide variety of phosphors, such as those used in fluorescent lamps, have been developed around apatite doped with transition metals as well as group IV and V elements, including: Sb[18-22], Mn[23-26], Ce[27], as well as thermoluminescence of

undoped apatite[28,29]. Several rare earth and transition metal doped apatites have been optically characterized and show promise as laser materials: Cr^{4+}:$Ca_5(PO_4)_3F$ (FAP or C-FAP)[30], Tb^{3+}:$Ca_{10-2x}Na_xTb_x(PO_4)_6F_2$ ($0 \leq x \leq 2$)[31], Eu^{3+}:$Sr_5(PO_4)_3F$ (S-FAP)[32], Eu^{3+}:$M_5(PO_4)_3X$ (M=Ca^{2+}, Sr^{2+}, Ba^{2+}, X=F^-,Cl^-,Br^-,OH^-)[33,34], Tm^{3+}:S-FAP[35], Er^{3+}:S-FAP[27,36], Er^{3+}:C-FAP saturable absorber[37], Dy^{3+}:S-FAP[38], Pr^{3+}:C-FAP[39,40], Pr^{3+}:S-FAP[36], and Ho^{3+}:S-FAP (has been lased)[41-43]. Recently, apatites (mostly fluorapatites) have been used as hosts for rare earth doped lasers (namely neodymium (Nd^{3+}) and ytterbium (Yb^{3+})), including: Nd^{3+} doped $Sr_5(VO_4)_3Cl$[44], $Ba_5(PO_4)_3F$[45], $Sr_xCa_{5-x}(PO_4)_3F$ (x = 0, 1, 2, 3, 4, and 5)[46], C-FAP[47-51], $Sr_5(VO_4)_3F$ (S-VAP)[52-58], and S-FAP[44,55,59-67].

The apatites studied in this dissertation have formulas given by $A_5(PO_4)_3F$, where A is given by Sr, Ba, or Ca and belongs to the crystal class 6/m or the hexagonal point group C_{6h}. The unit cell (shown in Fig. 2) contains two formula units with lattice parameters *a* (the length of one of the hexagonal edges), and *c* (the distance between hexagonal planes), where $Ca_5(PO_4)_3F$[68,69] has a = 9.38 and c = 6.89. Charge balance is necessarily required when a RE^{3+} ion substitutes for an A^{2+} cation in the $A_{10}(MO_4)_6X_2$ matrix. The long recognized charge compensation mechanism[70], which does not require any compensating ions to be specifically introduced, is the substitution of (RE^{3+} + O^{2-}) for (A^{2+} + X^-) at the A_{II} site. Ignoring the formation of defects or doping into the A_I site, there can be only two such RE^{3+} substitutions in a unit cell, since there are only two fluorine ions available.

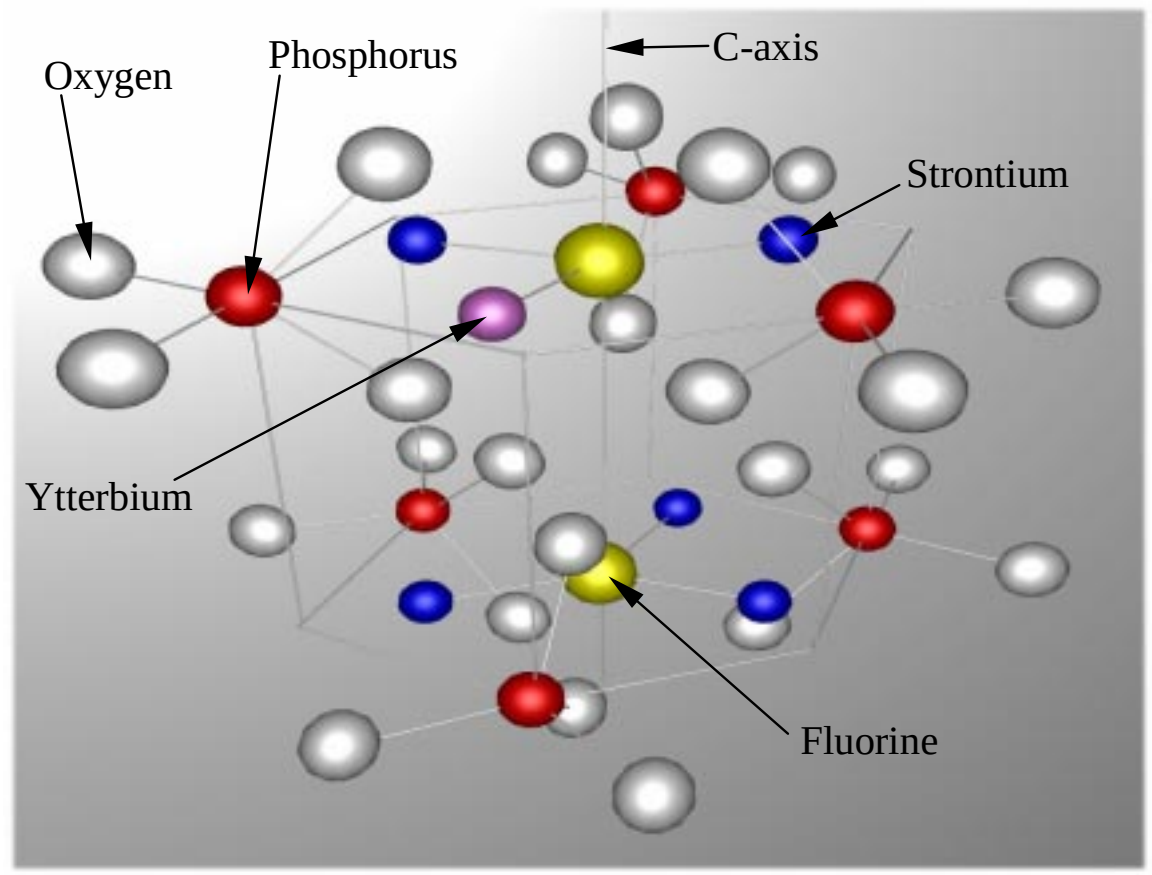

Fig. 2. Partial view of the $A_{10}(PO_4)_6F_2$ crystal structure showing the environment of the A_{II} ions about the c-axis of the crystal and the shared bonding F anions. A_I ions are omitted for clarity since their position lies along the c-axis between the trigonal planes defined by the fluorine ions

III. Ytterbium doped apatites

Ytterbium doped apatites represent the fusion of an efficient laser ion with a stable host that is capable of a variety of substitutions and strong fluorescence. In a comparative spectroscopic study of a large sample of ytterbium doped materials, DeLoach et. al.[71] identified Yb^{3+}:C-FAP as the most favorable material, producing the highest emission cross section and lowest intensity required to reach lasing threshold. Further investigation of Yb^{3+}:C-FAP[72-75] and its host variants include: Yb^{3+} doped $Ca_4Sr(PO_4)_3F$[72], $Ca_3Sr_2(PO_4)_3F$[72], S-VAP[72,73], $Ba_5(PO_4)_3F$ (B-FAP)[73], $Ca_5(PO_4)_3Cl$ (C-ClAP)[73], and S-FAP[76-80]. Yb^{3+}:S-FAP, having the best laser characteristics to date, was

further developed into a Q-switched oscillator[81-83], a mode-locked oscillator[84], a slab amplifier[85], and a scalable diode-pumped gas-cooled-slab laser[86]. Based on favorable laser and spectroscopic results, Yb:S-FAP was chosen as the optimal laser material to be used in an advanced design of a diode-pumped solid-state laser driver for inertial fusion energy[87].

IV. Growth of Ytterbium doped apatites

Ytterbium doped apatites are typically boule grown at high temperature (approximately 1700 °C) using the Czochralski technique[88,89]. This method uses induction heating to melt the raw materials in a crucible from which a boule is grown by pulling a rotating seed crystal from the surface (Fig. 3). The geometry of the liquid and heat flow in the crucible follows the general trends shown in Fig. 4. The heat and liquid flow gradients effect the shape and rate of growth of the boule melt interface and the stability of these gradients is critical to growing defect free crystals. Therefore, the crystals grown in this experiment and in most current Czochralski growth stations use computer control, where the inductive currents and pulling rates are stabilized to decrease changes in heat and liquid gradients thereby producing constant and/or ramped growth rate. Temperature and current stability required for low loss crystals are ±0.1 °C and ±1% respectively, which is challenging at 1700 °C. The pull rate is typically between 0.5 and 1.5 mm/hr. and the rotation rate is between 5 and 50 rpm. This corresponds to a growth rate of about an inch a day. If one includes the initial melting time (hot loading the crucible takes 1-16 hrs) and cool down of the boule (approximately 24 hrs..), a 6 inch boule can take between 1-2 weeks to grow. A picture of the typical growth station used for producing the fluorapatite crystals is shown in Fig. 5. The crystals are grown in an

inert atmosphere of dry nitrogen. During the growth process large amounts of SrF_2 can vaporize during the growth process. Consequently, the initial charge in the crucible typically has SrF_2 concentrations in excess of the stoichiometric amounts necessary to produce the fluorapatite. Changes to the initial charge also effect the growth rates, distribution coefficients (which is the ratio of the concentration of dopant in a grown boule to the dopant concentration of the initial charge in the crucible), temperatures of different phase transitions, and the crystalline structure of the material. The extreme thermal and liquid stability requirements, melt stoichiometric evolution, convection driven flow, and material phase transitions, make this multivariable process complex, slow, and challenging to optimize for high-quality crystal growth.

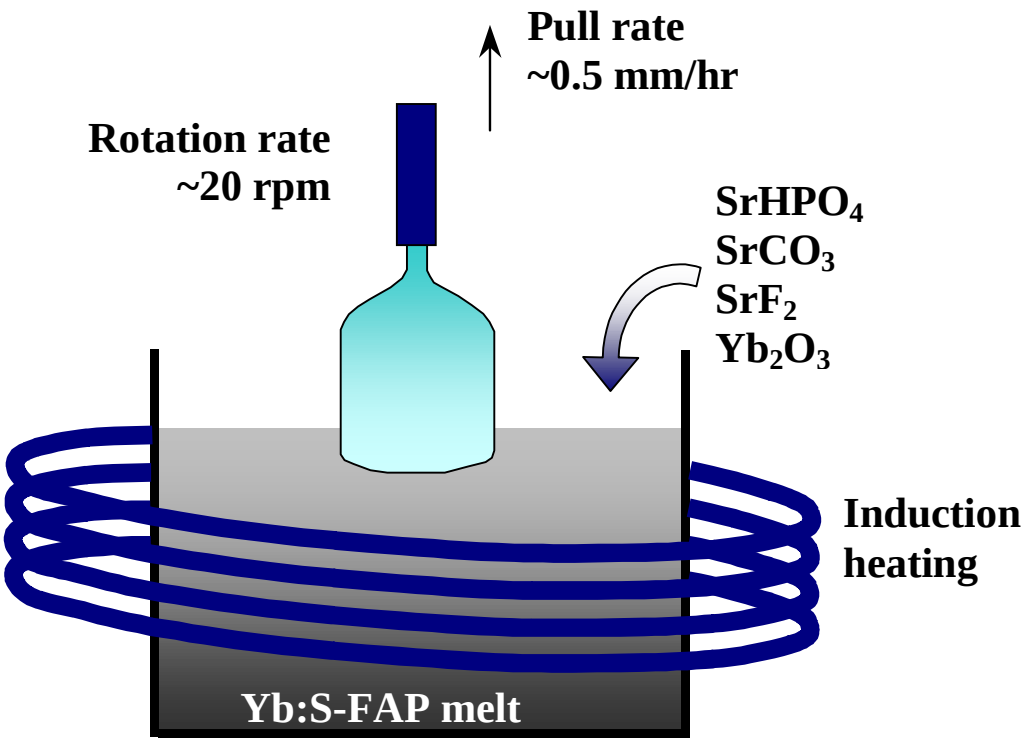

Fig. 3. Schematic of Czochralski growing apparatus

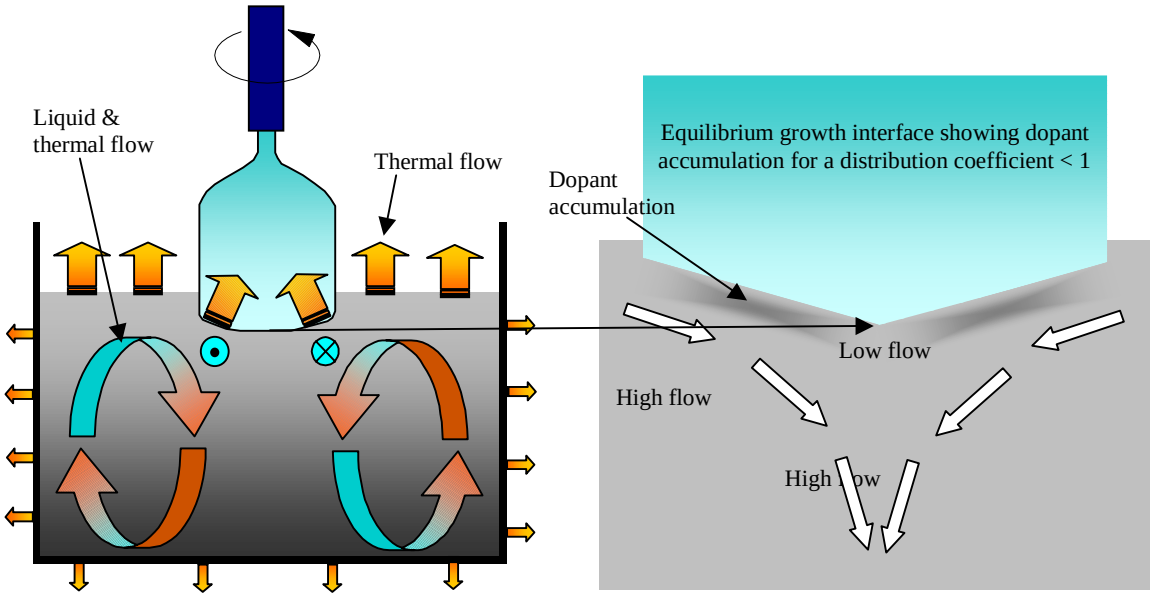

Fig. 4. a) Schematic of liquid flow and thermal gradients present in a Czochralski crucible. b) Magnified view of the boule/melt interface showing a low flow buffer zone as well as a dopant accumulation near the boule surface for doped boules grown with a distribution coefficient (= concentration of Yb^{3+} in boule/concentration of Yb^{3+} in initial charge) less than unity.

Fig. 5. Picture of an LLNL computer controlled (diameter control) Czochralski growth station with a stainless steel cooling jacket for better thermal gradient control, and a scale attached to the pull rod for continuous mass monitoring. (Courtesy of K. Schaffers)

V. The Mercury Laser System

A major motivation behind this work is the 1 kW Mercury Laser system currently being built at Lawrence Livermore National Laboratory (LLNL), which was proposed as a scalable, diode-pumped, repetition rated, inertial confinement fusion (ICF) laser driver (shown in Fig. 6). In a theoretical paper by Orth and Payne, Yb:S-FAP was employed in a multistage amplifier scheme for an advanced fusion driver concept[90]. The Mercury laser[91] is aimed at experimentally validating many of the concepts addressed in that paper. This diode-pumped solid state laser will provide 100 J pulses at 10 Hz with temporal pulsewidths between 2 and 10 ns, a 5 times diffraction limited beam, and a 10% wallplug efficiency.

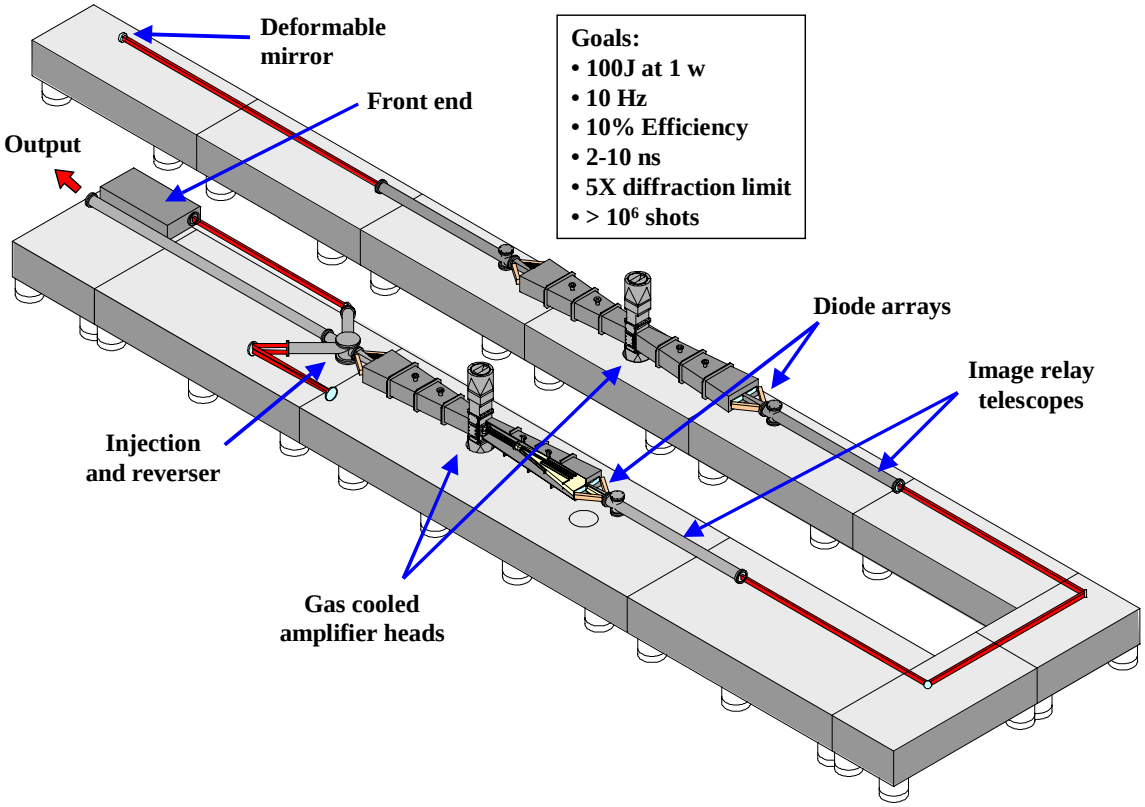

Fig. 6 The Mercury laser system employing split diode array back-plane allowing in line pumping and extraction.

The repetition rate and efficiency of this scalable laser system currently sets it apart from all other laser ICF drivers. Most large laser systems such as Nova (LLNL), Omega (University of Rochester), and Gekko (Japan), which are used primarily for target plasma physics, are highly energetic, but have very low repetition rates and wallplug efficiencies. For example, the National Ignition Facility (NIF), which is the forefront of laser ICF technology, operates at 6.9×10^{-5} Hz (one shot every 4 hrs.) and a 1% wallplug efficiency. For fusion power to be a usable power source, the driver would need to operate at the efficiencies and repetition rates of the Mercury laser but at a larger scale yielding mega-joule energies.

The high repetition rate achieved in Mercury is possible due to active gas cooling, decreased thermal loading by using efficient diode-lasers rather than flash lamps, and Yb:S-FAP crystals which provide better thermomechanical properties and less quantum defect than traditional Nd:glass amplifiers. The Yb:S-FAP parallel slab amplifiers (shown in Fig. 7) are cooled by helium flowing at mach 0.1 through 1 mm channels yielding turbulent flow conditions, which maximize the heat removal from the amplifier surface.

The cooling system for the laser was designed such that the heat removal direction is the same as the laser propagation direction (and the diode pump delivery direction), which minimizes the distortion due to thermal loading and further enhances the ability to operate at high repetition rates. The high efficiency of this laser system is in part due to the diode arrays. Each of the four arrays contains 70 tiles of 23 diode bars each for a total of 1610 diode bars, each of which can produce 100 W peak power for a total of 161 kW of peak power per diode array. Each diode pump pulse will deliver 121 J of pump

energy. The 900 nm pump laser energy has a 10 nm FWHM bandwidth that is similar to the absorption bandwidth of Yb:S-FAP, thus minimizing extraneous spectral components that could cause heating. Along with an efficient diode laser system, the Yb:S-FAP amplifiers offer high absorption of the pump light and a high emission cross section. The high emission cross section leads to a low saturation fluence allowing efficient extraction of the amplifiers below typical average damage thresholds (approximately 10 J/cm^2 for 10 ns pulses at 1 micron).

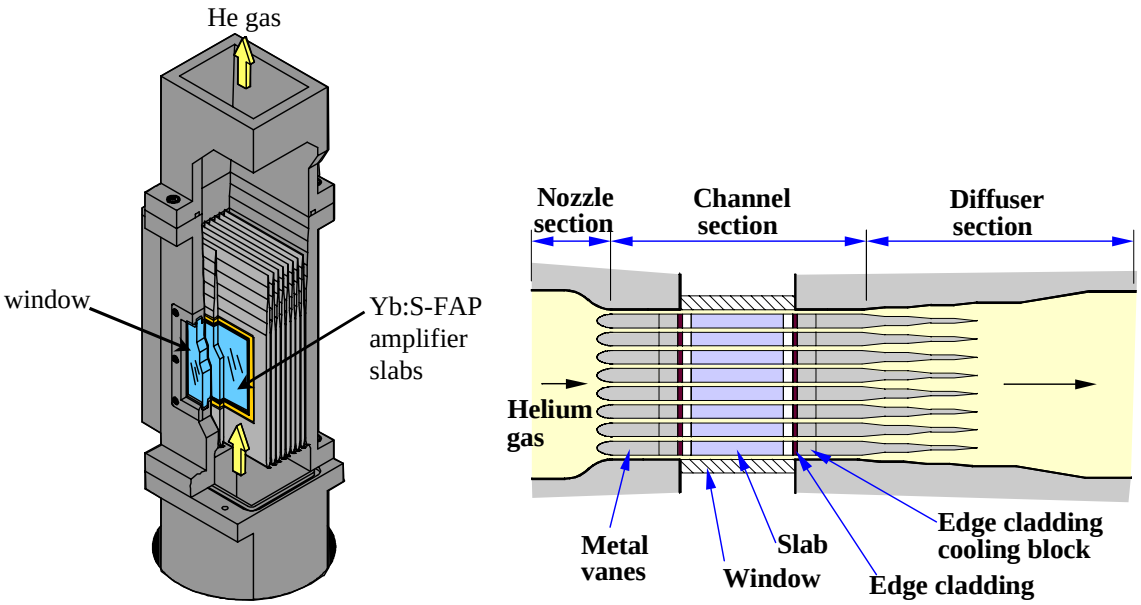

Fig. 7 a) The full gas cooling head carrying seven Yb:S-FAP slabs (4 x 6 x 0.75 cm), and b) a cut-away picture of the gas cooling system.

Finally, the architecture of the laser itself has been designed with efficiency and scalability in mind. The Mercury laser is an angularly multiplexed 4-pass laser system (shown in Fig. 6), which performs the small signal amplification as well as saturated extraction on the two amplifier heads. The beam is injected in the front end and passes through two diode-pumped amplifier heads before hitting the deformable mirror where some of the wavefront distortion induced by the optics is removed. The beam then

retraces its path to the injector/reverser optics which send the beam back through the system for the third and fourth passes through the amplifiers to give the final output laser pulses. The split diode array allows all of the optical components to be placed in line and would allow stacking of amplifiers in future diode-pumped ICF driver systems. In this advanced laser system where efficiency and technology are simultaneously pushed to their limits, crystal growth of Yb:S-FAP is paramount to success of the Mercury laser system. Yb:S-FAP must be an efficient absorber of the pump light and a high gain, efficient emitter of the laser light. It must also have high optical homogeneity, low scatter loss, and low thermal distortion to give the low wavefront distortion necessary for the 5 times diffraction limited beam. Finally, nonlinear loss mechanisms present at the high intensities achieved during extraction must be minimized.

Chapter 2. CHARACTERIZATION OF $Yb^{3+}:Sr_{5-x}Ba_X(PO_4)_3F$ CRYSTALS FOR DIODE-PUMPED LASERS

First published as: *A.J. Bayramian, C.D. Marshall, K.I. Schaffers, and S.A. Payne, "Characterization of $Yb^{3+}:Sr_{5-x}Ba_x(PO_4)_3F$ crystals for diode-pumped lasers," IEEE J. Quantum Electronics, **35**, pp. 665-674, 1999.*

I. Introduction

Ytterbium doped materials[1-3] have sparked a great deal of interest in the last couple of years due to their utility as diode pumped solid-state lasers. The interest lies in the long storage lifetimes of ytterbium doped materials, which are approximately four times longer than their neodymium doped counterparts. These long lifetimes are suited to low-power diode pumping schemes. Ytterbium also has a simple electronic structure in the near infrared (NIR), leading to a low quantum defect, excited state absorption (ESA), and nonradiative decay. The well known thermal and laser characteristics of yttrium aluminum garnet (YAG), including well understood growth techniques and high crystal quality, make YAG a good choice for high power applications. High power ytterbium doped YAG (Yb:YAG) lasers have been demonstrated[4-6]. Yb:YAG systems have been Q-switched[7], operated singe mode[8], and integrated into ultrashort pulse systems producing femtosecond pulses[9]. Applications include the development of diode-pumped tunable Yb:YAG miniature lasers[10], and laser operation of a planar ion-implanted Yb:YAG waveguide[11]. The great utility of optical fiber waveguides has led to the development of high-power ytterbium doped silica fiber lasers[12] and the spectroscopic evaluation of ytterbium doped glasses[13].

The fluorapatite family of crystalline host materials has recently shown much promise for medium power applications, where attention has been focussed on neodymium and

ytterbium doped crystals. Neodymium doped $Sr_5(VO_4)_3F$ (S-VAP), $Sr_5(VO_4)_3Cl$, $Ba_5(PO_4)_3F$ (B-FAP), $Ca_5(PO_4)_3F$ (C-FAP), and $Sr_5(PO_4)_3F$ (S-FAP) have been characterized spectroscopically and lased[14-22]. Likewise, a family of Nd: $Ca_{5-x}Sr_x(PO_4)_3F$ (CS-FAP)[23] have been characterized and lased for x = 0,1,2,3,4 and 5. Several ytterbium doped fluorapatite materials have been considered including: $Ca_5(PO_4)_3F$ (C-FAP), $Sr_5(PO_4)_3F$ (S-FAP), $Sr_5(VO_4)_3F$ (S-VAP), and $Ca_{5-x}Sr_x(PO_4)_3F$ (CS-FAP)[24-26]. Although YAG has better thermomechanical properties, making it better for high thermal loading in high power applications, the fluorapatites require greatly reduced pump intensities to lase efficiently but are limited to moderate thermal loading. These ideas have been demonstrated in the diode pumped laser performance of Yb:S-FAP[1]. Using a scalable, diode-pumped, high-power, gas-cooled-slab geometry, Marshall[27] measured 50 W of continuous wave (cw) optical power at 1047 nm with a laser slope efficiency of 51% with respect to absorbed diode pump power. The diode pump source was a high-power laser diode array with operating wavelength centered at 900 nm and a bandwidth of 5.5 nm FWHM. The complication arises here, in matching the pump bandwidth (5-10 nm) to the relatively narrow absorption bandwidth (approximately 5 nm in S-FAP). Specific applications may also require a greater bandwidth in the emission. These reasons led us to consider the families of mixed crystals $Ca_{5-x}Sr_x(PO_4)_3F$ and $Sr_{5-x}Ba_x(PO_4)_3F$, which show homogeneous and inhomogeneous broadening due to cation variation. An initial assay of the absorption spectra of materials in each of these categories led us to choose $Sr_{5-x}Ba_x(PO_4)_3F$ (SB-FAP) family of crystals as a starting point. The reasons for this choice lie in the similarity between the absorption spectra of S-FAP and B-FAP, which lead to moderate bandwidth and cross section changes.

II. Crystal Growth

Crystals of SB-FAP (x = 0, 0.25, 0.5, 1, 2, 5) up to 2.8 cm in diameter and 10 cm in length were grown using the Czochralski method as described by Schaffers[28]. The crystals were grown in a nitrogen atmosphere at a pull rate of 1 mm/hr and a rotation rate of 20 rpm. The crystals, as grown, are cloudy and therefore require a post-growth annealing process in which the boule is suspended over the melt for up to 7 days in a temperature zone of the growth furnace that is approximately 300 °C below the melting point. A constant starting concentration for ytterbium of 1 atomic percent or number density of approximately 16.8×10^{19} cm^{-3} in the melt $[Yb]_{melt}$ was used throughout the growth experiments. Ytterbium number densities in the crystal were then determined by using inductively coupled plasma mass spectrometry (ICP MS). Results of the mass spectral analysis were in weight percent of the pure material. The number density of ytterbium was then calculated using eqn. 1, where ρ is the density of the host material, A_{Yb} is the atomic weight of ytterbium, and N_{Av} is Avogadro's number. The densities for the SB-FAP crystals were interpolated from the densities of S-FAP and B-FAP[29] using a weighted average.

$$[Yb]_{crys} = \frac{(wt.\%)\rho}{100A_{Yb}} N_{Av} \qquad (1)$$

Using the number densities of ytterbium in the crystal and the initial charge in the melt, $[Yb]_{melt}$, the distribution coefficient, d, can be calculated using $d = [Yb]_{crys}/[Yb]_{melt}$. The distribution coefficients for all of the SB-FAP crystals are plotted in Fig. 1, where the dashed line through the data points is an empirical fit. We observe that the addition of barium to the host lattice facilitates the incorporation of ytterbium into the crystal.

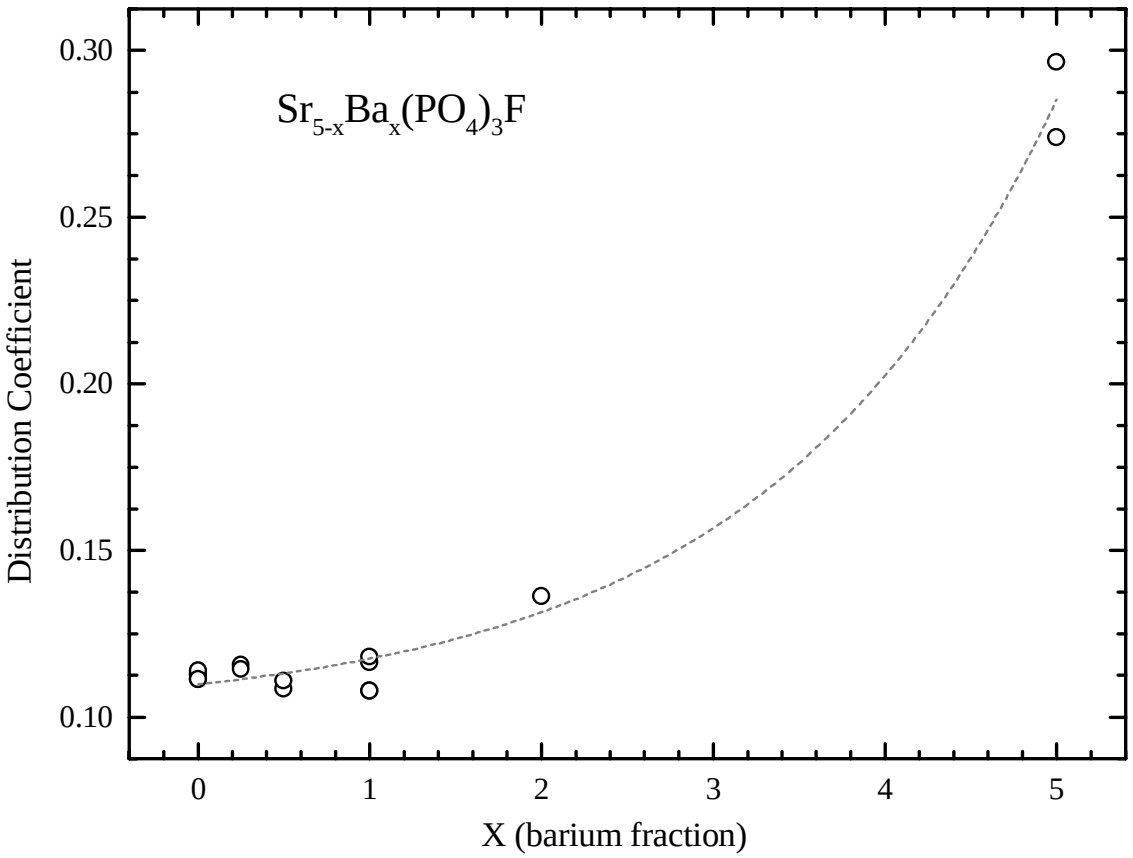

Fig. 1. Plot of the distribution coefficient measured for crystals of Yb^{3+}:$Sr_{5-x}Ba_x(PO_4)_3F$ where $0 \leq x \leq 5$.

III. Experimental Methods

Spectroscopic characterization consisted of absorption spectra, emission spectra, and emission lifetime measurements. Polarized absorption spectra were taken on a Perkin Elmer Lambda 9 spectrophotometer with a resolution of approximately 0.8 nm over the wavelength range of interest, 860 to 1200 nanometers. The absorbance value given by the spectrophotometer was then converted to absorption cross section using $\sigma_{abs} = [(\ln(10))*A]/\ell N_{Yb}$, where A is the absorbance (optical density) , ℓ is the length of the sample, and N_{Yb} is the ytterbium number density. Polarized emission spectra were taken using a diode-pump source to excite the SB-FAP crystals, then the emission was imaged

through a polarizer onto the entrance slit of the monochromator. The pump source consisted of a 100 W peak power microchannel cooled diode bar array[1], driven by a Specra Diode Labs Quasi-CW Laser Driver (model# SDL928-25), with $\lambda \sim 900$ nm at T = 15 °C. The grating used in the monochromator was a McPherson 600 groove/mm blazed at 1.0 μm. The signal was detected at the exit slit of the monochromator using a Judson Infrared, Inc. germanium detector (model#J16D-M204-R05M). To correct for the detector response, a black body spectrum was taken using a tungsten lamp, where the filament temperature was read using an optical pyrometer. The absolute wavelength was calibrated using a Nd:YLF laser with emission at 1047.6 nm and the zero-line of S-FAP at 985.5 nm[29]. The emission spectra were taken at a resolution of 0.6 nm. Radiative lifetimes were measured using a pulsed laser source to excite the SB-FAP crystals, and the fluorescent decay was observed using a Electro Optics Technology (EOT) photodetector (model# ET4000) and a digitizing oscilloscope. The pump source was a pulsed Cr:LiSAF laser tuned to 900 nm operated at 1 Hz with a pulsewidth of 200 μs and a maximum energy of 600 mJ. With the basic spectroscopy in hand, we then selected crystals for the laser experiments. The number of samples was narrowed to x=0,0.25,0.5, and 1 at this point because the quality of the boules precluded any large samples for x=2 and 5. Crystals with x=0.25,0.5, and 1 were cut into cubes approximately 1 cm thick and with end faces polished within 0.5' parallel and with $\lambda/4$ flat.

The small signal gain experiment was conducted using the pump-probe method employing the counterpropagating beam configuration shown in Fig. 2. All gain measurements used π–polarized pump and π–polarized probe beams, since the maximum absorption and emission for Yb:SB-FAP crystals occurs for the π–polarization direction

(see Fig. 4). The pump source was the same as for the lifetime experiments, and the probe source was a Spectra Physics diode-pumped Nd:YLF head operated CW and attenuated to very low power. The Cr:LiSAF beam was passed through a $\lambda/2$ plate and polarizer pair which was used as a variable attenuator. The Cr:LiSAF pump beam, which has an approximately top-hat intensity profile, was then focused by a lens to a 2 mm diameter spot in the SB-FAP crystals. The Fresnel reflection from the surface of a wedge was calibrated to monitor the incident fluence using a Molectron energy detector (Model# J-25). The Nd:YLF beam was counter propagated through a bandpass filter to prevent any pump light from entering the Nd:YLF oscillator, then passed through a polarizer and focused onto the crystal to a beam diameter of 150 μm. All beam diameters were measured using a Cohu CCD camera (Model#4800) operated using Coherent Beamview Analysis system. The Nd:YLF beam transmitted by the SB-FAP crystal reflects off the wedge, and passes through a lens, several irises, and bandpass filters, which serve to reduce stray pump light and amplified spontaneous emission (ASE) or fluorescence. The resulting signal was then detected using and a photodetector (Electro Optics Technology Model#ET4000) and sent to a digitizing oscilloscope. The experimental small signal gain was then measured based on Eqn. 2, where $S_{p\&p}$ is the signal with both the pump and probe lasers, S_{pump} is the signal with just the Cr:LiSAF laser, S_{probe} is the signal with just the Nd:YLF laser, and S_{back} is the signal with no laser sources. The absence of any probe gain saturation was verified by reducing the Nd:YLF power by an order of magnitude and observing identical gain.

$$G = \frac{S_{p\&p} - S_{pump}}{S_{probe} - S_{back}} \tag{2}$$

The laser experiments were performed using the experimental setup in Fig. 3. An Spectra-Physics argon ion laser (model#171) was used to pump the Spectra Physics Ti:Sapphire laser (model#3900) which was tuned to 900 nm with less than 0.2 nm FWHM for pumping the Yb:SB-FAP crystals. The tuned wavelength was measured and monitored by using a Spectra Physics Fizeau Wavelength Meter (model#7711).

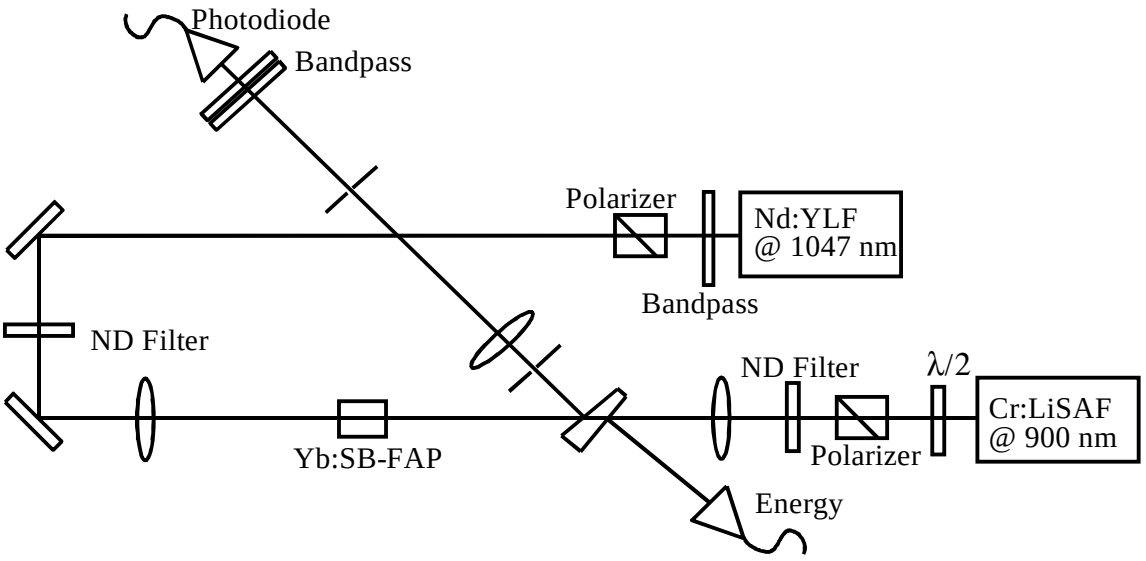

Fig. 2. Small signal gain experimental setup (ND = neutral density)

The roughly TEM_{00} output beam of the Ti:Sapphire laser passes through a telescope used to down collimate the beam 2X, followed by a λ/2 plate and polarizer pair used for pump beam attenuation and to establish the polarization direction. The Fresnel reflection from the wedge was detected using a Newport Multifunction Optical Meter (model#1835-c) with a germanium detector (model#818-IR), which allowed continuous monitoring of input pump power. The pump beam is focused by a 10 cm lens to a Gaussian intensity profile of ~100 μm diameter (1/e) in the Yb:SB-FAP crystal sample. The nearly concentric cavity consisted of two 5 cm radius of curvature mirrors separated by approximately 9.5 cm. The output of the cavity was then passed through either a long-

pass or a short-pass filter, depending on whether the laser or pump signal needed to be monitored, and detected by another Newport germanium detector.

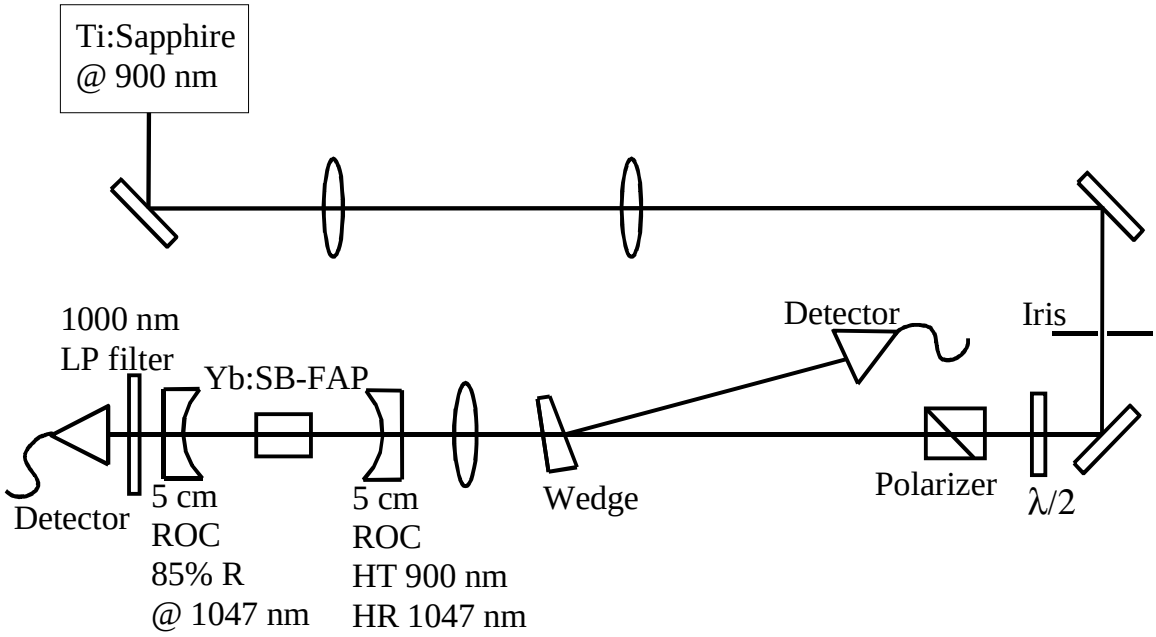

Fig. 3. Laser pumped laser experimental setup (LP = long pass, ROC = radius of curvature, HT = high transmission, HR = high reflectivity)

IV. Spectroscopy

The polarized absorption and emission cross sections of Yb:$Sr_4Ba(PO_4)_3F$ are shown in Fig. 4, which are similar to the spectral shape and position of all of the Yb:SB-FAP crystals. The basic structure of these spectra consists of transitions from the bottom of the $^2F_{7/2}$ manifold to the $^2F_{5/2}$ states as shown in Fig. 5. Since the apatites are anisotropic, there exists a polarization dependence to the absorption and emission spectra, with the π polarization of the crystal having both the stronger absorption and emission. The other smaller features are weak acoustic and vibrational modes as identified by DeLoach, et al.[29].

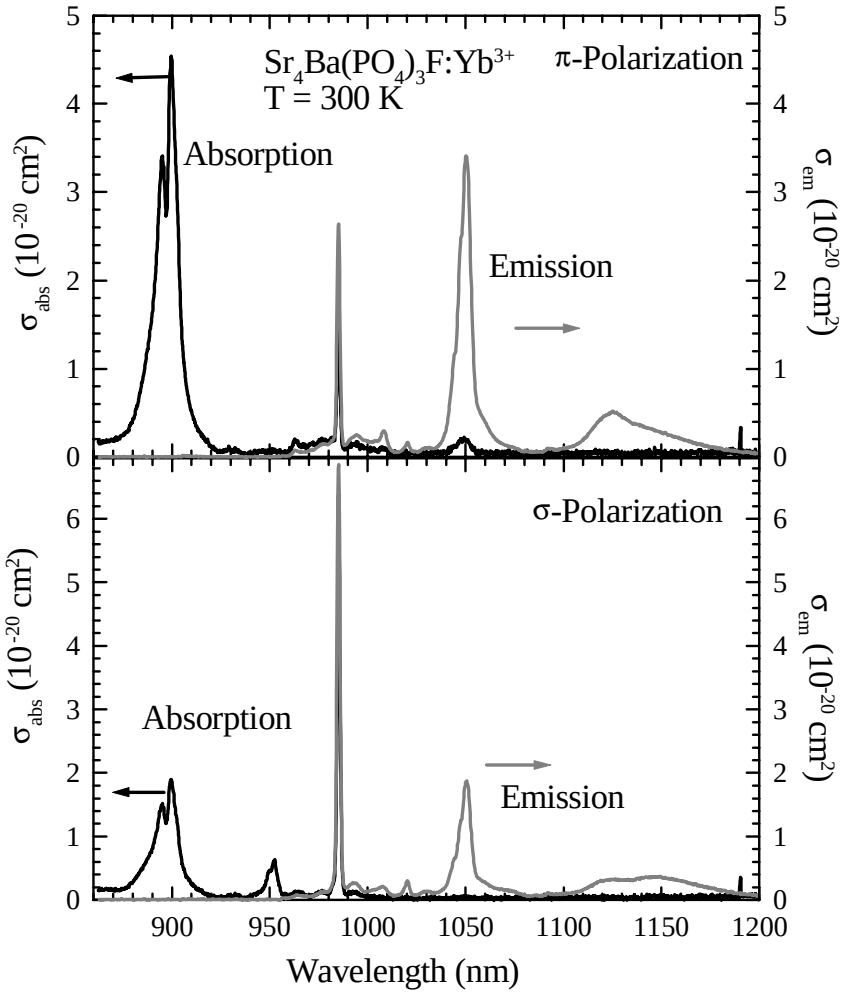

Fig. 4. Polarized absorption and emission cross sections of Yb:$Sr_4Ba(PO_4)_3F$. Fig. 5 shows the approximate electronic levels corresponding to the spectral peaks shown here.

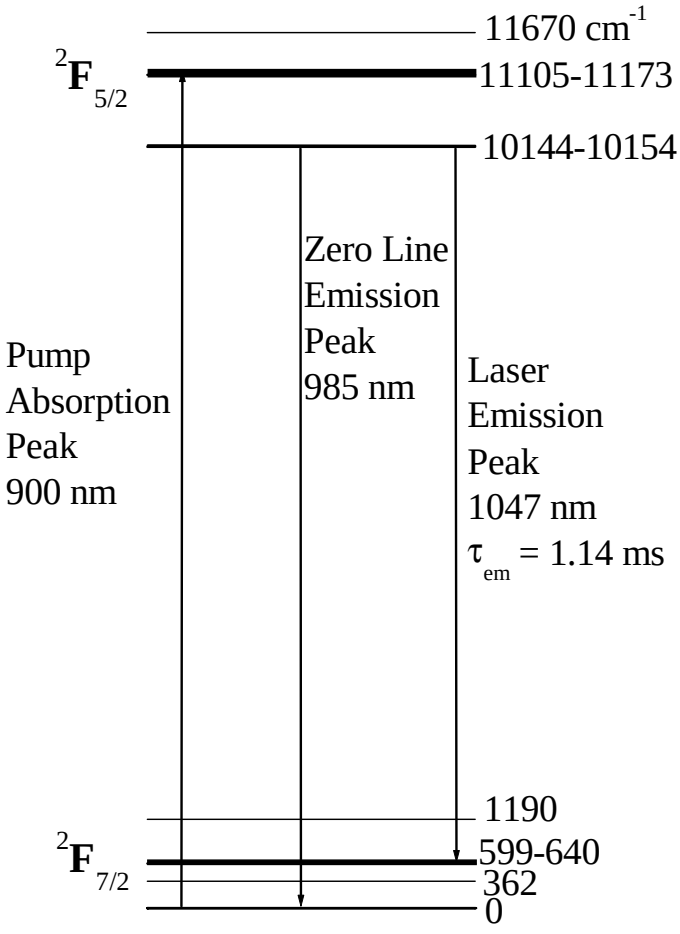

Fig. 5. Energy level structure of Yb:SB-FAP

Our interest lies in the shape and width of the 900 nm absorption feature in the π polarization direction. The absorption in this spectral region for all of the SB-FAP crystals has been overlaid in Fig. 6. Clearly, as the concentration of barium in the host lattice increases, the 900 nm absorption feature is broadened. Although not shown here due to poor crystal quality, B-FAP has its absorption peak at 895 nm and a minor peak at 900 nm, while S-FAP (shown) has the reversed situation. Thus the observed broadening can be partially attributed to a decrease in the pure S-FAP character of the crystal and a corresponding rise in the B-FAP character of the crystal, which will be discussed further at the end of this paper. The observed decrease in the area of the absorption cross section

for this spectral region as barium is added to the host lattice corresponds to a slight shift in oscillator strengths as pure S-FAP becomes pure B-FAP. The overall linewidth of the absorption feature, which has been defined here by the FWHM of a Gaussian best fit of the lineshape, increases from 4.7 nm for Yb:S-FAP to 15.9 nm for Yb:$Sr_3Ba_2(PO_4)_3F$, corresponding to equal heights of the two peaks.

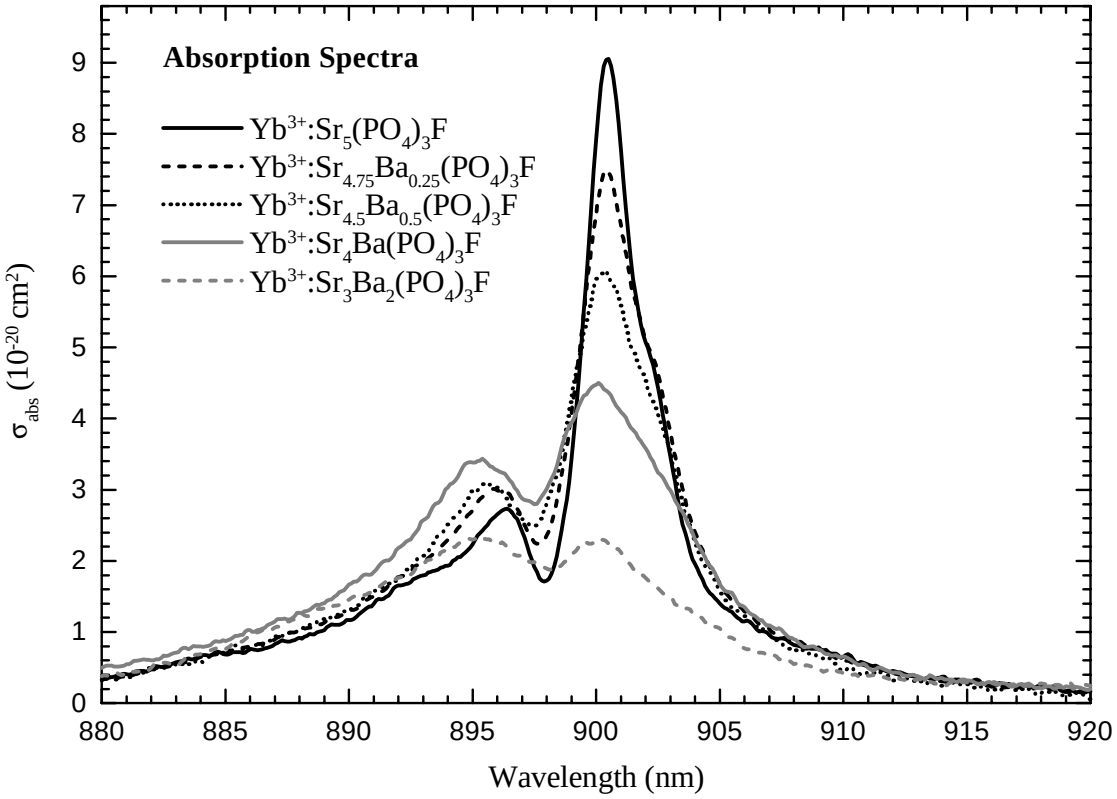

Fig. 6. Π polarized absorption cross sections for the ytterbium doped SB-FAP crystals.

Since the desired broadening has been achieved in the absorption cross section, we turn our attention to the corresponding broadening of emission cross sections and lineshapes. There are three methods of calculating and thus confirming the emission cross section: reciprocity, the Einstein method, and small signal gain. The first two methods are spectroscopic and will be covered in this section while the latter will be covered in the next section. Using reciprocity, the emission cross section can be

calculated using only the absorption cross section, and some knowledge of the energy level structure of ytterbium in SB-FAP as illustrated in Fig. 5. The emission cross section obtained by the reciprocity method is given by[3]:

$$\sigma_{em}^{\alpha}(\lambda) = \sigma_{abs}^{\alpha}(\lambda)\frac{Z_l}{Z_u}\exp[(E_{ZL} - hc/\lambda)/kT] \tag{3}$$

$$\text{where } Z = \sum_i d_i \exp(-E_i/kT) \tag{4}$$

Here $\alpha = \pi$ or σ, the polarization, λ is the wavelength, $\sigma_{abs}(\lambda)$ is the absorption cross section as a function of wavelength, Z_l is the partition function for the ground state, Z_u is the partition function for the excited state, and E_{ZL} is the zero line energy defined as the energy of the transition from the lowest level of the ground state to the lowest level of the excited state, k is the Boltzmann constant, and T is temperature. For all of the SB-FAP crystals the partition function ratio was taken to be 1.1 as was found previously by DeLoach[3] for C-FAP, and E_{ZL} was read from the absorption spectra itself, generally in the 985 nm region of the spectra for all of the SB-FAP crystals. For the transition at 1047 nm, this method has a rather large error since the high signal-to-noise of the absorption spectrum is exponentially compromised by the energy difference between the zero line and the spectral region of interest. In fact, emission cross sections calculated by reciprocity lose much of their spectral shape due to noise thereby only serving as a check of the other methods.

The Einstein method is much more accurate since the cross section value depends directly on the emission spectral lineshape, and inversely on the radiative lifetime. Since this method uses the actual emission of the sample, losses such as ESA, and lattice defects directly effect the emission lineshape and are thus taken into account. The

polarized emission cross sections, which will be dependent on pump wavelength for inhomogeneous absorption, using the Einstein method[3] are given by:

$$\sigma_{em}^{\alpha}(\lambda) = \frac{\lambda^2 g^{\alpha}(\lambda)}{8\pi n^2 \tau_{rad}} \tag{5}$$

Where α is the polarization, ν is the frequency, λ is wavelength, n is the index of refraction, τ_{rad} is the radiative lifetime, and $g^{\alpha}(\lambda)$ is the normalized lineshape function:

$$g^{\pi}(\lambda) = \frac{3S^{\pi}(\nu)}{[1+2\beta]\int S^{\pi}(\nu)d\nu}$$

$$g^{\sigma}(\lambda) = \frac{3S^{\sigma}(\nu)}{[\beta^{-1}+2]\int S^{\sigma}(\nu)d\nu} \tag{6}$$

The lineshape function is defined by $S^{\alpha}(\nu)=(\lambda/\nu)S^{\alpha}(\lambda)$, the black-body-corrected emission spectrum, and β which is the ratio of the total emission σ-polarized to the total emission π-polarized. The emission cross sections were calculated and the spectral lineshape of the laser transition near 1047 are shown in Fig. 7. The cross sections shown are all calculated from emission spectra of crystals pumped at a center wavelength of 896.5 ± 0.5 nm with a linewidth of 4 nm FWHM. Once again, the spectra are broadened by the addition of barium, from 4.9 nm (FWHM of a Gaussian best fit) for pure S-FAP to 10 nm for Sr_3Ba_2-FAP. In general, the Einstein method-derived cross sections are dependent on pump wavelength, since inhomogeneous spectral lineshapes will change with pump wavelength.

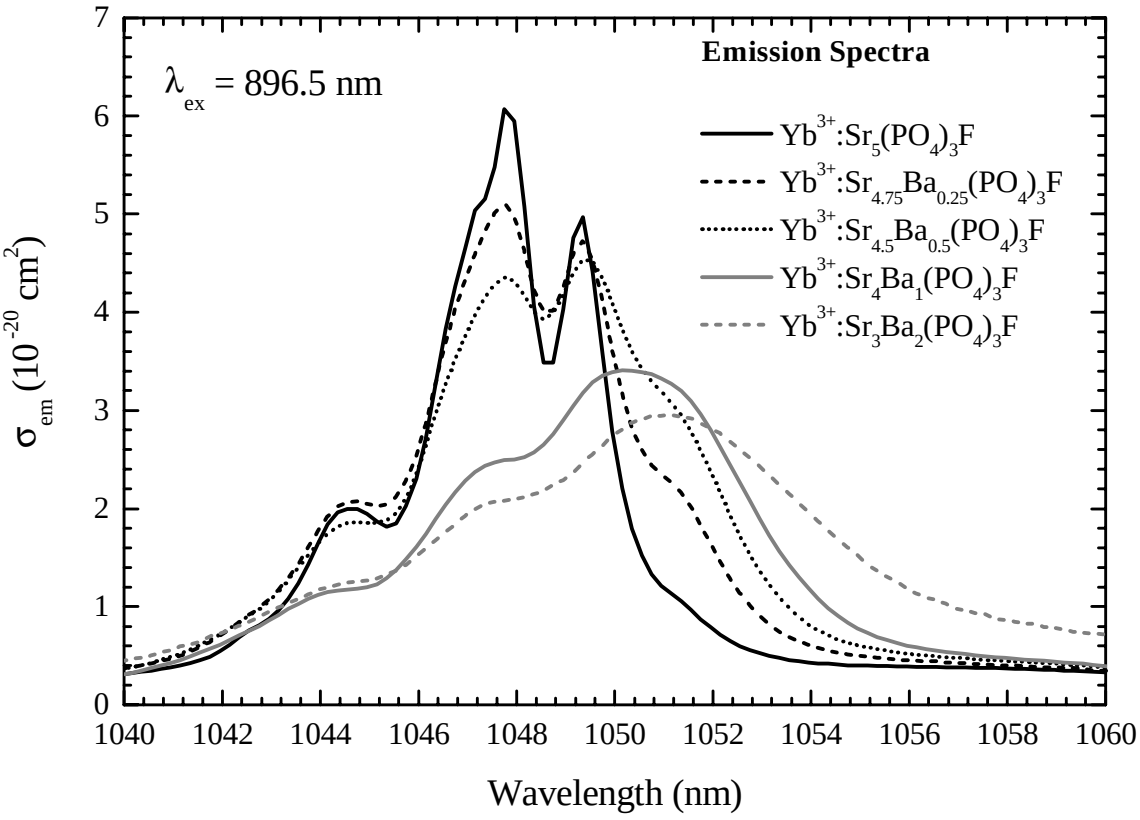

Fig. 7. Π polarized emission cross sections of ytterbium doped SB-FAP crystals using the Einstein method.

Since efficient extraction is a concern, the presence of any inhomogeneity and its relative magnitude in the SB-FAP crystals is important. Using an external cavity tunable diode laser with a linewidth less than 0.2 nm, emission spectra of $Sr_4Ba(PO_4)_3F$ were taken at a series of wavelengths between 893 and 903 nm. Fig. 8 shows that for the minimum and maximum pump wavelengths, the emission line shows some movement, which indicates some fraction of inhomogeneity within the crystal structure. Similar studies of the other SB-FAP crystals also showed inhomogeneity for the $Sr_3Ba_2(PO_4)_3F$ crystal, while the $Sr_{4.5}Ba_{0.5}(PO_4)_3F$, $Sr_{4.75}Ba_{0.25}(PO_4)_3F$, and $Sr_5(PO_4)_3F$ crystals showed little or no inhomogeneity. This experiment generated the maximum inhomogeneity by pumping into the wings of the absorption feature.

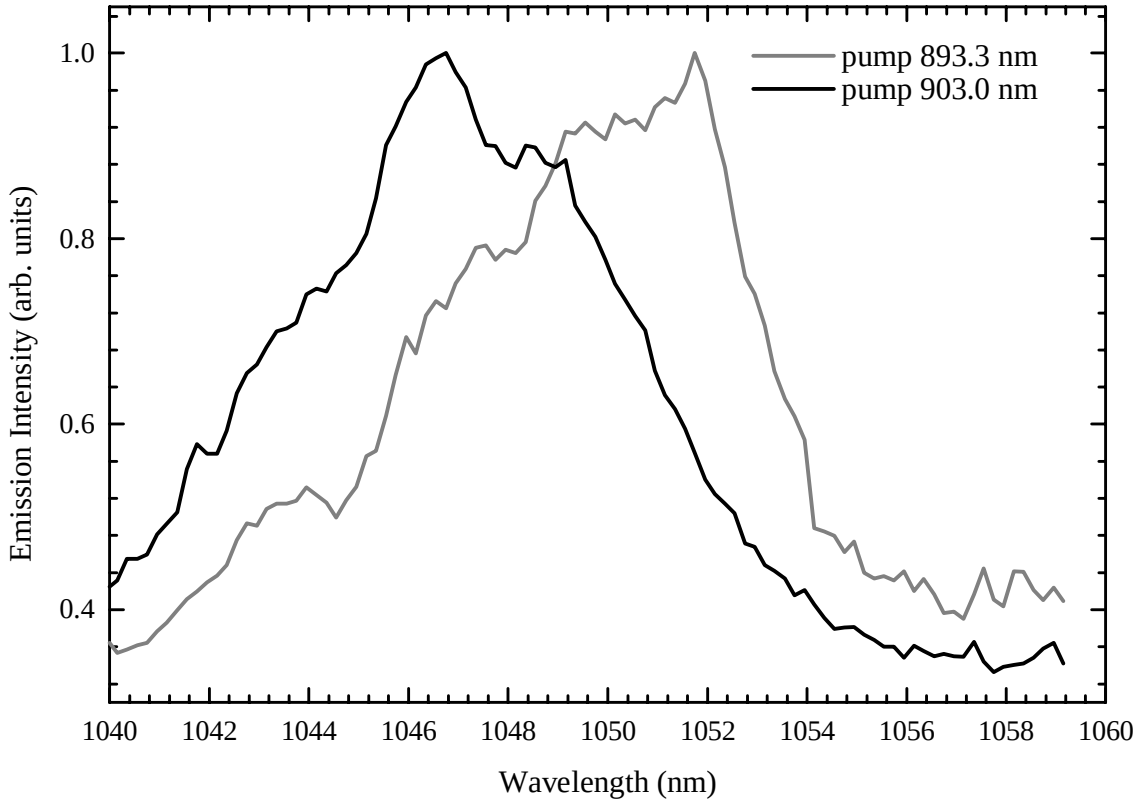

Fig. 8. The changing emission lineshape of Yb: $Sr_4Ba(PO_4)_3F$ with pump wavelength indicates inhomogeneous broadening.

The final basic spectroscopic measurement to be made is the radiative lifetime. The high absorption and emission cross sections at the zero line (ZL) in these materials mean radiation trapping will have a significant effect on the measured radiative lifetime as was observed by Marshall, et al.[30]. Eqn. 7 below provides an approximation to the equation in ref. 30 and 31 for small volumes, establishing a linear relationship between radiative lifetime and the $V^{1/3}$, where V is the volume of the crystal sample, and ξ is a constant for a given ytterbium concentration. The y-intercept then gives us the intrinsic radiative lifetime for an infinitely small crystal sample with no radiation trapping.

$$\tau_{meas} \cong \tau_o + \xi V^{1/3} \tag{7}$$

Table 1. The intrinsic radiative lifetime of the ytterbium doped SB-FAP crystals.

Material	Intrinsic Lifetime (msec)
$Sr_5(PO_4)_3F$	1.14
$Sr_{4.75}Ba_{0.25}(PO_4)_3F$	1.13
$Sr_{4.5}Ba_{0.5}(PO_4)_3F$	1.12
$Sr_4Ba(PO_4)_3F$	1.11
$Sr_3Ba_2(PO_4)_3F$	0.98
$Ba_5(PO_4)_3F$	0.94

Table 1 shows the radiative lifetime decreasing with increasing barium content in the lattice to a minimum lifetime for B-FAP. However, for the SB-FAP crystals with barium fraction less than one, the change is only 3%, leaving the energy storage lifetime basically unaffected at low barium fraction.

V. Small Signal Gain

The third determination of the emission cross sections is the small signal gain measurements. The relevant coupled two level rate equations are given by eqn. 8 and 9. A two-level rate equation can be used since the emission at the pump feature is very low.

$$\frac{dN_{gnd}(z,t)}{dt} = -\frac{dN_{ex}(z,t)}{dt}$$

$$= \frac{-\sigma_{abs}(\omega_p)N_{gnd}(z,t)I_p(z,t)}{\hbar\omega_p} + \frac{N_{ex}(z,t)}{\tau} \qquad (8)$$

$$\frac{dI_p(z,t)}{dz} = -\sigma_{abs}(\omega_p)N_{gnd}(z,t)I_p(z,t) \qquad (9)$$

N_{gnd} is the ground state population, N_{ex} is the excited state population, ω_p is the pump frequency, σ_{abs} is the absorption cross section, I_p is the pump intensity, and τ is the emission lifetime. Note that the emission cross section at the pump wavelength has been omitted since it is small compared to the absorption cross section. The pump source for

these experiments had a pulsewidth of 200 μs FWHM, which is a significant fraction of the radiative lifetime and must be taken into account. A simulation code was written in C^{++} that modeled the transient energy level populations described by Eqns. 8 and 9 (Appendix I.). The sample was divided into discrete spatial slices and the pump pulse into temporal intervals, and these temporal slices were propagated consecutively through the spatial slices. The new population values in each spatial slice were stored as dummy variables to be used as the new input populations for the next temporal pulse. In this way, the steady-state solutions for short times and spatial distances can be used to build up the temporally and spatially transient excited state population solution to eqn. 8. The transient small signal gain can then be calculated using:

$$G = \exp((N_{ex}\sigma_{em}(\omega_{gain}) - N_{gnd}\sigma_{abs}(\omega_{gain}))\ell) \tag{10}$$

where ω_{gain} is the frequency of the gain measurement, and ℓ is the crystal length. Since the experiments measured peak gain, the time was chosen such that excited state population and thus the gain was maximized. There are only three adjustable parameters in this pump code: the peak absorption cross section, number density, and peak emission cross section. By fitting measured pump transmission, the values for N_o ($N_o = N_{gnd} + N_{ex}$), the number density, and σ_{abs}, the absorption cross section, can be fixed. Note that fitting N_o controls the absolute intercept of the fit curve, and σ_{abs} controls the curvature, making it possible to independently fit these variables. With N_o and σ_{abs} fixed by the pump transmission measurement, the fit of the small signal gain has only one adjustable parameter, the emission cross section itself. The results of the pump transmission and small signal gain experiments as well as the transient pump code fits of these points are

given in Fig. 9, where the results from eqn. 10 are normalized to 1 at zero fluence to match experimental conditions (i.e. $G = G/\exp(-N_o\sigma_{abs}(\omega_{gain})\ell)$.

The results of all three methods of calculating emission cross section, the two methods for absorption cross section, and two methods for number density are summarized in table 2. Clearly, the number densities and absorption cross sections closely agree, especially given the vastly different experimental methods used to achieve these values. However, there is a slight spread in the emission cross sections values. As described earlier, reciprocity-method-derived emission cross sections have a low signal to noise and generally overestimate cross section values. The Einstein-method derived emission cross sections have the highest signal to noise ratio and take into account most of the losses, although the emission lineshape depends on the pump wavelength and linewidth due to inhomogeneity of the line. The small signal gain measurements are the most direct since all issues are inherently included in this method. However, it is important to note that the pump source for small signal gain is much narrower (~ 0.2 nm) than the pump source for the Einstein method (~ 4nm), and the extraction source is narrow as well (~ 0.1 nm), both of which exacerbate the inhomogeneous character of the measured gain. As the barium fraction increases, this effect is manifested by the gain cross sections decreasing relative to the Einstein emission cross sections.

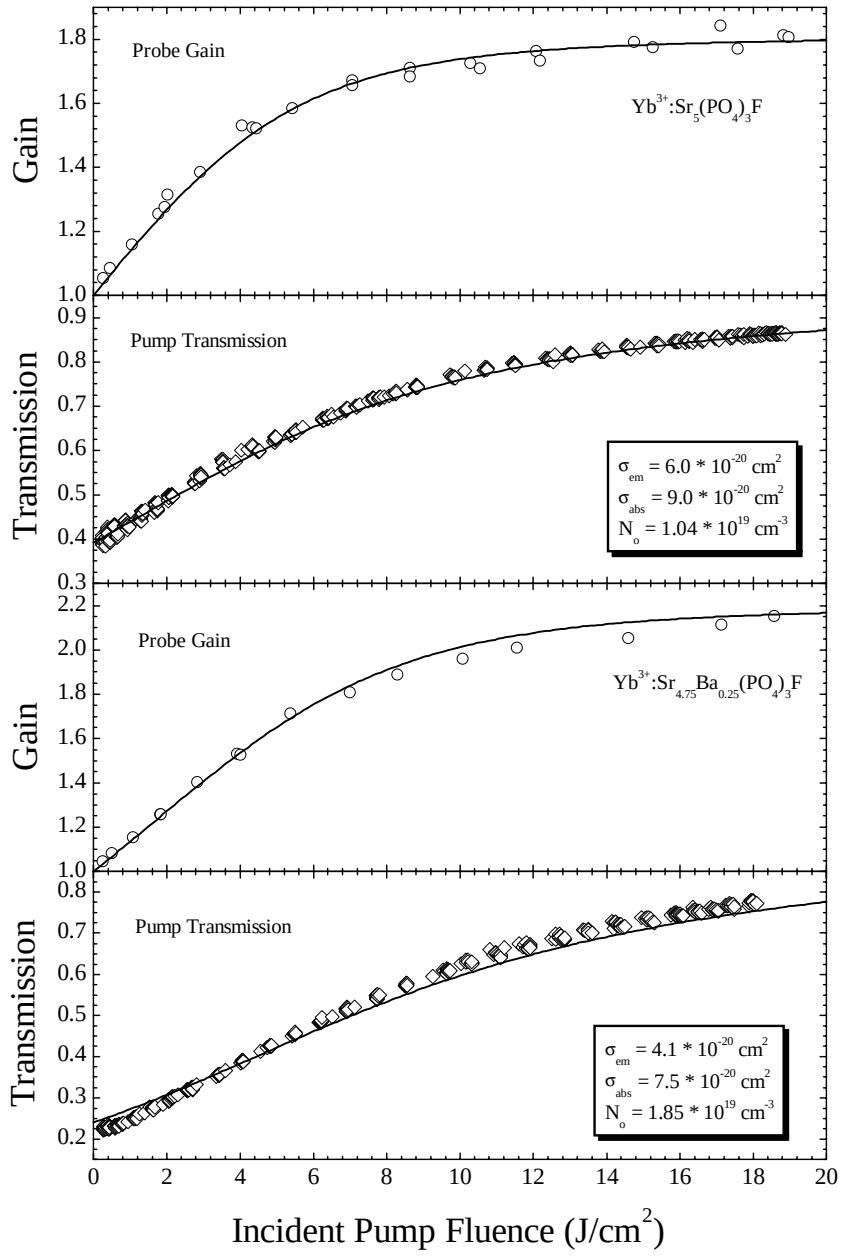

Fig. 9a. Pump transmission and small signal gain with the fitted values for σ_{abs}, σ_{em}, and N_o using transient pump code for ytterbium doped $Sr_5(PO_4)_3F$ and $Sr_{4.75}Ba_{0.25}(PO_4)_3F$.

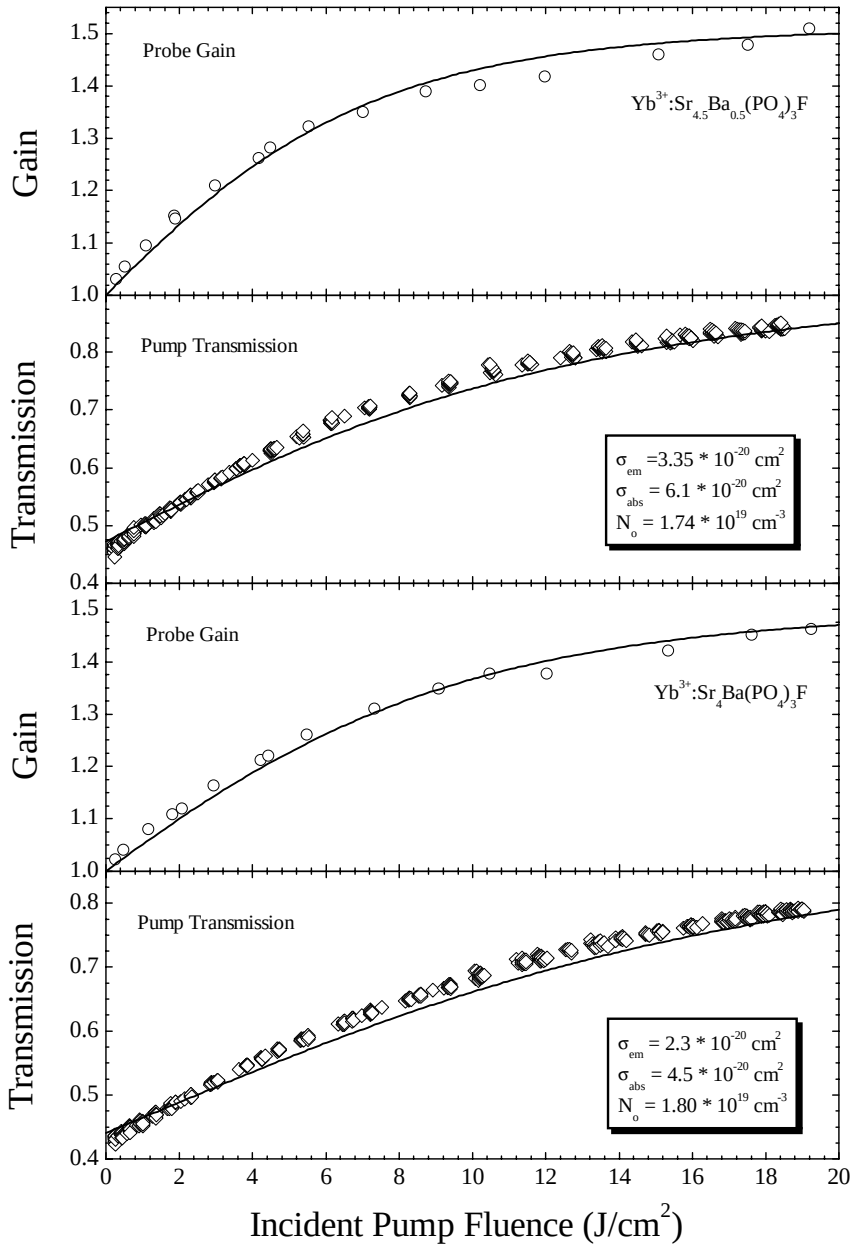

Fig. 9b. Pump transmission and small signal gain with the fitted values for σ_{abs}, σ_{em}, and N_o using transient pump code for ytterbium doped $Sr_{4.5}Ba_{0.5}(PO_4)_3F$ and $Sr_4Ba(PO_4)_3F$.

Table 2. Results of experimental measurements of polarized peak absorption and peak emission cross sections, and the dopant number density for ytterbium doped SB-FAP crystals.

$Sr_{5-x}Ba_x(PO_4)_3F$	$\sigma_{em}(10^{-20}\ cm^2)$			σ_{abs} $(10^{-20}\ cm^2)$		N_{Yb} $(10^{19}\ cm^{-3})$	
Barium Fraction	Reciprocity	Einstein	Gain	Spec.	Gain	Mass Spec.	Gain
0.00	7.0±1.0	6.1±0.6	6.0±1.0	9.1±0.2	9.0±0.8	1.14±0.2	1.04±0.3
0.25	6.0±1.0	5.1±0.6	4.1±1.0	7.5±0.2	7.5±0.8	1.91±0.2	1.85±0.3
0.50	5.2±1.0	4.5±0.6	3.4±1.0	6.1±0.2	6.1±0.8	1.81±0.2	1.74±0.3
1.00	3.8±1.0	3.4±0.6	2.3±1.0	4.5±0.2	4.5±0.8	1.93±0.2	1.80±0.3
2.00	3.3±1.0	2.9±0.6	N/A	2.2±0.2	N/A	2.14±0.2	N/A

VI. Laser Characterization

With the basic spectroscopy of the SB-FAP crystals in hand, we investigated the performance of these materials in a laser cavity. The pump saturation intensity, given by eqn. 11 is increased from 2.1 kW/cm^2 for S-FAP to 4.4 kW/cm^2 for Yb:$Sr_4Ba(PO_4)_3F$:

$$I_{sat} = \frac{hc}{\lambda_{abs}\sigma_{abs}\tau_0} \tag{11}$$

where λ_{abs} and σ_{abs} are the peak absorption wavelength and cross section values in the 900 nm spectral region. These values are on the same order of magnitude as the intensities of the pump light, which leads to bleaching of the absorption. Thus, the fraction of light absorbed will change as a function of intensity. However, when the crystal is lasing, the net gain in the cavity becomes clamped, implying the excited state population and thus the fraction absorbed is clamped as well. To obtain the F_l, the fraction absorbed while lasing, we use eqn. 12 which necessitates measurement of the F_{nl} (the fraction absorbed while the system is not lasing), as well as the pump power transmitted by the output coupler while lasing, P_l and while not lasing, P_{nl}. With F_l known, we can use the power incident on the crystal to calculate absorbed pump power, thereby allowing measurement of the slope efficiency of these materials [26]:

$$(1-F_l)=\frac{P_l}{P_{nl}}(1-F_{nl}) \tag{12}$$

Using the experimental setup described in section 2, we report lasing for the first time in the following ytterbium doped $Sr_{5-x}Ba_x(PO_4)_3F$ crystals for x = 0.25, 0.5 and 1. The slope efficiencies were measured for these materials as well as for ytterbium doped S-FAP using four different output couplers. A typical example of slope efficiency data, and least squares linear fit, are given in Fig. 10.

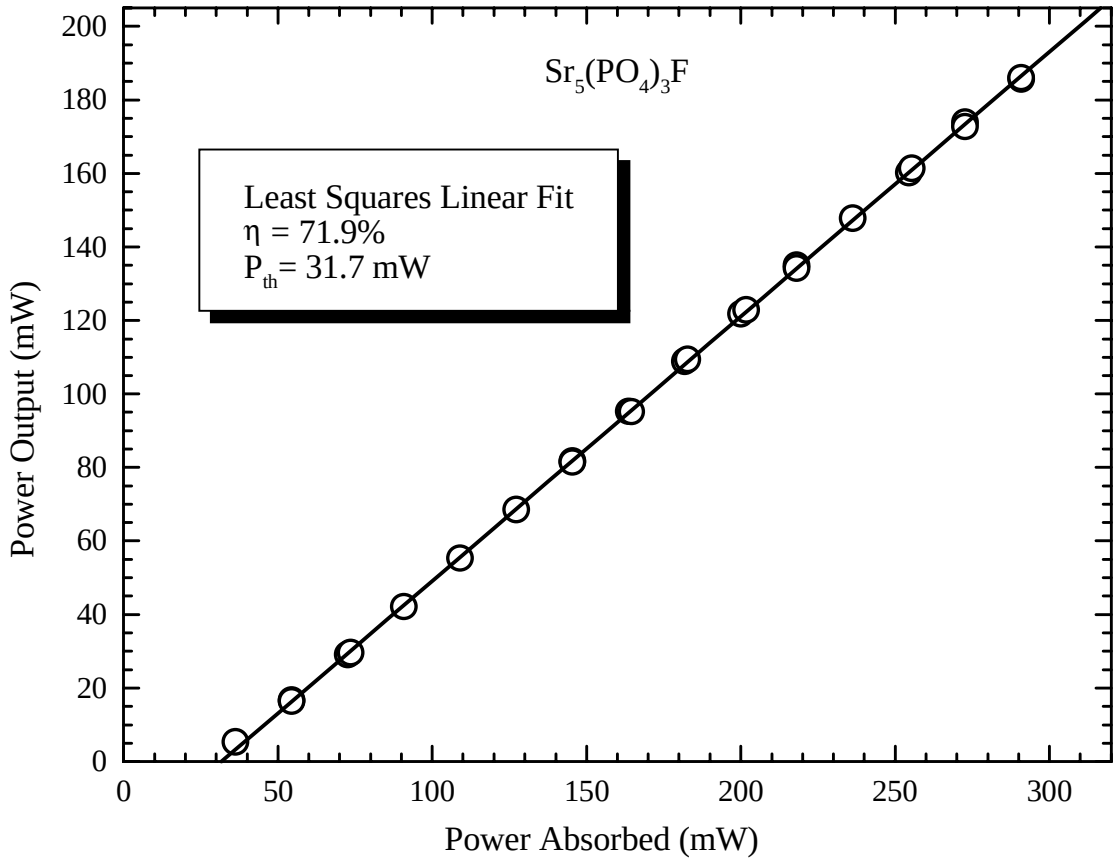

Fig. 10. Slope efficiency of Yb:S-FAP for a 19.8% output coupler .

The results of all of the slope efficiency studies are summarized in table 3 which gives the average of 2 to 3 slope efficiencies for each of the four output coupling values. The general rise in slope efficiency for each crystal with increasing output coupling is a

consequence of passive loss in the cavity. The highest experimentally measured slope efficiency was 71.9% with a 19.8% output coupler for S-FAP, but clearly for barium fractions up to 0.5, one could expect this high slope for any of the crystals.

Table 3. Average slope efficiencies vs. output couplings for the Yb:SB-FAP crystals.

Barium Fraction	Average Slope Efficiencies (± 0.02)			
	19.8% OC	9.7% OC	4.4% OC	3% OC
0.00	0.70	0.61	0.47	0.40
0.25	0.69	0.60	0.46	0.36
0.50	0.70	0.63	0.51	0.42
1.00	0.66	0.61	0.52	0.46

To better understand this data, we will use a "Caird plot" methodology[26,32] from which the double-pass loss, L_d, and the intrinsic efficiency (which in the absence of cavity mode mismatch, excited state absorption, and other nonlinear losses will equal the quantum defect), η_o, are deduced as shown by the equation:

$$\frac{1}{\eta} = \frac{1}{\eta_0} + \left(\frac{L_d}{\eta_0}\right)\frac{1}{T} \tag{13}$$

where T is the transmission and η is the measured slope efficiency. We see that there exists a linear relationship between η^{-1} and T^{-1} with an intercept of η_o^{-1} and a slope of L_d/η_o. The intrinsic slope efficiency, then, is the slope efficiency for zero loss in the cavity. We can use this equation to perform a least squares linear fit of the slope efficiency data points, yielding values for L_d and η_o. Fig. 11 shows a typical example of one of these Caird plots, showing the data points and the least squares fit. The anomalous data point, $\eta^{-1} = 3.03$, from one of our initial measurements was included to show how the Caird method also gives us a consistency check. Given the highly quantitative

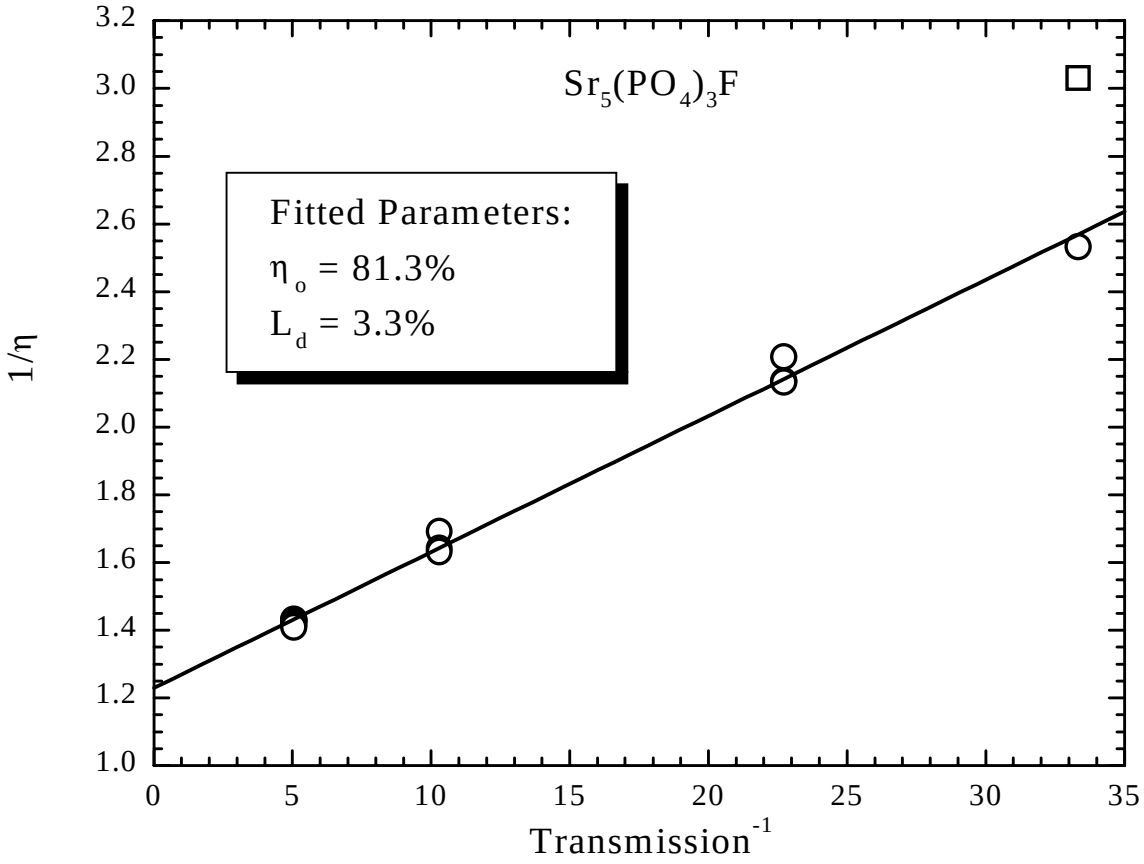

Fig. 11. Caird plot of Yb:S-FAP. The square point was omitted for the fit.

nature of these measurements, the subtle impacts of slight misalignments or other changes in the experimental setup are not readily apparent, but the Caird method allows a self consistent check of the experiment since the slope efficiency of any non-optimized laser cavity will deviate from the straight line defined by those which are optimized, thus eliminating all systematic errors from a measurement. We have summarized the results of the Caird plot analyses in Table 4, which depicts the fitted values for intrinsic slope efficiency, and for the double-pass loss. The single-pass losses for these materials are on the order of 1% for all of the crystals, which is reasonable considering the crystal samples are all early growth runs. To get a better handle on the intrinsic slope efficiencies, consider the quantum defect limit defined by the laser photon energy divided by pump

photon energy or $\lambda_{pump}/\lambda_{extract} \approx 0.86$ for the Yb:SB-FAP crystals. This limit implies every pump photon will create a laser photon, giving the theoretical limit for a perfect laser with these pump and extraction wavelengths. Clearly, S-FAP and the other SB-FAP crystals with barium fraction less 1 are very close to this limit indicating that the total losses are almost exclusively passive. In fact, the difference in the intrinsic efficiency of Yb:S-FAP with the quantum defect could be attributed entirely to a slight mode mismatch between the pump and cavity fields (which would be an example of a systematic error as described earlier). However, there is a significant decrease in the intrinsic slope efficiency as the barium fraction rises from 0.5 to 1. This reduction can be explained by the partially inhomogeneous nature of the SB-FAP absorption and emission lineshapes, which will be discussed in the following paragraph. It is interesting to note this same decrease in intrinsic slope efficiency from 84% for Yb:$Ca_5(PO_4)_3F$ to 65% for Yb:$Ca_3Sr_2(PO_4)_3F$ as the strontium fraction increased and the lines became inhomogeneous[24].

Table 4. The intrinsic slope efficiencies and double pass losses for Yb:SB-FAP crystals

Barium Fraction	Intrinsic Slope Efficiency, η_o	Double Pass Loss, L_d
0.00	81.3%	3.2%
0.25	81.2%	3.4%
0.50	79.1%	2.5%
1.00	70.6%	1.6%

To get a better qualitative understanding of the extent of inhomogeneity for the absorption features, we chose to model the absorption as totally inhomogeneous, in order to provide a worst case estimate of the effects of inhomogeneity on the laser slope efficiency. To accomplish this, the lineshape of the Yb:S-FAP and Yb:B-FAP absorption

in the spectral region from 880-920 nm were fitted using a 5 Gaussian function fit for each lineshape. These fits were then used as the base functions for the construction of the Yb:SB-FAP absorption lineshapes from 880-920 nm. There are two adjustable parameters for each of the lineshape functions, an amplitude factor for the lineshape given by A_S for S-FAP, and A_B for B-FAP, and a factor multiplying the width of every Gaussian in the lineshape fits given by Q_S for S-FAP, and Q_B for B-FAP to account for broadening. The full fitting function, where all of the a_i, λ_i, W_i, a_j, λ_j, W_j are constants defined by the fitted S-FAP and B-FAP lineshapes, is given by eqn. 14:

$$\sigma_{abs}^{SB}(\lambda) = A_S \sum_{i=1}^{5} a_i \exp\left[-\left(\frac{\lambda-\lambda_i}{Q_S W_i}\right)^2\right] + A_B \sum_{j=1}^{5} a_j \exp\left[-\left(\frac{\lambda-\lambda_j}{Q_B W_j}\right)^2\right] \qquad (14)$$

Using eqn. 14 to then fit the lineshape of the SB-FAP crystals gives the results for the four adjustable parameters (A_S, Q_S, A_B, Q_B) in table 5. The general trends are an increase in B-FAP amplitude as well as broadening of the overall width of the spectra as barium is added to the host lattice. To understand how these inhomogeneities would effect the overall slope, we must consider the pumping and lasing conditions. The slope efficiency studies employed a Ti:Sapphire laser tuned to 900.0 nm with a linewidth less than 0.2 nm, and the SB-FAP lasers operated narrow linewidth at their respective emission peaks. If these lines are totally inhomogeneous, any pump light that is absorbed into the B-FAP spectral site will emit at the B-FAP spectral site and will not be included in the laser extraction. That is, any light absorbed to the B-FAP site is a loss, since there is no extraction of the B-FAP spectral site. Table 5 lists the fitted relative loss induced by absorption to the B-FAP spectral site, which is defined as the ratio of the B-FAP absorption intensity relative to the total absorption intensity at the pump wavelength.

Clearly, as the barium fraction increases, the fitted relative loss increases as well. Next, we will define the experimental relative loss as the change in intrinsic slope efficiency relative to the intrinsic slope efficiency of S-FAP from our Caird analysis in table 4. Comparing the experimental and fitted relative losses, we can see that the experimental relative loss is much less (<0.3x) than the absorptive loss assuming totally inhomogeneous spectra. Qualitatively then, the spectra are a combination of homogeneous and inhomogeneous broadening induced by barium introduction into the lattice. The homogeneous broadening of ytterbium in the apatite structure was addressed in Ref. 29, where DeLoach et al. considered vibrational couplings causing homogeneous broadening of the pure electronic levels. When Yb^{3+} is doped into any of the fluorapatites, it replaces the divalent metal ion (Sr^{2+} or Ba^{2+}) involving the charge compensation scheme ($Yb^{3+} + O^{2-}$) for ($Sr^{2+} + F^{-}$). The presence of local vibrations in these Yb-O bonds coupled with the pure electronic states of Yb^{3+} has been shown to produce the observed lineshape structure. The homogeneous broadening associated with this vibrational interaction must therefore be responsible for the greater share of the broadening in the observed lineshapes of Yb:SB-FAP.

Table 5. The amplitude and width factors involved in fitting the lineshape of the Yb:SB-FAP crystals, and the comparison of the absorptive loss due to pumping a completely inhomogeneous line (i.e. S-FAP and B-FAP sites only), with the reduction in the intrinsic slope efficiency.

Barium Fraction	A_S	Q_S	A_B	Q_B	Absorptive Loss to B-FAP	Experimental Relative Loss
0.00	1.0	1.0	0.0	1.0	0%	0%
0.25	0.74	1.25	0.21	1.0	6%	0.1%
0.50	0.53	1.58	0.34	1.0	12%	2.2%
1.00	0.28	2.1	0.53	1.2	34%	10.7%

VII. Discussion

The broadened absorption and emission bands of the ytterbium doped $Sr_{5-x}Ba_x(PO_4)_3F$ crystals could serve a variety of useful applications. As was mentioned earlier, the broader absorption bandwidth enhances our ability to couple pump sources. For example, high power diode arrays can have greater bandwidth due to the individual diodes having slightly different center frequencies. Temperature chirp of the output wavelength during the pump pulse can also become a problem for compact pump sources due to cooling mechanisms. Broadening of the emission bandwidth can be even more crucial. Emission bandwidth is important when considering materials for chirped pulse amplification where the minimum output pulse length is governed by $\Delta\nu_{FWHM}\Delta\tau_{FWHM} \approx 0.44$ for a transform-limited Gaussian pulse, where $\Delta\nu_{FWHM}$ and $\Delta\tau_{FWHM}$ are the FWHM spectral and temporal pulsewidths, respectively[33]. For example, if we choose a total gain of 30000, then the bandwidths of emission spectra in Fig. 7 will be gain narrowed to a certain extent. The bandwidths and minimum pulsewidths will be approximately 75 GHz and 5.9 ps for Yb:S-FAP versus 305 GHz and 1.4 ps for $Yb:Sr_4Ba(PO_4)_3F$. For a low gain of 1, as for a laser, the bandwidths and minimum pulsewidths are 1 THz, 440 fs for Yb:S-FAP and 1.88 THz and 226 fs for $YB:Sr_4Ba(PO_4)_3F$. Another application of bandwidth is for beam smoothing of the driver beam of Inertial Confinement Fusion (ICF) for uniform target illumination to minimize seeding of Rayleigh-Taylor instabilities in the target. One of the methods of beam smoothing is Smoothing by Spectral Dispersion (SSD)[34] in which the coherence is reduced by a spectrally dispersing a frequency modulated beam, effectively smoothing the beam by moving the speckled intensity pattern. The normalized Root-Mean-Square (rms) intensity at the target is then

given by $\Delta I_{rms} \geq 1/(\Delta\nu\tau)^{1/2}$, where $\Delta\nu$ is the bandwidth, and τ is the integration time (~ 1.0 ns for ICF applications). Clearly, the broader-bandwidth mixed crystals enhance this beam smoothing method.

VIII. Summary

We have successfully grown a new family of ytterbium doped $Sr_{5-x}Ba_x(PO_4)_3F$ crystals. The basic spectroscopic properties of these materials have been measured including: absorption and emission cross sections, and radiative lifetimes. As expected, the absorption linewidth in the 900 nm spectral region was found to broaden with increasing barium fraction in the host lattice from 4.7 nm to a maximum of 15.9 nm FWHM. Consequently, the emission spectra were also found to broaden with increasing barium fraction in the host lattice from 4.9 nm to a maximum of 10 nm FWHM. The emission cross section, perhaps the most crucial spectroscopic parameter, was verified through three different methods, and these values were found to agree within experimental error. We have lased ytterbium doped $Sr_{4.75}Ba_{0.25}(PO_4)_3F$, $Sr_{4.5}Ba_{0.5}(PO_4)_3F$, and $Sr_4Ba(PO_4)_3F$ for the first time. The slope efficiencies for these crystals, including Yb:S-FAP, were measured for a variety of output couplers, and the intrinsic slope efficiencies calculated. Crystals with barium fraction less than 1 were found to have nearly unchanged slope efficiencies and intrinsic slope efficiencies, while the Yb:$Sr_4Ba(PO_4)_3F$ suffered from loss effects due to increased inhomogeneity of the lineshape. The extent of the inhomogeneity was qualitatively modeled and the crystals were found to have partially inhomogeneous lineshapes, where the inhomogeneity increased with increasing barium fraction in the host lattice.

Chapter 3. GAIN SATURATION MEASUREMENTS OF YTTERBIUM DOPED $Sr_5(PO_4)_3F$

First published as: *A.J. Bayramian, C. Bibeau, K.I. Schaffers, C.D. Marshall, and S.A. Payne, "Gain saturation measurements of ytterbium doped $Sr_5(PO_4)_3F$," Applied Optics, **39**, 982-985, 2000.*

I. Introduction

Knowing that we can engineer the host medium to match diode-pumping bandwidths, we now turn our attention to the extraction of the diode-pump energy that is absorbed. Perhaps the most important number associated with efficient extraction of energy in a laser amplifier system is the saturation fluence, which directly effects the output fluence necessary for efficient extraction. Ytterbium doped $Sr_5(PO_4)_3F$ (S-FAP) has been shown to be an ideal laser material for medium-power high-energy applications such as diode-pumped solid-state laser oscillator[1-5] and amplifier[6] systems. In a theoretical paper by Orth and Payne, Yb:S-FAP was employed in a multistage amplifier scheme for an advanced fusion driver concept[7]. An experimental validation of many of the concepts addressed in that paper is proposed in a diode-pumped solid-state laser (DPSSL) named Mercury[8].

The ytterbium ion[9-13] is attractive as a laser ion due to its simple electronic structure (shown in Fig. 1 in S-FAP), long radiative lifetimes, and high quantum defect efficiency, $\eta_q = \lambda_{pump}/\lambda_{laser}$, where λ_{pump} is the pump laser wavelength, and λ_{laser} is the laser wavelength. Neodymium, on the other hand has a complex electronic structure leading to concentration quenching, a shorter radiative lifetime, and lower quantum defect efficiency at the 1 μm transition when compared to ytterbium. The other factor involved in generating an efficient amplifier material is the host. If we compare the new host, S-

FAP, to YAG, a well known and very developed material, we find that Yb:S-FAP also has a lower saturation fluence (~3.3 J/cm^2) compared with Yb:YAG (9.5 J/cm^2)[14] thereby allowing efficient energy extraction at fluences less than the damage threshold of many materials/coatings (approximately 10 J/cm^2 for nanosecond pulses). For additional comparison of Yb:S-FAP with other popular one micron laser materials see table 1.

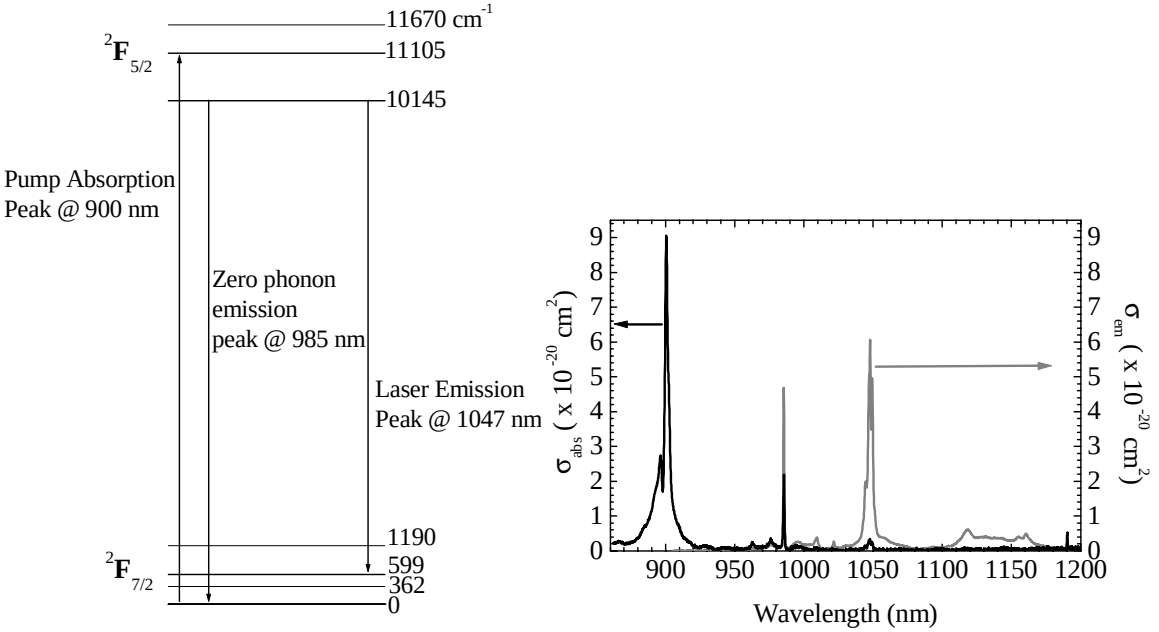

a) b)

Fig. 1 a) Energy level structure of Yb:S-FAP, b) Absorption and emission spectroscopy of Yb:S-FAP

Table 1. Comparison spectroscopic propertied of Yb^{3+} doped and Nd^{3+} doped laser materials

Dopant	Yb^{3+}		Nd^{3+}	
Host	**S-FAP[15]**	**YAG[14]**	**YAG[16]**	**phosphate glass[16]**
Lifetime (ms)	**1.1**	**1.0**	**0.23**	**~0.32**
Emission cross section ($\times$ 10^{-20} cm^2)	**6.0 (1047 nm)**	**2.0 (1029 nm)**	**28 (1064 nm)**	**~4.2 (1054 nm)**
Saturation Fluence (J/cm^2)	**3.2**	**9.6**	**0.67**	**4.5**
Quantum defect [λ_{Pump} (nm)/λ_{Laser} (nm)]	**0.86 (900/1047)** **0.94 (985/1047)**	**0.88 (912/1030)** **0.91 (940/1030)**	**0.82 (875/1064)** **0.76 (808/1064)**	**0.83 (875/1054)** **0.77 (808/1054)**

The saturation fluence can be written as:

$$F_{sat} = \frac{h\nu}{\sigma_{em}} k[F_{out}, \tau] \quad (1)$$

where σ_{em} is the gain cross section, ν is the laser frequency, and k is a dimensionless parameter representing the deviation from pure two-level homogeneous extraction, which can be a function of the output fluence (F_{out}) and the laser temporal pulsewidth (τ)[17]. To properly model gain and extraction of Yb:S-FAP amplifier systems as well as understand the effect of the emission lineshape, the value of the k factor, or equivalently the saturation fluence that needs to be measured. We report the experimental measurement of the saturated gain of Yb^{3+}:$Sr_5(PO_4)_3F$ at the 1047 nm laser line as a function of pump fluence and probe energy. The emission line was accurately modeled as a single homogeneous extraction, yielding values of 6.2×10^{-20} cm^2 for the emission cross section, and 3.3 J/cm^2 for the saturation fluence.

II. Gain Saturation Experiment

The gain saturation measurements utilized a high fluence pulsed source, shown below in Fig. 2 (top). A Q-switched Nd:YLF head (Spectra Physics Model 7960-L4-E) tuned for 1047 nm emission (coincident with the Yb:S-FAP emission peak) was amplified in a double pass Nd:YLF amplifier. The amplifier was a flash lamp pumped Nd:YLF rod (0.25” x 3.0") mounted in a Kigre pump chamber (FC-253-KK). The maximum energy output of the amplifier was approximately 40 mJ at 1047 nm, with a temporal pulsewidth of 8.1 ns Full-Width at Half Maximum (FWHM) as shown in Fig. 3a. The spatial profile of the output of the probe beam was measured using a Cohu CCD camera (Model#4800) and a Coherent Beamview Analysis system to be an elliptical gaussian beam with $1/e^2$ widths of 820 and 780 microns at the Yb:S-FAP crystal location as shown in Fig. 3b.

The system displayed shot to shot noise of as much as 10 % in the pulse energies, which could be managed with averaging (60 shot average for data points).

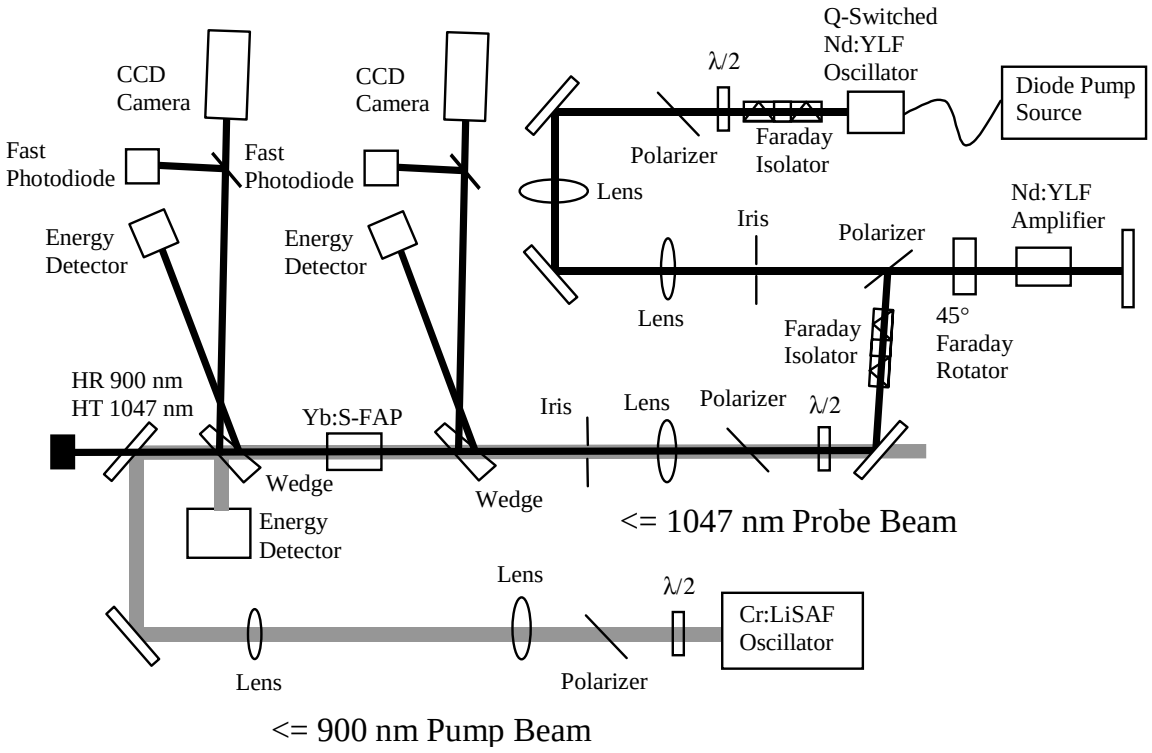

Fig. 2 Saturated gain experiment

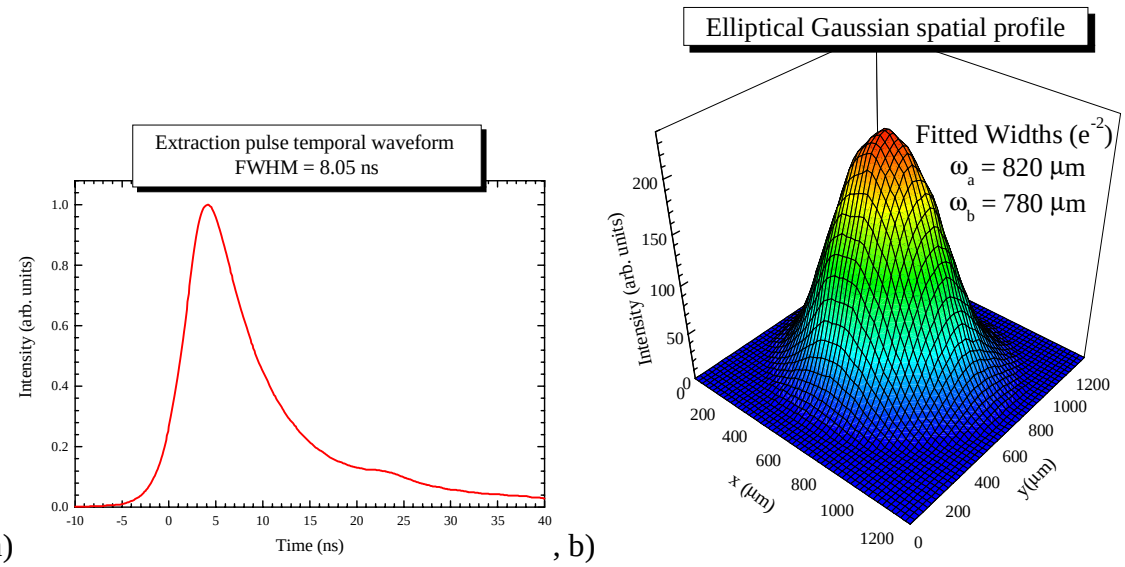

a) , b)

Fig. 3 a) Nd:YLF MOPA temporal pulsewidth, and b) far-field spatial profile

Gain saturation studies were conducted using the experimental setup shown in Fig. 2 (bottom). The S-FAP is pumped by a flashlamp pumped Cr:LiSAF laser tuned to the 900 nm S-FAP absorption peak, with a maximum energy of 0.6 J, a temporal pulsewidth of 162 μs FWHM, and a spatial profile that was roughly flat topped with a $1/e^2$ diameter of 2.03 mm FWHM. Energy measurements were made using Molectron detectors for probe light (model J-9) and pump light (model J-25), while temporal measurements were made using an Electro-Optics Technology photodetector (model ET2000). Wedges at both the input and output ends of the crystal allowed simultaneous measurement of pump input, probe input, and probe output energy, as well as probe temporal and spatial profiles. The S-FAP sample is 1 atomic percent (at. %) ytterbium doped and approximately 3 cm long. The timing of the probe pulse was set to occur near the end of the pump pulse when the gain in the crystal was maximized. For these experiments, the gain was measured both as a function of pump fluence and as a function of extraction energy (recalling that the gaussian spatial profile of the probe beam represents a continuum of different fluences and must be treated numerically). Gain values at the output energy detector were measured relative to a null pump shot so that all passive losses (Fresnel reflections, scatter, and ytterbium absorption at the probe wavelength) are normalized.

III. Gain Saturation Modeling

A simulation code[15] was written in C++, which modeled the transient energy level populations and gain in the transiently pumped, transiently probed Yb:S-FAP system (see Appendix II). The relevant coupled two-level rate equations are given by eqns. 2 and 3. A two-level rate equation can be used since the emission at the pump feature is very low (see Fig. 1).

$$\frac{dN_{gnd}(z,t)}{dt} = -\frac{dN_{ex}(z,t)}{dt}$$

$$= \frac{-\sigma_{abs}(\omega_p)N_{gnd}(z,t)I_p(z,t)}{\hbar\omega_p} + \frac{N_{ex}(z,t)}{\tau} \quad (2)$$

$$\frac{dI_p(z,t)}{dz} = -\sigma_{abs}(\omega_p)N_{gnd}(z,t)I_p(z,t) \quad (3)$$

N_{gnd} is the ground state population, N_{ex} is the excited state population, ω_p is the pump frequency, σ_{abs} is the absorption cross section, I_p is the pump intensity, and τ is the emission lifetime. Note that the emission cross section at the pump wavelength has been omitted since the upper and lower levels are assumed to thermalize instantaneously (the upper level has an instantaneous Boltzmann population = 0.99 (of the full upper manifold population))[6,15]. Using the code to model eqns. 2 and 3, the S-FAP sample was divided into discrete spatial slices and the pump pulse into temporal intervals, and these temporal slices were propagated consecutively through the spatial slices. The new population values in each spatial slice were stored as temporary variables to be used as the new input populations for the next temporal slice. In this way, the steady-state solutions for short times and spatial distances can be used to build up the temporally and spatially transient excited state population solution to eqn. 2. The transient small signal gain can then be calculated using:

$$G_0 = \exp[N_{ex}\sigma_{em}(\omega_L)\ell - N_{gr}\sigma_{abs}(\omega_L)\ell] \quad (4)$$

where N_{ex} and N_{gnd} are the excited and ground state populations respectively, σ_{em} and σ_{abs} are the emission and absorption cross sections of Yb:S-FAP[15] at the laser frequency, and ℓ is the crystal length. Since the experiments measured peak gain, the calculation was terminated when excited state population and thus the small signal gain were maximized.

The gaussian spatial profile of the probe pulse presents a small problem, since the extraction part of the calculation requires a fluence value. By discretizing the gaussian into a set of concentric shells of constant amplitude, the profile can be approximated to arbitrary accuracy. Each of these shells has a constant fluence, and can therefore be propagated through the next portion of the code that models the gain saturation. Since the extraction pulses are short compared to the emission lifetime, a Franz-Nodvik[18] approach was used employing Eqn. 5 to model the extraction:

$$G = \frac{F_{out}}{F_{in}} = \frac{F_{sat}}{F_{in}} \ln\left[(1 + G_0\left(\exp\left(\frac{F_{in}}{F_{sat}}\right) - 1\right)\right] \tag{5}$$

where G is the saturated gain, F_{out} is the output fluence, F_{sat} is the saturation fluence, G_0 is the small signal gain, and F_{in} is the input fluence. The fluence shells are then reassembled at the output of the code to give the total output energy and gain for a given input energy. The gain was normalized to one at zero pump fluence to match experimental conditions, and the results of the experiment and the modeling are given in Fig. 3, with the data points represented as large gray-scale spheres and the model fit points as a mesh. Taken as a whole, this plot displays all of the population dynamics between pumping and extraction. With very little probe energy (and fluence), the gain is not perturbed, so that one observes increasing gain with pump fluence and saturation as the population is totally inverted. Likewise, for maximum pump fluence, one observes decreasing gain with increasing probe energy (and fluence) as the gain saturates down to one. Gain saturation and the gain saturation fluence data are shown for F_{pump} = 18 J/cm^2 with the probe energy varied. Small signal gain and the corresponding pump saturation fluence data are shown for E_{probe} = 0.0001 J with the pump fluence varied. The larger

disparity between data and fit in the small signal gain regime is a result of the small signal, which occurs at the energy detector's lower limits (where signal to noise is low). The fit value for the gain cross section is 6.2×10^{-20} cm^2 which corresponds to a saturation fluence of 3.3 J/cm^2.

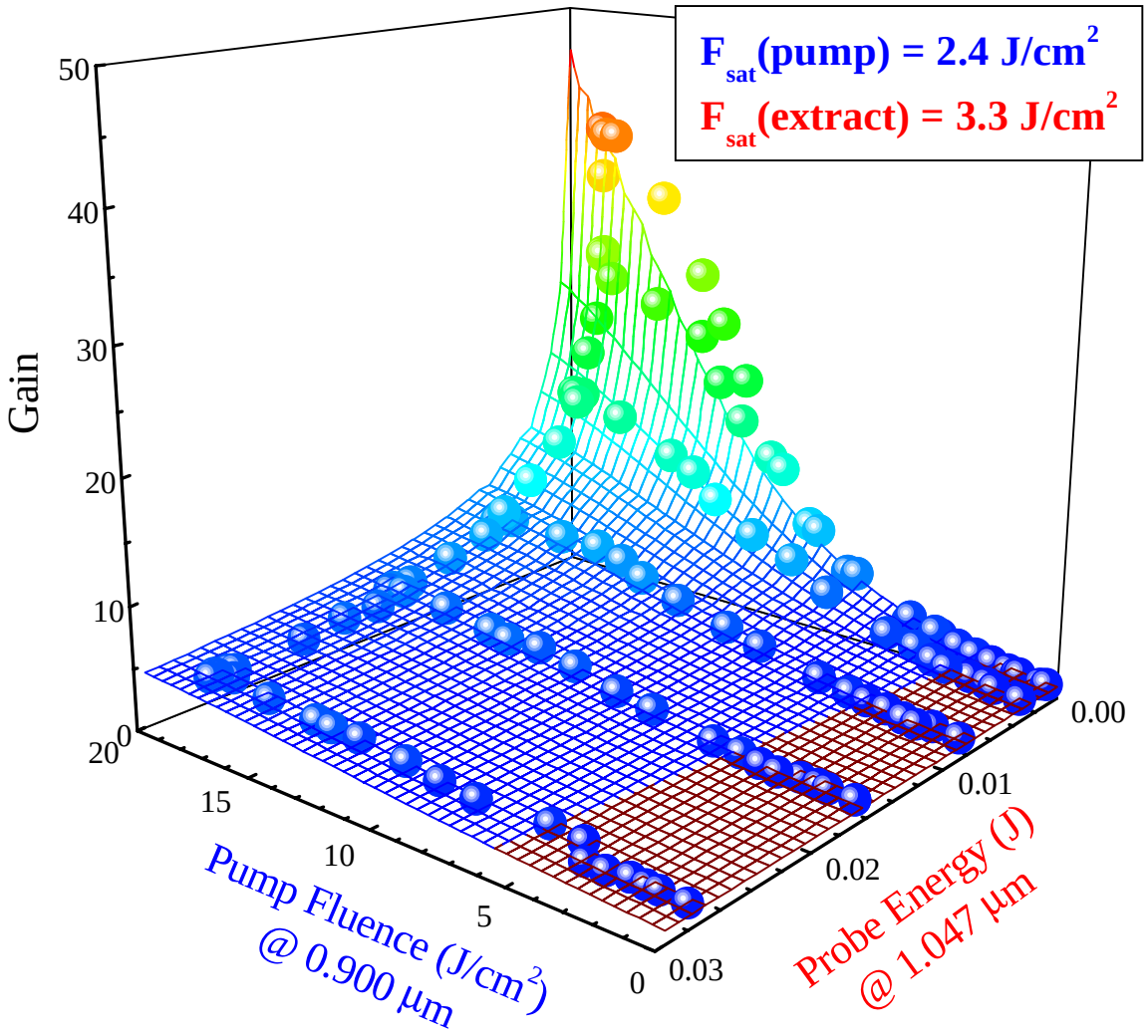

Fig. 3 Gain versus pump fluence and probe energy

Although an inhomogeneous model was initially employed in anticipation of an inhomogeneous extraction due to the double peaked shape of the absorption and emission features, the data fit to a single homogeneous extraction (or $k[F_{out}, \tau] = 1$) cross section as

shown in Fig. 4. Note that a fit line was not used for the data points since the data were not all taken with identical pump fluences, making point by point fitting necessary. When amplifying short (nanosecond) pulselengths, the only other critical parameter that must be taken into account is the lower level lifetime. If the pulses to be amplified are on the order of this lifetime, the lower laser level will bottleneck when stimulated emission occurs thereby reducing the expected gain and the extraction efficiency of the amplification. Bibeau et.al. measured the lower level lifetime for a similar material $Ca_5(PO_4)_3F$ or C-FAP[19] to be 200 ps for an energy gap of 1251 cm^{-1}. For the 1047 nm transition in S-FAP, the lower level gap is approximately 600 cm^{-1}. The lower level lifetime follows an energy gap law in which the lifetime is exponentially dependent on the energy gap. Since the energy gap is half that of C-FAP, and the S-FAP crystalline structure is nearly identical C-FAP, the lower level lifetime is expected to be much less than 200 ps, which will not effect amplification of nanosecond length pulsewidths.

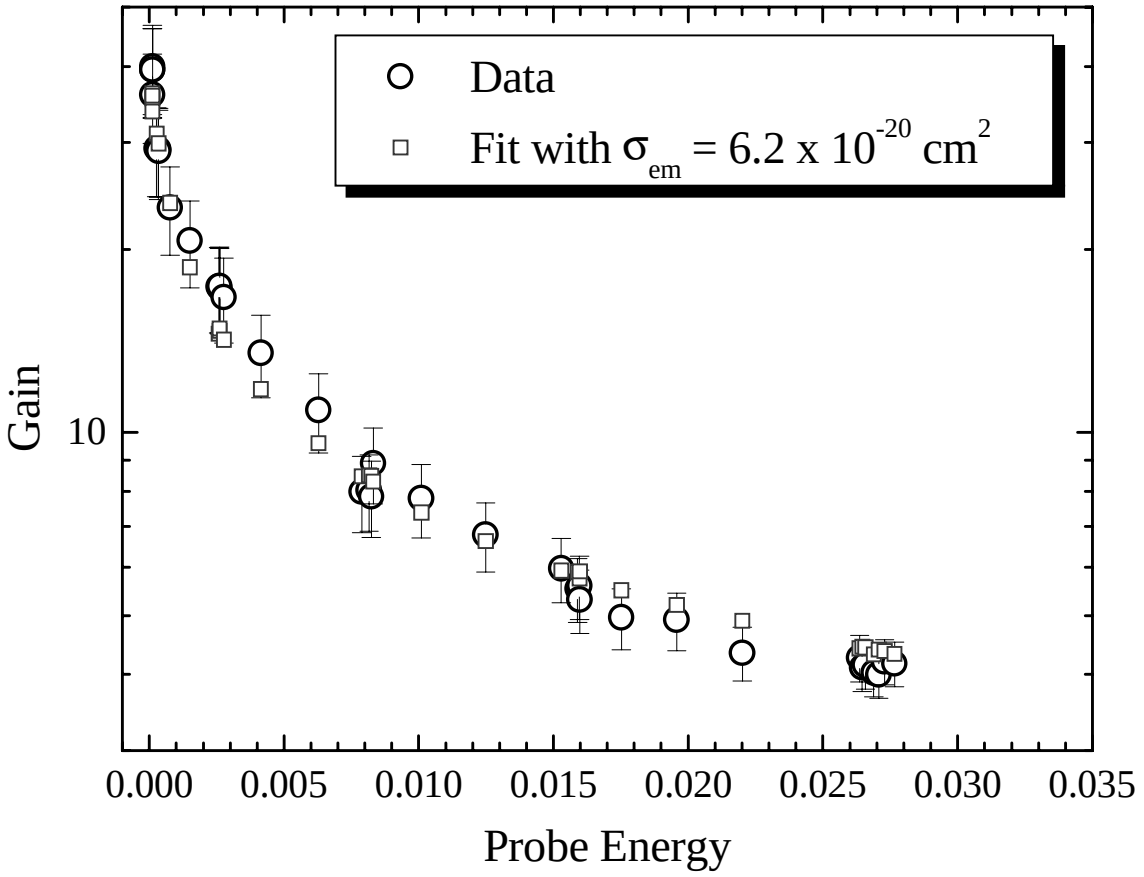

Fig. 4 Gain versus probe energy at peak pump fluence = 18 J/cm^2 with error analysis

IV. Summary

In conclusion the gain characteristics of Yb:S-FAP have been measured and modeled with a code that includes the spatial and temporal characteristics of the pump and probe beams. The theoretical fit to the data suggests that the extraction follows a homogeneous description of the saturation characteristics with a saturation fluence of 3.3 J/cm^2 at the 1047 nm gain peak.

Chapter 4. MATERIALS GROWTH AND OPTICAL PROPERTIES OF $Yb^{3+}Sr_5(PO_4)_3F$

First published as: *A.J. Bayramian, C. Bibeau, K.I. Schaffers, J.K. Lawson, C.D. Marshall, and S.A. Payne, "Development of ytterbium doped Sr5(PO4)3F for the Mercury Laser Project," OSA Trends in Optics and Photonics Series, **26**, pp. 635-641, 1999.*

I. Introduction

With efficient absorption and emission under control, the next most important issue is the beam quality in a pulsed laser system which not only effects the ability to focus the final output beam, but also effects phase modulation on the extraction beam in the amplifier system. Phase modulation can lead (in a variety of ways) to optical damage. The causes of phase modulation lie in the quality of the optics and Yb:S-FAP amplifiers, and the effect of thermal loading on the optics and amplifying medium. Ytterbium doped $Sr_5(PO_4)_3F$ (S-FAP) has been shown to be a robust laser material ideal for medium power applications such as diode-pumped solid-state laser oscillator[1] and amplifier[2] systems. Currently ytterbium doped S-FAP is being considered for the gain medium in a diode-pumped laser for advanced fusion driver. The first phase of this project is the Mercury laser described in Chapter 1. To accomplish this task, 4 x 6 x 0.75 cm slabs of S-FAP are required. Crystals of Yb:S-FAP, grown using the Czochralski (CZ) method, have been hampered by optical defects such as cracking, cloudiness, bubble core (which will be defined in the next section), grain boundaries, and anomalous absorption, which are detrimental to energy extraction. Current Yb:S-FAP Czochralski growth runs have yielded crystals with promising optical quality as well as an understanding of defect formation. The optical homogeneity of bulk S-FAP has been measured using

interferometry and quantified with power spectral density (PSD) spectra, which displays the discrete spatial frequency spectrum of the phase map. Recent growth runs have shown PSD spectra with amplitudes nearly that of high quality fused silica optics. Optical bonding has also been investigated, where the bond is invisible both on the phase map and the PSD spectrum. The effect of thermal loading can be modeled using basic physical properties such as thermal expansion (α), change in index of refraction with temperature ($\partial n/\partial T$), and the stress-optic coefficients. The stress-optic coefficients for S-FAP pertinent to slab amplifier geometry thermal loading were measured for the first time with values: $q_{33} = 0.308 \times 10^{-12}$ Pa^{-1} and $q_{31} = 0.936 \times 10^{-12}$ Pa^{-1}.

II. Crystal Growth

Improvement in the crystal quality of CZ grown Yb:S-FAP has been attributed to a better understanding of the defects and refinement of growth conditions[3]. Cracking (Fig. 1a) has been attributed to large thermal gradients and strain from defect sites in the crystals. Cloudiness (Fig. 1d) in the crystals is caused by second phase precipitation from unstable growth conditions such as fluctuations at the growth interface and variations in melt composition due to the evaporation of SrF_2 at the melt surface. Methods of maintaining a stable melt composition are being engineered to compensate for evaporation induced composition changes which occur during growth. The boules also experience a post-growth annealing process over the melt, which further reduces cloudiness. Annealing is achieved by simply suspending the crystal over the melt after growth is finished to allow gases to diffuse in and out of the crystal thus reducing defects. Another method, which eliminates the post-growth anneal is the addition of excess SrF_2 to the initial melt composition. This method yields clear crystals with no annealing and

less overall defects. The amount of excess SrF_2 is another variable in the growth process, which has varied from 0% to 100% excess SrF_2. The best results have been obtained with 33% of excess SrF_2.

Perhaps the most difficult defect to eliminate is the bubble core (Fig. 1c), which has been traced to constitutional supercooling caused by instability at the growth interface that leads to trapped pockets (bubbles) of low melting temperature liquid. These bubbles generally first occur at the center of the boule growth interface due to the low flow zone that exists at the position (see Ch. 1 Fig. 4). Absorption spectra of the core defects indicate that they contain increased concentrations of ytterbium relative to the surrounding medium. The spectra are identical to absorption of defect free Yb:S-FAP indicating the ytterbium has a local environment identical to the surrounding medium (with an increased dopant concentration). The observed bubble core appear to grow (propagate) along the c-axis of the boules, regardless of the orientation of the growth. Stabilization of the growth interface through controlling thermal gradients, power fluctuations, and composition changes have greatly reduced the bubble core defects. Recently, the use of a very high thermal gradient furnace has been used to give a sharper growth interface and enhance the confinement of the bubble core to the center of the boule where the defects are initiated by the low flow (stagnant) conditions as shown in Ch. I, Fig. 4.

The final issue is the formation of low-angle grain boundaries or slip dislocations (Fig 1b), which are planar groups of dislocations that separate neighboring grains with crystallographic misorientation of $< 5°$ and are visible to the naked eye as refractive index striations, which are oriented perpendicular to the c-axis, through the S-FAP

crystals. These boundaries can be nucleated from the above defects as well as by propagation from the seed to the crystal. One method of reducing these defects is to grow the defects out of the seed using seed extension. The seed is extended by growing a long narrow boule that narrows to a waist before increasing the diameter to grow the full-diameter usable boule. This method works if the gain boundaries occur at an angle to the growth direction. However, since the grain boundaries are roughly perpendicular to the c-axis, this method has limited results with a-axis grown boules.

a), b)

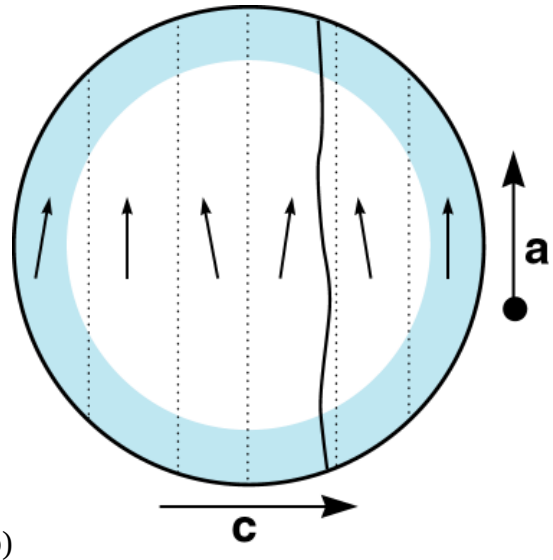

c),

d)

Fig. 1 Examples of various types of growth related crystalline defects including: a) cracking, b) grain boundaries (slip dislocations), c) bubble core, and d) cloudiness

Recent absorption spectra have uncovered a fifth kind of defect, which will be called anomalous absorption. This defect does not seem to effect the optical quality (although they may be linked), but it does effect the absorption and thus the dopant concentration in the crystals. Fig. 2 shows the absorption of a crystal with the anomalous absorption defect with a defect free absorption overlaid for comparison. The spectral region from 900-1020 nm contains the anomalous absorption site. Since rare earth ions are difficult to separate, one possible source for this anomalous absorption could be another impurity doping with the ytterbium. However, absorption of the visible and UV show no other absorption features, which eliminates the possibility of another impurity dopant causing the absorption. The two absorption features were also determined to be inhomogeneous, since excitation at 900 nm produced only non-anomalous emission, while excitation at 965 nm in the anomalous absorption feature showed emission duplicating the anomaly as well as normal S-FAP emission due to the anomaly's overlap with the zero line of the non-anomalous absorption (shown in Fig. 3). This anomaly is currently thought to be ytterbium doping into the nine coordinate oxygen polyhedron A_I site as identified in the Chapter I., where ytterbium has a local environment of oxygen atoms that are part of phosphate groups. In this environment one might expect the spectroscopy of ytterbium in this site to be very similar to ytterbium doped phosphate glass. Indeed, comparison of the anomalous absorption and emission with that of ytterbium doped phosphate glass[4] shows high similarity.

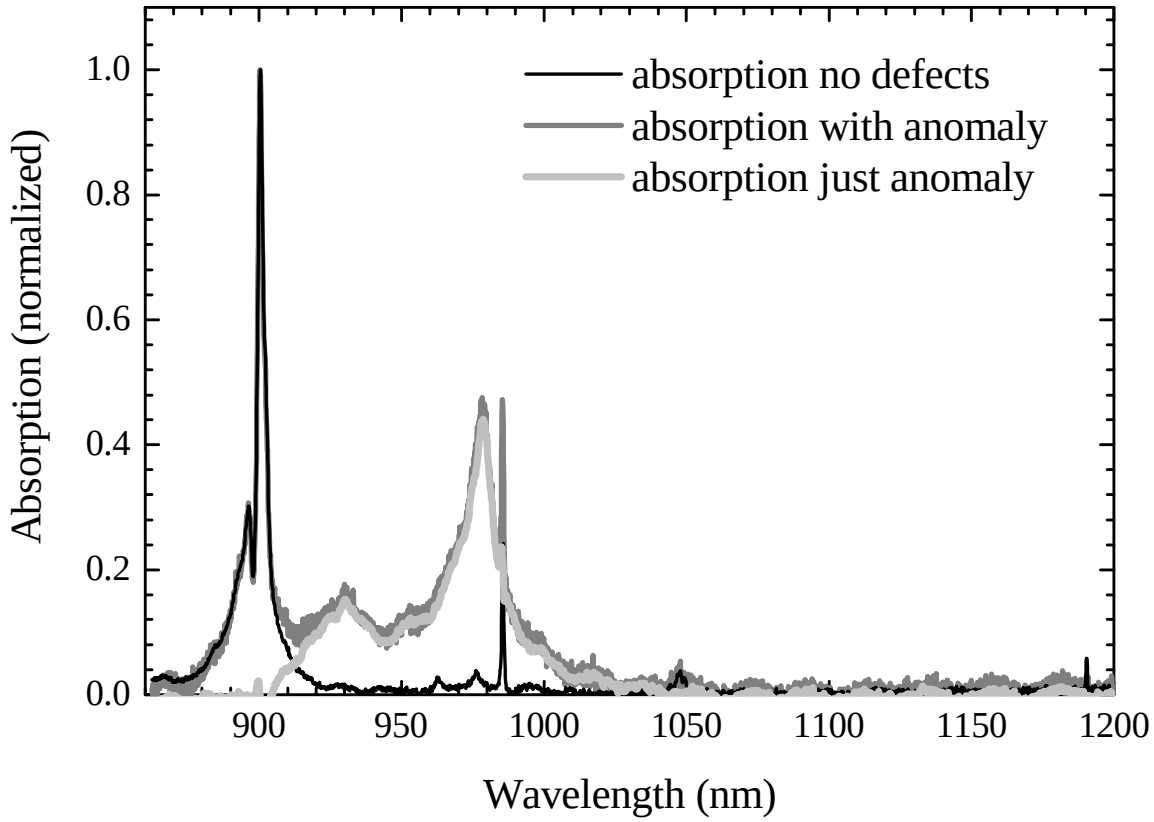

Fig. 2. Anomalous absorption defect of Yb:S-FAP with a defect-free spectrum overlaid for comparison.

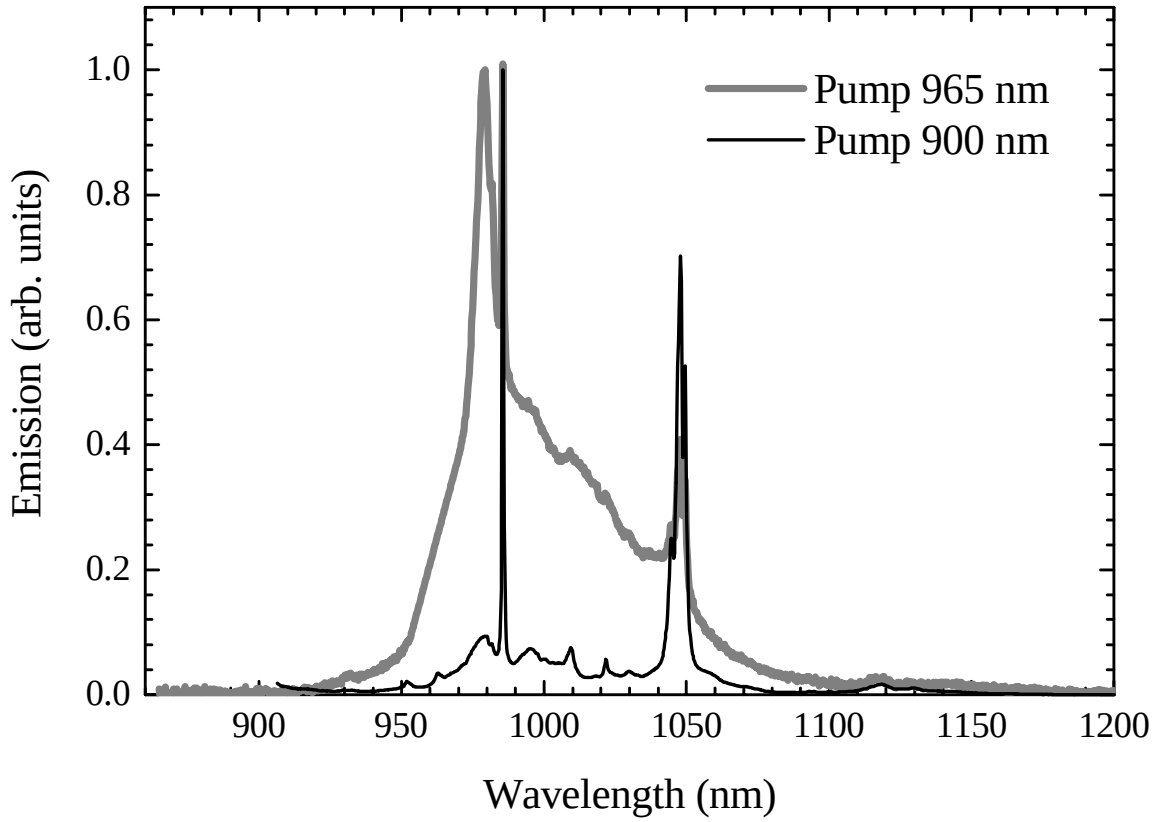

Fig. 3 Emission intensity for selected excitation of a crystal displaying anomalous absorption

The growth of this anomaly has been empirically determined from a large number of Yb:S-FAP boule growths to be dependent on the orientation of the growth axis of the boule with respect to the c-axis of the crystal. To date, anomalous absorption has only been found in a-axis growth boules (the long dimension of the boule is along the a-axis). The anomalous absorption is absent in most boules grown at 45° to the c-axis and so far in all c-axis growth boules. Table I summarizes the defects which were characterized, the proposed solutions and the outcome of growth trials using these new techniques. By implementing more stable growth conditions, we have been able to produce Yb:S-FAP crystals with sufficient optical quality to meet the Mercury laser specifications (an example is shown in Fig. 4).

Table I. Issues and defects in Yb:S-FAP crystal growth and their respective solutions.

Issues	Physical understanding	Solution	Outcome
Cracking	• Results from high thermal gradients and internal defects	• Reduce thermal gradients • Cool crystals in the melts • Reduce core defects	• Crack-free large-diameter crystals (≤ 5 cm)
Cloudiness	• Second phase precipitation on line defects	• Add excess SrF_2 • Perform post-annealing	• Clear crystals
Bubble Core	• Caused by constitutional supercooling	• Stabilize the growth interface • Minimize abrupt diameter changes • Higher thermal gradient furnace • Grow along a different axis	• A reduced number of core defects • defects limited to central region
Grain Boundaries	• Planar groups of dislocations that propagate from the seed or originate at the core	• Use defect-free seeds • Stabilize the growth interface • Perform seed extensions • Reduce bubble core	• Crystals have been grown with less than two grain boundaries
Anomalous absorption	• Yb^{3+} in a different type of site	• avoid a-axis growth	• Yb:S-FAP spectra free of anomalous absorption
Size	• Current growth capability limits crystal diameter to ~4-5 cm	• diffusion bond smaller pieces to make a full size slab	• Full size Mercury slabs possible

Fig. 4 An example of a 2 x 2.5 x 0.5 cm slice from a boule of S-FAP which is free of defects.

III. Bulk Homogeneity Measurement

Progress in bulk homogeneity has been monitored by mapping the transmitted phase of several Yb:S-FAP crystals using an interferometer. The phase maps of the homogeneity are converted to Power Spectral Density (PSD) plots, which are the square of the 2-D Fourier amplitude spectrum of the phase map divided by the width of the frequency intervals (see Eqn. 1). The maximum tolerable PSD in any frequency interval is defined by the desired beam characteristics at the output of the laser system and affects the diffraction limited spot size possible with a given beam. Phase maps have confirmed our theory that a core of higher index occurs at the center of the boule due to slightly higher ytterbium concentration, as well as showing that grain boundaries or any imperfection visible to the naked eye have an undesirable affect on the transmitted wavefront. Fig. 5 displays the phase map of a slice from the best Yb:S-FAP boule to date. To achieve the phase plot in Fig. 5, the phase front of the slice had to be

subapertured to eliminate the core of the boule. The two dimensional PSD plot of the phase map in Fig. 5 was then integrated according to Eqn. 1 to give the 1-D PSD plot in Fig. 6.

$$PSD(\nu_x) = \int PSD(\nu_x, \nu_y) d\nu_y = \int \frac{\left|\Phi(\nu_x, \nu_y)\right|^2}{\Delta\nu_x \Delta\nu_y} d\nu_y \quad (1)$$

where $PSD(\nu_x)$ is the 1-D PSD, $PSD(\nu_x, \nu_y)$ is the 2-D PSD, $\Phi(\nu_x, \nu_y)$ is the discrete Fourier transform of the phase map, $\Delta\nu_x$ and $\Delta\nu_y$ are the frequency steps, and x, y can be rotated to any directions of interest. Since the measurement is taken with a camera having a finite array of pixels with finite pixel size, very low and very high frequencies cannot be accurately measured. The PSD plots shown in this thesis show the data that is valid to the camera resolution between vertical lines. Data outside these lines is not valid data and is a result of Fourier transforming the data with a quasi-infinite set of spatial frequencies. The high frequency valid data limit is defined as half of the maximum frequency which can be displayed by the pixels of the camera (i.e. a full wave is five pixels). The low frequency data valid line is defined as six times the lowest frequency which can be displayed by the phase map, a half wave over the full aperture. The lowest frequencies are also not valid since the removal of focus and tilt from the phase data changes the value of the PSD for these frequencies. The straight line through the data corresponds to a fractal model[5] given by Eqn. 2:

$$F(\nu) = \alpha\nu^{-\beta} \quad (2)$$

where $F(\nu)$ is the specification function, ν is the spatial frequency, α = 1nm^2 mm (this value partially controls the final diffraction limit of the beam), and β = 1.55 (this value was empirically established by the actual measurement of many high quality optics).

This line is defined by the diffraction limited beam requirements at the output of the Mercury laser, which has been specified as approximately 5 times diffraction limited for the long axis of the 5-cm x 3-cm beam. To meet this specification, all of the PSD data points must lie below this line (which makes the output beam 5 time diffraction limited or better). Since the boules grown so far have had apertures less than this requirement, we have investigated the idea of bonding together smaller crystals to achieve the required size. The core and any other defective parts of a crystal can be removed by cutting the crystals and bonding the defect-free pieces together as shown in Fig. 7. Onyx Optics, Inc. in Dublin, CA, have made all of the crystal bonds to date with great success. The bonds are invisible to the naked eye and have a negligible negative impact on the phase maps, while allowing vast improvement of the overall transmitted phase of the crystal, since the best parts of a boule can be bonded together. Fig 8 shows the phase map of a typical bonded S-FAP crystal, while Fig. 9 compares the 1-D PSD of the unbonded part of the crystal with the 1-D PSD of the whole crystal including the bond. Clearly, bonding has almost no discernable impact on the 1-D PSD and therefore the diffraction limited beam quality of the Mercury output beam.

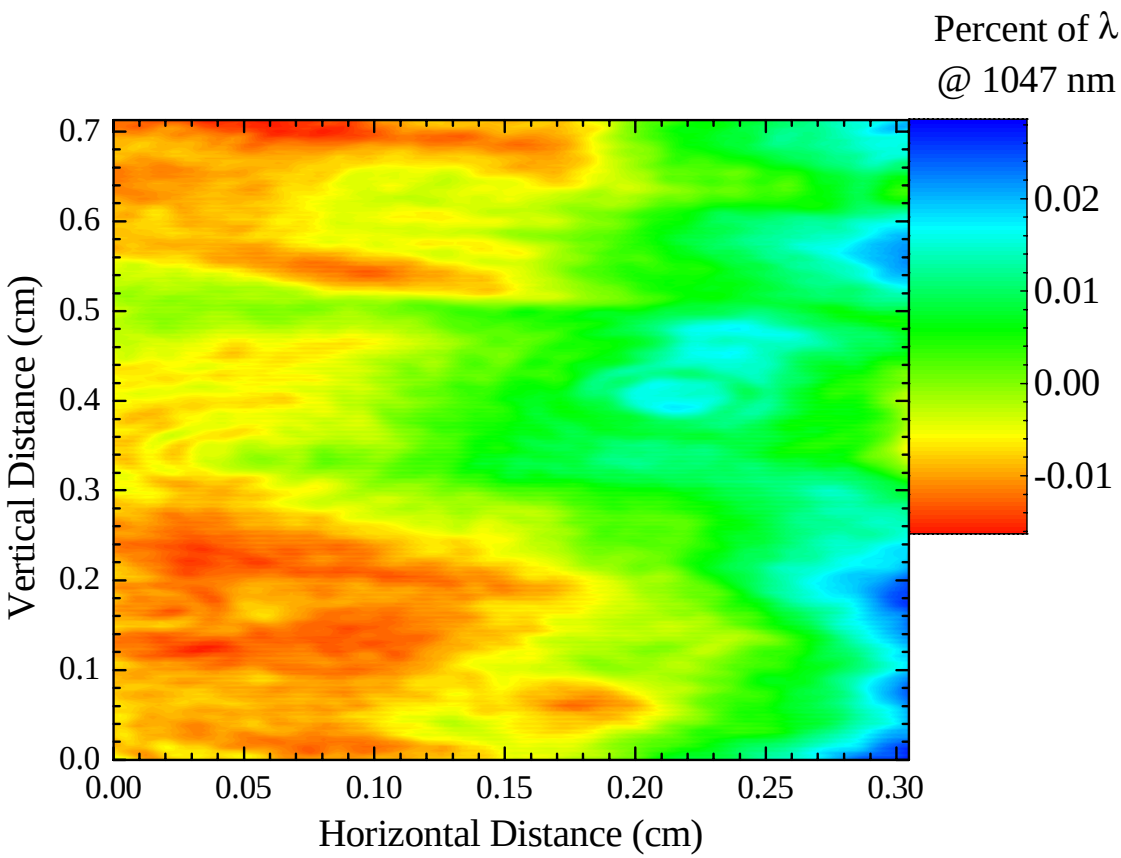

Fig. 5 Phase map of Yb:S-FAP crystal 6.54 mm thick

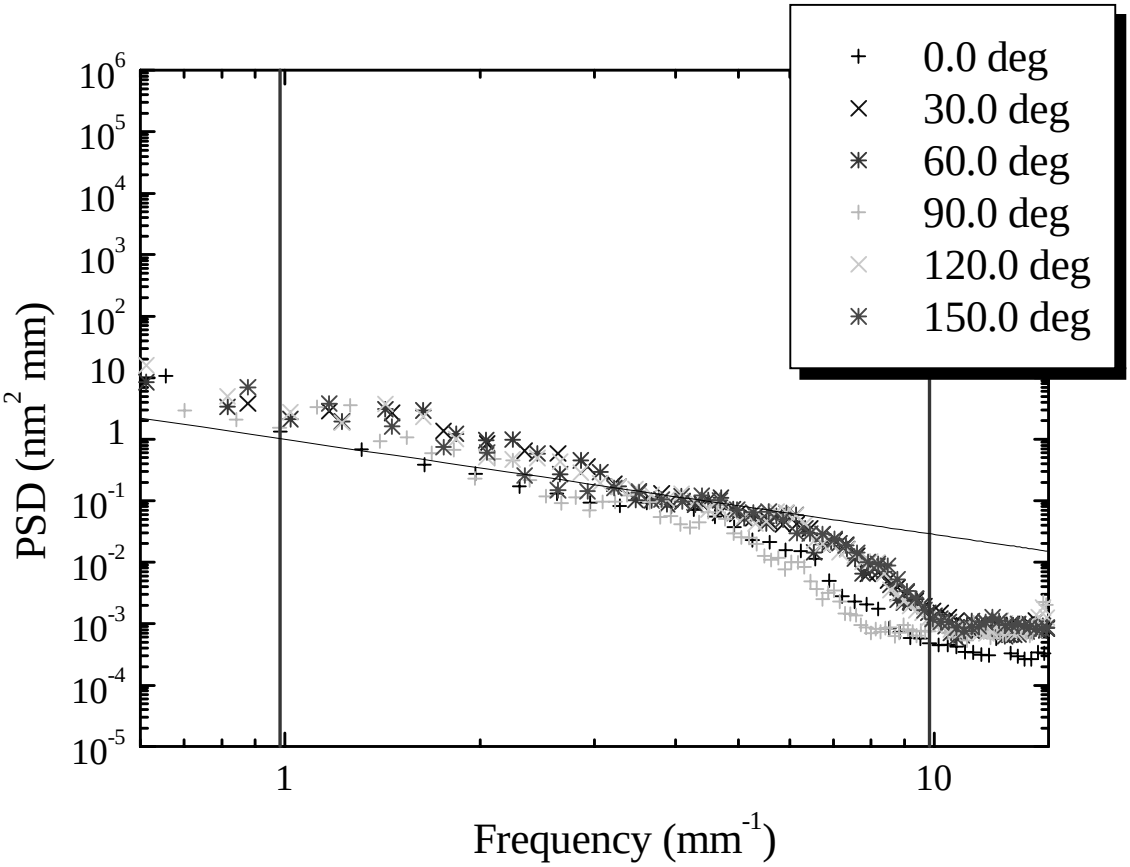

Fig. 6. Power Spectral Density (PSD) plot of Yb:S-FAP crystal 6.54 mm thick

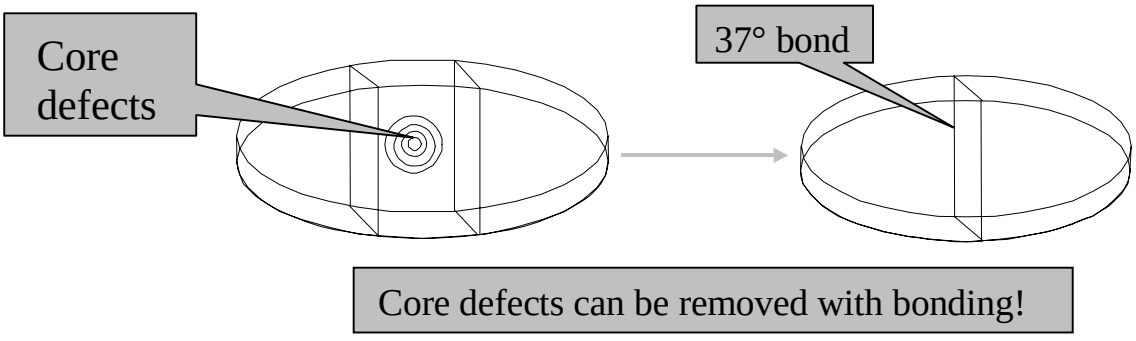

Fig. 7 Illustration showing how bonding can be used for defect removal

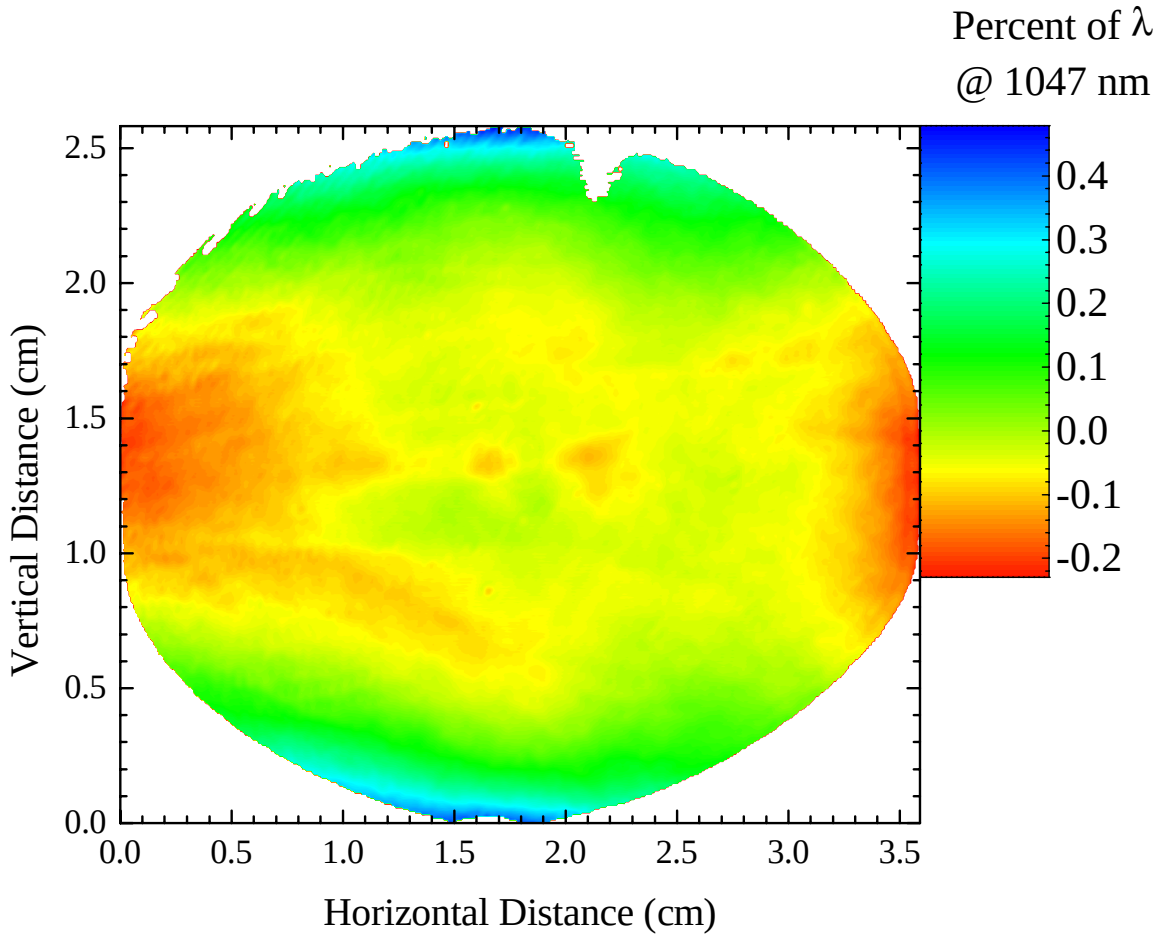

Fig. 8. Phase map of bonded S-FAP crystal

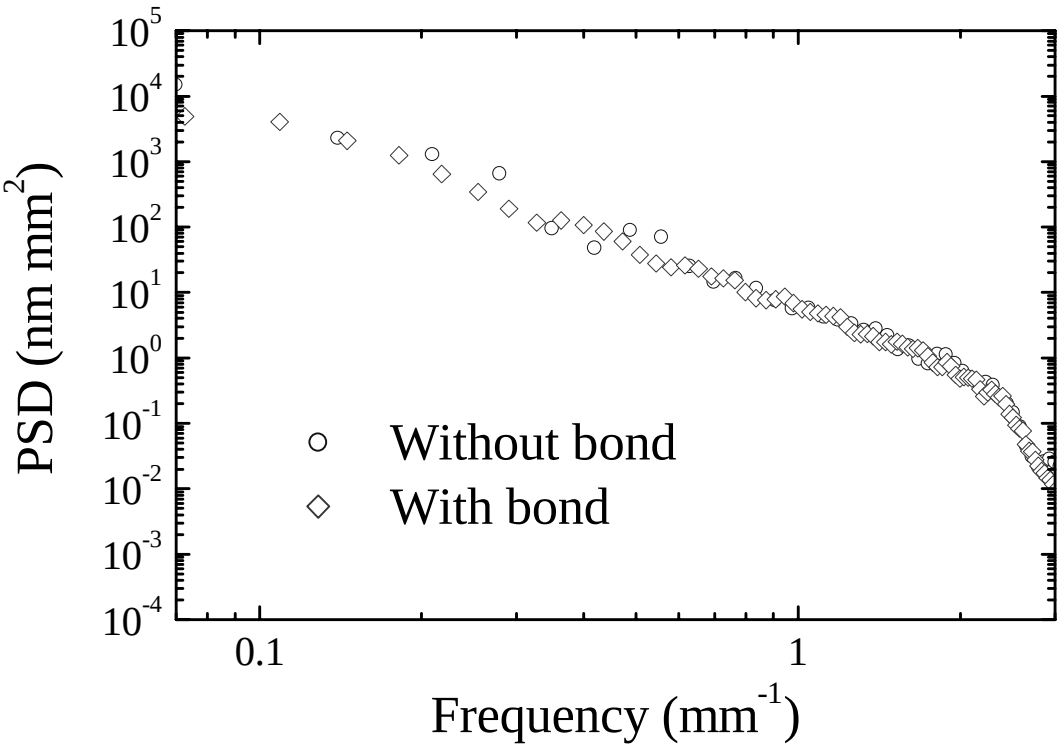

Fig. 9. 1-D PSD comparing the crystal phase map in Fig. 3 before and after bonding.

IV. Thermo-optic distortion

Another large source of beam aberration in an amplifier system is due to thermal loading of the optical materials from absorption. These distortions are entirely defined by the geometry of the heat sources and sinks. Perhaps the most well known thermal aberration is the formation of a thermal lens in laser rods. In this case, the geometry of interest is a long thin rod (i.e. the length is much greater than the rod diameter), where heat is deposited radially in the rod, whether by end-pumping or side-pumping. The rod's major heat sink is the sides of the rod. This yields a radially symmetric steady-state thermal gradient. There are three major optical distortions resulting from this heating: physical expansion, stress induced by uneven expansion, and change in the index of refraction with temperature. In a rod geometry this corresponds to physical bulging or

cupping of the rod end faces, radially induced index variations due to thermal stress, and a radially dependent index of refraction. These effects taken together will yield an effective lens with focal length, f, which is dependent on the thermal loading of the material as given by[6]:

$$f = \frac{KA}{P_a}\left(\frac{\alpha r_0 (n_0 - 1)}{L} + \alpha C_{r,\phi} n_0^3 + \frac{1}{2}\frac{dn}{dT}\right)^{-1} \quad (3)$$

where f is the thermal lens focal length, K is the thermal conductivity, A is the rod cross-sectional area, P_a is the total heat dissipated in the rod, α is the thermal coefficient of expansion, r_0 is the rod radius, n_0 is the index of refraction, L is the length of the rod, $C_{r,\phi}$ are the elasto-optical coefficients of the material, and $\partial n/\partial T$ is the change in index with temperature. These thermal lenses can be very strong, with thermal focal lengths so short (< 1 μm) that thermally induced waveguiding or self-focusing results. Thus, consideration of these thermal induced distortions is very important when designing and modeling a new optical system. For temperature distributions in "real world" geometries as well as non uniform heat loading, the optical distortion is not straight forward and needs to be calculated for the boundary conditions and thermal loading of each individual application. While the thermal coefficient of expansion and the change of refractive index with temperature are known, the stress optic coefficients for S-FAP have not been well documented, yet are required for understanding and development of this material in thermally loaded environments such as the Mercury laser.

V. Stress Optic measurement in S-FAP

The photoelastic effect is observed when an optical material is subjected to an applied force and develops internal stresses (σ) or strains (η) which in turn cause a change in

the refractive index of the material. The equations governing this effect are defined according to the dielectric impermeability tensor, B, which is the inverse of the relative dielectric tensor, ε. The components of ε are simply the coefficients of the index ellipsoid associated with an anisotropic solid. Along any principle axis, B identically equals $1/n^2$. The generalized equation for the photoelastic effect is[7]:

$$\Delta B_{ij} = q_{ijkl}\sigma_{kl} \tag{4}$$

where q is the piezooptic tensor, and σ is the applied stress. The full tensor form of eqn. 1 for Yb^{3+}:S-FAP, which has hexagonal symmetry (crystal class 6/m) is given by eqn. 5, where the reduced (Voigt) notation 1 = xx, 2 = yy, 3 = zz, 4 = yz, 5 = xz, and 6 = xy is used[7]:

$$\begin{bmatrix}\Delta B_1\\ \Delta B_2\\ \Delta B_3\\ \Delta B_4\\ \Delta B_5\\ \Delta B_6\end{bmatrix} = \begin{bmatrix} q_{11} & q_{12} & q_{13} & 0 & 0 & 2q_{16}\\ q_{12} & q_{11} & q_{13} & 0 & 0 & -2q_{16}\\ q_{31} & q_{31} & q_{33} & 0 & 0 & 0\\ 0 & 0 & 0 & q_{44} & q_{45} & 0\\ 0 & 0 & 0 & -q_{45} & q_{44} & 0\\ -q_{16} & q_{16} & 0 & 0 & 0 & q_{11}-q_{12}\end{bmatrix}\begin{bmatrix}\sigma_1\\ \sigma_2\\ \sigma_3\\ \sigma_4\\ \sigma_5\\ \sigma_6\end{bmatrix} \tag{5}$$

Since the light is always polarized along the "c" or “zz” axis for the Mercury laser system (reduced notation 3), the relevant portion of this equation becomes:

$$\Delta B_3 = \Delta\left(\frac{1}{n_3^2}\right) = q_{31}\sigma_1 + q_{31}\sigma_2 + q_{33}\sigma_3 \tag{6}$$

Solving for Δn_3 and making the approximation that the magnitude of the index of refraction is basically unchanged by the applied stress ($n_{3i} \sim n_{3f}$), eqn. 6 can be rewritten to give the index change of:

$$\Delta n_3 = \frac{-n_3^3}{2}\left(q_{31}\sigma_1 + q_{31}\sigma_2 + q_{33}\sigma_3\right) \tag{7a}$$

or path length change of:

$$\Delta p_3 = \Delta n_3 \ell_2 = \frac{-n_3^3}{2}\left(q_{31}\sigma_1 + q_{31}\sigma_2 + q_{33}\sigma_3\right)\ell_2 \qquad (7b)$$

From eqn. 7, we can see that two independent stress measurements are needed to evaluate the two unknown photoelastic coefficients, q_{31} and q_{33}. The geometry of the experiments needed to measure q_{33} and q_{31} are as follows:

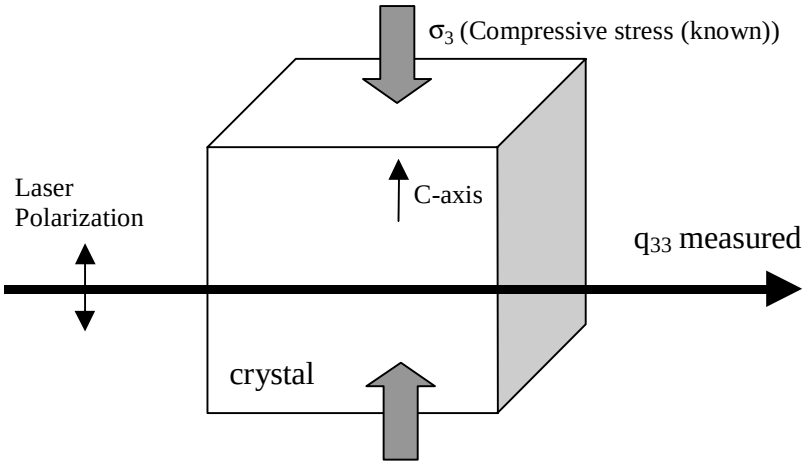

Fig. 10. Compressive stress geometry for a-axis propagation and c-axis polarization to measure q_{33}

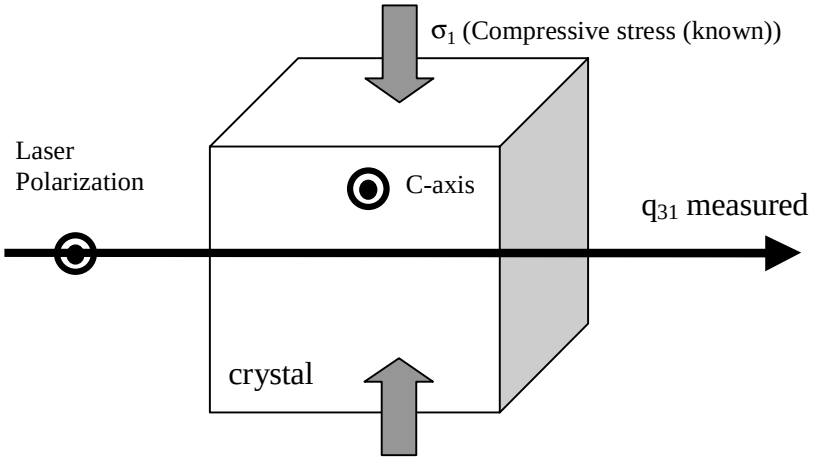

Fig. 11. Compressive stress geometry for c-axis propagation and a-axis polarization to measure q_{31}

In addition to photoelastic effects, a solid also changes shape when subjected to an applied stress. For small stresses, below the elastic limit, the body returns to its original shape when the stress is removed, and the amount of strain (deformation) is proportional to the applied stress according to Hooke's Law (eqn. 8)[7]. For a simple isotropic solid put under tensile stress, the longitudinal strain, ε, equals $\Delta\ell/\ell$ where $\Delta\ell$ is the increase in length, and ℓ is the original length[7]. For anisotropic solids the strain relation to applied stress can be written as[7]:

$$\varepsilon_{ij} = s_{ijkl}\sigma_{kl} \tag{8}$$

where ε_{ij} is the homogenous strain, s_{ijkl} is the elastic compliance (which is the inverse of the elastic stiffness constant c_{ijkl}, also known as Young's Modulus), and σ_{kl} is again the applied stress. Once again, the full tensor form of eqn. 8 for Yb^{3+}:S-FAP, using the reduced (Voigt) notation is[7]:

$$\begin{bmatrix}\varepsilon_1\\ \varepsilon_2\\ \varepsilon_3\\ \varepsilon_4\\ \varepsilon_5\\ \varepsilon_6\end{bmatrix} = \begin{bmatrix} s_{11} & s_{12} & s_{13} & 0 & 0 & 0\\ s_{12} & s_{11} & s_{13} & 0 & 0 & 0\\ s_{13} & s_{13} & s_{33} & 0 & 0 & 0\\ 0 & 0 & 0 & s_{44} & 0 & 0\\ 0 & 0 & 0 & 0 & s_{44} & 0\\ 0 & 0 & 0 & 0 & 0 & 2(s_{11}-s_{12}) \end{bmatrix}\begin{bmatrix}\sigma_1\\ \sigma_2\\ \sigma_3\\ \sigma_4\\ \sigma_5\\ \sigma_6\end{bmatrix} \tag{9}$$

The strain in Eqn. 9 can be simplified for these experiments since propagation is only along the "yy" direction or 2 for these two geometries to give:

$$\varepsilon_2 = \frac{\Delta\ell_2}{\ell_2} = s_{12}\sigma_1 + s_{13}\sigma_3$$

$$\Rightarrow \Delta p_3 = (n_3 - 1)\Delta\ell_2 = (n_3 - 1)(s_{12}\sigma_1 + s_{13}\sigma_3)\ell_2 \tag{10}$$

Together, the photoelastic effect and Hooke's Law deformation fully describe the wavefront distortion of an optical material that is subject to small stresses in an

isothermal environment. The optical distortion due to the two stress geometries will be measured interferometrically by observing fringe movement in the experimental setup in Fig. 12. The magnitude of the stress-optic coefficients will be determined by the number of fringes (waves) which move across the field of view as the stress is applied (Fig. 13).

The sign of these coefficients depends on whether the fringes move to the right or left. The following procedure is used to calibrate the fringe movement to a known direction. With the no applied stress to the crystal, the interferometer is initially aligned such that only a single fringe is visible. Mirror #1 is then tilted in a clockwise direction about the vertical axis producing a set of vertical fringes at the camera position. The sign of the stress-optic coefficients is then determined by the direction that the fringes move as the stress is applied. For example, if the stress induced distortion caused a decrease in path length, the angled wavefront from Mirror #1 shown in Fig. 13 will move forward relative to the flat wavefront from Mirror #2, which will cause the fringes to move to the left.

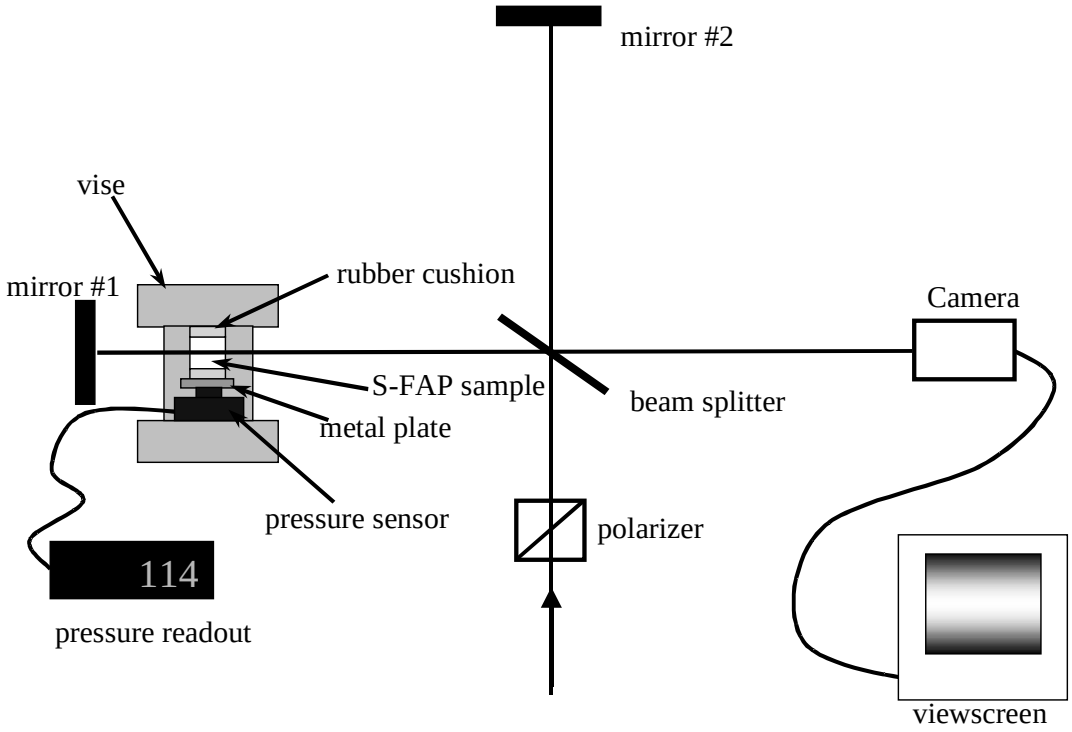

Fig. 12. Experimental arrangement for interferometrically determining the path length change due to stress.

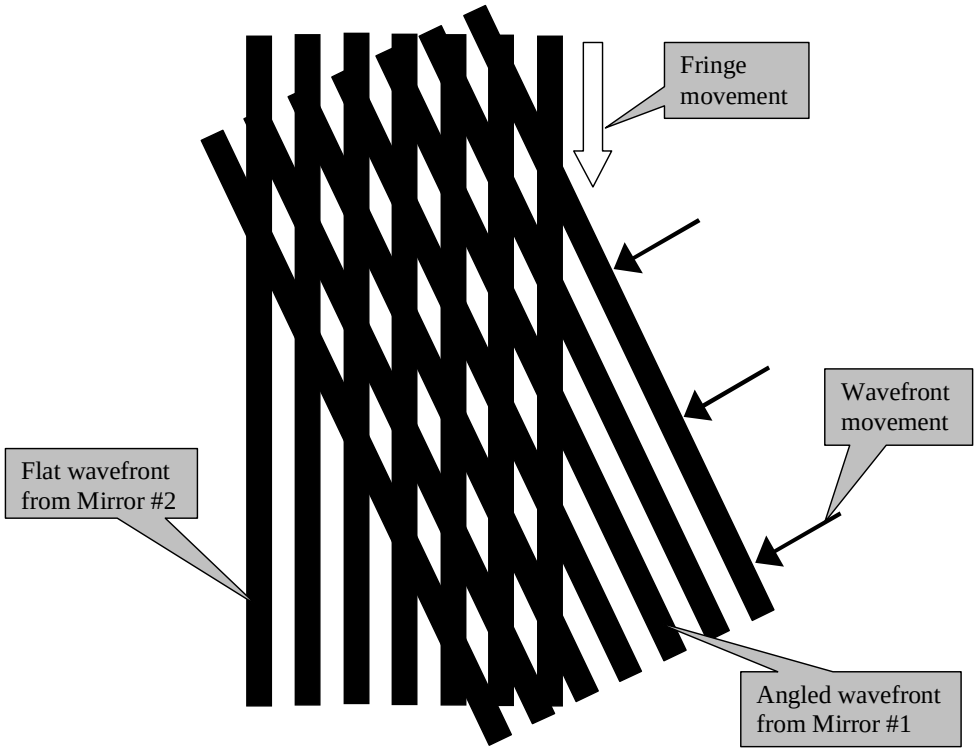

Fig. 13 Diagram depicting fringe movement dependent on sign of stress induced path length change

Noting that the above mathematics define squeezing stress as negative, we expect path length changes of:

$$\Delta p_3^c = \frac{-n_3^3}{2} q_{33}\sigma_3 \ell_2 + (n_3 - 1)s_{13}\sigma_3 \ell_2 \tag{11a}$$

for squeezing along the c-axis (3) and polarized along c (3) (Fig. 10), and

$$\Delta p_1^c = \frac{-n_3^3}{2} q_{31}\sigma_1 \ell_2 + (n_3 - 1)s_{12}\sigma_1 \ell_2 \tag{11b}$$

for squeezing along the a-axis (1) and polarized along c (3) (Fig. 11). Data were taken by varying the applied stress and observing the direction the fringes move as well as the magnitude of distortion, or fringe movement, normalized to wavelength ($\Delta p/\lambda$). Due to signal to noise issues, the our measurement of the magnitude of distortion is still under investigation. However, the current experiment does give the sign (direction of fringe movement) of the distortion. Using magnitude values from a NASA experiment where the sign was ambiguous in conjunction with the sign determined in our experiments allows a proper calculation of the stress optic coefficients. The NASA distortion ($\Delta p/\lambda$) values are given in table 1:

Table 1. NASA experimental results

σ_3 (10^6 Pa)	$\Delta p_3^c/\lambda$	σ_1 (10^6 Pa)	$\Delta p_1^c/\lambda$
-3.32	**-0.172**	**-1.21**	**-0.233**
-7.55	**-0.459**	**-3.75**	**-0.460**
-11.33	**-0.759**	**-5.85**	**-0.758**
-12.00	**-0.772**	**-8.06**	**-0.952**
		-9.68	**-1.133**

We define m as the number of waves of optical path length induced per unit stress ($m = (\Delta p/\lambda)/\sigma$), which can be obtained from the slope of a linear regression of the data in table 1. Note that the actual experimental configuration involves a double-pass arrangement. With these corrections, Eqns. 11a and 11b can be solved for q_{31} and q_{33} yielding:

$$q_{33} = \frac{1}{n_3^3}\left[2(n_3 - 1)s_{13} - \frac{m_3^c \lambda}{\ell_1}\right] \tag{12a}$$

$$q_{31} = \frac{1}{n_3^3}\left[2(n_3 - 1)s_{12} - \frac{m_1^c \lambda}{\ell_1}\right] \tag{12b}$$

Table 2 gives material properties and calculated results. Note that the elastic compliances for S-FAP have not been measured, but were instead extrapolated from measurements on C-FAP[8,9] using eqn. 13. For an isotropic material, s = 1/E where s is the elastic compliance and E is Young's modulus. This equality can be approximated for an anisotropic material by using the averaged Young's modulus.

$$s_{ij}^{S-FAP} = s_{ij}^{C-FAP}\frac{E_{Ave(C-FAP)}}{E_{Ave(S-FAP)}} \tag{13}$$

Table 2 Material properties and calculated results:

Property	LLNL Values	NASA Values
c_{Ave}(C-FAP)[10]	**119**	**119**
c_{Ave}(S-FAP)[11]	**109**	**109**
s_{13} (x 10^{-12} Pa^{-1})	**-2.29, -2.63**	**-2.29**
s_{12} (x 10^{-12} Pa^{-1})	**-1.91, -2.33**	**-1.91**
λ (m)	**5.43 x 10^{-7}**	**5.43 x 10^{-7}**
n_1	**1.631**	**1.631**
n_3	**1.626**	**1.626**
ℓ_2 (m)	**8.77 x 10^{-3}**	**8.77 x 10^{-3}**
m_3^c (x 10^{-8} Pa^{-1})	**-7.1**	**7.1**
m_1^c (x 10^{-8} Pa^{-1})	**-10.8**	**10.8**
q_{33} (x 10^{-12} Pa^{-1})	**0.308**	**-1.692**
q_{31} (x 10^{-12} Pa^{-1})	**0.936**	**-2.107**

VI. Summary

Progress has been made on many of the growth initiated defects that inhibit the production of large aperture clear crystals. The use of active diameter control, power conditioning, oriented seeds, seed extension, and excess SrF_2 doping has produced clear nearly defect free crystals. The crystal quality was monitored interferometrically, quantified with PSD analysis of the phase map, and found to have satisfactory distortion for Mercury requirements. Bonding of crystals was investigated in the event that large diameter clear crystals can not be grown with adequate crystal quality, and was found to produce bonds nearly invisible to phase analysis (and the naked eye). Finally, the pertinent photoelastic constants for c-axis polarized laser geometry of S-FAP were measured.

Chapter 5a. CONSIDERATION OF STIMULATED RAMAN SCATTERING IN YB:S-FAP LASER AMPLIFIERS

First published as: *A.J. Bayramian, C. Bibeau, R.J Beach, C.D. Marshall, and S.A. Payne, "Consideration of Stimulated Raman Scattering in Yb:S-FAP laser amplifiers," to be published Applied Optics, 2000.*

I. Introduction:

With the amplifier system running efficiently and with good beam quality, the next issue lies in possible nonlinear losses induced by high intensity laser pulses interacting with the Yb:S-FAP amplifiers. The 100 J, 1-10 ns operating regime of the Mercury laser necessitates the consideration of other nonlinear optical loss mechanisms beyond B-integral effects[1] (a cumulative measure of the nonlinear interaction (self-phase modulation) of a pulse with an optical material) such as stimulated Raman scattering (SRS). We report the first quantitative measurement of the SRS gain coefficient in Yb:$Sr_5(PO_4)_3F$ to be 1.23 ± 0.12 cm/GW at 1053 nm. This data, along with surface and bulk losses, feedback due to surface reflections, gain saturation, and bandwidth have been applied to a quantitative model that predicts the effects of SRS within a laser amplifier system where the laser gain medium shows SRS gain. Limitations and impact to the laser amplifier performance are discussed, along with possible techniques to reduce SRS loss.

SRS is based on the spontaneous Raman effect, which was discovered by C.V. Raman in 1928[2]. Spontaneous Raman scatting is a weak, nearly isotropic inelastic scattering from vibrational modes. Upon scattering, incident radiation frequencies are shifted to a Stokes (lower) frequency or an Anti-Stokes (higher) frequency as illustrated in Fig. 1, where g is the ground state, n is an excited vibrational state, ω is the incident radiation

frequency, ω_S is the Stokes frequency, and ω_A is the Anti-Stokes frequency. The dashed line is a virtual level associated with some higher lying electronic state. Under typical laboratory conditions, the Stokes transition is preferred, since the electronic populations in levels in n and g must obey Boltzmann statistics (i.e. the ratio of populations in n versus g is $\exp(-\hbar\omega_{ng}/kT)$, where $\hbar$ is Plank's constant, ω_{ng} is the n→g transition frequency , k is Boltzmann's constant, and T is the temperature). Under excitation by an intense laser beam, the spontaneous Raman scattering process becomes a stimulated process as the photon occupation number in the Stokes mode becomes much greater than one[2]. SRS causes nonlinear growth of the Stokes mode with incident laser intensity and propagation distance in the Raman active medium, which in turn depletes the laser mode. For these reasons, SRS is a suspect loss in any Raman active material where high intensity laser beams are concerned.

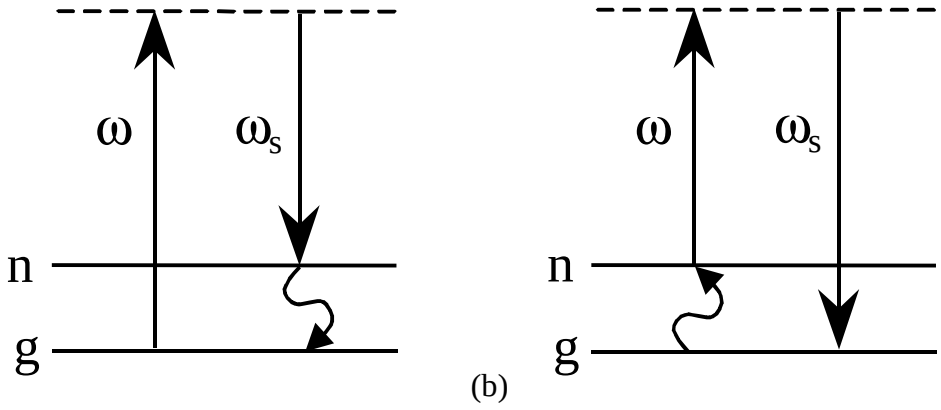

Fig. 1 Energy level diagrams showing Raman (a) Stokes, and (b) Anti-Stokes scattering

Raman transitions have been observed in $Sr_5(PO_4)_3F$ (S-FAP), with the strongest transition occurring at $\nu = 950\ cm^{-1}$, which corresponds to the symmetric breathing mode of the PO_4 group (tetrahedral symmetry)[3]. An energy-level diagram of the Yb^{3+} ion in

the S-FAP host lattice and its corresponding Raman transition is depicted in Fig. 2. Due to the large energy level separation between the V_1 (the vibrational excited state) and the ground state, the excited state population of this mode will be ~1% under the nominal operating conditions (300K). Therefore, a stimulated Stokes Raman shift of the 1047 nm input to 1163.4 nm is expected to dominate below threshold. Threshold in this paper is defined as a condition in which the conversion of laser light to an SRS process exceeds a given percentage usually ranging 0.1% to 10%[4]. Hereafter, we will use 1% as the threshold condition.

II. SRS gain coefficient:

To model and understand the growth of the SRS signal, we must establish the source term as well as the SRS gain coefficient for S-FAP. When the input Stokes intensity is small compared to the pump intensity, and the pump depletion is small (i.e. $I_{Raman}(0)\, e^{gI_{pump}\ell} << I_{pump}(0)$), the equation for steady-state SRS gain is given by[4]:

$$\begin{aligned} I_{Raman}(\ell) &= \frac{h\nu_{Raman}\eta_{Raman}(\ell)}{A\tau_p} \\ &= \frac{h\nu_{Raman}\eta_{Raman}(0)}{A\tau_p}\exp[g(\nu_{pump})I_{pump}\ell] \end{aligned} \tag{1}$$

where I_{Raman} is the Raman intensity, ν_{Raman} is the Stokes frequency, η_{Raman} is the number of Raman photons, ℓ is the length of the gain medium, A is the area of the beam, τ_p is the temporal Raman pulsewidth, g is the Raman gain coefficient, ν_{pump} is the pump frequency, and I_{pump} is the pump laser intensity. The two unknowns then in our equation are the number of noise photons, $\eta_{Raman}(0)$, and the Raman gain coefficient, g.

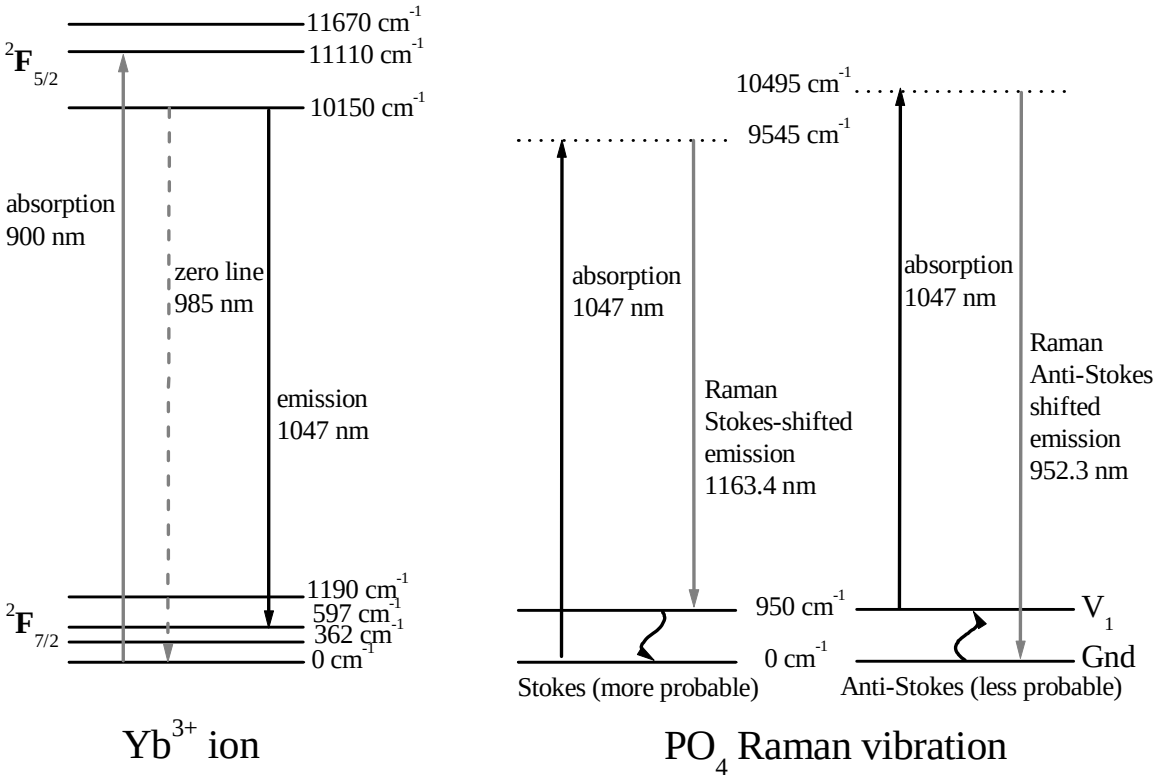

Fig. 2. Energy level diagram of Yb^{3+} and the Raman transition associated with the laser emission line in the $Sr_5(PO_4)_3F$ (S-FAP) host medium.

The source term, or $\eta_{Raman}(0)$, represents the number of Raman photons arising from zero point fluctuations, and is given by Eqns. 2, 3, and 4[4]:

$$\eta_{Raman}(0) = N_{modes} = N_{spatial} N_{temporal} \tag{2}$$

$$N_{spatial} = F^2 = \left(\frac{A_{pump}}{\lambda_{Raman} L} \right)^2 \tag{3}$$

$$N_{temporal} \approx \begin{cases} 1, & \tau_p \le \dfrac{G_{total}}{\pi \Delta\nu_{Raman}} \\ \dfrac{\tau_p \pi \Delta\nu_{Raman}}{G_{total}}, & \tau_p >> \dfrac{G_{total}}{\pi \Delta\nu_{Raman}} \end{cases} \tag{4}$$

where N represents the number of modes, F is the Fresnel number of the system, A_{Raman} is the area of the Raman beam, L is the interaction length, τ_p is the pump temporal

pulsewidth, $\Delta\nu_{Raman}$ is the Raman linewidth, and G_{total} is the product $gI_{pump}\ell$. Since the intensity profile across the aperture of the amplifiers is a top hat, the area of the Raman beam will be the same as the pump beam. To determine the peak Raman gain coefficient for S-FAP, we make use of[5]:

$$g(\nu_0) = N\left(\frac{d\sigma}{d\Omega}\right)_{90}^{0} \frac{2\lambda_{Raman}^2\lambda_{pump}}{3\pi hcn^2} \tag{5}$$

where ν_0 is the Raman emission line center, N is the number density of Raman generators, $(d\sigma/d\Omega)_{90}^{0}$ is the peak spontaneous Raman cross section at 90 degrees to the propagation direction, λ_{Raman} is the Raman wavelength, λ_{Pump} is the pump laser frequency, and n is the index of refraction at the Stokes wavelength. This gives the frequency dependence of the gain coefficient, but the scattering cross section itself has frequency dependence. The frequency dependence of the differential Raman scattering cross section is given by[6]:

$$\left(\frac{d\sigma}{d\Omega}\right) = \frac{2\pi^2 h n_{Raman}}{mc^4 n_{Laser}\lambda_{Raman}^4\Omega_{Raman}}\left(\frac{\partial\alpha}{\partial q}\right)^2 = \frac{\sigma}{\lambda_{Raman}^4} \tag{6}$$

where h is Planks constant, n_{Raman} is the index of refraction at the Raman wavelength, m is the reduced mass of the Raman vibration, c is the speed of light, n_{Laser} is the index of refraction at the laser wavelength, λ_{Raman} is the Raman (Stokes) wavelength, Ω_{Raman} is the Raman vibration frequency, $\partial\alpha/\partial q$ is the normal mode derivative of the polarizability tensor, and σ is everything in the central part of eqn. 6 except λ_{Raman}. Combining Eqns. 5 and 6, and defining $(d\sigma/d\Omega)_{90}^{0} = \sigma/\lambda^4$, gives:

$$g(\nu_0) \propto \frac{N\sigma\lambda_{pump}}{n^2\lambda_{Raman}^2} \tag{7}$$

Recently, Basiev et.al[7] published a comparative study of several crystals and determined the polarized $(d\sigma/d\Omega)_{90}{}^{0}$ value relative to that of diamond, which they normalized to 100. To make quantitative use of these results, a quantitative measurement for a single gain coefficient is needed. The gain coefficient for S-FAP can then be found by scaling a particular reference material measured relative to S-FAP with a known quantitative gain coefficient as shown in eqn. 8.

$$g^{0}_{S-FAP} = g^{0}_{Mat}\left(\frac{N\sigma_{S-FAP}\lambda^{2}_{Raman(Mat)}n^{2}_{Mat}\lambda_{pump(S-FAP)}}{N\sigma_{Mat}\lambda^{2}_{Raman(S-FAP)}n^{2}_{S-FAP}\lambda_{pump(Mat)}}\right) \tag{8}$$

Using Eqn. 8 to convert the gain coefficients of SiO_2[2], $LiNbO_3$[2], diamond[8], $CaCO_3$[6], $KGd(WO_4)_2$[9], $Ba(NO_3)_2$[10], gives a spread in the extrapolated gain coefficient for S-FAP reflecting experimental errors in Basiev's relative cross section measurement as well as the experimental measurement of the gain coefficients. The results of this comparative study are presented in Table 1. The average scaled gain coefficient for S-FAP is 1.08 ± 0.41 cm/GW. Since the magnitude of the error in the g values is too large to produce a reasonable prediction in the modeling for the Mercury laser, an experiment was designed to directly measure the Raman gain coefficient, g.

The experimental arrangement is shown in Fig. 3. A flashlamp-pumped 100 J Nd:glass laser was used to generate 1-2 ns pump pulses with intensities up to 3.6 GW at 1.053 μm. The experiment employed three crystals in series to generate a Raman pulse (total crystal length = 6.024 cm). The pump light was polarized parallel to the c-axis of the crystal, which is identical to the polarization of maximal laser gain in Yb:S-FAP[11]. Since the pump light and the SRS light are collinear after exiting the last crystal, the colors were separated using a prism. The SRS energy detector was shielded by a

longpass filter with OD = 5 at 1.053 μm and approximately 80% transmission at 1.170 μm, the Stokes-shifted wavelength (Part # 11100 REFLP, Omega Optical, Inc.). The results of the experiment with error bars are plotted in Fig. 4. In the displayed plot, a straight line representing 1.053 μm transmitted light has been subtracted from the data, partially eliminating a noise floor in the original data at low intensities. This leaves the exponential growth of the SRS signal clearly visible in the data.

Theoretical predictions of the SRS signal were generated using Eqn. 1 for values of the Raman gain coefficient ranging from 1.2 to 1.4 cm/GW (shown in Fig. 4). The data roughly fit to the theory curve (which has no adjustable parameters) for a gain coefficient of 1.3 cm/GW, which is within the error of our earlier theoretical prediction of 1.08 cm/GW. One can see that small changes in the Raman gain coefficient (8%) in the theory curves cause nearly order of magnitude changes in the generated SRS signal indicating extreme sensitivity of SRS signal to the magnitude of g. Note that the logarithm of Eqn. 1 can be approximated to give the equation for a straight line with slope $g(\nu_{pump})\ell$ (Eqn. 9), where C is a constant. A least-squares fit of the data (shown as a dotted line in Fig. 4) gives a value of $g = 1.23 \pm 0.12$ cm/GW, allowing an independent check of the validity of our model.

$$\ln[I_{Raman}(\ell)] = \ln\left[\left(\frac{1}{I}\right)\left(\frac{h\nu_{Raman}\tau_p\pi\Delta\nu_{Raman}}{g(\nu_{pump})\ell A_{pump}\tau_p}\right)\left(\frac{A_{pump}}{\lambda_{Raman}L}\right)^2\right] + g(\nu_{pump})\ell I$$

$$\approx C + [g(\nu_{pump})\ell]I \qquad (9)$$

Table 1. Raman spectroscopic values and gain coefficients for S-FAP and various other materials. The calculated range of gain values varies from 0.39 up to 2.22 cm/GW thus emphasizing the need for experimental verification.

Material	S-FAP	Diamond	$KGd(WO_4)_2$	$CaCO_3$	$Ba(NO_3)_2$	SiO_2	$LiNbO_3$
λ_{pump} (μm)	**1.0476**	**0.694**	**1.064**	**0.532**	**0.532**	**0.694**	**0.694**
Ω_{Raman} (cm^{-1})	**950.3**	**1332.9**	**768.0**	**1086.4**	**1048.6**	**464.5**	**256.0**
λ_{Raman} (μm)	**1.163**	**0.765**	**1.159**	**0.565**	**0.563**	**0.717**	**0.707**
$\Delta\nu_{Raman}$ (cm^{-1})	**2.8**	**2.7**	**6.4**	**1.2**	**0.4**	**7.0**	**23.0**
n	**1.614**	**2.400**	**2.033**	**1.658**	**1.580**	**1.544**	**2.183**
σ (relative)	**3.80**	**100.00**	**37.00**	**10.60**	**63.00**	**1.20**	**22.00**
$g_{(meas)}$ (cm/GW)	-	**6.9**	**6.0**	**5.5**	**47.0**	**0.80**	**8.9**
$g_{S\text{-}FAP(calc)}$ (cm/MW)	-	**0.38**	**0.96**	**0.97**	**1.26**	**1.33**	**1.57**

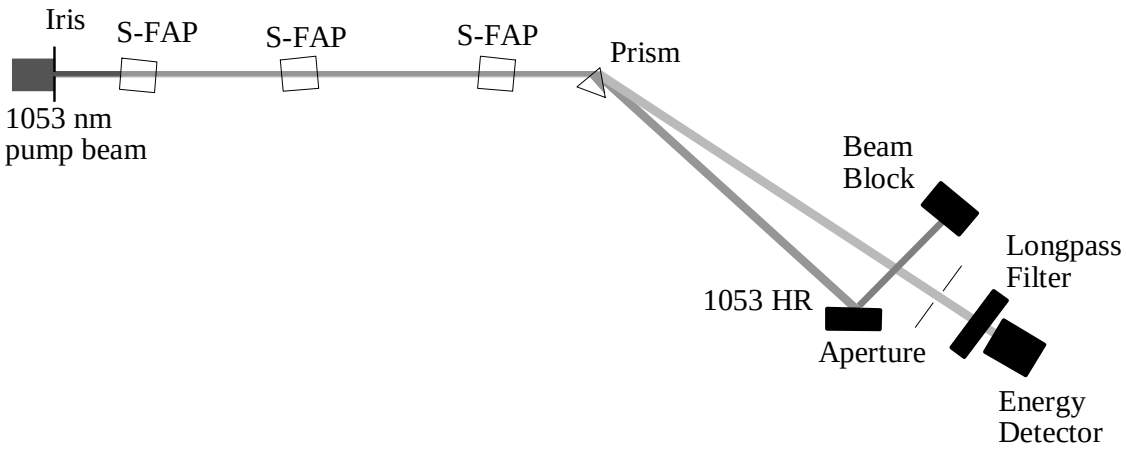

Fig. 3. Experimental arrangement for the first measurement of the SRS gain coefficient.

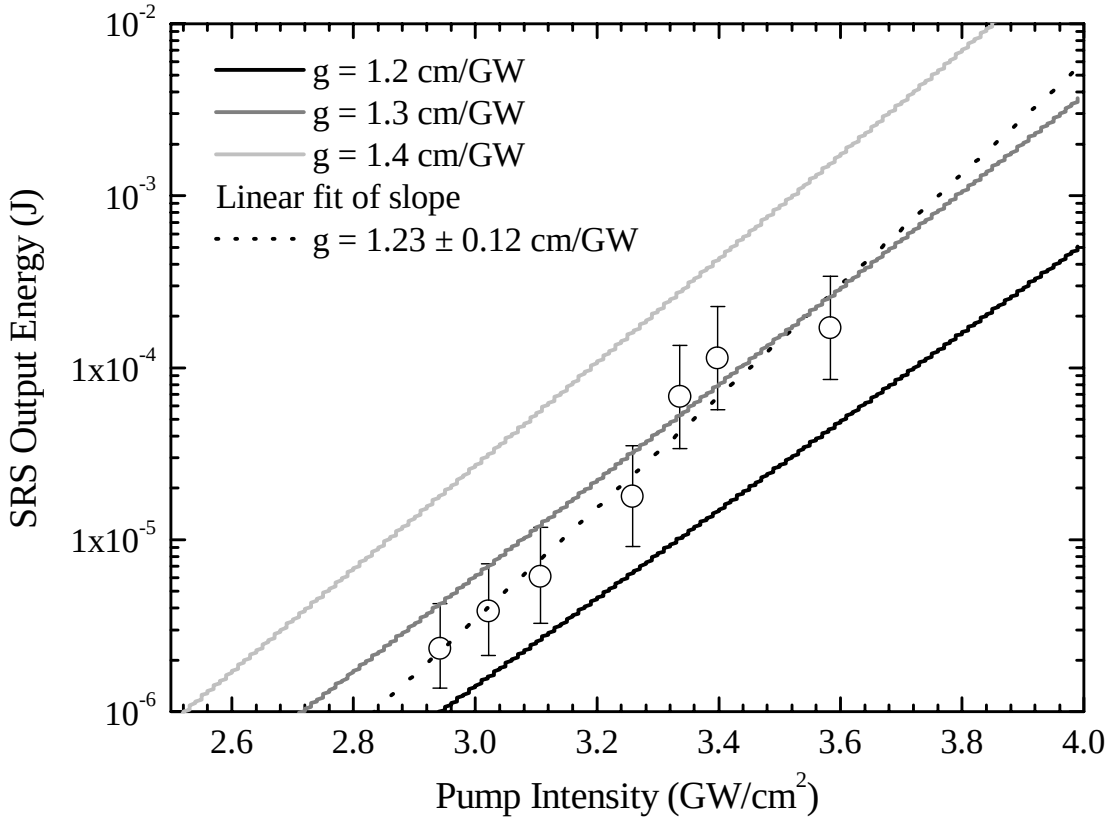

Fig. 4. Output stokes energy as a function of pump intensity with the experimental data plotted as circles with approximate error bars, and theoretical fits using values for the SRS gain coefficient between 1.2 and 1.4 cm/GW, as well as a linear fit of the data.

III. Modeling SRS in a single pass amplifier system

To begin to understand the magnitude of SRS loss, we begin with a simple amplifier system as shown in Fig. 5. If we first assume the reflectivity of the surfaces is zero at the Raman wavelength, and an amplifier thickness of 5 cm, then the typical gIL threshold is about 22, where threshold is defined at 1% conversion of laser energy to Raman energy. Note that this calculation assumes an undepleted pump (where the pump is the laser beam) since we are modeling SRS loss in laser amplifiers. Therefore, this calculation breaks down when the SRS intensity becomes greater than approximately 10 % of the laser intensity.

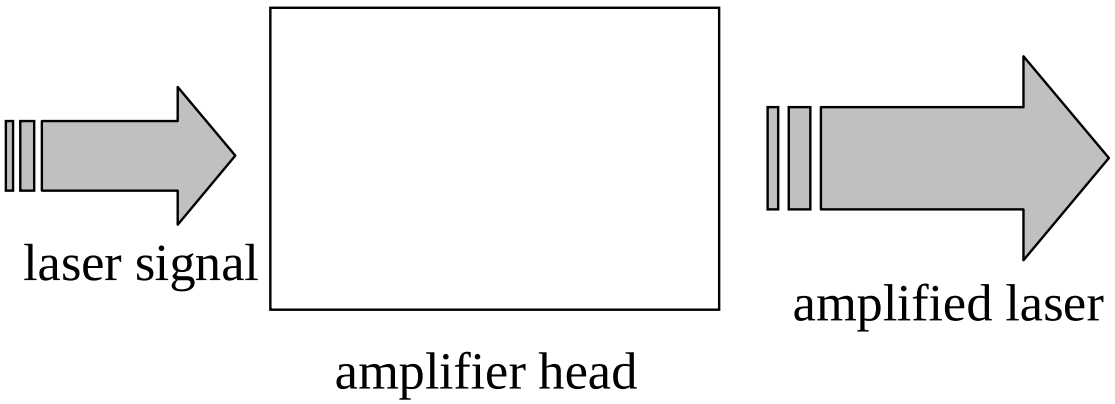

Fig. 5. Schematic of a simple single pass amplifier

The results of this calculation are given in Fig. 6 in units of normalized Raman intensity, which is defined as the ratio of the Raman to the laser intensity. The solid line curve reflects the best case scenario where no Raman light is reflected from the surfaces. If the reflectivity of the surfaces is increased above zero, the SRS threshold is reduced and the slope is increased. This occurs because the reflections effectively increase the path length (by the ratio of the laser pulsewidth to the 1-way transit time through the amplifier). The surface losses reduce the SRS gain multiplicatively, while the path length increase enters exponentially. At the other extreme where the surfaces form an etalon cavity (the dotted curve in Fig. 6), the slope remains the same since the path length is still the same, while the intercept decreases since there is now almost no reflection loss. This case is essentially a quasi-CW Raman laser since the laser pulsewidth is 100 times the Raman lifetime, defined as $(\pi\Delta\nu_{Raman})^{-1}$ = 3.79 ps. The deleterious effects of surface reflections bring SRS thresholds down and increase the slope of the gain curve which can severely effect the operation of large scale amplifier systems.

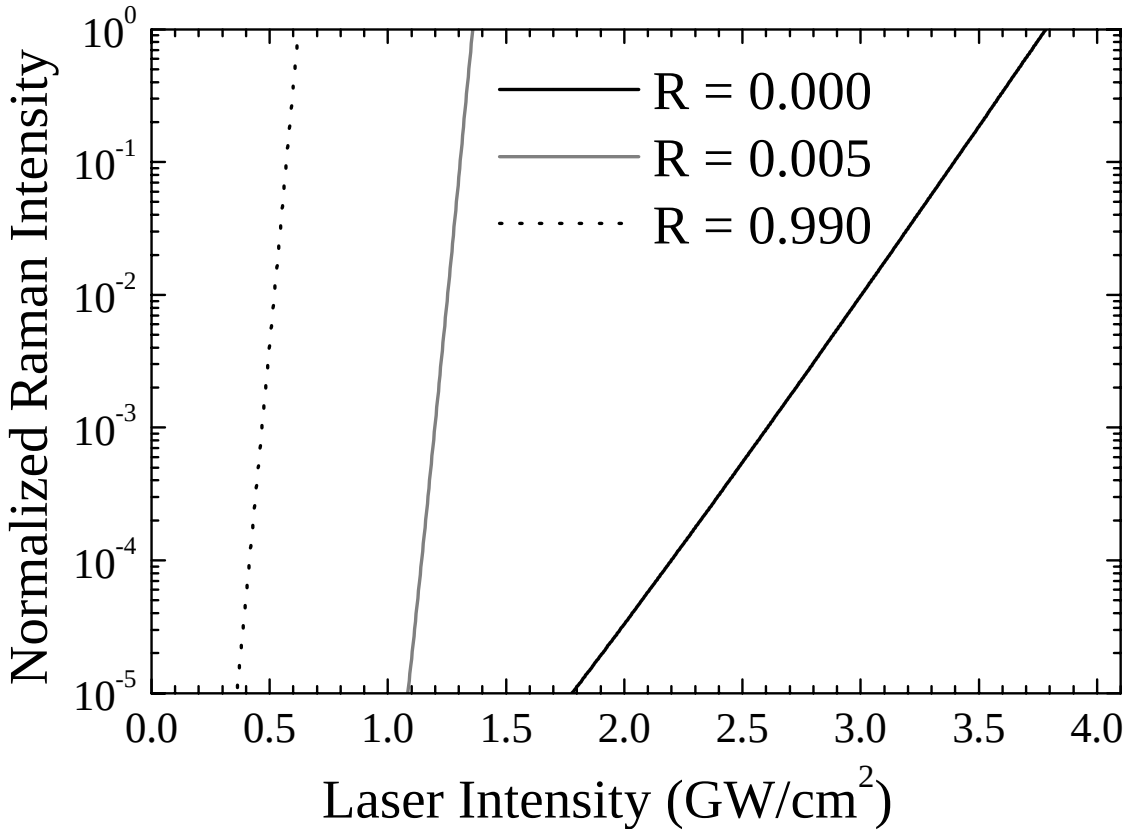

Fig. 6. Normalized SRS intensity versus laser intensity for L = 5 cm, τ = 2 ns, and different surface reflectivity (R).

IV. Modeling SRS in a large scale laser amplifier system:

In sections III and IV, the modeling efforts are presented in a general study. However, to illustrate the sensitivity of various key parameters, a specific S-FAP laser system needs to be considered. We chose the geometry of an actual system being built (the Mercury Laser system[12]) whose general layout is shown in Fig. 7.

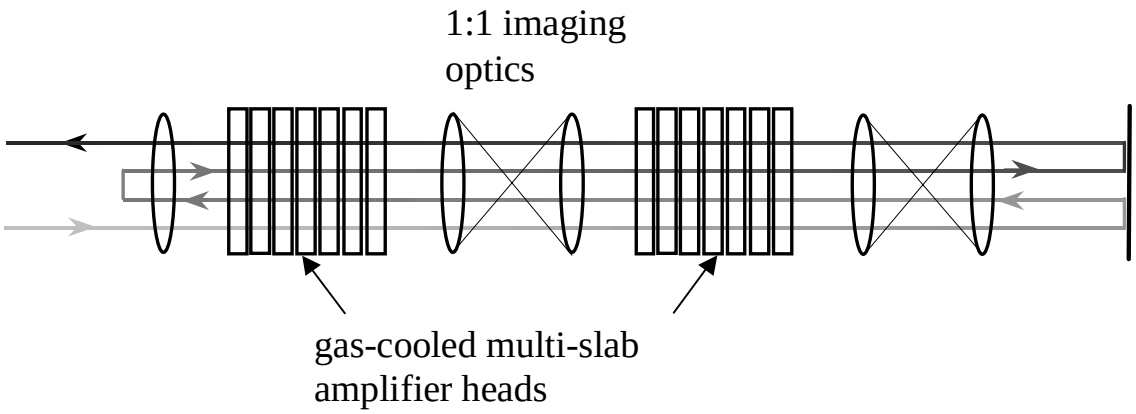

Fig. 7. Schematic of the 4-pass mercury amplifier system

The relevant parameters in the model are: the Fresnel number (Eqn. 3) which effects the number of modes available, the output fluence of the amplifier system which leads to exponential Raman gain, and the degree of laser gain saturation. Note in Fig. 8 that the saturated case (top curve) exacerbates the SRS problem by allowing more gain medium to interact near maximum fluence (highest Raman gain). With the magnitude of the gain coefficient in hand, the SRS gain can be modeled in the geometry of a specific laser amplifier system. A code was used to calculate the laser gain for the amplifier chain, including pump absorption, laser gain saturation, and laser bandwidth effects (see table 2 for modeling parameters and Appendix IIIa). In Fig. 7 and later figures, the output will be plotted as the normalized fluence, which is defined as the output fluence, F_{out}, divided by the saturation fluence, $F_{sat} = h\nu_{laser}/\sigma_{em}$, where h is Plank's constant, ν_{laser} is the laser frequency, and σ_{em} is the emission cross section at the laser wavelength.

Fig. 8 shows the normalized laser fluence in Mercury calculated as a function of the normalized distance through the amplifier defined as the distance, x, divided by the total length of gain medium, L, including all bulk and surface losses for several narrow line front-end input fluences. While the saturated case is optimal for efficient energy

extraction, the SRS loss from the intensity length product in Eqn. 1 makes the top curve the least desirable. Since SRS is exponentially dependent on the laser intensity, consideration must be made balancing optimum energy extraction in the amplifiers, the temporal pulsewidth and the threshold for SRS generation.

Table 2. Modeling parameters

Parameter	Value
SRS gain coefficient (cm/GW)	**1.3**
Laser wavelength (nm)	**1047**
SRS Stokes wavelength (nm)	**1163.4**
Raman bandwidth, $\Delta\nu$ (GHz)	**84**
# of slabs in an amplifier head	**7**
Slab thickness (cm)	**0.75**
Gap between slabs (cm)	**0.1**
Area of slab (cm^2)	**15**
Scatter loss in gain medium (cm^{-1})	**0.005**
Anti-reflection coating reflectivity	**0.0025**

There are three basic SRS gain mechanisms which are important in a laser amplifier system which has multiple amplifiers and/or multiple passes through a single amplifier (in order of decreasing loss): multi-pass on a single amplifier head (by way of surface reflections), single pass through the entire chain, and single pass on a single amplifier head. The single pass gain mechanisms are simply the single pass amplification of the quantum noise generated by spontaneous emission, while the multi-pass gain begins with the noise photons but then grows from the Fresnel reflections from the amplifier and/or nearby optical surfaces. In both of these geometries the Fresnel number used for the calculation of noise photons is adjusted based on apertures in the amplifier chain and the effective path length change upon reflection.

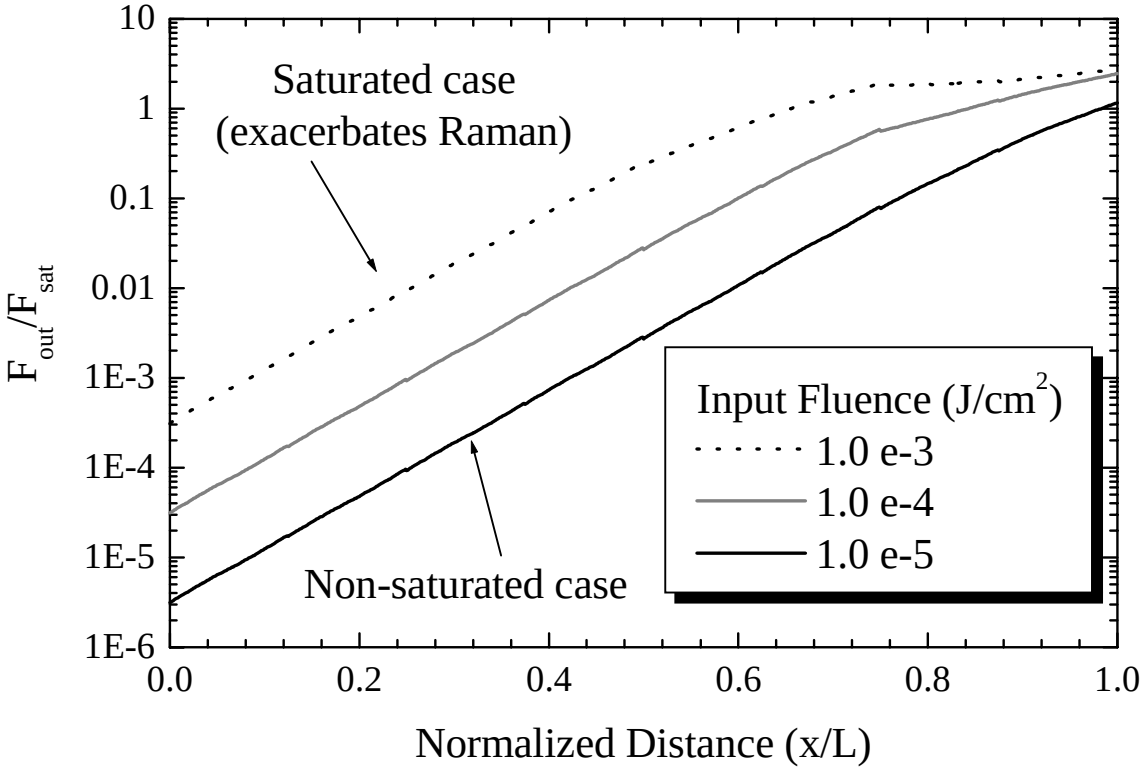

Fig. 8. Normalized fluence, including all Fresnel losses, as a function of normalized distance through the Mercury amplifier chain ($G_0 \sim 1.5 \times 10^6$). Three different front-end input fluences are plotted to show different saturation behaviors.

To more accurately model SRS generation in a multi-segment amplifier system, the initial SRS calculation is modified by temporal and etalon corrections. Temporal corrections, a consequence of the finite temporal length of the output pulse (and SRS gain), account for the lower gain length seen by the trailing edge of the SRS signal (Fig. 9 left). Etalon corrections, as a consequence of having multiple slabs (surfaces) in an amplifier head, create coherent signal feedback between multiple surfaces in the amplifier head (Fig. 9 right). These corrections are important to consider, however in our particular case the net effect was negligible (approximately 1%) to the SRS threshold.

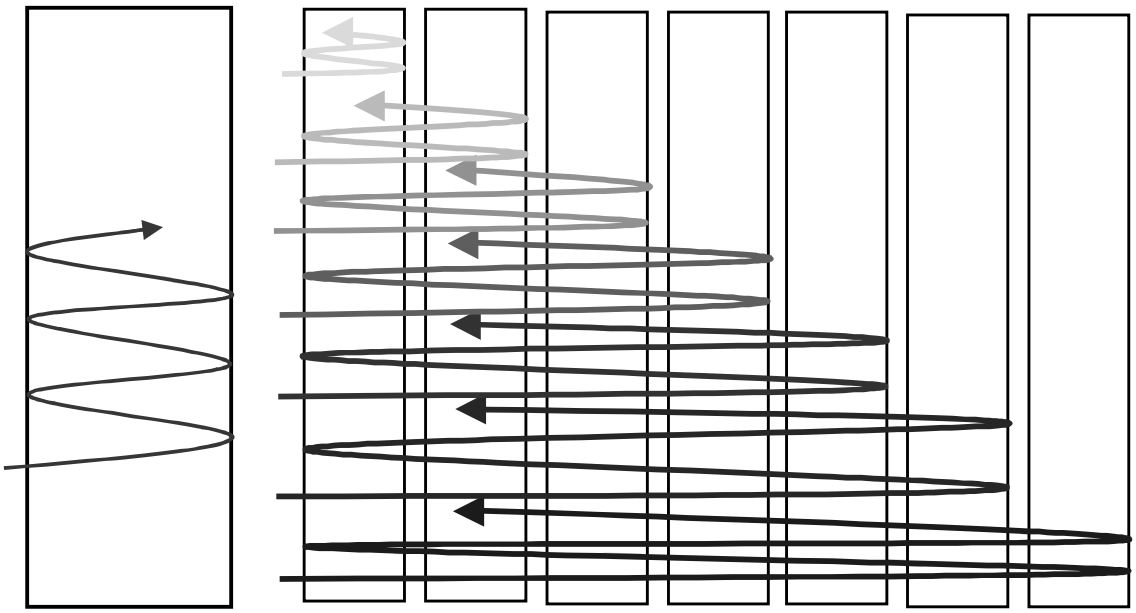

Fig. 9. Diagrams of temporal (left) and etalon (right) corrections to the SRS code

Incorporating both of these effects into the model, we calculated the operating point for the amplifier system which corresponds to the Raman threshold condition stated earlier as 1% conversion of the output energy. The results of this calculation are presented in Fig. 10, where the three traces represent propagation of a narrowline-input spectrum (narrow (≤ 1 GHz) with respect to the Raman transition (84 GHz)) with the Raman gain coefficient varied. For example, operating the Mercury laser with F_{out}/F_{sat} = 2.02 (100-J pulses), narrowline input, and the Raman gain coefficient, g = 1.3 cm/GW, the pulsewidths must be greater than 4.2 ns for the SRS loss to be less than 1%. Clearly, SRS output needs to be considered when operating Mercury. The small Fresnel reflections coupled with strong Raman gain at the laser output intensity create a condition in which Raman must be suppressed. The effect of the corrections shown in Fig. 9 can be seen in Fig. 11, which compares the g = 1.3 cm/GW line from Fig. 10 overlaid with a plot of the SRS output from just the last amplifier head with no temporal correction, etalon

corrections, or SRS signals from earlier in the amplifier chain. Fig. 12 is similar to Fig. 10 except the gain coefficient is held constant at g = 1.3 cm/GW and the surface reflectivity is varied, showing critical sensitivity to high-quality low-reflectivity coatings. Fig. 13 is again similar to Fig. 10 except the size of the extraction beam is varied, showing relative insensitivity to the scale of the laser amplifier system. However, it is important to note that transverse SRS plays an increasingly important role in the threshold calculation as the area of the beam increases (the transverse dimension becomes large enough to achieve SRS conversions approaching threshold). For example, if the area is increased to 1000 cm^2, transverse SRS dominates the SRS loss.

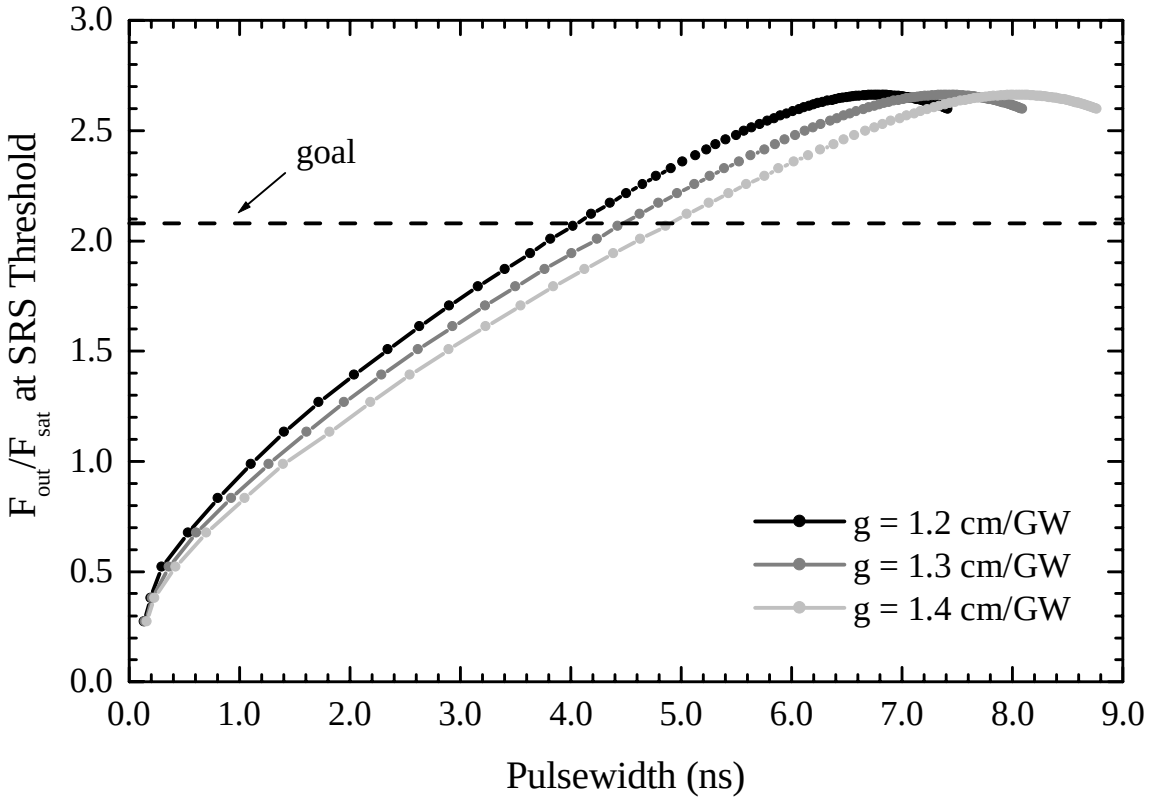

Fig. 10. The normalized fluence at SRS threshold (defined as 1% conversion) versus temporal pulsewidth. Traces show narrowband extraction with the gain medium surface reflectivity, R = 0.0025, and the SRS gain coefficient varied.

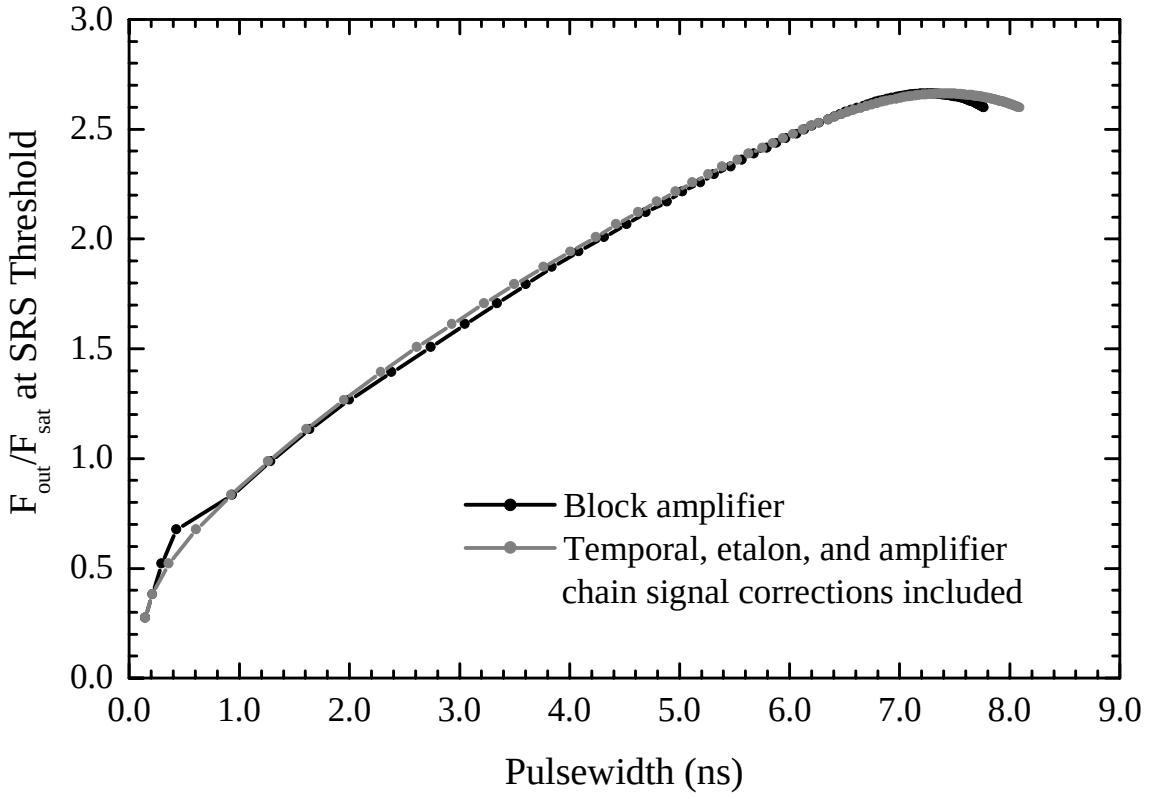

Fig. 11. The normalized fluence at SRS threshold (defined as 1% conversion) versus temporal pulsewidth showing the negligible effect of correcting for pulse-length, multiple reflections between slabs within head as well as input from SRS earlier in the chain.

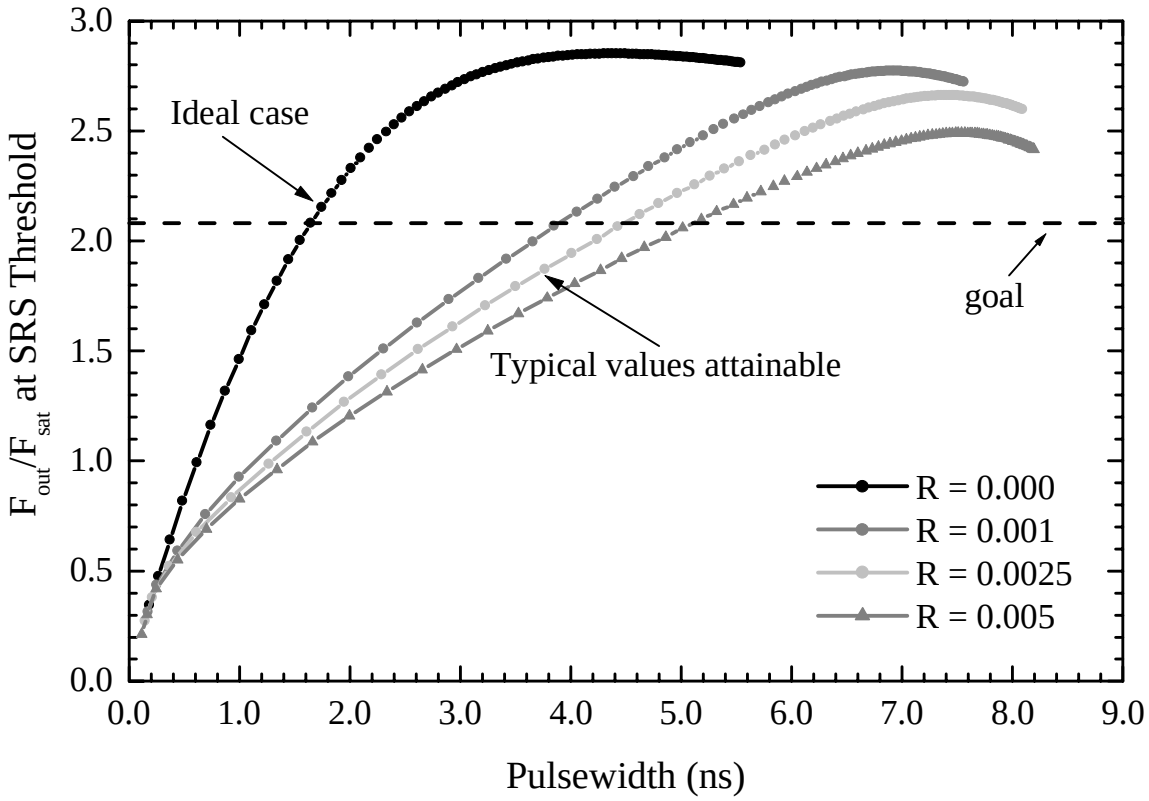

Fig. 12. The normalized fluence at SRS threshold (defined as 1% conversion) versus temporal pulsewidth. Traces show narrowband extraction with g = 1.3 cm/GW with the gain medium surface reflectivity varied.

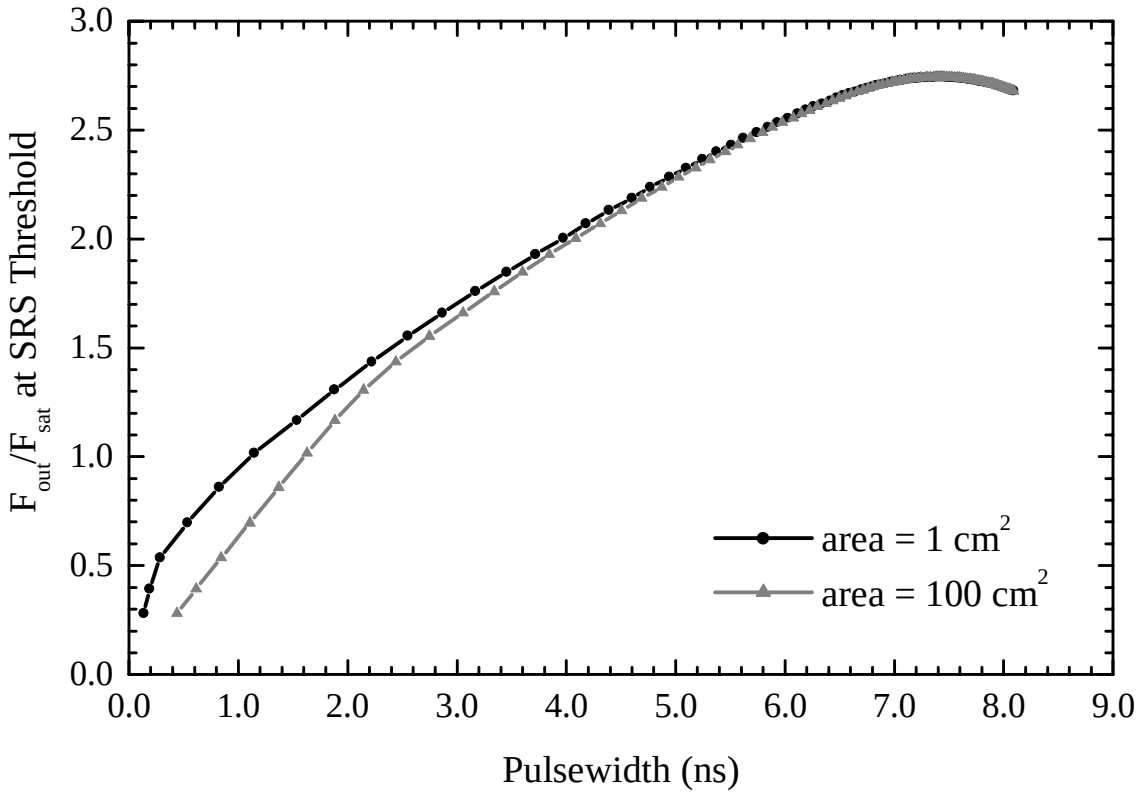

Fig. 13. The normalized fluence at SRS threshold (defined as 1% conversion) versus temporal pulsewidth. Traces show narrowband extraction with g = 1.3 cm/GW, R = 0.0025, area of extraction (laser beam area) varied.

V. Methods for Reducing SRS:

There are several ways in which the above SRS losses can be significantly reduced. The simplest solution is to run the system with longer pulsewidths and/or lower output fluences. Another important option is the addition of bandwidth to the laser beam. In the forward propagation direction, the addition of bandwidth does not significantly effect the SRS gain due to a narrowline input spectrum, G_{Narrow}. However, in the backward direction, the addition of bandwidth does effect the narrowband SRS gain as shown in Eqn. 10 (which is also valid for the forward direction) [13,14]:

$$\frac{G_{Broad}}{G_{Narrow}} = F = \frac{1}{2}\left[1-\left(1+\frac{\Delta\nu_R}{\Delta\nu_P}\right)\frac{L_g}{L_d}\right]+\sqrt{\frac{1}{4}\left[1-\left(1+\frac{\Delta\nu_R}{\Delta\nu_P}\right)\frac{L_g}{L_d}\right]^2+\frac{\Delta\nu_R L_g}{\Delta\nu_P L_d}} \qquad (10)$$

where G_{Broad} is the broadband gain, G_{Narrow} is the monochromatic gain, F is the bandwidth gain reduction factor, $\Delta\nu_R$ is the Raman linewidth (84 GHz), $\Delta\nu_p$ is the pump laser linewidth, the gain length, $L_g = (gI)^{-1}$ is the length over which the Stokes intensity grows by a factor of e with a monochromatic pump, and L_d is the Raman coherence length defined by Eqn. 11[13,15]:

$$L_{df} = \frac{c}{4\Delta n\Delta\nu_p} \approx 52.4 \text{ cm}, \qquad L_{db} = \frac{c}{4n_S\Delta\nu_p} \approx 0.04 \text{ cm} \qquad (11)$$

where L_{df} is the forward SRS coherence length, L_{db} is the backward SRS coherence length, c is the speed of light, Δn is the difference between the pump and Stokes indices of refraction, and n_s is the index of refraction at the Stokes wavelength. Using values from table 1 as well as $\Delta n \approx 0.0013$, gives L_{df} = 52.4 cm and L_{db} = 0.04 cm for a pump bandwidth of 110 GHz. Incidentally, the transverse SRS coherence length has roughly the same form as backward scatter ($L_{dt} \sim L_{db}/2$ = 0.08 cm), and can thereby be drastically reduced with the implementation of bandwidth which may be an issue for large aperture systems (long transverse dimension). For intensities > 1 GW/cm^2, the ratio F is > 0.985 for forward SRS making $G \sim G_{Narrow}$, while for intensities < 5 GW/cm^2 (that is 10 J/cm^2 for 2 ns pulses), F < 0.470 for backward SRS making $G < 0.470*G_{Narrow}$ (this is a significant effect since G_{Narrow} is in nepers). For multiple passes due to surface (normal incidence) reflections, the SRS gain mechanism alternates between forward SRS (monochromatic gain) and backward SRS (reduced gain with bandwidth). Incorporating this effect into the modeling code (see Appendix IIIb), the operating point for Mercury

which corresponds to the Raman threshold was calculated versus temporal pulsewidth for several normalized front end input bandwidths ($\Delta\nu_{Laser}/\Delta\nu_{Raman}$) as shown in Fig. 14 with the narrow line input data overlaid for comparison. Thus, the addition of bandwidth has a favorable effect on the operating point of the Mercury laser, and any amplifier where Fresnel reflections contribute to the SRS signal.

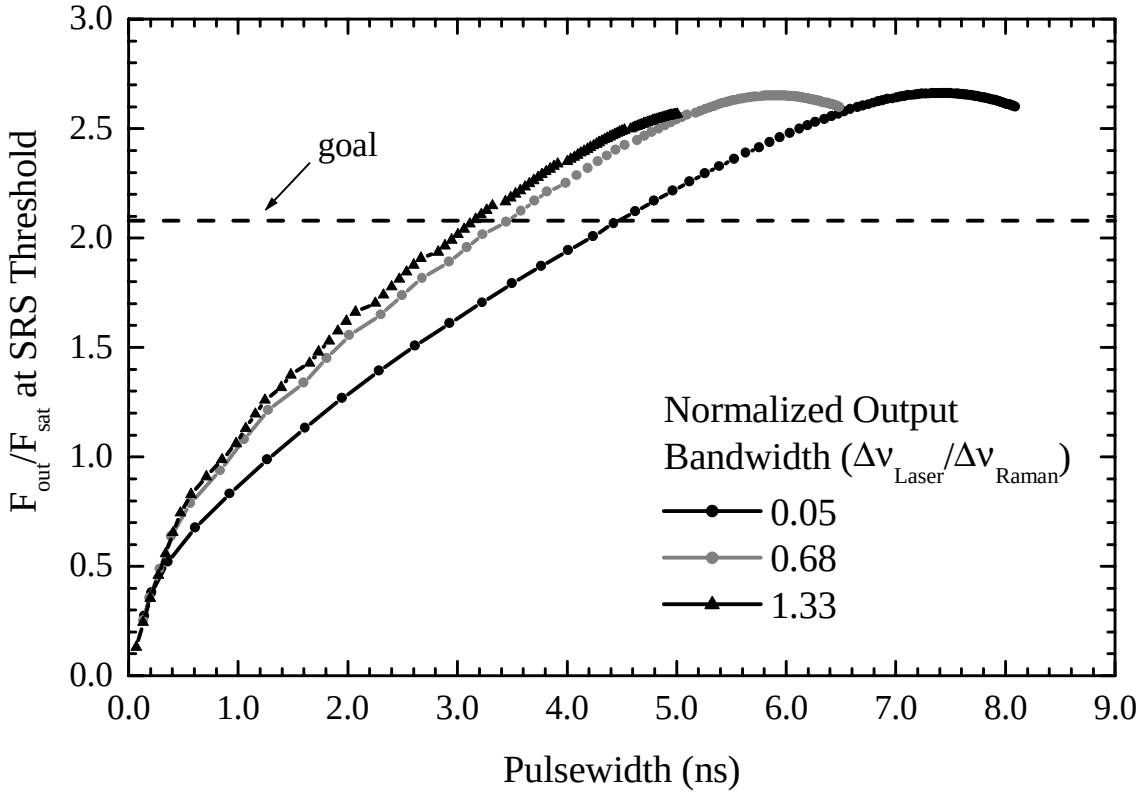

Fig. 14. The normalized fluence at SRS threshold (defined as 1% conversion) versus temporal pulsewidth. Colored traces show extraction with g = 1.3 cm/GW, R = 0.0025, with the input bandwidth varied.

One may ask, how is the SRS gain effected if the SRS direction is not exactly in the forward or backward direction? To answer this question, the SRS coherence length given

by Eqn. 11 must be derived for arbitrary angles. The SRS coherence length is given in general by[15]:

$$L_{coh} = \frac{\pi}{\Delta k} = \frac{\pi}{\left|\vec{k}_L - \vec{k}_S\right|} \tag{12}$$

By choosing our k vectors as in Eqn. 13, the coherence length can be derived for arbitrary angle q with respect to the direction of the laser light given by Eqn. 14:

$$k_L = \frac{2\pi n_L}{\lambda_L} = \frac{2\pi n_L \nu_L}{c}\hat{i}$$

$$\vec{k}_S = \frac{2\pi n_S}{\lambda_S}\left[\cos(\theta)\hat{i} + \sin(\theta)\hat{j}\right] = \frac{2\pi n_S \nu_S}{c}\left[\cos(\theta)\hat{i} + \sin(\theta)\hat{j}\right] \tag{13}$$

$$L_d(\theta) = \frac{c}{2\sqrt{\left[n_L\Delta\nu_L - n_S\Delta\nu_S\cos(\theta)\right]^2 + \left[n_S\Delta\nu_S\sin(\theta)\right]^2}} \tag{14}$$

This derivation gives slightly different values for the coherence length for θ = 0°, 90°, and 180° from Murray[13], with the approximation that $\Delta\nu_S \approx \Delta\nu_L$ = 84 GHz for θ = 0°, 90°, and 180°, and $n_S \approx n_L$ = 1.6252 for θ = 90°, and 180°. However, the more important parameter from the point of view of SRS gain is the F factor given by Eqn. 10. Eqn. 14 gives a coherence length twice as long as Eqn. 11 for θ = 0°, but results in only a 2 % change in F. The angular dependence of F for a laser signal with a normalized output bandwidth of unity is shown in Fig. 15.

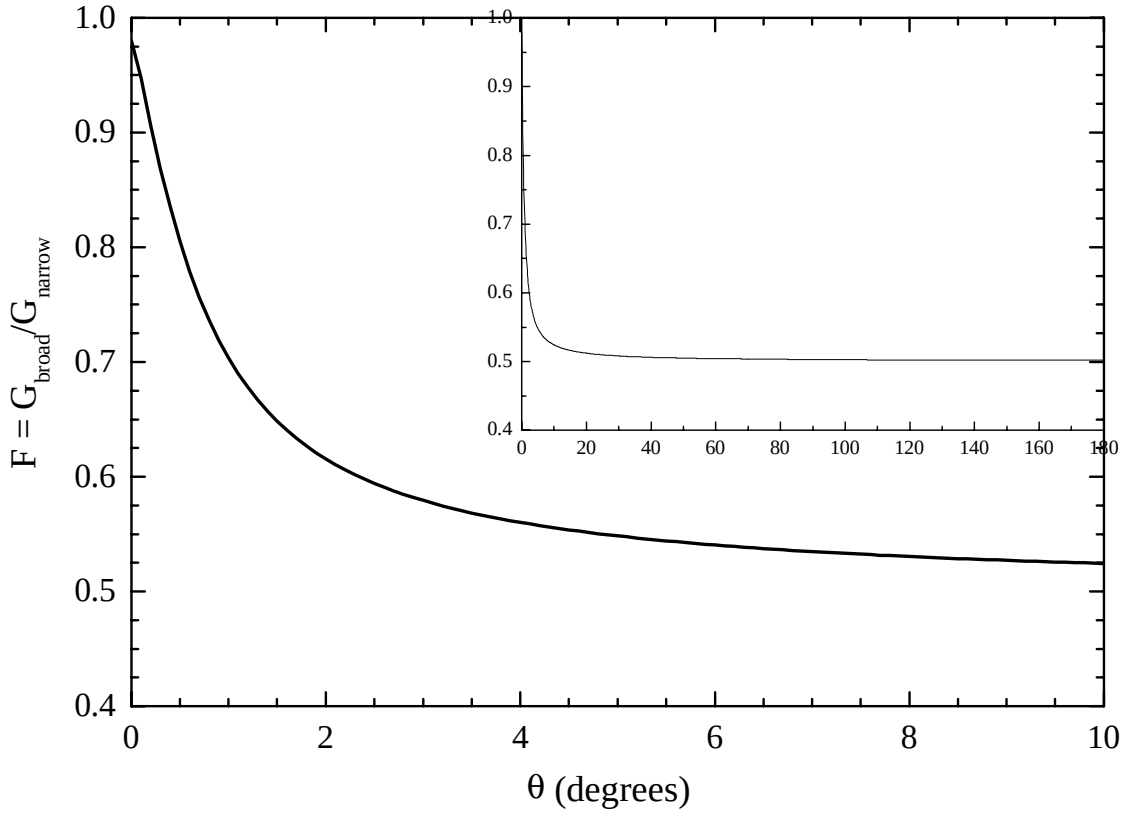

Fig. 15. The gain factor, $F = G_{Broad}/G_{Narrow}$, as a function of the angle between $\vec{k}_S$ and $\vec{k}_L$. The inset shows this same graph with the same axis on a smaller scale.

The use of pinholes or baffles at all laser foci in the amplifier chain can also help suppress SRS. The pinholes/baffles serve to block high Fresnel number modes from propagating down the chain thus impacting the Fresnel number used in the calculation of noise photons which seed the SRS loss. SRS signal gain can also be eliminated by the introduction of a dichroic mirror between the two amplifier heads to kick out the SRS beam, thereby reducing the problem of SRS buildup to just a single head. If air gaps exist between the slabs of the amplifier head (as in the Mercury system), the introduction of an absorber gas, such as methane can also be used to reduce the intra-head gain.

Likewise, the thickness of these gaps can be increased, thereby decreasing the SRS gain to loss ratio when etaloning occurs.

Since the largest portion of the SRS signal is often due to internal reflections of a single amplifier head, one possible way to reduce SRS is to reduce the number of allowed reflections by wedging the surfaces of the slabs as shown in Fig. 16. The SRS model was adjusted to include losses due to changes in Fresnel number with angle, and beam walk-off beyond the extraction aperture (see Appendix IIIc). The total wedge angle between all slabs is denoted as Ω. The results of the calculation are shown in Fig. 17 as the operating point for system which corresponds to the Raman threshold condition versus the temporal pulsewidth for a variety of total wedge angles, Ω. The intra-head and temporal corrections have a larger effect in this case since the number of Fresnel reflections is effected. Finally, by using bandwidth in conjunction with the tilt methods, suppression of SRS is further enhanced. A wedged amplifier head (or even a non-wedged amplifier head at Brewster's angle) ensure that Fresnel reflections occur at angles where the F factor (shown in Fig. 15) is significantly below unity thereby maximizing the suppressive effects of bandwidth.

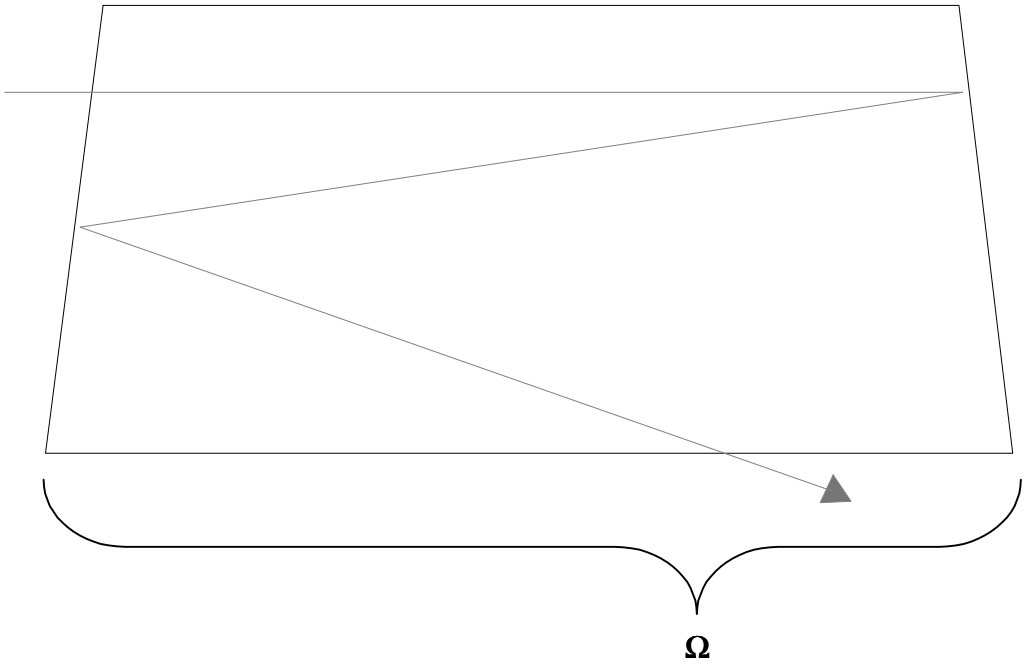

Fig. 16. Possible amplifier head geometry employing wedged slabs to reduce SRS buildup by reducing the number of possible intra-head reflections.

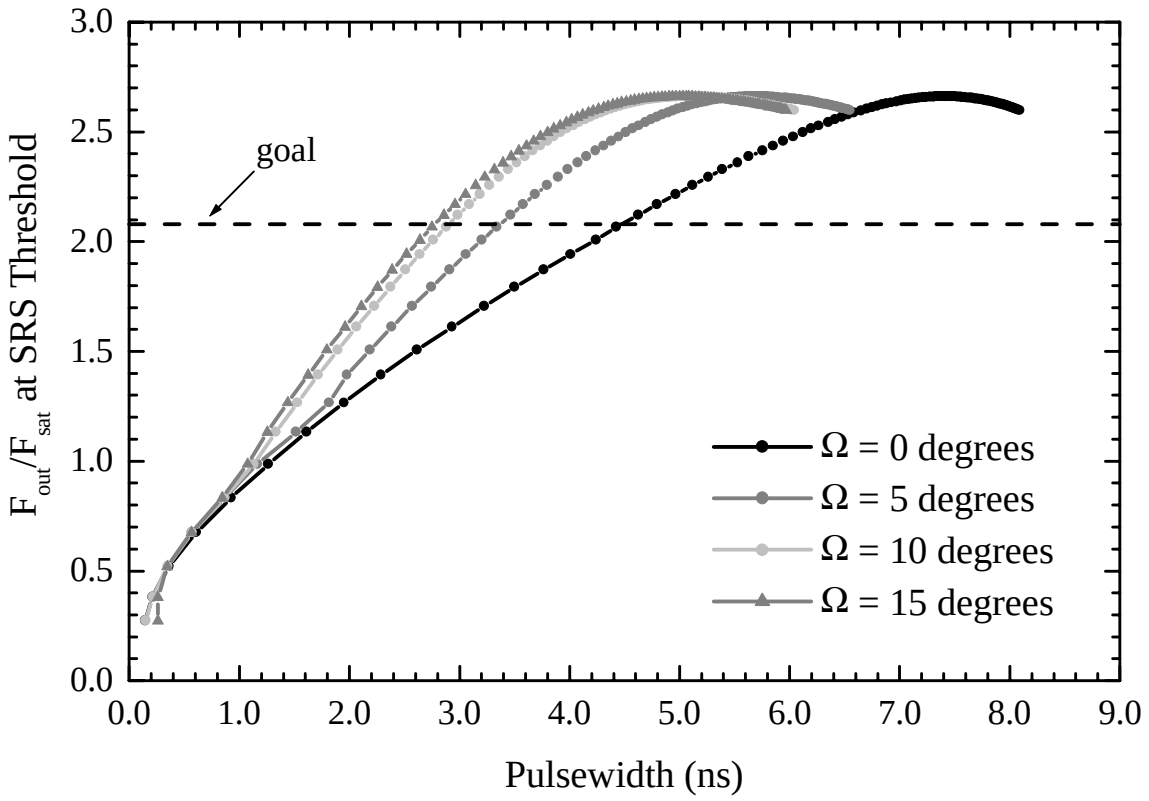

Fig. 17. The normalized fluence at SRS threshold (defined as 1% conversion) versus temporal pulsewidth. Colored traces show narrowband extraction with g = 1.3 cm/GW, R = 0.0025, with the total wedge angle, Ω, varied.

VI. Discussion

The SRS loss model used in these calculations is a good starting point for getting the operating point of the amplifier to first order. However, there are several assumptions made to simplify these calculations which may not always be true. The first assumption is that the spatial profile of the laser beam is a flat-top and the temporal profile is square. Real laser pulses will of course not match these assumptions, and since deviations from the assumption represent changes in intensity which nonlinearly effects SRS generation. When considering new systems or geometries, even relatively small deviations from the above assumptions need to be examined. On the plus side, consider a gaussian spatial and temporal profile laser pulse with identical energy to the square pulse. Only the center

portion of the beam is at the peak intensity and the SRS gain falls off exponentially from this point. Therefore, assuming the peak intensity is the same for the two cases, the SRS loss will be much less in the Gaussian case since the effective area of high intensity is greatly reduced. The next caveat comes from the nature of the amplifier geometry in Mercury. The many parallel surfaces in the amplifier not only lead to Fresnel reflections of the SRS light but also the laser light. Although these reflections are individually small, when they coherently add the resultant intensity from even a 0.25% reflectivity coating on 18 surfaces (7 amplifier slabs plus two windows with 2 surfaces each) can lead to local intensity peaks a factor of two higher than the intensity would be without the Fresnel reflections. These local high intensity laser peaks become local high Raman gain peaks leading to increased SRS loss. The exact magnitude, position, and size of these peaks is difficult to ascertain not only computationally, but experimentally as well, since the wavefront of each surface must be precisely known to predict the coherent interference pattern present within the gain medium. The Raman gain was also calculated with only 8 surfaces to simplify calculations. To first order the reflectivity of the other 10 surfaces can be decreased to zero and the remaining 8 surfaces increased accordingly. The effect of the extra surfaces will be to put the threshold on a higher reflectivity curve as shown on Fig. 12. For example, if the surface reflectivity, $R = 0.001$, the curve which includes the sixteen surfaces will be somewhere between $R = 0.002$ and $R = 0.003$. The exact solution is challenging, since the path through Raman gain medium as well as the other media can undergo many permutations. Another approximation lies in the slab tilt model for SRS reduction used in this thesis, which calculates the number of reflections or path length using a ray which starts at the narrow end of the wedge and

works its way towards the wide end as shown in Fig. 18. This ray, which is parallel to the edge face, was chosen since its path length represents something of a mean between rays initially pointed toward the wide end of the wedge (shorter path length), and those rays initially pointed at the narrow end of the wedge (longer path length which is limited to the path length of the pulse). Detailed ray tracing would be required to confirm the wisdom of this choice, which favors temporal pulsewidths that are short relative to the amplifier width.

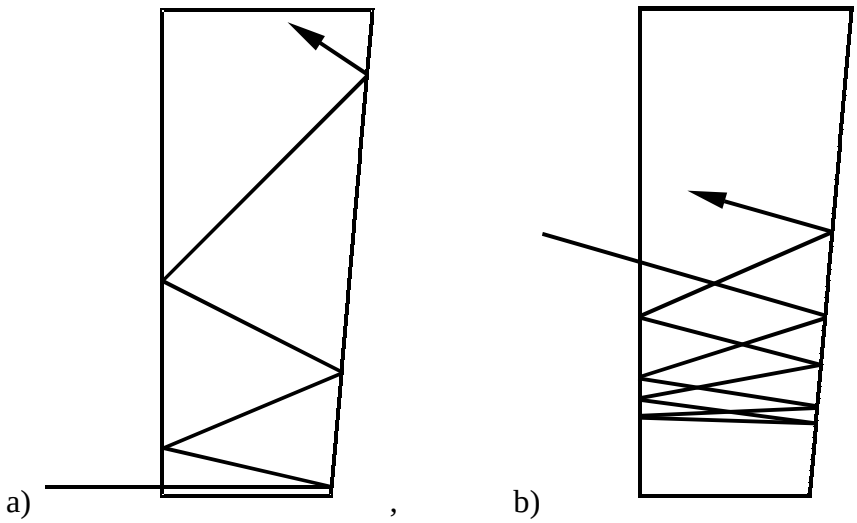

Fig. 18 a) Chosen ray for calculating slab tilt path length changes, b) The path of the "lucky" ray whose path length is not effected by the wedge (and is only limited by the temporal pulsewidth)

Transverse SRS has not been mentioned in the modeling to this point because the single pass transverse SRS is much less that the Fresnel reflected forward and backward SRS. For this statement to be true, there must be no Fresnel reflections from the edges of the amplifier. This can be accomplished with absorbers, although the reflection from the interface between the S-FAP and the absorber would have to be much less than 0.25%, else transverse SRS would build from Fresnel reflections just as the forward and

backward SRS did. The other possibility is to wedge the amplifier edges so that transverse SRS is kicked out of the gain path. Finally, there exists the possibility of total internal reflection modes (since anti-reflection coatings are usually only anti-reflective over a narrow range of angles) building from high angle reflection from the anti-reflection coatings. The gain coefficient is also slightly suspect since for anisotropic crystals like S-FAP, the SRS gain will be depolarized relative to the initially polarize laser beam. The experiment shown in Fig. 3 only measures the effective combined gain in both polarizations. The SRS energy exiting the crystal is then calculated by assuming only p-polarized SRS emission (since the depolarization ratio is not known for S-FAP), then backing out the losses of the prism and filters. SRS depolarization will obviously skew the magnitude of the answer (by a possible factor of 2 or 3, which when viewed on a log scale makes almost no difference), while the slope of the line in log space will be preserved. With these caveats in mind, the SRS model developed here for large amplifier systems can probably predict the SRS threshold pulsewidth to within 20% (where this error could be decreased with more accurate measurement of the SRS gain coefficient, and extensive ray tracing analysis to back up the aforementioned assumptions).

VII. Summary

The SRS gain coefficient for S-FAP has been measured experimentally to be 1.3 cm/GW, which agrees with the average value derived from the Basiev[7] results and the independently measured SRS gain coefficients of six other materials. To properly model the SRS gain in an amplifier system, a code was developed which calculates the laser fluence through an amplifier system as a function of distance, including spectral and temporal characteristics of the pulse. Another code was also developed to model the SRS

gain, which included temporal, intra-head oscillation, full chain effects, bandwidth, and slab-tilt corrections to accurately model SRS buildup during a laser pulse. The results of several calculations indicate that the SRS signal is extremely sensitive to the magnitude of the SRS gain coefficient and the surface reflectivity of the amplifier heads. Possible methods for reducing SRS included the addition of bandwidth to the laser signal and tilting and/or wedging the amplifier head with respect to the laser propagation direction. Both of these solutions significantly decrease the minimum pulsewidth possible at SRS threshold.

Chapter 5b. CONSIDERATION OF STIMULATED BRILLOUIN SCATTERING IN YB:S-FAP LASER AMPLIFIERS

I. Introduction

Another nonlinear loss associated with high intensity laser amplifier systems is Stimulated Brillouin Scattering (SBS), which is inelastic scattering from acoustic waves which are launched by the laser pulse. In this chapter, the SBS gain coefficient is evaluated theoretically and used to analyze SBS loss in S-FAP optical amplifier systems such as the Mercury laser. Methods of reducing SBS in S-FAP amplifiers is discussed in light of the results given in the previous chapter for Stimulated Raman Scattering. SBS in optical materials arises from scattering due to time dependent fluctuations in the optical properties of the material, such as the index of refraction. Simply stated, Brillouin scattering occurs when photons are scattered by acoustic waves traveling in a medium. Since acoustic waves are of much lower frequency than phonons or light waves, the Brillouin linewidths (0.007 cm^{-1}) and Brillouin frequency shifts (~0.2 cm^{-1}) are much smaller than Raman linewidths (~2 cm^{-1}) and frequency shifts (~1000 cm^{-1}). Like SRS, there is a spontaneous version of Brillouin scattering that is weakly dependent on thermal fluctuations or quantum-mechanical zero-point fluctuations, which induce index variations. SBS is initiated when intense laser radiation (frequency ω_L) interferes with Stokes radiation, ω_S (which can be from spontaneous Brillouin scattering or intentionally seeded) to launch an acoustic wave Ω with frequency equal to ω_L-ω_S (see Fig. 1).

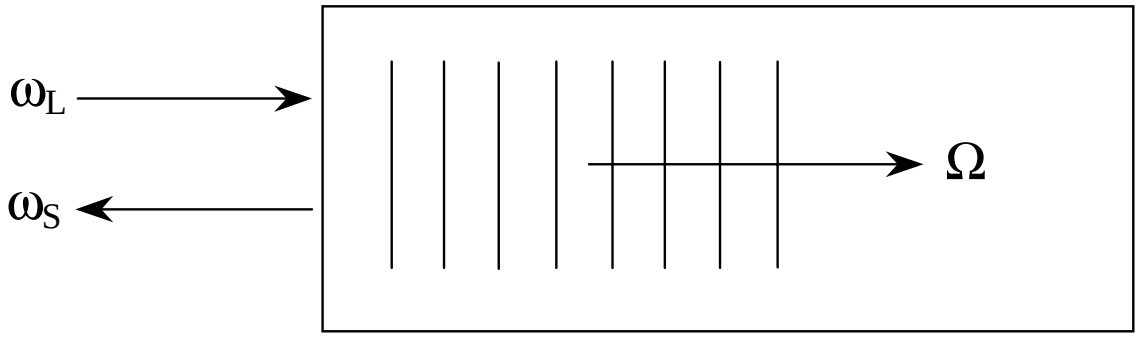

Fig.1 The stimulated Brillouin scattering (SBS) process

The acoustic wave causes fluctuations in the optical properties of the material, namely the index, thereby creating a moving Bragg grating which scatters the laser frequency. The laser light is Doppler shifted by Ω as Stokes light, ω_S. This positive feedback 3-wave mixing process results in exponential gain with input laser intensity and can lead to nearly 100% scattering of the laser light as Stokes light. Note that the SBS threshold shall be defined as 1% conversion of pump (laser) energy into Stokes energy. SBS is caused by two physical mechanisms, namely optical absorption and electrostriction. The first mechanism, optical absorption, operates by generating heat in the high intensity portions of the interference pattern which leads to thermal expansion. The density variations induced by the expansion can then excite the acoustic disturbance at frequency Ω. Electrostriction, the second mechanism, is the tendency of optical materials to become denser in regions of high optical intensity. The laser-Stokes interference can then drive an acoustic wave at Ω. Clearly, SBS is a concern for any high-intensity laser system employing a Brillouin active medium.

II. Theoretical gain coefficient

The equations governing SBS are in many ways similar to those governing stimulated Raman scattering (SRS). The equation for undepleted, steady state Brillouin gain is:

$$I_{Stokes}(z) = I_{Stokes}(L)\exp[g_B I_{Laser}(L-z)] \quad (1)$$

where I_{Stokes} is the Stokes wave intensity, L is the length of the medium, g_B is the Brillouin gain coefficient, and I_{Laser} is the laser intensity. Note that this equation assumes the Stokes wave is seeded from the point z = L and experiences exponential growth in the reverse direction. The Stokes wave can be intentionally seeded with an input Stokes signal, or build up from thermal spontaneous Brillouin scattering. Unlike SRS, SBS is highly directional and is actually attenuated in the forward direction (in fact the Doppler effect increases the laser frequency in the forward direction to give the Anti-Stokes wave, $\omega_{AS} = \omega_S + \Omega$).

The thermal noise factor for eqn. 1 can be expressed in terms of the thermal noise power into a given solid angle $d\Omega = \pi\theta^2/4$ and is given by[2]:

$$I_{Stokes}(L) = \frac{p_{noise}(\theta)}{A} = \frac{\omega_S}{\omega_A} k_b T \Delta\nu_B \frac{4\pi\theta^2}{\lambda^2} \quad (2)$$

where A is the area of the beam, and k_b is the Boltzmann constant.

The gain coefficient for counterpropagating pump and Stokes waves in an anisotropic solid can be expressed as[3]:

$$g_B = \frac{k_S \cdot k_A \cdot n_S^2 \cdot n_P^3 \cdot p'^2}{2 \cdot c \cdot \rho \cdot \upsilon_A \cdot \Gamma_B} \quad (3)$$

$$k_S = n_S\omega_S/c, \quad (4)$$

$$k_A = \Omega_B/\upsilon_A, \quad (5)$$

$$p' = p_{ik}\boldsymbol{\varepsilon}_{Pi}\boldsymbol{\varepsilon}_{Si}\boldsymbol{\kappa}_{Ak}\boldsymbol{\varepsilon}_{Ak}, \tag{6}$$

$$\Gamma_B = 2\pi\Delta\nu_B = \tau_B^{-1} \tag{7}$$

where g is the stimulated Brillouin scattering gain coefficient, k_S is the Stokes wavevector, k_A is the acoustic wavevector, n_S and n_P are the polarization dependent indices of refraction for Stokes and pump respectively, p' is the coupling constant between elastic and electric fields, c is the speed of light, ρ is the density of the optical medium, υ_A is the acoustic velocity, Γ_B is the Brillouin angular linewidth, ω_S is the Stokes angular frequency, Ω_B is the Brillouin angular frequency, p_{ik} are the elasto-optic coefficients in reduced tensor (Voigt) notation, $\boldsymbol{\varepsilon}_{Pi}$ is the pump polarized dielectric tensor, $\boldsymbol{\varepsilon}_{Sj}$ is the Stokes polarized dielectric tensor, $\boldsymbol{\kappa}_{Al}$ is the acoustic unit vector, $\boldsymbol{\varepsilon}_{Am}$ is the acoustic dielectric tensor, $\Delta\nu_B$ is the Brillouin bandwidth, and τ_B is the phonon lifetime. The elasto-optic coefficients can be related to the piezo-optic constants, q_{ij}, and the elastic compliance constants, s_{kl}, given in Ch.3 sec.5 using an equality given by Nye[4] in reduced matrix (Voigt) notation:

$$\Delta B_m = q_{mk}\sigma_{k,} \qquad q_{mk} = p_{ml}s_{lk,} \tag{8}$$

which can be solved for p_{ml} in terms of the two known constants q_{mk} and s_{lk} to give:

$$p_{ml} = q_{mk}s_{lk}^{-1} = q_{mk}c_{kl} \tag{9}$$

The elasto-optic coefficients are then:

$$P_{ij} = \begin{vmatrix} p_{11} & p_{12} & p_{13} & 0 & 0 & p_{16} \\ p_{12} & p_{11} & p_{13} & 0 & 0 & -p_{16} \\ p_{31} & p_{31} & p_{33} & 0 & 0 & 0 \\ 0 & 0 & 0 & p_{44} & p_{45} & 0 \\ 0 & 0 & 0 & -p_{45} & p_{44} & 0 \\ -p_{16} & p_{16} & 0 & 0 & 0 & \frac{1}{2}(p_{11}-p_{12}) \end{vmatrix} \tag{10}$$

$$p_{11} = \frac{q_{13}(-s_{11}+s_{12})s_{13} - q_{11}s_{13}^2 + q_{12}s_{13}^2 + q_{11}s_{11}s_{33} - q_{12}s_{12}s_{33}}{(s_{11}-s_{12})(-2s_{13}^2 + (s_{11}+s_{12})s_{33})}$$

$$p_{12} = \frac{q_{13}(-s_{11}+s_{12})s_{13} - q_{12}s_{13}^2 + q_{12}s_{11}s_{33} + q_{11}(s_{13}^2 - s_{12}s_{33})}{(s_{11}-s_{12})(-2s_{13}^2 + (s_{11}+s_{12})s_{33})}$$

$$p_{13} = \frac{q_{13}(s_{11}+s_{12}) - (q_{11}+q_{12})s_{13}}{-2s_{13}^2 + (s_{11}+s_{12})s_{33}}$$

$$p_{31} = \frac{-q_{33}s_{13} + q_{31}s_{33}}{-2s_{13}^2 + (s_{11}+s_{12})s_{33}}$$

$$p_{33} = \frac{q_{33}(s_{11}+s_{12}) - 2q_{31}s_{13}}{-2s_{13}^2 + (s_{11}+s_{12})s_{33}}$$

$$p_{44} = \frac{q_{44}}{s_{44}}$$

$$p_{45} = \frac{q_{45}}{s_{45}}$$

$$p_{16} = \frac{q_{62}}{s_{11}-s_{12}} \qquad (11)$$

It is important at this point to invoke some of the geometries typically used for S-FAP, namely the polarization of the 1047 nm emission peak is polarized parallel to the z (3) axis, and SBS gain is also typically due to longitudinal waves (i.e. $\kappa_A \bullet \varepsilon_A = 1$), which leaves the following equation for p':

$$p' = p_{31}(\varepsilon_{P3}\bullet\varepsilon_{S3})(\kappa_{A1}\bullet\varepsilon_{A1}) + p_{33}(\varepsilon_{P3}\bullet\varepsilon_{S3})(\kappa_{A3}\bullet\varepsilon_{A3}) + p_{44}(\varepsilon_{P3}\bullet\kappa_{A3})(\varepsilon_{S2}\bullet\varepsilon_{A2}) +$$

$$p_{44}(\varepsilon_{P3}\bullet\varepsilon_{A3})(\varepsilon_{S2}\bullet\kappa_{A2}) + p_{45}(\varepsilon_{P3}\bullet\varepsilon_{A3})(\varepsilon_{S2}\bullet\kappa_{A1}) + p_{45}(\varepsilon_{P3}\bullet\kappa_{A3})(\varepsilon_{S2}\bullet\varepsilon_{A1}) \qquad (12)$$

Eqn. 5 can be modified for arbitrary angle, θ, between the pump and Stokes waves to give:

$$k_A = (k_S^2 - 2\,k_S\,k_P\cos\theta + k_P^2)^{½} \qquad (13)$$

Using these equations, the gain coefficient can be calculated from the basic properties of an optical material. The known values for properties of S-FAP are given in Table 1.

Table 1. Properties used to calculate the SBS gain coefficient

Property			Value	
Laser wavelength, λ_P [$\times$ 10^{-4} cm]			**1.0477**	
Laser frequency, ω_P [$\times$ 10^{15} rad/s]			**1.799136**	
Laser index of refraction[5], n_P^o, n_P^e			**1.6176, 1.6126**	
Laser polarization (o,e)			**e**	
Laser wavevector, k_P^e [$\times$ 10^4 cm^{-1}]			**9.671128**	
Density[5], ρ [g/cm^3]			**4.14**	
Young's Modulus for S-FAP[5], K [GPa]			**109**	
Young's Modulus for C-FAP[6], K [GPa]			**119**	
Acoustic Velocity[1] ($\upsilon_A=(K/\rho)^{½}$) [$\times$ 10^5 cm/s]			**5.13**	
Brillouin frequency[1], ($\Omega_B = 2\ k_P^e\ \upsilon_A$) [$\times$ 10^9 rad/s]			**99.23**	
Brillouin wavevector[1], k_A, [$\times$ 10^5 cm^{-1}]			**1.93**	
Stokes Frequency, ω_S [$\times$ 10^{15} rad/s]			**1.799037**	
Stokes wavevector, k_S [$\times$ 10^4 cm^{-1}]			**9.670594**	
Stokes wavelength, λ_S [$\times$ 10^{-4} cm]			**1.04776**	
Stokes index of refraction, n_S^o, n_S^e			**1.6176, 1.6126**	
Elastic compliance constants for C-FAP[$\times$ 10^{-12} Pa][7,8]			Elastic compliance constants for S-FAP(scaled from C-FAP) [$\times$ 10^{-12} Pa]	
s_{11}	**8.68**	**9.06**	s_{11}	**9.48**	**9.89**
s_{12}	**-1.36**	**-2.14**	s_{12}	**-1.48**	**-2.34**
s_{13}	**-2.10**	**-2.42**	s_{13}	**-2.29**	**-2.64**
s_{33}	**6.96**	**7.19**	s_{33}	**7.60**	**7.85**
s_{44}	**22.9**	**19.1**	s_{44}	**25.00**	**20.85**
Piezo-optic constants for S-FAP [$\times$ 10^{-12} Pa]					
			q_{31}	**-2.1088**	
			q_{33}	**-1.6924**	

Unfortunately, some of the required information to calculate the SBS gain coefficient, including the Brillouin linewidth and some of the piezo-optic constants are missing. As a result, the measured gain coefficients of several solid Brillouin materials will be used to give an estimate of the magnitude of SBS generation in a large scale amplifier system employing S-FAP. The materials of choice are fused silica, potassium dihydrogen phosphate (KD*P), and CaF_2, which have their Brillouin parameters listed in table 2.

Table 2 Brillouin Parameters of selected materials[3].

Material	**fused silica**	**KD*P**	**CaF_2**
Pump Wavelength, λ_P [nm]	**1053**	**532**	**532**
Frequency Shift, Ω_B [GHz]	**32.65**	**30.52±0.156**	**37.164±1.185**
Linewidth, Γ_B [MHz]	**40.8**	**107.4±7.2**	**45.6±8.8**
Brillouin lifetime, τ_B [ns]	**3.90**	**1.48**	**3.49**
g_B [cm/GW]	**4.8**	**5.09±0.4**	**4.11±0.65**
SBS angle, θ [degrees]	**180**	**180**	**180**
index of refraction, n	**1.4496**	**1.5073**	**1.4354**
Density, ρ [g/cm^3]	**2.202**	**2.355**	**3.179**

We can see that for these three typical materials, the gain coefficient is nearly identical and the linewidth is a maximum for KD*P. Hereafter, the modeling will assume a worst case scenario by picking the largest gain coefficient and largest bandwidth as seen in KD*P as those closest to S-FAP's values.

III. Modeling SBS loss in S-FAP

In the absence of bandwidth on the pump laser, the intensity of the steady state SBS signal will grow according to eqn. 1. However, it is important to note that the equation governing steady-state SBS is valid for times greater than or equal to the Brillouin lifetime. Since Mercury operates between 2 and 10 ns, eqn. 1 will be valid for S-FAP as long as the Brillouin linewidth (which is the inverse of the Brillouin lifetime) is greater than 79.5 MHz. However, transient SBS shows growth which is less than steady state SBS, so eqn. 1 is still adequate as the worst case SBS loss estimate regardless of pulsewidth. For the Mercury geometry where the beam is 3 x 5 cm and the amplifier heads are 5.85 cm thick, $I_{Stokes}(L) = 7.59 \times 10^{-5}$ W/cm^2. Using the same computer code developed for SRS modeling in Ch. 4, the amplifier operating point at SBS threshold versus temporal pulsewidth was calculated. The results are shown in Fig. 2 as the

normalized output fluence at SBS threshold versus pump (laser) temporal pulsewidth, where normalized pump fluence is defined as the output fluence, F_{out}, divided by the saturation fluence, $F_{sat} = h\nu_{laser}/\sigma_{em}$, where h is Plank's constant, ν_{laser} is the laser frequency, and σ_{em} is the emission cross section at the laser wavelength. The data indicate that operation of the amplifier at a nominal normalized fluence of 2.02 (100 J), requires the temporal pulsewidth to be greater than 4.8 ns to stay below the SBS threshold.

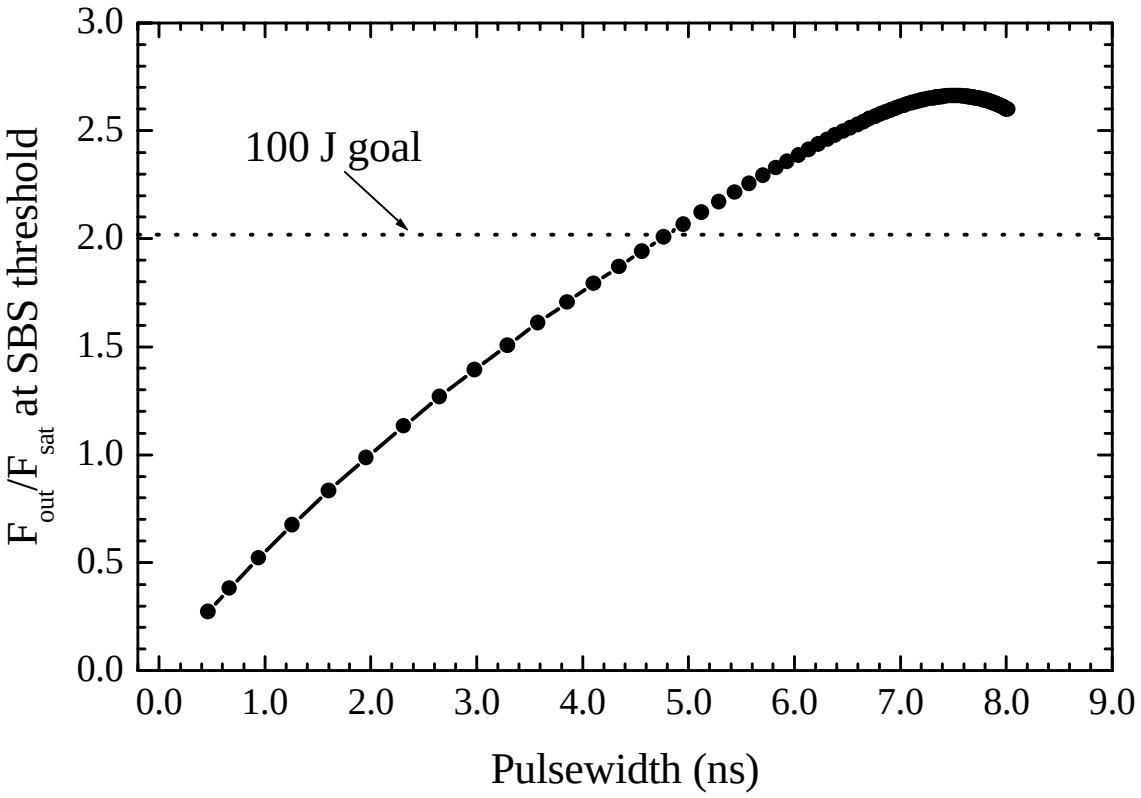

Fig. 2 The normalized fluence at SBS threshold (defined as 1% conversion) versus temporal pulsewidth for narrowband input.

IV. Countermeasures

The above SBS losses can be significantly reduced in several ways. The simplest solution is to run the system with longer pulsewidths and/or lower output fluences. A

much more difficult solution is to increase the ytterbium doping in S-FAP, thus allowing thinner amplifiers that preserve the laser gain while reducing the nonlinear interaction length in the S-FAP medium. The simplest solution, which doesn't involve changing the operating point or ordering new laser materials, is to increase the pump (laser) bandwidth. SBS gain suppression using pump bandwidth is governed by eqns. 10-14 in Ch.4. Eqn. 1 is then modified by the pump bandwidth:

$$I_{Stokes}(z) = I_{Stokes}(L)\exp[Fg_B I_{Laser}(L-z)] \tag{14}$$

where F is the bandwidth gain reduction factor defined in Ch. 4. Using eqn. 13, the normalized fluence at SBS threshold with pump (laser) bandwidth versus temporal pulsewidth is shown in Fig. 3 with Fig.2 overlaid for comparison. Here the addition of bandwidth leads to more than a factor of 2 change in the operating temporal pulsewidth, allowing greater peak power and intensity.

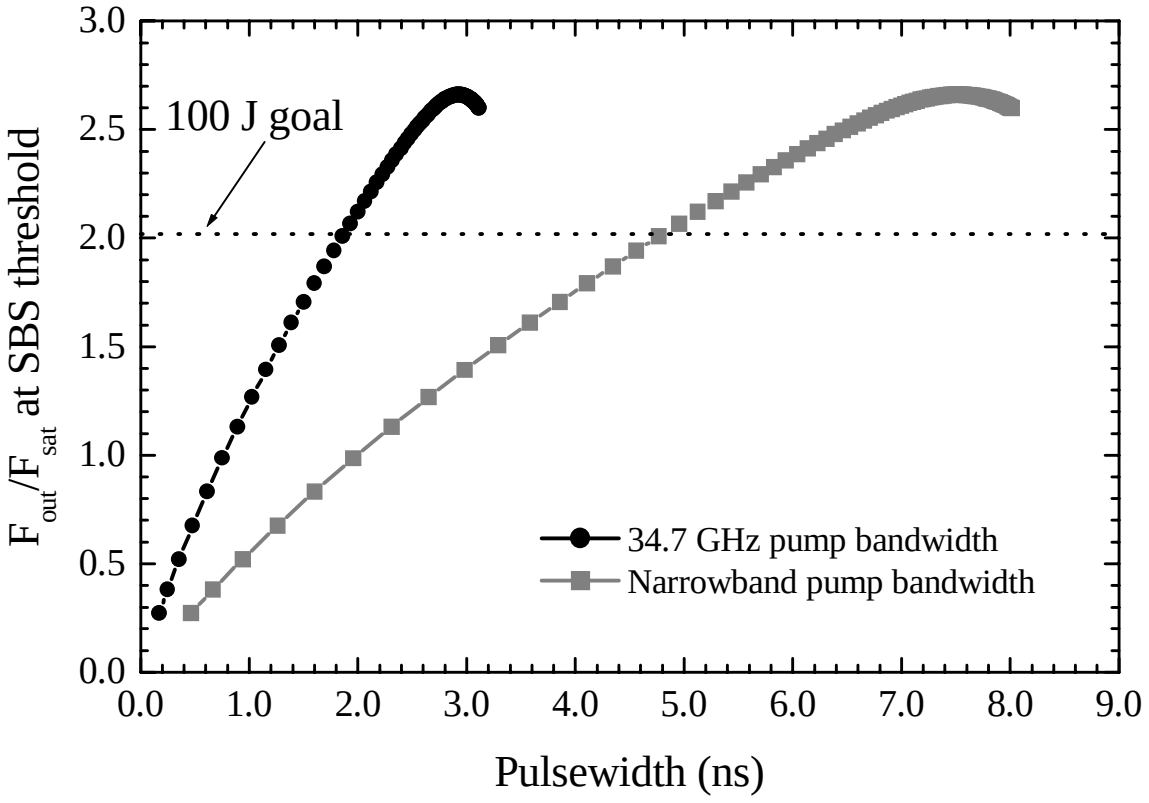

Fig. 3. The normalized fluence at SBS threshold (defined as 1% conversion) versus temporal pulsewidth for narrowband and 34.7 GHz laser output bandwidth.

IV. Summary

In conclusion, this simple estimation has shown SBS to be a problem at the nominal Mercury output energy (100 J) and below a temporal pulsewidth of 4.8 ns. The addition of bandwidth shows enhanced SBS suppression relative to SRS suppression due to the large disparity in spontaneous Brillouin linewidth versus spontaneous Raman linewidth.

Chapter 6a. THREE-LEVEL Q-SWITCHED LASER OPERATION OF YB:S-FAP AT 985 NM

First published as: *A.J. Bayramian, C. Bibeau, C.D. Marshall, S.A. Payne, and W.F. Krupke, "Three-Level Q-Switched Laser Operation of Yb:S-FAP at 985 nm," Optics Letters, **25**, 1-3, 2000.*

I. Introduction

With the spectroscopy, wavefront, and nonlinear losses in hand it is possible to fully understand and model Yb:S-FAP in an amplifier system like Mercury. We now turn our attention to new applications for Yb:S-FAP. While commercial applications exist for efficient diode-pumped Yb:S-FAP lasers at 1 micron, perhaps even more interesting is the transition at 985 nm, which would allow nonlinear conversion to the blue wavelengths. To accomplish this task, the 985 nm laser transition must first be developed. The enormous gain cross sections of ytterbium-doped apatites, which are unique among all ytterbium-doped materials[1], present a special opportunity for efficient Q-switched operation based on the zero-line wavelength of 985 nm. A quick spectroscopic and thermomechanical comparison (see table 1) of Yb:S-FAP with neodymium doped $Y_3Al_5O_{12}$ (Nd:YAG) and chromium doped Al_2O_3 (Ruby), which are two other well known 3-level laser systems, shows Yb:S-FAP to be the clear winner in terms of quantum efficiency, long lifetime for convenient diode-pumping, and high cross sections for efficient absorption and extraction. We report that ytterbium doped $Sr_5(PO_4)_3F$ was successfully lased at 985 nm in pulsed mode with a slope efficiency of 74% and an absorbed threshold energy of 18 mJ. Q-switched slope efficiencies of 21% were obtained with a maximum energy of 9.4 mJ in 8.8 ns pulses. The demonstration of Yb:S-FAP at 985 nm reported here makes possible a new class of compact, efficient,

diode-pumped, doubled and tripled lasers at 492 nm (blue-green) and 328 nm (ultraviolet), respectively.

Table 1. Comparison of Yb:S-FAP with 2 well known 3-level laser systems.

3-Level laser systems	$Yb^{3+}:Sr_5(PO_4)_3F$ (S-FAP)[2]	$Nd^{3+}:Y_3Al_5O_{12}$ (YAG)[3]	$Cr^{3+}:Al_2O_3$ Ruby[3]
Laser wavelength (nm)	**985**	**946**	**694**
Gain cross section ($\times\ 10^{-20}$ cm^2)	**10.0**	**4.0**	**2.5**
Fluorescent lifetime (ms)	**1.1**	**0.23**	**3.0**
Pump Wavelength (nm)	**900**	**808**	**404, 554**
Pump cross section ($\times\ 10^{-20}$ cm^2)	**9.0**	**4.0**	**20.6, 18.0**
Quantum defect ($\lambda_{Pump}/\lambda_{Laser}$)	**0.91**	**0.85**	**0.58, 0.80**
preferred pump source	**diode**	**diode**	**flashlamp**
Losses	**scatter**	**scatter, ESA, upconversion**	**scatter, ESA, upconversion**
Thermal Conductivity (W/cm K)	**0.02**	**0.14**	**0.42**
Specific Heat (J/g K)	**0.5**	**0.59**	**0.75**
Thermal Diffusivity (cm^2/s)	**0.0098**	**0.046**	**0.13**
Thermal Expansion ($\times 10^{-6}$ K^{-1})	**10**	**7.5**	**5.8**
$\partial n/\partial T$ ($\times 10^{-6}$ K)	**-10**	**7.3**	**12.6**

An energy level diagram of Yb:S-FAP (Fig. 1) highlights two possible laser transitions, where the three level operation at 985 nm is of interest in this chapter. The absorption and emission cross sections (Fig. 2) show the preferred pump absorption along the π-polarization direction, while lasing will be preferentially along σ–polarization with respect to the c-axis. Prior laser experiments with S-FAP at 1047 nm[4,5,6] and preliminary results at 985 nm in an apatite analog[7] indicate that the 985 nm emission cross section appears to be sufficient for lasing, although the absorption that is due to true three-level operation could limit the output.

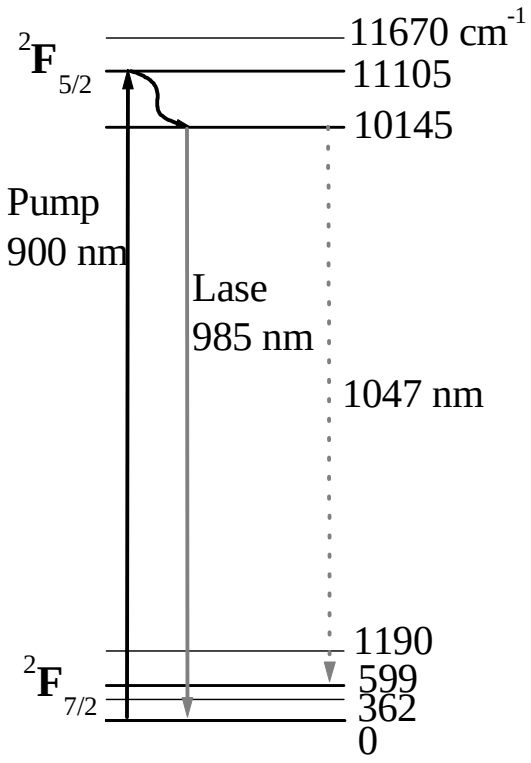

Fig. 1 Energy level diagram of Yb^{3+} in S-FAP

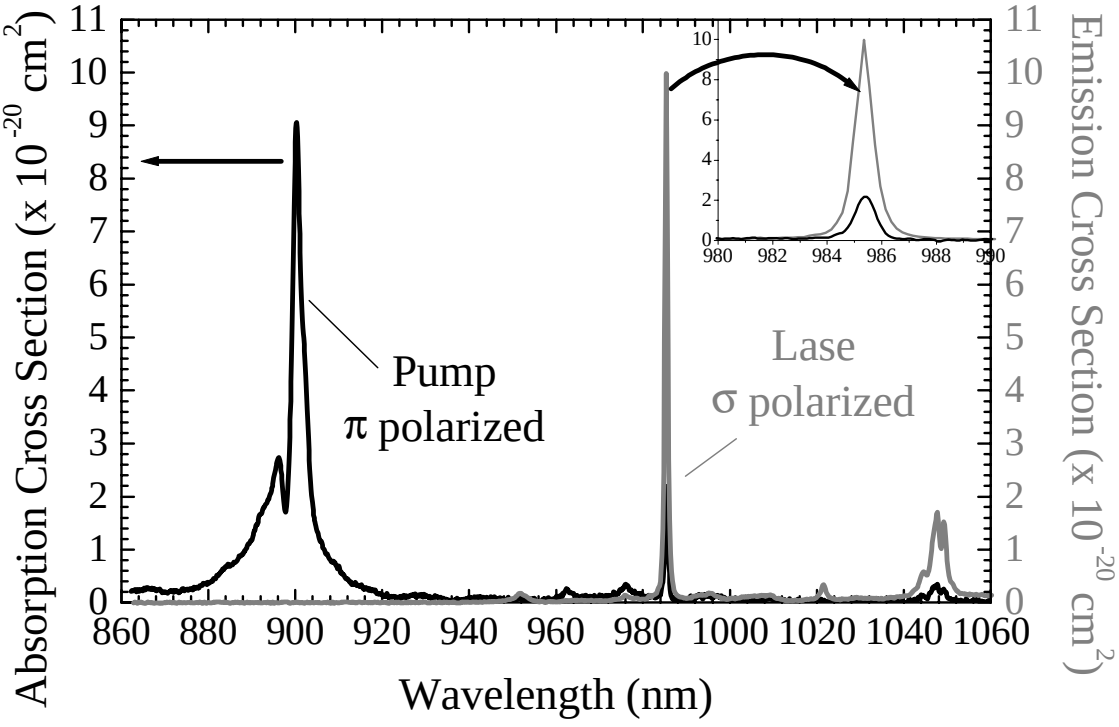

Fig. 2 Polarized absorption and emission cross-sections for Yb^{3+}:S-FAP.

II. Quasi-CW laser operation

The sample was end pumped in a hemispherical near-concentric cavity design (Fig. 3) with a flash-lamp-pumped Cr:LiSAF laser operated at 900 nm with a temporal pulse width of 200 μs. The flat-top spatial profile of the pump laser was focused to a spot size of 600 μm at the center of the crystal, with a maximum incident energy of 350 mJ, or a maximum fluence in the crystal of 124 J/cm^2. The pump power threshold was estimated by use of[8]

$$P_{th} = \frac{\pi h\nu_0(\varpi_0^2 + \varpi_P^2)}{2f_b\eta_0\tau_{em}(1-\exp(-N_0\sigma_{abs}L))}\left(\frac{L_d + T}{2\sigma_{em}} + f_a N_0 L\right), \quad (1)$$

The threshold power was then converted to threshold energy for pulse operation by use of[9]:

$$E_{th} = \frac{P_{th}\tau_P}{1-\exp(-\tau_p/\tau_{em})}, \quad (2)$$

where ν_p (3.33×10^{14} s^{-1}) is the pump laser frequency, ω_0 (3.2×10^{-2} cm) is the cavity mode size, ω_p (3.2×10^{-2} cm) is the pump spot size, L_d (0.02) is the double-pass loss, T (0.162) is the transmission loss due to output coupling, f_a (0.808) is the Boltzmann fraction in the ground state of the ground state manifold, N_0 (1.80×10^{19} cm^{-3}) is the number density, L (1.00 cm) is the crystal length, f_b (0.989) is the Boltzmann fraction with respect to the excited state manifold, η_p (1.00) is the pump quantum efficiency, τ_{em} (1.14 ms) is the emission lifetime, σ_{abs} (9.0×10^{-20} cm^2) is the absorption cross section at the pump frequency, σ_{em} (10×10^{-20} cm^2) is the emission cross section at the laser wavelength, and τ_p (0.20 ms) is the temporal pump pulse width. Using Eqns. (1) and (2), we estimate the energy threshold to be approximately 15 mJ, which is well below our

maximum incident pump power and at a fluence of 6.7 J/cm^2 is also below damage threshold for 200-μs pulses.

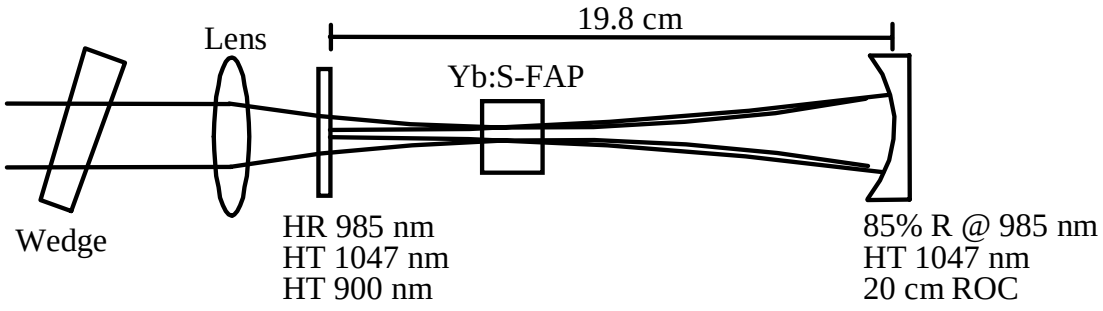

Fig. 3 Cavity design used for lasing at 985 nm. HR, high reflectivity; HT, high transmission; R, reflectivity; ROC, radius of curvature.

The cavity mirrors (Fig. 3), which were coated by Quality Thin Films, needed to be highly transmissive at 1047 nm to suppress oscillation at 1047 nm (where the threshold is only 2 mJ with the same parameters as the 985-nm laser). Upon alignment, lasing action with high mode quality was immediately observed. Verification of the wavelength was obtained with an optical spectrum analyzer (Ando Electric Co.), which indicated a peak wavelength of 984.7 nm. A Rigrod analysis[10] predicted an optimum output coupling of 18%. We observed a maximum slope efficiency of 74%, with a threshold of 16.6 mJ (Fig. 4) with our largest available output coupling of 16%.

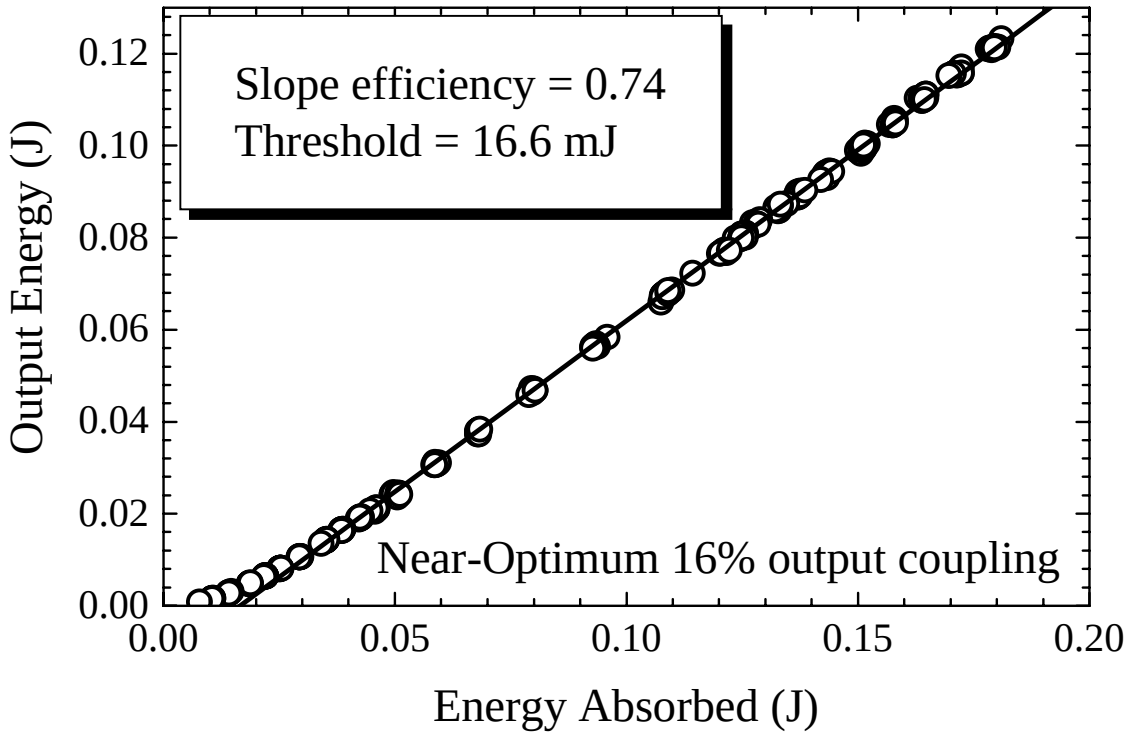

Fig. 4 Highest laser slope efficiency at 985 nm with a 16% output coupler.

By evaluating the slope efficiencies at two other output couplings, 5.7% and 0.86%, we can fit the losses as well as the intrinsic slope efficiency to the experimental points. Plotting the inverse of the slope efficiency versus the inverse of the output coupler transmission, also known as a Caird plot[11], we find that the losses are given by

$$\frac{1}{\eta} = \frac{1}{\eta_0} + \left(\frac{L_d}{\eta_0}\right)\frac{1}{T_{OC}}, \tag{3}$$

where η is the measured slope efficiency, η_0 is the intrinsic slope efficiency, L_d are the double pass losses, and T_{OC} is the transmission of the output coupler. The Caird plot is shown in Fig. 5, in which the double pass losses are shown to be 0.027% (0.017 cm^{-1}) and the intrinsic slope efficiency is shown to be 88%, which is nearly equal to the quantum-defect-limited efficiency of η_d = 91%.

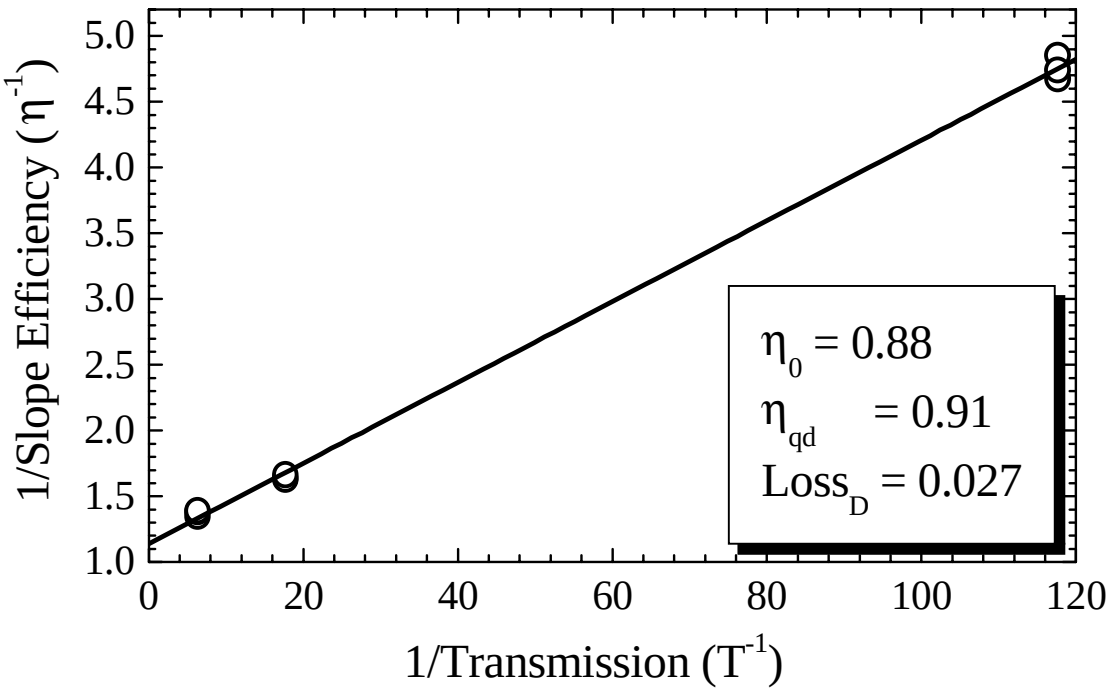

Fig. 5 Caird plot of the inverse slope efficiency versus inverse output coupling, showing the intrinsic slope efficiency close to the quantum defect.

III. Q-Switched Laser Operation

A modified version of the cw laser cavity (Fig. 6) employed a thin film polarizer (CVI Laser Corp.) and an electro-optic (E-O) modulator (Quantum Technology, Inc.) as a Q-switch. The surfaces of the S-FAP sample were antireflection coated to avoid premature oscillation from the uncoated S-FAP surfaces. Note that the E-O Q-switch is not in the best location in the cavity since the mode passing through the modulator is divergent. Rather its position was chosen to avoid passing pump light through the modulator. Fig 6 is not the optimal cavity design, however it is the simplest (requiring the fewest cavity elements) in light of the rather poor spatial beam quality of the pump laser. This cavity also allows large changes in the mode passing through the crystal with very small changes in the cavity. As the cavity length approaches 20 cm (neglecting optical path

length increase caused by intracavity optical elements) the mode passing through the crystal diverges.

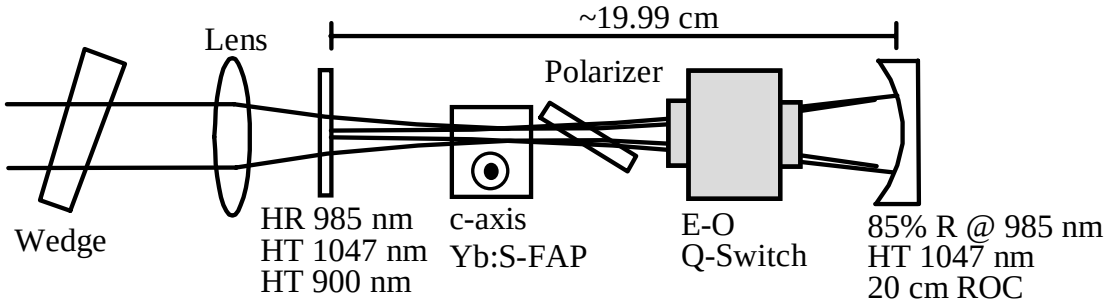

Fig. 6 Design of the Q-switched cavity. E-O, electro-optic.

Since this cavity will only output a single Q-switched pulse for every pump pulse, the maximum Q-switch energy will optimize for larger mode size. However, since the pump power is limited, the degree of inversion decreases with increasing mode size which will decrease the output Q-switched energy. Therefore, the maximum Q-switch energy will optimize for a specific mode size. To find the optimum mode size, a computer code was used to model the q-switched output energy from first principles (see Appendix IVa). The pump absorption and the resulting inversion were modeled as a two-level system with rate equations for the ground and the excited states, where pumping into the upper band is assumed to thermalize instantaneously within the excited state according to:

$$\frac{dN_{gnd}(z,t)}{dt} = -\frac{dN_{ex}(z,t)}{dt},$$

$$= \frac{-\sigma_{abs}(\omega_p)N_{gnd}(z,t)I_p(z,t)}{\hbar\omega_p} + \frac{N_{ex}(z,t)}{\tau}, \quad (4)$$

$$\frac{dI_p(z,t)}{dz} = -\sigma_{abs}(\omega_p)N_{gnd}(z,t)I_p(z,t), \quad (5)$$

where N_{gnd} is the ground state population, N_{ex} is the excited state population, ω_p is the pump frequency, σ_{abs} is the absorption cross section, I_p is the pump intensity, and τ is the emission lifetime. Note that the emission cross section at the pump wavelength has been omitted since the upper and lower levels are assumed to thermalize instantaneously (the lowest level of the excited state manifold has a Boltzmann population = 0.99)[2,6]. Using the code to model eqns. 4 and 5, the S-FAP sample was divided into discrete spatial slices and the pump pulse into temporal intervals, and these temporal slices were propagated consecutively through the spatial slices. The new population values in each spatial slice were stored as dummy variables to be used as the new input populations for the next temporal slice. In this way, the steady-state solutions for short times and spatial distances can be used to build up the temporally and spatially transient excited state population solution to eqn. 4. We can then use the initial inversion to predict the Q-switched extraction, following[12]

$$\Delta n_f = \Delta n_i \exp((\Delta n_f - \Delta n_i)/\Delta n_{th}), \tag{6}$$

$$E_{out} = \frac{(\Delta n_i - \Delta n_f) A_{Pump} l_s h\nu_L \ln(R)}{(f_a^e + f_b^e)\ln(T^2 R)},\ \Delta n_i > \frac{-\ln(T^2 R)}{2\sigma_{em} l_s}, \tag{7}$$

where Δn_f is the inversion after extraction, Δn_i is the inversion after pumping, Δn_{th} is the threshold inversion, A_{Pump} is the pump mode area, l_s is the gain medium length, ν_L is the laser frequency, R is the output coupler reflectivity, T is the one way cavity transmission, σ_{em} is the laser emission cross section, and f_b^e and f_a^e are the initial and final Stark level Boltzmann occupation factors, respectively, of the laser transition. We solve transcendental eqn. 6 to obtain Δn_f, which can then be used with Eqn. 7 to obtain Q-switched output energy. By inputting the maximum possible pump energy available and

varying the pumped spot size, the optimal output energy versus pump mode size was found (shown in Fig. 7). Clearly, the choice of mode size has a large effect on the output energy. The resulting output energy versus absorbed energy as shown in Fig. 8, where a small spot size (where the inversion is maximal) gives small output energy, while the larger spot sizes (smaller inversion) gives the optimum output energy. This effect is caused largely by saturation of the inversion, which is a strong effect in Yb:S-FAP due to the low saturation fluence (2.8 J/cm^2). The observed roll over of the individual curves is caused by scatter loss and residual absorption.

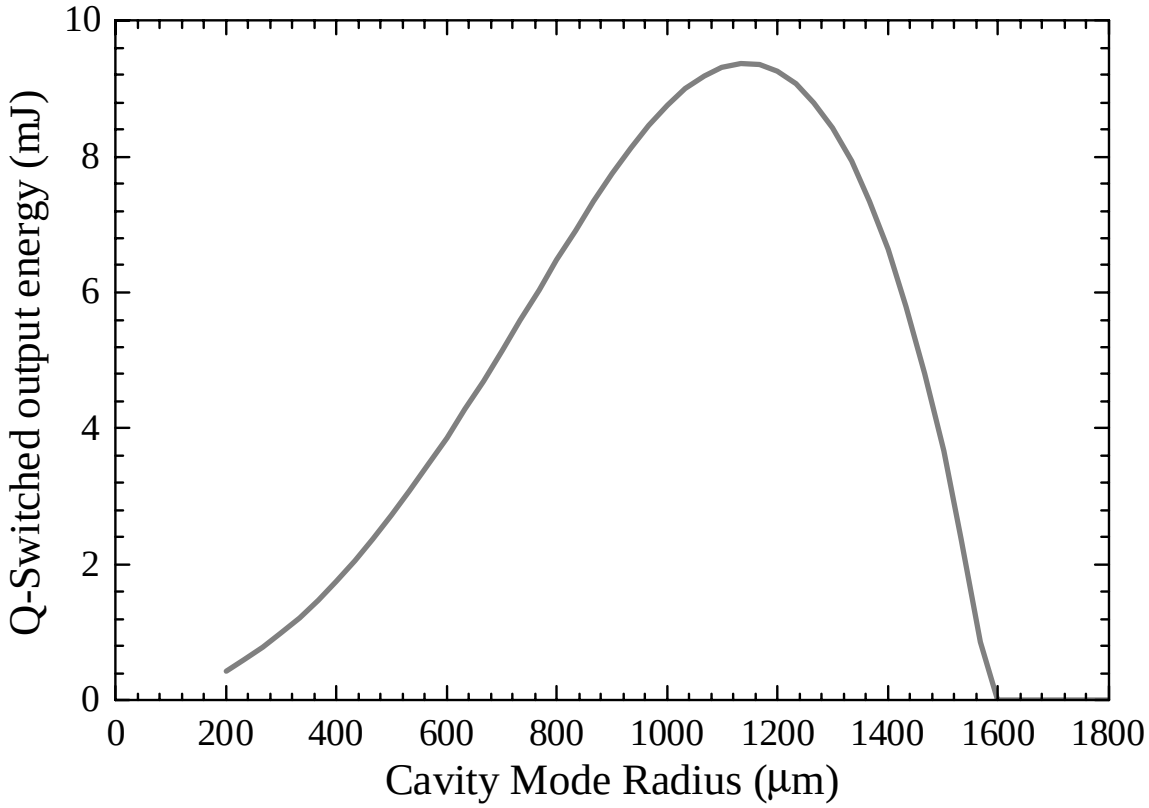

Fig. 7 Theory curve of Q-switched output energy for maximum pump energy (360 mJ incident) versus cavity mode radius showing optimum cavity mode size.

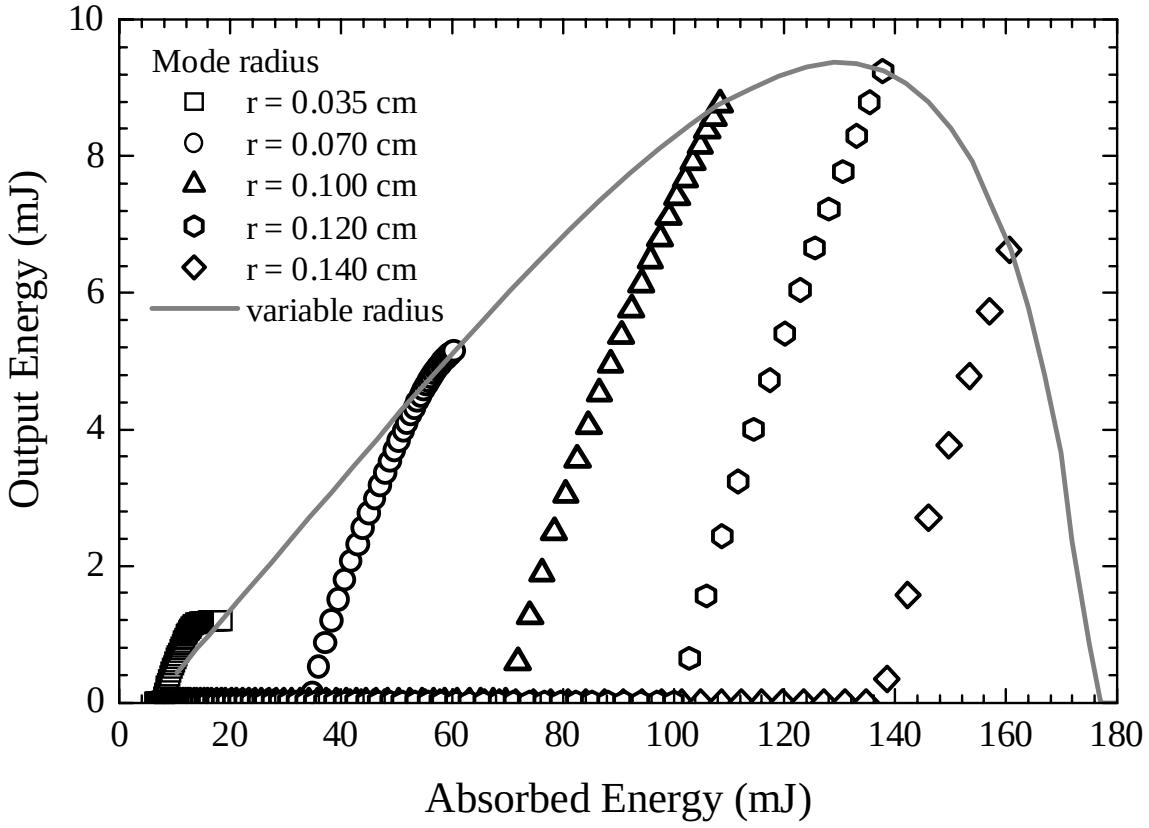

Fig. 8 Theory curves of Q-switched output energy versus absorbed pump energy for various fixed cavity mode radii, with Fig. 7 overlaid to show optimum.

Using the theoretical predictions in Fig. 7 and 8, the pump focusing and cavity length were adjusted such that the pump and cavity mode radii were 1000 μm. This optimized cavity produced Q-switched pulses with a maximum energy of 9.4 mJ and a pulsewidth of 9.4 ns. The slope efficiency was measured to be 21% with respect to absorbed power at a threshold of 75 mJ as shown in Fig. 9. The experimental points are shown as open circles, overlaid with a linear regression that is weighted by the high-output energy points, as well as a theoretical curve with no adjustable parameters (Appendix IVa).

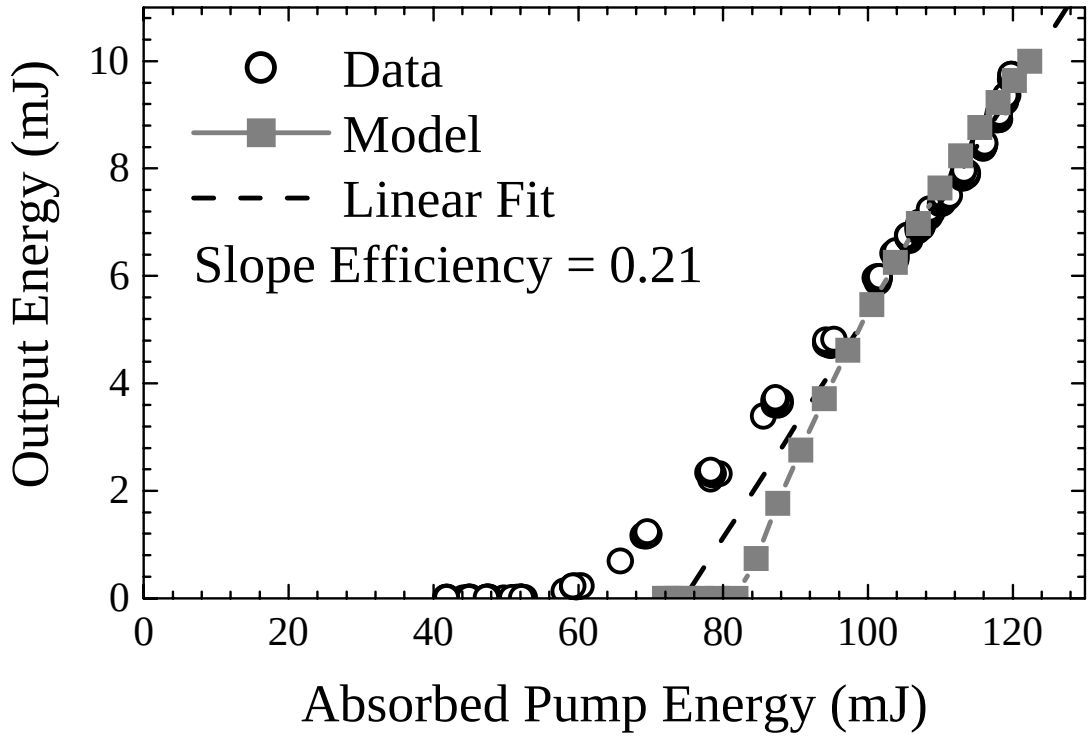

Fig. 9. Experimental and theoretical Q-switched slope efficiencies, showing nonlinear slope efficiency with a linear fit to high output as well as the theoretical model output.

The error between the model and the experimental data points near threshold appears to be due to the onset of different modes, since we increased the pumped mode volume to approximately 2 mm in diameter to allow greater energy extraction. This unstable behavior could also be induced by the non-uniform spatial profile of the pump laser. The Q-switched cavity losses are also much higher than in the cw cavity configuration. These additional losses can be attributed to two factors: passive losses from the polarizer and the Q-switch (approximately 14%), and only a single Q-switch pulse for every pump pulse. The intracavity passive losses could be decreased by using the polarizer in reflection mode and designing the cavity such that the E-O modulator was placed in a relatively collimated section of the intracavity mode. Another alternative would be to use an acousto-optic modulator as a Q-switch, which would allow us to take out the polarizer

altogether. The simplest system involves the use of a passive Q-switch, which could be as simple as a thin plate of saturable absorber material placed intracavity. However, both of these methods tend to produce Q-switched pulses with a much longer temporal pulsewidth. The low Q-switch rate acts as a loss since we must excite over half the ground state in order to reach inversion; which results in greater than 50% saturable loss, owing to the three-level nature of this system. One possible way of reducing the effect of this loss is to repetitively Q-switch for a single pump pulse (or cw pumping), where several pulses can be extracted within the emission lifetime of the excited state. It is then possible to share the saturable loss between the pulses and approach the slope efficiency of the quasi-cw cavity (further discussion available in Siegman[10]).

Another method for comparing the theory and experiment is to observe the pulse compression with increasing pump fluence. This mechanism can be easily understood when one considers two pump fluence cases: low pump fluence leading to low gain just above laser threshold, and high pump fluence leading to high gain which far exceeds laser threshold. The low gain (approximately 1) case will require the buildup of the Q-switched pulse from spontaneous emission to make many passes through the gain medium, which translates into long pulsewidth due to cavity roundtrip time. On the other hand, the high gain case leads to fast buildup and extraction, and translates into short temporal pulsewidths. The Q-switched pulsewidths were measured using a high speed silicon photodiode (Electro-Optics Technology, Inc.) and a digitizing oscilloscope. The experimental results are shown in Fig. 10 with a theory curve (Appendix IVb) having no adjustable parameters overlaid for comparison. Again, we find that the theory and experiment follow similar trends and agree at high pump fluence, while at low pump

fluence the curves diverge from on another. This divergence is caused by the same premature laser turn-on as observed in Fig. 9. The temporal pulsewidth diverges to infinity as the pump fluence drops below threshold. Fig. 11 shows the temporal profile of the fully compressed Q-switched pulse at 8.8 ns.

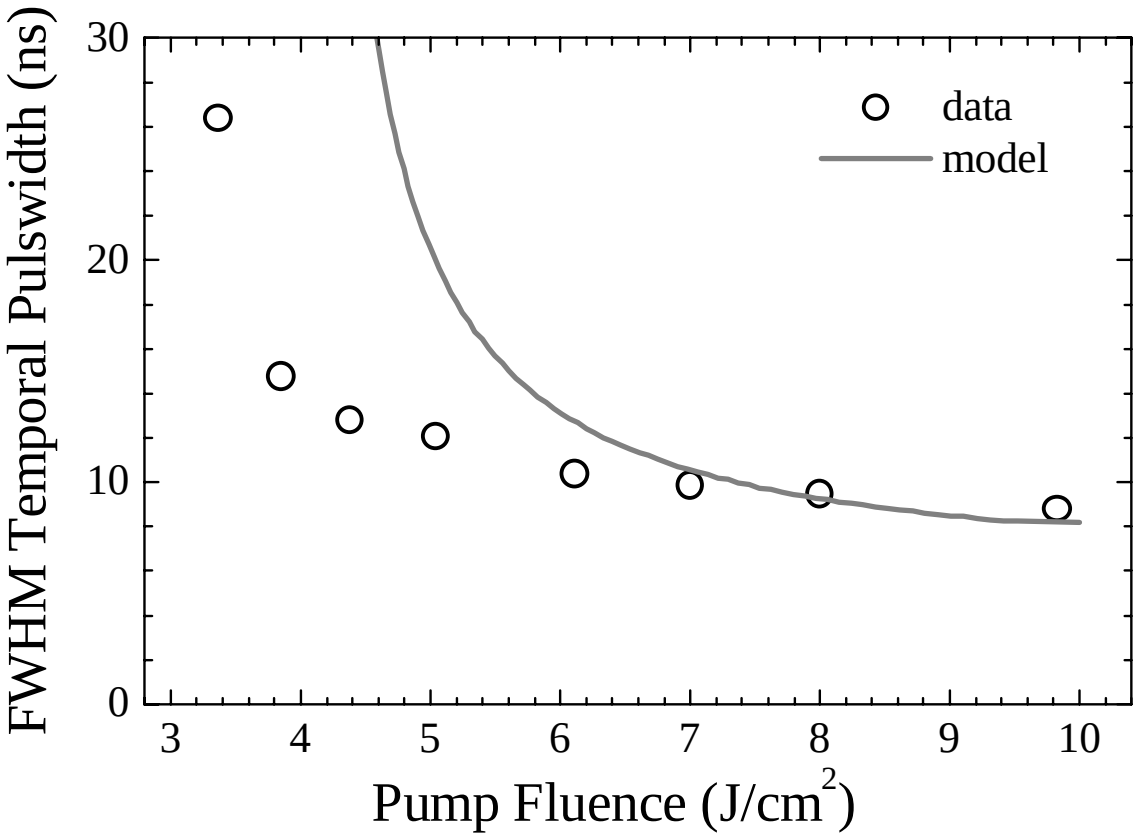

Fig. 10 The FWHM temporal pulsewidth versus pump fluence showing pulse compression with increasing stored gain.

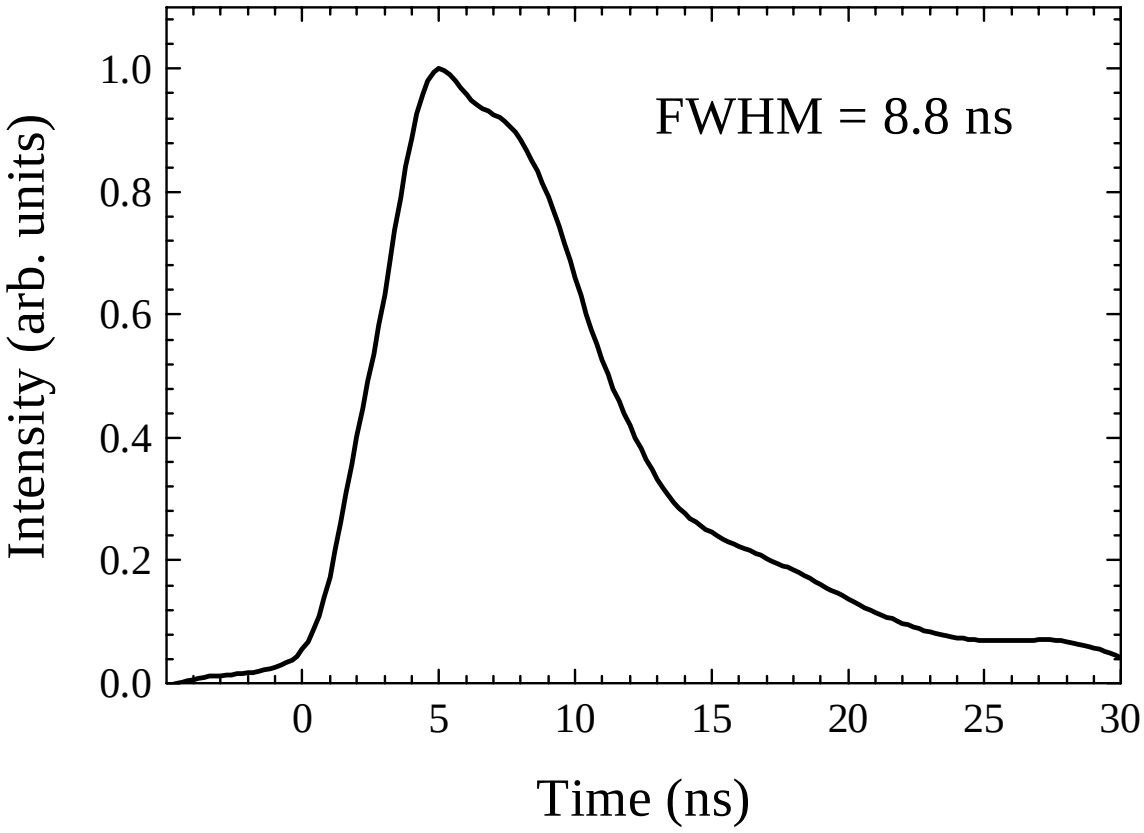

Fig. 11 The temporal profile of the 985 nm Q-switched pulse with maximum pump fluence.

One of the goals this project is to perform second harmonic conversion of the 985 nm beam. Efficient harmonic conversion requires high intensity and good beam quality. The beam quality factor[13] or M^2, of this oscillator was fitted to the variance versus distance from a beam waist,. as shown in Fig. 12, yielding $M_x^2 = 2.4$ and $M_y^2 = 2.8$. Where the M^2 Gaussian beam propagates according to

$$w_i(z) = w_0(z_0)\sqrt{1+\left(\frac{M^2\lambda(z-z_0)}{\pi w_0^2(z_0)}\right)^2} \tag{8}$$

where $w_i(z)$ is the beam size at position z, $w_0(z_0)$ is the waist size, M^2 is the beam quality factor, λ is the wavelength of propagation, and z_0 is the waist position.

The inset shows a gray-scale contour plot of the far-field beam profile -3.6 cm from the waist.

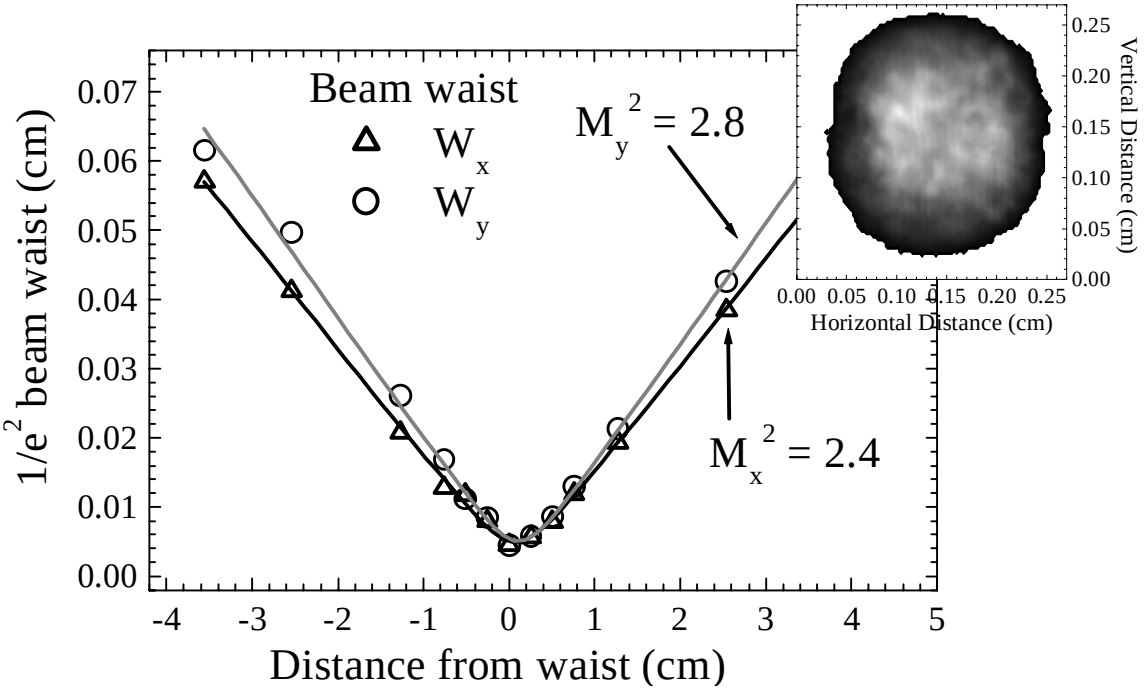

Fig. 12. M^2 analysis of the 985 nm Q-switched laser beam

IV. Summary

Yb:S-FAP has been successfully lased and Q-switched on the three level transition at 985 nm. The measured quasi-cw laser efficiencies are a maximum of 74% with a 16% output coupler and a Caird plot shows the intrinsic efficiency to be 88% near the quantum defect limit of 91%. As a Q-switched laser, the three level nature impacts the slope efficiency, which drops to 21%. The maximum Q-switched energy was measured to be 9.8 mJ in a 8.8 ns FWHM temporal pulse with an average M^2 of 2.6.

Chapter 6b. NONLINEAR FREQUENCY CONVERSION OF A YB:S-FAP LASER AT 985 NM

First published as: *A.J. Bayramian, C. Bibeau, C.A. Ebbers, C.D. Marshall, S.A. Payne, and W.F. Krupke, "Q-Switched Yb^{3+}:$Sr_5(PO_4)_3F$ three-level laser operation at 985 nm and efficient doubling at 492.5 nm," CLEO 2000 Technical Digest, CMD4, pp. 17-18.*

I. Introduction

The results of Chapter 6a show ytterbium doped $Sr_5(PO_4)_3F$ provides an efficient diode-pumped high power solid-state medium for generation of 985 nm laser light. Although the 985 nm laser is useful and efficient, perhaps more important are the doubled and tripled frequencies of this laser wavelength at 492 nm and 328 nm, respectively. Most blue-green and ultraviolet lasers are generally inefficient systems that use flashlamps. Typical non-solid-state systems, such as dye lasers, use poisonous laser dyes (which require another laser as a pump source) or bulky gas laser sources making them awkward and hazardous. The nonlinear medium used for second harmonic conversion is a relatively new material, namely yttrium calcium oxyborate, $YCa_4O(BO_3)_3$ (YCOB). This material was chosen for its relatively high effective nonlinear coefficient, d_{eff} = 1.14 pm/V (almost 3 times larger than KDP's d_{eff} = 0.384), and chemical stability[1]. We report the second harmonic conversion of 985 nm to 492.5 nm using YCOB, with a maximum efficiency of 32%. Peak output energies of 2 mJ in an 8 ns temporal pulsewidth were achieved at 492.5 nm.

II. Second Harmonic Conversion Modeling

Second harmonic conversion is based on materials which have a nonzero second order nonlinear susceptibility, $\chi^{(2)}$, which couples the square of the electric field at the fundamental frequency with a polarization at the second harmonic and drives the second

harmonic signal. Using Maxwell's equations, this process can be solved using coupled fundamental and second-harmonic waves propagating in the nonlinear medium. The solution is given by[2,3]:

$$\frac{P_{2\omega}}{P_{\omega}} = \tanh^2\left[\left(\frac{2\pi^2 d_{eff}^2 L^2 P_{\omega}}{\varepsilon_0 c n_{\omega}^2 n_{2\omega} \lambda_{2\omega}^2 A}\right)^{1/2} \frac{\sin(|\Delta k| L/2)}{(|\Delta k| L/2)}\right], \tag{1}$$

where $P_{2\omega}$ [W/m^2] is the second harmonic power, P_{ω} [W/m^2] is the fundamental power, d_{eff} [pm/V] is the effective nonlinear coefficient, L is the length of nonlinear medium [m], ε_0 is the permittivity of free space [8.854 $\times$ 10^{-12} C/Vm], c is the speed of light in vacuum [3.0 $\times$ 10^8 cm/s], n_{ω} is the fundamental index of refraction, $n_{2\omega}$ is the second harmonic index of refraction, $\lambda_{2\omega}$ is the second harmonic wavelength, A is the plane-wave beam area, and Δk is the phase mismatch, which for type I phase matching given by:

$$\Delta k = k_{\omega} + k_{\omega} - k_{2\omega} = \frac{4\pi}{\lambda_{\omega}}(n_{2\omega} - n_{\omega}) \tag{2}$$

where λ_{ω} is the fundamental wavelength. Eqn. 1 can be simplified for low conversion efficiencies or non-depleted pump to give[3]:

$$\frac{P_{2\omega}}{P_{\omega}} = \left(\frac{2\pi^2 d_{eff}^2 L^2 P_{\omega}}{\varepsilon_0 c n_{\omega}^2 n_{2\omega} \lambda_{2\omega}^2 A}\right) \frac{\sin^2(|\Delta k| L/2)}{(|\Delta k| L/2)^2} \tag{3}$$

Using eqn. 1 or 3, the output power or conversion efficiency can be calculated as a function of fundamental power incident on the nonlinear medium. The assumption for both equations is that the fundamental and harmonic light is composed of plane waves that have no temporal structure.

For these experiments, the incident beam will be pulsed and quasi-Gaussian. Therefore, the instantaneous power and intensity will vary for different spatial and temporal portions of the beam. Another complexity arises in that the beam must be focused into the crystal to enhance the fundamental intensity and optimize conversion efficiency. This results in a change in the Gaussian width as a function of position through the nonlinear medium. To properly model these effects a compute code was written (see Appendix V) which discretizes the Gaussian beam into a set of concentric shells of constant amplitude and slices the temporal profile into intervals with constant amplitude. In addition, the medium itself is discretized into a set of spatial slices that interact with a fixed-intensity temporal-spatial laser slices. Using these approximations, the intensity is constant over one slice of a temporal and spatial shell, and Eqn. 1 can be used to calculate the generated second harmonic energy. Summing the second harmonic energy from all shell-temporal-spatial slices gives the total second harmonic energy generated as well as the conversion efficiency for a pulsed Gaussian fundamental focussed through a nonlinear medium.

There are two additional issues that must be considered for a focussed Gaussian beam: phase mismatch, and beam walk-off. In general nonlinear crystals are oriented such that phase matching occurs, $\Delta k = 0$, so that maximum conversion occurs at a given input power. Phase matching typically occurs only at one angle of propagation through the crystal. The focussed Gaussian beam creates a complex k-distribution since not all light rays entering the nonlinear medium propagate in the same direction, which results in imperfect phase matching and decreased conversion efficiency for some portion of the beam. Beam walk-off occurs when the propagation direction of the fundamental or

harmonic beams do not propagate along a dielectric axis, causing double refraction. This means that the Poynting vector, the direction of power flow, and the wavevector are not collinear, but occur at a small angle. This walk-off angle has the effect of limiting the length over which conversion occurs, thereby effecting the conversion efficiency. The effect of the walkoff angle can be expressed as a reduction in the d_{eff}[4]:

$$d_{eff}^{2'} = \frac{d_{eff}^2}{1 + L\rho/\left(\omega_0\sqrt{\pi}\right)} \tag{4}$$

where ρ is the walk-off angle, and ω_0 is the beam waist size. The walk-off angle is given by[5] $\cos(\rho) = \cos(\rho_{2\omega})\cos(\rho_{\omega})$, where ρ_i are given by:

$$\tan(\rho) = n^2\left[\left(\frac{s_x}{n^{-2} - n_x^{-2}}\right)^2 + \left(\frac{s_y}{n^{-2} - n_y^{-2}}\right)^2 + \left(\frac{s_z}{n^{-2} - n_z^{-2}}\right)^2\right]^{-1/2}, \tag{5}$$

where n is the index along the phase matching direction, s_i are the unit vector components of the propagation direction vector **s**, and n_i are the indices of refraction along the dielectric axis. An initial fit was performed using eqns. 1 and 4 and setting $\Delta k = 0$ to model the experimental results.

III. Second Harmonic Conversion Experiments

The second harmonic conversion material $YCa_4O(BO_3)_3$ (YCOB), was grown by Czochralski method at approximately 1510°C[1] producing a clear boule with cracking at its base due to thermal stresses induced during growth and cooling. This biaxial crystal belongs to the space group C_m, which in turn belongs to the monoclinic system. The unit cell constants were found to be a = 8.046 Å, b = 15.959 Å, c = 3.517 Å, and β = 101.19°. The Sellmeier equations governing the dispersion of YCOB were found by Iwai[1] to be

$$n_x^2 = 2.81697 + \frac{0.022418}{\lambda^2 - 0.0149216} - 7.73709\times10^{-5}\cdot\lambda^2, \quad (6)$$

$$n_y^2 = 2.91924 + \frac{0.0252847}{\lambda^2 - 0.0130221} - 6.44657\times10^{-5}\cdot\lambda^2, \quad (7)$$

$$n_z^2 = 2.95452 + \frac{0.025835}{\lambda^2 - 0.0125276} - 7.64814\times10^{-5}\cdot\lambda^2, \quad (8)$$

where λ is the wavelength in microns. The boules are grown such that n_y lies along the length of the boule. This orientation allows for phase matching for a variety of wavelengths by propagation through the x-z plane of the boule. A slice of the boule was cut and oriented for type 1 phase matching of 985 nm doubling to 492.5 nm at 27° with respect to the n_z axis in the x-z plane to produce a crystal 5 x 5 x 16 mm as shown in Fig. 1.

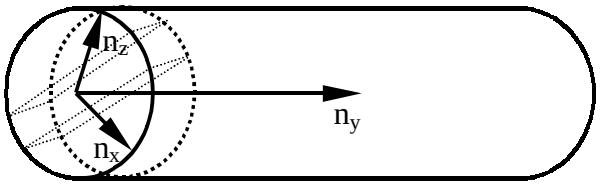

Fig. 1 Geometry of boule with respect to index ellipsoid and dashed lines showing cut of crystal for phase matching.

Since this demonstration is in part a proof of principle, the crystal was left uncoated and the second harmonic conversion was performed external to the 985 nm Q-switched cavity as shown in Fig. 2.

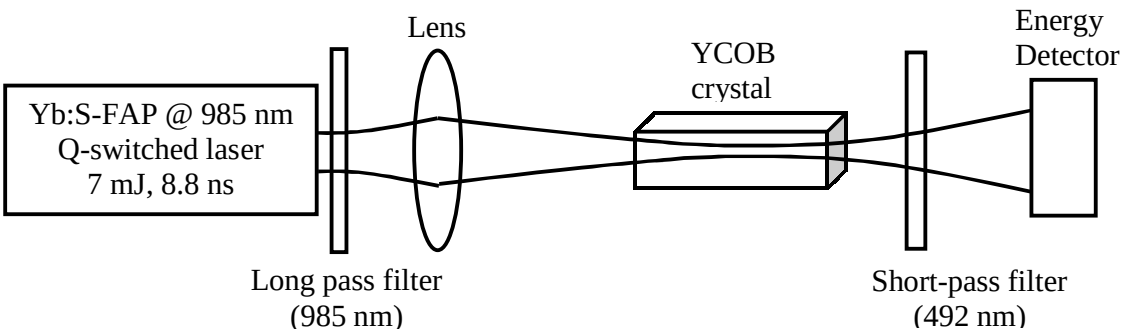

Fig. 2 Experimental arrangement for second harmonic generation measurements.

To achieve maximum conversion efficiency, the YCOB crystal was placed on a tilt and skew axis mount to allow fine-tuning of the phase matching direction. The focal length and focal spot position in the YCOB sample were adjusted to produce a maximum in the 492.5 nm harmonic energy. The harmonic wavelength was verified using an optical spectrum analyzer (Ando Electric Co.), which indicated a peak wavelength of 492.46 nm. The temporal pulsewidth of the 492.5 nm beam is shown in Fig. 3, where the 985 nm pulsewidth has been overlaid for comparison to show the decreased pulsewidth due to the nonlinear conversion with laser intensity. The harmonic conversion efficiency to 492 nm was measured as a function 985 nm input and the results are plotted in Fig. 4. The conversion efficiency was modeled using Eqn.1 and Eqn. 4 using the parameters given in Table 1. Clearly, the model does not fit the data as the fundamental 985 nm energy is increased. This can be traced back to our assumption that $\Delta k = 0$ for a conversion experiment using focused Gaussian beams. For $\Delta k \neq 0$, the harmonic light actually back-converts to the fundamental as the fundamental power is increased[6]. Using a computer code[7] that models plane wave propagation in nonlinear media from first principals, the harmonic conversion efficiency could be modeled with a variety of Δk's as a function of fundamental intensity. The output of these calculations could then be incorporated into

the Gaussian shell code to give conversion efficiency for focused Gaussian beams with an effective (averaged) Δk for the whole beam. The results of this effort are plotted in Fig.4 as the gray curve, where the effective phase mismatch, Δk_{ave}, for the whole beam has been empirically found to be 4.4 cm^{-1}, which is a reasonable value considering the far field beam angle would give a Δk value of 19.4 cm^{-1}. Fig.4 clearly shows the importance of backconversion when fitting experimental results of harmonic conversion of focussed high- intensity Gaussian beams.

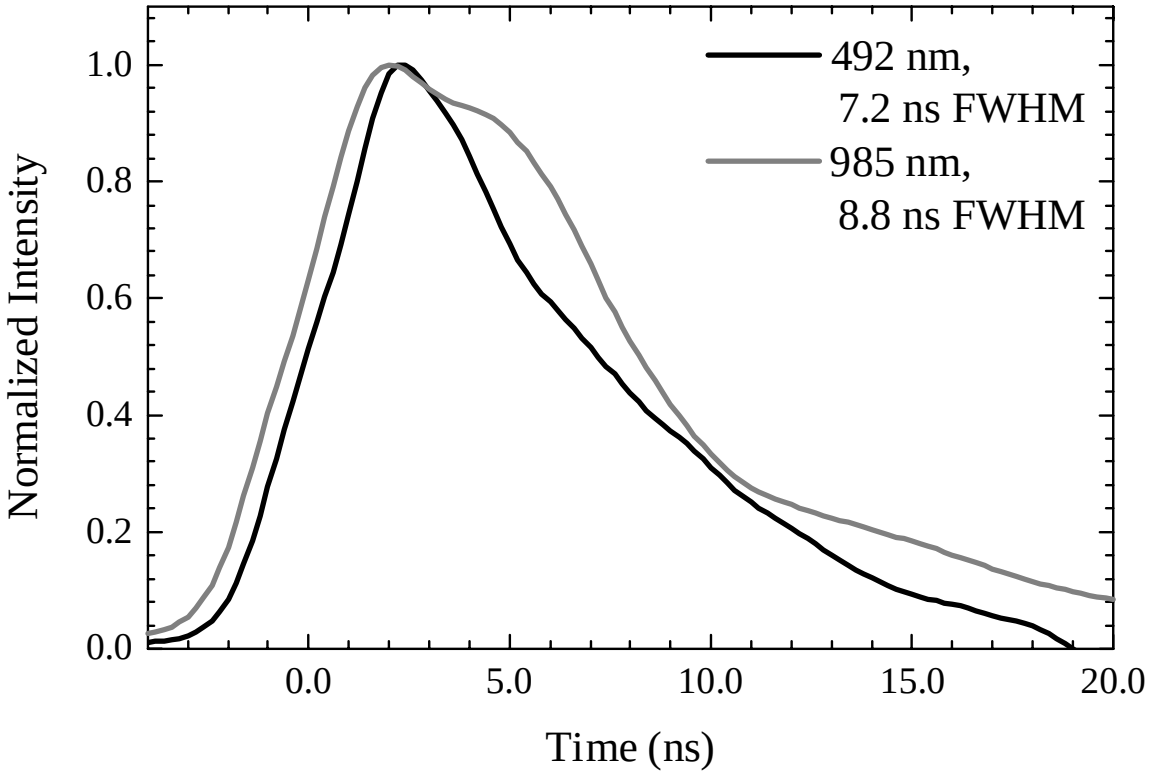

Fig. 3. Temporal profile of 492 nm harmonic and 985 nm fundamental beams showing temporal compression due to intensity driven conversion efficiency.

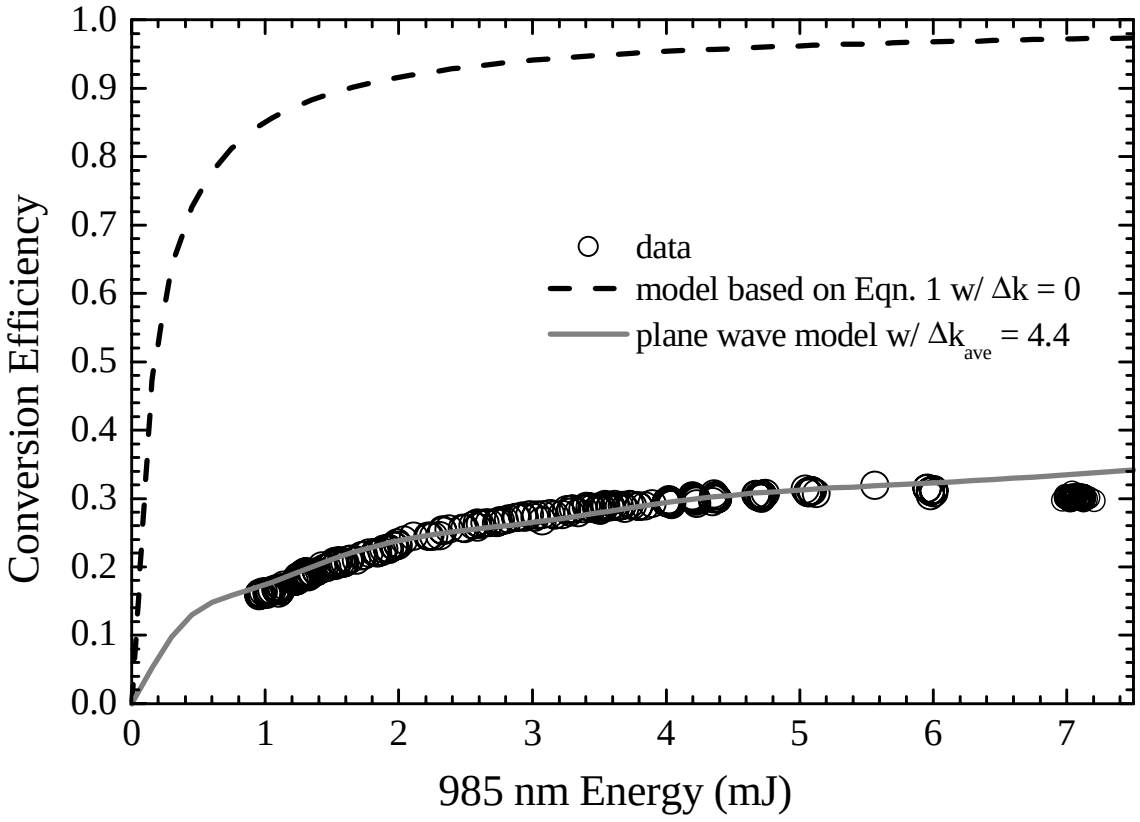

Fig. 4 Second harmonic conversion efficiency to 492.5 nm as a function of input fundamental energy at 985 nm, with model fit.

Table 1 Modeling parameters

Parameter	Value
Fundamental wavelength, λ_ω (nm)	**985**
Second Harmonic wavelength, $\lambda_{2\omega}$ (nm)	**492.5**
Fundamental index of refraction, n_ω	**1.71627**
Second harmonic index of refraction, $n_{2\omega}$	**1.71627**
Length of nonlinear medium, L (cm)	**2.66**
Effective nonlinear coefficient[8], d_{eff} (pm/V)	**1.14**
X waist radius ($1/e^2$), ω_{0x} (μm)	**58**
Y waist radius ($1/e^2$), ω_{0y} (μm)	**73**
Waist position, z_0 (cm)	**1.33**
Maximum input energy (mJ)	**7.5**
Walk-off angle, ρ (degrees)	**1.16**

IV. Summary

Efficient second harmonic conversion was successfully demonstrated in YCOB using type 1 phase matching and the 985 nm Q-switched laser described in Ch. 6 as the pump source. A maximum conversion efficiency of 32% was measured giving more than 2 mJ of 492.5 nm energy. The harmonic conversion process using pulsed, focusing Gaussian beams was successfully modeled with only one adjustable parameter and matches well with the experimental results.

SUMMARY

The experiments performed in this thesis provide a better understanding of ytterbium in the fluorapatite host and how this material performs in laser oscillators and amplifiers. The host lattice of Yb:S-FAP was modified by the addition of barium, which enhanced the absorption and emission bandwidths through homogenous broadening. Basic spectroscopy was performed on these crystals which showed absorption cross sections as high as 9×10^{-20} cm^2, emission cross sections as high as 6.2×10^{-20} cm^2 and radiative lifetimes as long as 1.14 ms. Crystals of $Yb^{3+}:Sr_{5-x}Ba_x(PO_4)_3F$ where $x < 1$ showed essentially homogeneous lines offering 8.4 nm (1.8 times enhancement) of absorption bandwidth and 6.9 nm (1.4 times enhancement) of emission bandwidth. The homogeneity of the lines was probed spectroscopically, as well as through oscillator experiments which showed efficient pumping and extraction with intrinsic slope efficiencies within 5% of the S-FAP intrinsic slope efficiency (81%). The gain saturation fluence of ytterbium doped $Sr_5(PO_4)_3F$ (S-FAP) was experimentally verified to be 3.2 J/cm^2 using a high fluence Q-switched probe pulse. This measurement allows accurate modeling of gain and output energy of laser amplifier systems such as the Mercury laser.

In an effort to improve the size and optical homogeneity of Yb:S-FAP crystals for the Mercury laser system, recent growths have shown the absence of nearly all defects (cracking, cloudiness, bubble core, slip dislocations, and anomalous absorption). Interferometry and power spectral density plots of transmission through S-FAP crystals have confirmed the ability to grow crystals suitable for propagation with low beam distortion. Optical bonding of smaller crystals to make composite larger ones was successfully demonstrated to the point where the bond is not even visible on an

interferogram. The stress optic coefficients needed for proper modeling of thermally loaded Yb:S-FAP crystals were also measured yielding $q_{33} = 0.308 \times 10^{-20}$ Pa^{-1}, and $q_{31} = 0.936 \times 10^{-20}$ Pa^{-1}.

Nonlinear losses were addressed by first examining stimulated Raman scattering (SRS), where the SRS gain coefficient was measured to be 1.3 cm/GW, which allows modeling of SRS losses in S-FAP lasers and amplifiers. The use of laser bandwidth and surface tilt to reduce Fresnel reflections were found to be effective methods of reducing SRS loss. In the absence of physical parameters necessary for an accurate quantitative evaluation of stimulated Brillouin scattering (SBS) losses, simple, order of magnitude estimates were made with known materials and the use of bandwidth as applied to the SRS losses found to be more than sufficient to suppress SBS.

Finally, ytterbium doped $Sr_5(PO_4)_3F$ was successfully lased on its three-level transition at 985 nm with a slope efficiency of 74% and then Q-switched with a slope efficiency of 21% to give a maximum output energy of 9.8 mJ in an 8.8 ns temporal pulse. Using a $YCa_4O(BO_3)_3$ crystal, the 985 nm Q-switched pulses were frequency doubled to 492 nm with a maximum conversion efficiency of 32% giving an output energy of 2 mJ. These results indicate that an efficient, diode pumped, all solid-state laser at 492 nm is possible.

There are several experiments in this thesis whose results would be enhanced by additional research. Of course the most important experiment is the operation of the Mercury laser which incorporates S-FAP as its amplifying medium. Validation of the SRS modeling on the Mercury laser system would not only verify the gain coefficient measurement, but also the validity and effect of Fresnel reflections in SRS loss buildup and countermeasures towards SRS loss suppression. Further measurement of S-FAP's

stress-optic and photoelastic coefficients would allow thorough modeling of thermal loading of S-FAP in all geometries as well as allow accurate modeling of SBS. Experimental measurement of SBS on the Mercury beam line could then confirm the SBS models. The Q-switched 985 nm laser could be greatly improved with the use of a passive Q-Switch, such as Cr:YAG, and CW (or quasi-CW) diode pumping. This would allow greatly improved efficiencies, simpler cavities, and much higher repetition rates. Improved beam quality from such a system would in turn allow more efficient doubling. Tripling of this system to 328 nm would make for a great diode pumped UV laser system, with efficiencies possibly much higher than existing Nd:YAG systems.

REFERENCES

Chapter 1

[1] H.W. Etzel, H.W. Gandy, and R.J. Ginther, *Appl. Opt.* **1**, 534 (1962).
[2] L.F. Johnson, J.E. Geusic, and L.G. Van Uitert, Appl. Phys. Lett. **7**, 127 (1965).
[3] A.R. Reinberg, L.A. Riseberg, R.M. Brown, R.W. Wacker, and W.C. Holton, *Appl. Phys. Lett.* **19**, 11 (1971).
[4] W.F. Krupke, and L.L.Chase, *SPIE* **1040**, 68 (1989).
[5] P. Lacovara, H.K. Choi, C.A. Wang, R.L. Aggarwal, and T.Y. Fan, *Opt. Lett.* **16**, 1089-1091 (1991).
[6] A.A. Kaplyanskii and E.G. Kuzminov, *Opt. Spect.* **29**(4), 376-381, 1970.
[7] T.Alekel, and D.A. Keszler, *Inor. Chem.*, **32**, 101-105, 1993.
[8] J.G. Fletcher, F.P. Glasser, and R.A. Howie, *Acta. Cryst.*, C**47**, 12-14, 1991.
[9] Roelandts, G.Y. Weber, and L. Quaglia,. *Nucl. Inst. Meth.*, **157**, 141-146, 1978.
[10] E.J. Oosthuyzen and A.J. Burger, *Earth Planet Sci. Lett.*, **18**, 29-36, 1973.
[11] R. Jayaprakash, V.V. Ratnam, and S.A. Durrani, *Nucl. Tracks,* **10**, 601-604, 1985.
[12] E. Bertel, *Phys. Rev. B*, **17**(12), 4544-4548, 1978.
[13] J.M. Powers, R.G. Craig, and K.C. Ludema, *Wear*, **23**, 209-224, 1973.
[14] M.C. Shea, Z.Li, and R.C. Bradt, *J. Appl. Phys.*, **75**, 7784-7787, 1994.
[15] S.V. Akimov, M.D. Volnyanskii, V.G. Monya, and E.F. Dudnik, *Sov. Phys. Tech. Phys.*, **49**, 1405-1406, 1979.
[16] T. Yano, Y. Nabeta, and A Watanabe, *Appl. Phys. Lett.*, **18**, 570-571, 1971.
[17] S.V. Dorozhkin, *Inorganic Materials*, **29**, 1187-1188, 1993.
[18] B.G. DeBoer, A. Sakthivel, J.R. Cagle, and R.A. Young, *Acta. Cryst.* , B**47**, 683-92, 1991.
[19] L.B. Moran, J.K. Berkowitz, and J.P. Yesinowski, *Phys. Rev. B.*, **45**, 5347-5360, 1992.
[20] R. Jayaprakash, and V.V. Ratnam, *Phys. Stat. Sol.*, **65**, 147-152, 1981.
[21] E.W.J.L. Oomen, W.M.A. Smit, and G. Blasse, *Mat. Chem. Phys.*, **19**, 357-368, 1988.
[22] R.C. Ropp, *J. Electrochem. Soc.*, **118**, 1510-1512, 1971.
[23] R. Jayaprakash, and V.V. Ratnam, *Phys. Stat. Sol.*, **61**, 259-264, 1980.
[24] P.R. Suitch, J.L. LaCout, A. Hewat, and R.A. Young, *Acta. Cryst.*, B**41**, 173-179, 1985.
[25] D. Lapraz, F. Guame, and M. Barland, *Phys. Stat. Sol.*, **89**, 249-253, 1985.
[26] M.A. Scott, B. Henderson, H.G. Gallagher, and T.P.J. Han, *J. Phys.: Cond. Matter*, **9**, 9893-9908, 1997.
[27] C.F. Chenot, A.F. Kasenga, and R.E. Pappalardo, *J. Lum.*, **24/25**, 95-98, 1981.
[28] V.V. Ratnam, R. Jayaprakash, and N.P. Daw, *J. Lum.*, **21**, 417-424, 1980.
[29] D. Lapraz, and A. Baumer, *Phys. Stat. Sol.*, **80**, 353-366, 1983.
[30] J.B. Gruber, C.A. Morrison, D.C. Harris, M.D. Seltzer, T.H. Allik, J.A. Hutchinson, and M.P. Scripsick, *J. Appl. Phys.*, **77**, 2116-2123, 1995.
[31] M. Tachihante, D. Zambon, A. Arbus, M. Zahir, A. Sadel, and J.C. Cousseins, *Mat. Res. Bull.*, **28**, 605-613, 1993.
[32] A.O Wright, M.D. Seltzer, J.B. Gruber, and B.H.T. Chai, *J. Appl. Phys.*, **78**, 2456-2467, 1995.
[33] M. Kottaisamy, R. Jagannathan, P. Jeyagopal, R.P. Rao, and R.L. Narayanan, *J. Phys D: Appl. Phys.*, **27**, 2210-2215, 1994.

[34] R. Jagannathan, and M. Kottaisamy, *J. Phys.:Cond. Matt.*, **7**, 8453-8466, 1995.
[35] J.B. Gruber, A.O. Wright, M.D. Seltzer, B. Zandi, L.D. Merkle, J.A. Hutchinson, C.A. Morrison, T.H. Allik, and B.H.T. Chai, *J. Appl. Phys*, **81**, 6585-6598, 1997.
[36] J.B. Gruber, M.D. Seltzer, M.E. Hills, T.H. Allik, J.A. Hutchinson, C.A. Morrison, and B.H.T. Chai, *Opt. Mat.*, **3**, 99-113, 1994.
[37] K. Spariosu, R.D. Stultz, M. Birnbaum, T.H. Allik, and J.A. Hutchinson, *Appl. Phys. Lett.*, **62**, 2763-2765, 1993.
[38] J.B. Gruber, B. Zandi, and L. Merkle, *J. Appl. Phys.*, **83**, 1009-1017, 1998.
[39] Caprez, P. Mikhail, C. Schwecke, and J. Hulliger, *J. Mat. Res.*, **12**, 3210-3213, 1997.
[40] A.O. Wright, M.D. Seltzer, J.B. Gruber, B. Zandis, L.D. Merkle, and B.H.T. Chai, *J. Phys. Chem. Solids*, **57**, 1337-1350, 1996.
[41] K.B. Steinbruegge, T. Henningsen, R.H. Hopkins, R. Mazelsky, N.T. Melamed, E.P. Riedel, and G.W. Roland, *Appl. Opt.*, **11**, 999-1012, 1972.
[42] R.H. Hopkins, and R.G. Seidensticker, *J. Crys. Growth*, **11**, 97-98, 1971.
[43] J.B. Gruber, B. Zandi, M.D. Seltzer, *J. Appl. Phys.*, **81**, 7506-7513, 1997.
[44] L.D. DeLoach, S.A. Payne, B.H.T. Chai, and G. Loutts, *Appl. Phys. Lett.*, **65**, 1208-1210, 1994.
[45] G.B. Loutts, C.Bonner, C. Meegoda, H. Ries, M.A. Noginov, N. Noginov, M. Curley, P. Ventkateswarlu, A. Rapaport, and M. Bass, *Appl. Phys. Lett.*, **71**, 1997.
[46] N. Faure, C. Borel, R. Templier, M. Couchaud, C. Calvat, and C.Wyon, *Opt. Mat.*, **6**, 293-303, 1996.
[47] J.B. Gruber, C.A. Morrison, M.D. Seltzer, A.O. Wright, M.P. Nadler, T.H. Allik, J.A. Hutchinson, and B.H.T. Chai, *J. Appl. Phys.*, **79**, 1746-1758, 1996.
[48] E.A. Tsvetkov, *Phys. Stat. Sol.*, **46**, 311-314, 1978.
[49] Z. Shao, Y. Chen, J.C. Bergquist, *Chinese Phys.*, **11**, 391-393, 1991.
[50] F.C. Cruz, B.C. Young, and J.C. Bergquist, *Appl. Opt.*, **37**, 7801-7804, 1998.
[51] X.X. Zhang, G.B. Loutts, M. Bass, and B.H.T. Chai, *Appl. Phys. Lett.*, **64**, 10-12, 1994.
[52] D.K. Sardar, and P.D. Bella, *Phys Rev. B*, **55**, 2859-2862, 1997.
[53] J.L. Dallas, *Appl. Opt.*, **33**, 6373-6376, 1994.
[54] M.A. Scott, H.G. Gallagher, T.P.J. Han, and B. Henderson, *Rad. Eff. Def. Solids*, **136**, 47-50, 1995.
[55] P. Hong, X.X. Zhang, R.E. Heale, H. Weidner, M. Bass, and B.H.T. Chai, *J. App. Phys.*, **77**, 294-300, 1995.
[56] R.E. Peale, P.L. Summers, H. Weidner, B.H.T. Chai, and C.A. Morrison, *J. Appl. Phys.*, **77**, 270-276, 1995.
[57] D. Shen, C. Wang, Z. Shao, X. Meng, and M. Jiang, *Appl. Opt.*, **35**, 2023-2025, 1996.
[58] D.L. Corker, B.H.T. Chai, J. Nicholls, and G.B. Loutts, *Acta. Crys.*, C**51**, 549-551,1995.
[59] X.X. Zhang, P. Hong, G.B. Loutts, J. Lefaucheur, M. Bass, and B.H.T. Chai, *Appl. Phys. Lett.*, **64**, 3205-3207, 1994.
[60] X.X. Zhang, M. Bass, B.H.T. Chai, P.J. Johnson, and J.C. Oles, *J. Appl. Phys.*, **80**, 1280-1286, 1996.
[61] S. Zhao, Q. Wang, X. Zhang, S. Wang, L. Zhou, L. Sun, and S. Zhang, *Appl. Opt.*, **36**, 7756-7759, 1997.
[62] Q. Wang, S. Zhao, X. Zhang, L. Sun, and S. Zhang, *Opt. Comm.*, **128**, 73-75, 1996.

[63] S. Zhao, Q. Wang, X. Zhang, S. Wang, L. Zhao, L. Sun, and S. Zhang, *Opt. Eng.*, **36**, 3107-3110, 1997.
[64] X. Zhang, S. Zhao, Q. Wang, L. Sun, S. Zhang, G. Yao, and Z. Zhang, *Opt. Comm.*, **155**, 55-60, 1998.
[65] S. Zhao, Q. Wang, X. Zhang, L. Sun, and S. Zhang, *Opt. Laser. Tech.*, **28**, 477-480, 1996.
[66] S. Zhao, Q. Wang, X. Zhang, S. Wang, L. Zhao, L. Sun, and S. Zhang, *Opt. Laser Tech.*, **29**, 207-209, 1997.
[67] H. Zhang, X. Meng, L. Zhu, C. Wang, P. Wang, Z. Yang, Y.T. Chow, and J. Dawes, *Jpn. J. Appl. Phys.*, **38**, 1510-1513, 1999.
[68] P.E. Mackie and R.A. Young, *J. Appl. Cryst.*, **6**, 26-31, 1973.
[69] M.E. Fleet, and Y. Pan, *Amer. Miner.*, **82**, 870-877, 1997.
[70] J.L. Ouweltjes, *Modern Materials*, Vol.**5** (Academic Press, New York, 1965), p.161
[71] L.D. DeLoach, S.A. Payne, L.L. Chase, L.K. Smith, W.L. Kway, and W.F. Krupke, *IEEE J. Quant. Elec.*, **29**, 1179-1191, 1993.
[72] R. Scheps, J.F. Myers, and S.A. Payne, *IEEE Phot. Lett.*, **5**, 1285-1288, 1993.
[73] S.A. Payne, L.K. Smith, L.D. DeLoach, W.L. Kway, J.B. Tassano, and W.F. Krupke, *IEEE J. Quant. Elec.*, **30**, 170-179, 1994.
[74] S.A. Payne, L.D. DeLoach, L.K. Smith, W.L. Kway, J.B. Tassano, W.F. Krupke, B.H.T. Chai, and G. Loutts, *J. Appl. Phys.*, **76**, 497-503, 1994.
[75] L.D. DeLoach, S.A. Payne, W.L. Kway, J.B. Tassano, S.N. Dixit, and W.F. Krupke, *J. Lum.*, **62**, 85-94, 1994
[76] L.D. DeLoach, S.A. Payne, L.K. Smith, W.L. Kway, and W.F. Krupke, *J. Opt. Soc. Am. B*, **11**, 269-276, 1994.
[77] C.D. Marshall, L.K. Smith, R.J. Beach, M.A. Emmanuel, K.I. Schaffers, J. Skidmore, S.A. Payne, and B.H.T. Chai, *IEEE J. Quant. Elec.*, **32**, 650-656, 1996.
[78] M.R. Dickinson, L.A.W. Gloster, N.W. Hopps, and T.A. King, *Opt. Comm.*, **132**, 275-278, 1996.
[79] S.A. Payne, R.J. Beach, C. Bibeau, C.A. Ebbers, M.A. Emmanuel, E.C. Honea, C.D. Marshall, R.H. Page, K.I. Schaffers, J.A. Skidmore, S.B. Sutton, and W.F. Krupke, *IEEE J. Sel. Top. Quant. Elec.*, **3**, 71-81, 1997.
[80] V.P. Orlovskii, B.M. Zhigarnovskii, G.V. Rodicheva, Y.M. Popov, N.M. Romanova, and V.F. Kharsika, *Inorg. Mat.*, **34**, 391-394, 1998.
[81] Bibeau, I.L. Bass, R.J. Beach, L.K. Smith, C.D. marshall, S.C. Mitchell, and S.A. Payne, *OSA TOPS on Adv. Sol. State Lasers*, **1**, 19-21, 1996.
[82] J.W. Pierce, and R.D. Mead, *SPIE* **2986**, 19-28, 1997.
[83] L.A.W. Gloster, P. Cormont, A.M. Cox, T.A. King, and B.H.T. Chai, *Opt. Comm.*, **146**, 177-180, 1998.
[84] L. Xiao, R. Shuangchen, and T. Yhu-Ping, *Acta. Phot. Sinica*, **26**, 1007-1014, 1997.
[85] C.D. Marshall, S.A. Payne, L.K. Smith, H.T. Powell, W.F. Krupke, and B.H.T. Chai, *IEEE J. Sel. Top. Quant. Elec.*, **1**, 67-77, 1995.
[86] C.D. Marshall, L.K. Smith, S.Sutton, M.A. Emmanuel, K.I. Schaffers, S. Mills, S.A. Payne, and W.F. Krupke, *OSA TOPS on Adv. Sol. State Lasers*, **1**, 208-212, 1996.
[87] C.D. Orth, S.A. Payne, and W.F. Krupke, *Nuc. Fus.*, **36**, 75-116, 1996.
[88] J. Czochralski, *Z. Physik. Chem.* **92**, 219-221, 1918.

[89] P. Hartman, ed., Crystal growth: an introduction, American Elsevier Publishing Co., New York, pp. 212, 1973.
[90] C.D. Orth, S.A. Payne, and W.F. Krupke, *Nuc. Fus.* **36**, 75, 1996.
[91] Marshall, C. Bibeau, A. Bayramian, R. Beach, C. Ebbers, M. Emanuel, B. Freitas, S. Fulkerson, E. Honea, B. Krupke, J. Lawson, C. Orth, S. Payne, C. Petty, H. Powell, K. Schaffers, J. Skidmore, L. Smith, S. Sutton, and S. Telford, *OSA TOPS*, **19**, 318, 1998.

Chapter 2

[1] C.D. Marshall, L.K. Smith, R.J. Beach, M.A. Emanuel, K.I. Schaffers, J. Skidmore, S.A. Payne, and B.H.T. Chai, *IEEE J Quan. Elec.*,**32**, 650-656, 1996.
[1] K.I. Schaffers, A.J. Bayramian, C.D. Marshall, J.B. Tassano, and S.A. Payne, *OSA Trends in Optics and Photonics, Advanced Solid-State Lasers*, Pollock, C.R. and Bosenberg, W.R., Editors, **10**, 420-424, 1997.
[2] L.D. DeLoach, S.A. Payne, L.L. Chase, L.K. Smith, W.L. Kway, and W.F. Krupke, *IEEE J. Quantum Electron.*, **29**, 1179-1191, 1993.
[3] H. Bruesselbach, and D.S. Sumida, *Opt. Lett.*, **21**, 480-482, 1996.
[4] U. Brauch, A. Giesan, M. Karszewski, C. Stewen, and A. Voss, *Opt. Lett.*, **20**, 713-715, 1995.
[5] C. Bibeau, R.J. Beach, S.C. Mitchell, M.A. Emanuel, C.A. Ebbers, S.B. Sutton, and K.S. Jancaitis, *IEEE J. Quantum Electron.*, **34**, 2010-2019, 1998.
[6] T.Y. Fan, S. Klunk, and G. Henein, *Opt. Lett.*, **18**, 423-425, 1993.
[7] T.Y. Fan, and J. Ochoa, *IEEE Phot. Tech. Lett.*, **7**, 1137-1138, 1995.
[8] C. Honninger, G. Zhang, U. Keller, and A. Giesan, *Opt. Lett.*, **20**, 2402-2404, 1995.
[9] T. Taira, J. Saikawa, T. Kobayashi, and R.L. Byer, *IEEE J. Sel. Top. Quantum Electron.*, **3**, 100-104, 1997.
[10] D.C. Hanna, J.K. Jones, A.C. Large, D.P. Shepard, A.C. Tropper, P.J. Chandler, M.J. Rodman, P.D. Townsend, and L. Zhang, *Opt. Comm.*, **99**, 211-215, 1993.
[11] H.M. Pask, R.J. Carman, D.C. Hanna, A.C. Tropper, C.J. Mackechnie, P.R. Barber, and J.M. Dawes, *IEEE J. Sel. Top. Quantum Electron.*, 1, 2-13, 1995.
[12] X. Zou, and H. Toratani, *Phys. Rev. B*, **52**, 15889-15897, 1995.
[13] P. Hong, X.X. Zhang, R.E. Peale, H. Weider, M. Bass, and B.H.T. Chai, *J. App. Phys.*, **77**, 294-300, 1995.
[14] D. Shen, C. Wang, Z. Shao, X. Meng, and M. Jiang, *Appl. Opt.*, **35**, 2023-2026, 1996.
[15] R.E. Peale, P.L. Summers, H. Weidner, B.H.T. Chai, and C.A. Morrison, *J. All. Phys.*, **77**, 270-276, 1995.
[16] L.D. DeLoach, S.A. Payne, B.H.T. Chai, and G. Loutts, *Appl. Phys. Lett.*, **65**, 1208-1210, 1994.
[17] G.B. Loutts, C. Bonner, C. Meegoda, H. Ries, M.A. Noginov, N. Noginova, M. Curley, P. Venkateswarlu, A. Rapaport, and M. Bass, *Appl. Phys. Lett.*, **71**, 303-305, 1997.
[18] X.X. Zhang, M. Bass, B.H.T. Chai, P.J. Johnson, and J.C. Oles, *J. Appl. Phys.*, **80**, 1280-1286, 1996.
[19] X.X. Zhang, P. Hong, G.B. Loutts, J. Lefaucheur, M. Bass, and B.H.T. Chai, *Appl. Phys. Lett.*, **64**, 3205-3207.
[20] X.X. Zhang, G.B. Loutts, M. Bass, and B.H.T. Chai, *Appl. Phys. Lett.*, **64**, 10-12, 1994.

[21] J.B. Gruber, C.A. Morrison, M.D. Seltzer, A.O. Wright, M.P. Nadler, T.H. Allik, J.A. Hutchinson, and B.H.T. Chai, *J. Appl. Phys.,* **79**, 1746-1758, 1996.
[22] N. Faure, C. Borel, R. Templier, M. Couchaud, C. Clavat, and C. Wyon, *Opt. Mat.,* **6**, 293-303, 1996.
[23] S.A. Payne, L.D. DeLoach, L.K. Smith, W.L. Kway, J.B. Tassano, and W.F. Krupke, *J. App. Phys.,* **76**, 497-503, 1994.
[24] S.A. Payne, L.K. Smith, L.D. DeLoach, W.L. Kway, J.B. Tassano, and W.F. Krupke, *IEEE J. Quantum Electron.,* **30**, 170-179, 1994.
[25] L.D. DeLoach, S.A. Payne, L.K. Smith, W.L. Kway, and W.F. Krupke, *J. Opt. Soc. Am. B.*, **11**, 269-276, 1994.
[26] C.D. Marshall, L.K. Smith, S. Sutton, M.A. Emanuel, K.I. Schaffers, S. Mills, S.A. Payne, and W.F. Krupke, *OSA Trends in Optics and Photonics, Advanced Solid-State Lasers*, Payne, S.A. and Pollock, C.R., Editors, **1**, 208-212, 1996.
[27] K.I. Schaffers, L.D. DeLoach, C.A. Ebbers, and S.A. Payne, *IEEE J. Quantum Electron.,* **32**, 741-748, 1996.
[28] L.D. DeLoach, S.A. Payne, W.L. Kway, J.B. Tassano, S.N. Dixit, and W.F. Krupke, *J. Lum.*, **62**, 85-94, 1994.
[29] C.D. Marshall, S.A. Payne, L.K. Smith, H.T. Powell, W.F. Krupke, and B.H.T. Chai., *IEEE J. Sel. Top. Quantum Electron.,* **1**, 67-77, 1995.
[30] J.A. Caird, A.J. Ramponi, and P.R. Staver, *J. Opt. Soc. Am. B,* **8**, 1391-1403, 1991.
[31] J.A. Caird, S.A. Payne, P.R. Staver, A.J. Ramponi, L.L. Chase, and W.F. Krupke, *IEEE J. Quantum Electron.,* **24**, 1077-99, 1988.
[32] A.E. Siegman, Lasers. California: University Science Books, 1986.
[33] S. Skupsky, R.W. Short, T. Kessler, R. S. Craxton, S. Letzring, and J.M. Soures, *J. Appl. Phys.,* **73**, 3456-3462, 1989.

Chapter 3

[1] C.D. Marshall, L.K. Smith, R.J. Beach, M.A. Emanuel, K.I. Schaffers, J. Skidmore, S.A. Payne, and B.H.T. Chai, *IEEE J. Quan. Elec*., **32**, 650, 1996.
[2] M.R. Dickinson, L.A.W. Gloster, N.W. Hopps, and T.A. King, *Opt. Comm*., **132**, 275, 1996.
[3] J.W. Pierce, and R.D. Mead, *Solid State Lasers VI, Proc. of SPIE,* **2986**, 19, 1997.
[4] L. Xiao, R. Shuangchen, and T. Yhu-Ping, *Acta Photonica Sinica*, **26**, 1007, 1997.
[5] L.A.W. Gloster, P. Cormont, A.M. Cox, T.A. King, and B.H.T. Chai, *Opt. Comm.* **146**, 177, 1998.
[6] C.D. Marshall, S.A. Payne, L.K. Smith, H.T. Powell, W.F. Krupke, and B.H.T. Chai, *IEEE J. Sel. Top. Quan. Elec.* **1**, 67, 1995.
[7] C.D. Orth, S.A. Payne, and W.F. Krupke, *Nuc. Fus.* **36**, 75, 1996.
[8] C. Marshall, C. Bibeau, A. Bayramian, R. Beach, C. Ebbers, M. Emanuel, B. Freitas, S. Fulkerson, E. Honea, B. Krupke, J. Lawson, C. Orth, S. Payne, C. Petty, H. Powell, K. Schaffers, J. Skidmore, L. Smith, S. Sutton, and S. Telford, *OSA TOPS*, **19**, 318, 1998.
[9] H.W. Etzel, H.W. Gandy, and R.J. Ginther, *Appl. Opt.,* **1**, 534, 1962.
[10] L.F. Johnson, J.E. Geusic, and L.G. Van Uitert, *Appl. Phys. Lett.,* **7**, 127, 1965.
[11] A.R. Reinberg, L.A. Riseberg, R.M. Brown, R.W. Wacker, and W.C. Holton, *Appl. Phys. Lett.,* **19**, 11, 1971.

[12]W.F. Krupke, and L.L.Chase, High Power and Solid State Lasers II, G. Dube, Ed., *SPIE,* **1040**, 68, 1989.
[13]P. Lacovara, H.K. Choi, C.A. Wang, R.L. Aggarwal, and T.Y. Fan, *Opt. Lett.* **16**, 1089-1091, 1991.
[14]L.D. DeLoach, S.A. Payne, L.L. Chase, L.K. Smith, W.L. Kway, and W.F. Krupke, *IEEE J.Quan. Elec.*, **29**, 1179, 1993.
[15]A. J. Bayramian, C. D. Marshall, K. I. Schaffers, and S. A. Payne, *IEEE J Quan. Elec.* **35**, 665-674, 1999.
[16]W. Koechner Solid-State Laser Engineering, Springer-Verlag, New York, NY, 1996, pp. 49-55.
[17]S. M. Yarema, and D. Milam, *IEEE J. Quan. Elec.*, **18**, 1155-1163, 1982.
[18]L. M. Frantz and J. S. Nodvik, *J. Appl. Phys.*, **34**, 2346-2349, 1963.
[19]C. Bibeau, S.A.Payne, and H.T. Powell, *J. Opt. Soc. Am. B*, **12**, 1981-1992, 1995.

Chapter 4

[1] C.D. Marshall, L.K. Smith, R.J. Beach, M.A. Emanuel, K.I. Schaffers, J. Skidmore, S.A. Payne, and B.H.T. Chai, *IEEE J. Quan. Elec.* **32**, 650-656, 1996.
[2] C.D. Marshall, S.A. Payne, L.K. Smith, H.T. Powell, W.F. Krupke, and B.H.T. Chai, *IEEE J. Sel. Top. Quan. Elec.* **1**, 67-77 1995.
[3] K.I. Schaffers, J.B. Tassano, S.A. Payne, R.L. Hutcheson, R.L. Equall, and B.H.T. Chai, *OSA Trends in Optics and Photonics, Advanced Solid-State Lasers*, **19**, 437-441, 1998.
[4] X. Zou, and H. Toratani, *Phys. Rev. B*, **52**, 15889-15897, 1995.
[5] E.L. Church, *Applied Optics*, **27**, 1518-1526, 1988.
[6] W. Koechner, Solid State Laser Engineering, Springer-Verlag, New York, 1996,
[7] J.F. Nye, Physical Properties of Crystals, Oxford University Press, Oxford, UK, 1983, pp.131-149, 241-254.
[8] H.S. Yoon and R.E. Newnhan, *Amer. Mineral.*, **54**, 1193, (1969).
[9] S.K. Tan, *Dissertation Abstr. Intern. B*, **34**, 2862, (1973).
[10]S.A. Payne, L.K. Smith, L.D. DeLoach, W.L. Kway, J.B. Tassano, and W.F. Krupke, *IEEE J. Quantum Electron.*, **30**, 170-179, (1994).
[11]L.D. DeLoach, S.A. Payne, L.K. Smith, W.L. Kway, and W.F. Krupke, *J. Opt. Soc. Am. B.*, Vol. **11**, 269-276, (1994).

Chapter 5a

[1] A.E. Siegman, Lasers, University Science Books, Mill Valley, Ca, 1986, pp. 385.
[2] R.W. Boyd, Nonlinear Optics, Academic Press, San Diego, 1992, pp. 287-298, 365-397.
[3] L.C. Kravitz, J.D. Kingsley, and E.L. Elkin, *J. Chem. Phys.*, **49**, 4600-4610, 1968.
[4] CRC Handbook of Laser Science and Technology, Supplement 2: Optical Materials, M.J. Weber, editor, CRC Press, Inc., Boca Raton, FL, 1995, pp.334-364.
[5] J.T. Verdeyen, Laser Electronics, 3rd ed., Prentice-Hall, Inc., New Jersey, 1995, pp. 651-660.

[6] CRC Handbook of Laser Science and Technology, Vol.3 Optical Materials Part 1, M.J. Weber, editor, CRC Press, Inc., Boca Raton, FL, 1995, pp.283-294.
[7] T.T. Basiev, A.A. Sobol, P.G. Zverev, L.I. Ivleva, V.V. Osiko, and R.C. Powell, *Opt. Mat.*, **11**, 307-314, 1999.
[8] A.K. McQuillan, W.R.L. Clements, and B.P. Stiocheff, *Phys. Rev. A*, **1**, 628-635, 1970.
[9] I.V. Mochalov, *Opt. Eng.* **36**, 1660-1669, 1997.
[10] S.N. Karpukhin, and A.I. Stepanov, *Sov. J. Quantum Electron.*, **16**, 1027-1031, 1986.
[11] C. D. Marshall, L. K. Smith, R. J. Beach, M. A. Emanuel, K. I. Schaffers, J. Skidmore, S. A. Payne, and B. H. T. Chai, *IEEE J. Quan. Elec.*, **32**, 650-656, 1996.
[12] C. Marshall, C. Bibeau, A. Bayramian, R. Beach, C. Ebbers, M. Emanuel, B. Freitas, S. Fulkerson, E. Honea, B. Krupke, J. Lawson, C. Orth, S. Payne, C. Petty, H. Powell, K. Schaffers, J. Skidmore, L. Smith, S. Sutton, and S. Telford, *OSA Trends in Optics and Photonics Series*, **19**, 318-325, 1998.
[13] J.R. Murray, J.R. Smith, R.B. Ehrlich, D.T. Kyrazis, C.E. Thompson, T.L. Weiland, and R.B. Wilcox, *J. Opt. Soc. Am. B*, **6**, 2402-2411, 1989.
[14] S.A. Akhmanov, Y.E. D'yakov, and L.I. Pavlov, *Sov. Phys. JETP*, **39,** 249-256, 1974.
[15] W.R. Trutna, Y.K. Park, and R.L. Byer, *IEEE J. Quantum. Electron.*, **15**, 648-655, (1979).

Chapter 5b

[1] R.W. Boyd, Nonlinear Optics, Academic Press, San Diego, 1992, pp. 325-360.
[2] M.J. Weber, Ed., CRC Handbook of Laser Science and Technology, CRC Press, Ann Arbor, MI, 1995, pp. 346-364.
[3] G.W. Faris, L.E. Jusinski, and A.P. Hickman, *J. Opt. Soc. Am. B.*, **10**(4), 587-599, 1993.
[4] J.F. Nye, Physical Properties of Crystals, Oxford University Press, New York, 1993, pp. 131-149, 235-254.
[5] L.D. Deloach, S.A. Payne, L.K. Smith, W.L. Kway, and W.F. Krupke, *J. Opt. Soc. Am. B*, **11**, 269-276, 1994.
[6] S.A. Payne, L.K. Smith, L.D. Deloach, W.L. Kway, J.B. Tassano, and W.F. Krupke, *IEEE J. Quant. Elec.*, **30**, 170-179, 1994.
[7] H.S. Yoon, R.E. Newnham, *Amer. Miner.*, **54**, 1193-1197, 1969.
[8] S.K. Tan, *Dissertation Abstr. Intern.*, B**34**, 2862, 1973.

Chapter 6a

[1] J.R. Armitage, R. Wyatt, B.J. Ainslie, and S.P. Craig-Ryan, *OSA Proc. on Tunable Solid-State Lasers*, Eds. M.L. Shand and H.P. Jenssen, **5**, 346-349, 1989.
[2] A.J. Bayramian, C.D. Marshall, K.I. Schaffers, and S.A. Payne, *IEEE J. Quan. Elec.*, **35**, 665-674, 1999.
[3] W. Koechner, Solid State Laser Engineering, Springer-Verlag, New York, 1996, pp. 39-53.
[4] L.D. DeLoach, S.A. Payne, L.L. Chase, L.K. Smith, W.L. Kway, and W.F. Krupke, *IEEE J. Quan. Elec.*, **29**, 1179-1191, 1993.

[5] C.D. Marshall, L.K. Smith, R.J. Beach, M.A. Emanuel, K.I. Schaffers, J. Skidmore, S.A. Payne, and B.H.T. Chai, *IEEE J. Quan. Elec.* **32**, 650-656, 1996.
[6] C.D. Marshall, S.A. Payne, L.K. Smith, H.T. Powell, W.F. Krupke, and B.H.T. Chai, *IEEE J. Sel. Top. Quan. Elec.* **1**, 67-77, 1995.
[7] S.A. Payne, L.D. Deloach, L.K. Smith, W.L. Kway, J.B. Tassano, W.F. Krupke, and B.H.T. Chai, *J. Appl. Phys.* **76**, 497-503, 1994.
[8] T.Y. Fan, and R.L. Byer, *IEEE J. Quan. Elec.* **23**, 605-612, 1987.
[9] P.F. Moulton, *IEEE J. Quan. Elec.* **21**, 1582-1595, 1985.
[10] A.E. Siegman, Lasers, University Science Books, Mill Valley, CA, 485, 1024-1033, 1986.
[11] J.A. Caird, S.A. Payne, P.R. Staver, A.J. Ramponi, L.L. Chase, and W.F. Krupke, *IEEE J. Quantum Electron.*, **24**(6), 1077-99, 1988.
[12] R.J. Beach, *IEEE J. Quant. Elec.*, **31**(9), 1606-1613, (1995).
[13] A.E. Siegman, "New developments in laser resonators," *Proc. of SPIE*, **1224**, 7-13, (1990).

Chapter 6b

[1] M. Iwai, T. Kobayashi, H. Furuya, Y. Mori, and T. Sasaki, *Jap. J. Appl. Phys.*, **36**,276-279, 1997.
[2] V.G. Dmitriev, G.G. Gurzadyan, and D.N. Nikogosyan, Handbook of Nonlinear Optical Crystals, Springer-Verlag, New York, 1997, pp. 50-51.
[3] W. Koechner, Solid-State Laser Engineering, Springer-Verlag, New York, 1996, pp. 564-578.
[4] H.P. Weber, E. Mathieu, K.P. Meyer, *J. Appl. Phys.*, **37**, 3584, 1966.
[5] F. Brehat and B. Wyncke, *J Phys. B: At. Mol. Opt. Phys.*, **22**, 1891-1898, 1989.
[6] J.A. Armstrong, N. Bloembergen, J. Ducuing, And P.S. Pershan, *Phys. Rev.*, **127**, 1918-1939, 1962.
[7] Code written by Chris Ebbers
[8] J.J. Adams, C.A. Ebbers, K.I. Schaffers, and S.A. Payne, submitted *Opt. Lett.*, May 2000.

APPENDIX

This appendix contains the many computer codes used for modeling the results of experiments described in the thesis. The C^{++} computer codes require only data files (such as temporal pulse data and/or emission and absorption spectroscopy) to run, assuming one has C^{++} installed on their system. As I progressed on my thesis, I found C^{++} to be somewhat inefficient and time consuming for error checking for the quick calculations I wanted to run. I turned to VisualBasic for my programming needs since it is seamlessly integrated into the Microsoft Excel program, thus allowing programming in a "spreadsheet physics" environment. Unfortunately, this means the programs given in the appendices are not complete in themselves, rather they require a spreadsheet (which has its own embedded formulas) to operate. I have given the VisualBasic codes along with example spreadsheets where they are necessary.

I: CW gain

The following code is written in Borland C^{++} and was run on a PC running Windows 95. The code typically runs in less than a minute. This program calculates the 900 nm pump depletion of a spatially infinite plane wave with an arbitrary input temporal pulse shape for the Yb:S-SAP gain medium. Small signal gain from stimulated emission at a specified probe wavelength is included, i.e. no change in excited state populations.

```
/* CW Gain revision 4, Andy Bayramian, copyright February 24, 1998 */
/* Based on a program by Chris Marshall */

#include "stdio.h"
#include "math.h"
#include "stdlib.h"
#include "conio.h"

/* Defining Parameters */
FILE *infile, *outfile;
char fname[20];
char swap[20];
char run[20];
char ext[20] = ".dat";

char material[20] = "Sr5-FAP";      /* Material being tested */
char pumpin[20] = "pulse1.dat";     /* External Input pump pulse shape file */
char pumpint[20] = "900in.dat";     /* Internal Input pump pulse shape file */
char absfile[20] = "abs056.dat";    /* Absorption cross section data file (lambda, p-pol, s-pol) */
char emfile[20] = "em056.dat";      /* Emmision cross section data file (lambda, p-pol, s-pol) */
char pumpout[20] = "900out_707_";/* Output pump pulse shape file */
char fluout[20] = "fluout_707_";    /* Output Transmission, fluorescence, and Nex files */
char gainfil[20] = "gain_707_";     /* Output Gain file */
char n3vst[20] = "N3vs-T_707_";  /* Populations versus time  (t, N1t,N3t) */
char n3vsz[20] = "N3vs-Z_707_";  /* N3 versus space (z, N3z) */
char param[20] = "parameter.dat"; /* A printout log of the parameters used in a particular calculation */
char tst = 'g';                     /* Pump pulse shape, can be g/s/e Gaussian, Square or External */
char pumpsp = 'p';                  /* 900 nm pump polarization (p/s) */
char probesp = 'p';                 /* 1047 nm probe polarization (p/s) */
char gainpass = 's';                /* Single or double pass gain (s/d) */
char pumppass = 's';                /* Single or double pass pumping (s/d) */
char ppar = 'y';                    /* Print parameters? (y/n) */
char fflu = 'y';                    /* Print output transmission, flourescence, and Nex files? (y/n) */
char ppout = 'n';                   /* Print output temporal pump pulse? (y/n) */
char nvst = 'n';                    /* Print populations vs. time? (y/n) */
char nvsz = 'n';                    /* Print N3 vs space? (y/n) */
float FI900_0 = 18.90;              /* Peak pump fluence, note an increase requires increasing stepfactor */
float stepfactor = 190;             /* The width divided by the step factor gives time step */
float width900 = 188e-6;            /* Width of 900 pump pulse (seconds) */
float ABS_peak = 9.0e-20;           /* Absorption cross section (cm^2) at the spectral peak */
float EM_peak = 6.00e-20;           /* Emission cross section (cm^2) at the spectral peak */
float pumpwav = 900.2;              /* Pump wavelength used in calculation (nm) */
float probewav = 1047.6;            /* Probe wavelength used in calculation (nm) */
float N1_t0 = 2.16e19;              /* Number density of dopant atoms in crystal (cm-3) */
float d = 3.37;                     /* Thickness of crystal (cm) */
float scatter = 0.01;               /* pump beam scatter loss cm-1 for poor TIR down rod */
float Rs1 = 0.0567;                 /* Reflectivity of first surface at 900 nm */
```

```
float hc = 1.9878e-16;              /* hc/(1e-9) to be divided by a wavelength in nm to give hv (Joules) */
float tau = 1.14e-3;                /* Fluorescent lifetime of the excited state (seconds) */
float abpeak_p = 9.054e-20;         /* Experimental absorption cross section peak p-pol. */
float empeak_p = 6.068e-20;         /* Experimental emission cross section peak p-pol. */
float abpeak_s = 3.87e-20;          /* Experimental absorption cross section peak s-pol. */
float empeak_s = 2.7e-20;           /* Experimental emission cross section peak s-pol. */
int timepoints = 500;               /* Only used for internally generated pump pulse */
int Inpts = 100;                    /* Inpts = number of Intensity points, max = 400 */

int offset;                         /* Time offset for internally generated pulses */
int tpk;                            /* i = tpk + iwidth when N3 peaks */
int zpts;                           /* zpts = number of z slices in crystal */
int tpts;                           /* tpts = number of time points, max = 4000 */
int abpts;                          /* number of absorption data points, max = 4000 */
int empts;                          /* number of emmision data points, max = 4000 */
int i, j, k, pts, stop;

float t[4002];                      /* time, slices = 4002 */
float z[101];                       /* position is the distance into the sample in cm, spatial slices = 101 */
float N1[4002][101];                /* Number density of ground state as a function of time */
float N3[4002][101];                /* Number density of excited state as a function of time */
float N1t[4002];                    /* time dependent ground state density */
float N3t[4002];                    /* time dependent excited state density */
float I900[4002];                   /* 900 output temporal profile */
float I900_inc[4002];               /* 900 input incident profile */
float I900_tmp[4002];               /* temporary 900 Intensity */
float N3z[101];                     /* Number density of excited state vs. position at Fmax */
float N1old[101], N3old[101];       /* number density of states in the previous time slice */
float Fluence[1000];                /* Fluence */
float Trans[1000];                  /* Transmission */
float Fluor[1000];                  /* flourescence spectrum */
float N1ave[1000];                  /* Average gound state density */
float N3ave[1000];                  /* Average excited state density */
float Ntot[1000];                   /* Total number density averaged over the crystal vs. pump intensity */
float Gain[1000];                   /* Small signal gain at specified wavelength */
float ABSpump;                      /* 900 nm absorption cross section (cm^2) used in calculation */
float EMpump;                       /* 900 nm emission cross section (cm^2) used in calculation */
float ABSprobe;                     /* probe wavelength absorption cross section used in calculation */
float EMprobe;                      /* probe wavelength emission cross section used in calculation */
float delt;                         /* time slice (s) */
float delz;                         /* thickness of crystal slice (cm) */
float R900_s1;                      /* pump intensity reflectivity at pump wavelength for 1st surface S1 */
float R900_s2;                      /* pump intensity reflectivity at pump wavelength for 2nd surface S2 */
float I900_0;                       /* peak 900 nm Intensty in W/cm2 */

float delta, Nmax, intarea, intarea2;
float x[4002], y[4002], x1[4002], yp[4002], ys[4002];
float tmp, tmp1, tmp2, C1, C2, C3;

/*************************************************************/

void errexit() /* This routine exits program when error occurs */
{
    printf("\n\n!!!!!!!ERROR!!!!!!\n\n");
    printf("Now exiting to system\n\n");
    exit(0);
```

```
}

int filecreation()
{
    stop = 0;
    for(i=0;i<20;i++)
    {
        if(swap[i] == NULL) break;
        fname[i] = swap[i];
    }
    stop = i;
    for(i=0;i<20;i++)
    {
        if(run[i] == NULL) break;
        fname[i + stop] = run[i];
    }
    stop = stop + i;
    for(i=0;i<20;i++)
    {
        if(ext[i] == NULL) break;
        fname[i + stop] = ext[i];
    }
    return(0);
}

int readxy() /* Routine to read a 2 column, space delimited, file (w/ max 4000 pts) in arrays x[i], y[i] */
{
    char buf[100];
    infile = fopen(fname, "r+") ;
    pts = 0 ;
    while(fgets(buf, 100, infile) != (NULL)) pts = pts + 1 ;
    pts = pts + 1;
    fclose(infile) ;
    if(pts < 1 || pts>4000)
    {
        printf("\n!!!! ERROR !!!!\n\nTHE DATA FILE DID NOT OPEN CORRECTLY\n");
        printf("\nOR THE NUMBER OF POINTS IS TOO LARGE\n");
        printf("\nPRESS RETURN TO CONTINUE\n");
        errexit();
    }
    infile = fopen(fname, "r+");
    for(i=0;i<pts;i++) fscanf(infile, "%G %G", &x[i], &y[i]);
    fclose(infile);
    delta = x[1] - x[0];
    return(0);
}

int normy() /* This routine normalizes input y[i] of (x,y) data */
{
    intarea = 0.0;
    for(i=0;i<pts;i++)  intarea = intarea + y[i] * (delta);
    for(i=0;i<pts;i++) y[i] = y[i] / intarea;
    return(0);
}

int readxyy() /* Routine reads a 3 column, space delimited file (max 4000 pts) in arrays x1[i], yp[i], ys[i] */
```

```
{
    char buf[100];
    infile = fopen(fname, "r+") ;
    pts = 0 ;
    while(fgets(buf, 100, infile) != (NULL)) pts = pts + 1 ;
    pts = pts + 1;
    fclose(infile) ;
    if(pts < 1 || pts>4000)
    {
        printf("\n!!!! ERROR !!!!\n\nTHE DATA FILE DID NOT OPEN CORRECTLY\n");
        printf("\nOR THE NUMBER OF POINTS IS TOO LARGE\n");
        printf("\nPRESS RETURN TO CONTINUE\n");
        errexit();
    }
    infile = fopen(fname, "r+");
    for(i=0;i<pts;i++) fscanf(infile, "%G %G %G", &x1[i], &yp[i], &ys[i]);
    fclose(infile);
    delta = x[1] - x[0];
    return(0);
}

int gainprint()  /* Prints out gain vs. fluence file */
{
    for(i=0;i<20;i++) swap[i] = gainfil[i];
    filecreation();
    outfile = fopen(fname, "w+") ;
    for(k=0;k < Inpts; k++) fprintf(outfile, "%G %G \n", Fluence[k], Gain[k]);
    fclose(outfile);
    return(0);
}

int fluprint()  /* Prints out transmission, fluorescence, and Nex (Flu, T, Fluor, Nex) file */
{
    for(i=0;i<20;i++) swap[i] = fluout[i];
    filecreation();
    outfile = fopen(fname, "w+");
    for(k=0;k < Inpts; k++) fprintf(outfile, "%G %G %G %G \n", Fluence[k], Trans[k], Fluor[k],
N3ave[k]);
    fclose(outfile);
    return(0);
}

int pumprint()  /* Prints pump output temporal profile (t, I900) file */
{
    for(i=0;i<20;i++) swap[i] = pumpout[i];
    filecreation();
    outfile = fopen(fname, "w+");
    for(i=0;i < tpts; i++) fprintf(outfile, "%G %G \n", t[i], I900[i]);
    fclose(outfile);
    return(0);
}

int n_vs_t() /* Prints a file of populations versus time (t, N1t, N3t) */
{
    for(i=0;i<20;i++) swap[i] = n3vst[i];
    filecreation();
```

```
    outfile = fopen(fname, "w+");
    for(i=0;i<tpts;i++)
    {
        N1t[i] = 0;
        N3t[i] = 0;
        for(j=0;j<zpts;j++)
        {
            N1t[i] = N1t[i] + N1[i][j]*delz ;
            N3t[i] = N3t[i] + N3[i][j]*delz ;
        }
        fprintf(outfile, "%G %G %G \n", t[i], N1t[i], N3t[i]);
    }
    fclose(outfile);
    return(0);
}

int n_vs_z() /* Prints a file of populations versus space (z, N3z) */
{
    for(i=0;i<20;i++) swap[i] = n3vsz[i];
    filecreation();
    outfile = fopen(fname, "w+");
    for(j=0;j<zpts;j++) fprintf(outfile, "%G %G \n", z[j], N3z[j]);
    fclose(outfile);
    return(0);
}

int par()  /* Prints the parameters of this calculation to a file */
{
    for(i=0;i<20;i++) fname[i] = param[i];
    outfile = fopen(fname, "a+") ;
    fprintf(outfile, "%s, %s, ", run, material);
    fprintf(outfile, "%G, %G, %G, %d, %G, %G \n", ABS_peak, EM_peak, N1_t0, tpk, tau, scatter);
    fprintf(outfile, "%.3G, %.3G, %.3G, %.3G, %G, %G, ", ABSpump, EMpump, ABSprobe, EMprobe,
pumpwav, probewav);
    fprintf(outfile, "%G, %G \n", d, Rs1);
    fprintf(outfile, "%c, %c, %c, %c, %.3G", pumppass, gainpass, pumpsp, probesp, tmp1);
    fprintf(outfile, "\n \n \n");
    fclose(outfile);
    return(0);
}

/****************************************** Main ************************************/
main()
{
    printf("This program calculates the fractional transmission for the pump wavelength \n");
    printf("for an arbitrary temporal profile with pump depletion due to ground state \n");
    printf("absorption.  Output is automatically a Gain vs. Fluence file, and optional \n");
    printf("Transmission, Fluorescence, and N3 vs. fluence, Transmitted pump intensity, \n");
    printf("N1, and N3 vs. time, N3 vs. z, and param file that lists all constants used.\n");
    printf("All files are space delimited, with crystal and run number attached.\n");
    printf("Units are in J, cm, and s. \n");
    printf("\n\n  !!Note that NO ASE or reabsorption is included yet!! \n\n");
    printf("Please input the run number:  ");
    scanf("%s", &run);
    getchar();
    printf("\n %d Total Intensity Points", Inpts);
```

```
    printf("\n   Intensity Points Left");

/**************** Define single or double pass pumping and reflectivities *****************/
    if(pumppass == 's') /* single pass pumping */
    {
        R900_s1 = Rs1; /* includes TIR mismatch */
        R900_s2 = Rs1;
    }
    if(pumppass == 'd') /* double pass pumping */
    {
        R900_s1 = Rs1;
        R900_s2 = 0.95;
    }

    /***************************** Define the input pulse shape ************************/
    if(tst=='e')
    {
        for(i=0;i<20;i++)fname[i] = pumpin[i];
        readxy();
        normy();
        tpts = pts;
        for(i=0;i<tpts;i++)
        {
            t[i] = x[i];
            I900[i] = y[i];
            I900[i] = I900[i] * FI900_0;
        }
        delt = delta;
    }
    if(tst != 'e')
    {
        tpts = timepoints;
        delt = width900/stepfactor;
        offset = int(0.4*tpts);
        if(tpts>4000) errexit();
        if(tst == 'g')
        {
            for(i=0;i<tpts;i++)
            {
                t[i] = (i-200) * delt;
                I900_0 = FI900_0 / (0.886 * width900);
                I900[i] = I900_0 * exp(-4*(t[i]/width900) * (t[i]/width900));
            }
        }
        else  /* tst == "s"  */
        {
            for(i=0;i<tpts;i++)
            {
                t[i] = (i-200) * delt;
                I900[i] = 0.0;
                I900_0 = FI900_0 / width900;
                if((t[i] >= 0) && (t[i] <= width900)) I900[i] =  I900_0;
            }
        }
        /* Prints the internally generated input pulse to a file */
        for(i=0;i<20;i++) fname[i] = pumpint[i];
```

```
    infile = fopen(fname, "w+") ;
    for (i=1;i<tpts;i++) fprintf(infile, "\n %f %f", t[i], I900[i]);
    fclose(infile);
}
for(i=0;i<tpts;i++)
{
    I900_inc[i] = I900[i];
    I900_tmp[i] = I900_inc[i];
}

/*******************************Define the spatial slicing*************************/

zpts = 100;
delz = d/(float)zpts;  /* thickness of z slice */
for(j = 0; j <zpts; j++) z[j] = (float)j * delz;

/************************start of main calculation section*****************************/
/* Define cross sections and a few usefule consants */

/* Reading absorption cross section file */
for(i=0;i<20;i++)fname[i] = absfile[i];
readxyy();
for(i=0;i<pts;i++) yp[i] = yp[i] / (abpeak_p);
for(i=0;i<pts;i++) ys[i] = ys[i] / (abpeak_s);
abpts = pts;

/* Now define the absorption cross sections at pump and probe wavelengths */
for(i=0;i<abpts;i++) if(x1[i]>pumpwav) break;
if(pumpsp== 'p') ABSpump = yp[i-1] + (pumpwav-x1[i-1])*(yp[i]-yp[i-1])/(x1[i]-x1[i-1]);
if(pumpsp== 's') ABSpump = ys[i-1] + (pumpwav-x1[i-1])*(ys[i]-ys[i-1])/(x1[i]-x1[i-1]);
for(i=0;i<abpts;i++) if(x1[i]>probewav) break;
if(probesp== 'p') ABSprobe = yp[i-1] + (probewav-x1[i-1])*(yp[i]-yp[i-1])/(x1[i]-x1[i-1]);
if(probesp== 's') ABSprobe = ys[i-1] + (probewav-x1[i-1])*(ys[i]-ys[i-1])/(x1[i]-x1[i-1]);
ABSpump = ABSpump*ABS_peak;
ABSprobe = ABSprobe*ABS_peak;

/* Reading emission cross section file */
for(i=0;i<20;i++)fname[i] = emfile[i];
readxyy();
for(i=0;i<pts;i++) yp[i] = yp[i] / (empeak_p);
for(i=0;i<pts;i++) ys[i] = ys[i] / (empeak_s);
empts = pts;

/* Now define the emission cross sections at pump and probe wavelengths */
for(i=0;i<empts;i++) if(x1[i]>pumpwav) break;
if(pumpsp== 'p') EMpump = yp[i-1] + (pumpwav-x1[i-1])*(yp[i]-yp[i-1])/(x1[i]-x1[i-1]);
if(pumpsp== 's') EMpump = ys[i-1] + (pumpwav-x1[i-1])*(ys[i]-ys[i-1])/(x1[i]-x1[i-1]);
for(i=0;i<empts;i++) if(x1[i]>probewav) break;
if(probesp== 'p') EMprobe = yp[i-1] + (probewav-x1[i-1])*(yp[i]-yp[i-1])/(x1[i]-x1[i-1]);
if(probesp== 's') EMprobe = ys[i-1] + (probewav-x1[i-1])*(ys[i]-ys[i-1])/(x1[i]-x1[i-1]);
EMpump = EMpump*EM_peak;
EMprobe = EMprobe*EM_peak;

C1 = ABSpump *  delt * pumpwav / hc;
C2 = EMpump * delt * pumpwav / hc;
C3 = delt / tau;
```

```
/* Now start main calculation */
/* Intensity loop */
for(k=0;k < Inpts; k++)
{
    if(Inpts != 1) for(i=0;i<tpts;i++)
    {
        I900_inc[i] = I900_tmp[i]* (k+0.0001) / (Inpts-1);
        I900[i] = I900_inc[i];
    }
    else for(i=0;i<tpts;i++) /* for a single pump intensity point */
    {
        I900_inc[i] = I900_tmp[i];
        I900[i] = I900_inc[i];
    }

    if(Inpts != 1) Fluence[k] = FI900_0 * (k+0.0001) /(Inpts-1);
    if(Inpts == 1) Fluence[k] = FI900_0;
    /* initialize the populations before the pulse hits the first spatial slice */

    N1ave[k] = 0.0;
    N3ave[k] = 0.0;
    Fluor[k] = 0.0;

    for(j = 0; j < zpts; j++)
    {
        N1old[j] = N1_t0;
        N3old[j]  = 0.0;
    }

    for(i = 0; i < tpts-1; i++)  /* time loop */
    {
        if(pumppass == 's')
        {
            for(j = 0; j < zpts; j++) /* first pass spatial loop */
            {
                /* restructure the temporal pulse shape for each spatial slice */
                I900[i] = I900[i] * exp(-(N1old[j] * ABSpump + scatter) * delz);
                N1[i][j] = N1old[j] * (1 - C1 * I900[i] ) + C3 * N3old[j] + N3old[j] *  C2 * I900[i];
                N3[i][j] = N3old[j] * (1 - C3 - C2 * I900[i] ) + N1old[j] * C1 * I900[i];
                N3old[j] = N3[i][j];
                N1old[j] = N1[i][j];
                Fluor[k] =  Fluor[k] + N3old[j] / zpts / tpts;
            }/* end of first pass spatial loop */
            I900[i] = I900[i];  /* reflection from surface S2 */
        }
        if(pumppass == 'd')
        {
            for(j = 0; j < zpts; j++) /* first pass spatial loop */
            {
                /* restructure the temporal pulse shape for each spatial slice */
                I900[i] = I900[i] * exp(-(N1old[j] * ABSpump + scatter) * delz);
                N1[i][j] = N1old[j] * (1 - C1 * I900[i] ) + C3 * N3old[j] / 2 + N3old[j] *  C2 * I900[i];
                N3[i][j] = N3old [j]* (1 - C3 / 2 - C2 * I900[i] ) + N1old[j] * C1 * I900[i];
                N1old[j] = N1[i][j];
                N3old[j] = N3[i][j];
```

```
            }/* end of first pass spatial loop */
            I900[i] = I900[i];  /* Reflection off the second surface once */
            for(j = zpts-1; j > -1; j--) /* second pass spatial loop */
            {
                /* restructure the temporal pulse shape for each spatial slice */
                I900[i] = I900[i] * exp(-(N1old[j] * ABSpump + scatter) * delz);
                N1[i][j] = N1old[j] * (1 - C1 * I900[i] ) + C3*N3old[j] / 2 +N3old[j] *  C2 * I900[i];
                N3[i][j] = N3old [j]* (1 - C3 / 2 - C2 * I900[i] ) + N1old[j] * C1 * I900[i];
                N1old[j] = N1[i][j];
                N3old[j] = N3[i][j];
                Fluor[k] =  Fluor[k] + N3old[j] / zpts / tpts;
            }/* end of second pass spatial loop */
            I900[i] = I900[i];
        }
    }  /* end of time loop */
    tpk = 0;
    Nmax = 0.0;
    for(i=0;i<tpts-1;i++)
    {
        N3ave[k] = 0;
        for(j = 0; j < zpts; j++)
        {
            N3ave[k] = N3ave[k] + N3[i][j] / (zpts);
        }
        if(N3ave[k]>Nmax)
        {
            Nmax = N3ave[k];
            tpk = i;
        }
    }
    N3ave[k] = 0;
    N1ave[k] = 0;
    for(j = 0; j < zpts; j++)
    {
        N1ave[k] = N1ave[k] + N1[tpk][j] / (zpts);
        N3ave[k] = N3ave[k] + N3[tpk][j] / (zpts);
        N3z[j] = N3[tpk-20][j];
    }
    Ntot[k] = N1ave[k] + N3ave[k];
    if(gainpass == 's')
    {
        Gain[k] = exp(d * N3ave[k] * EMprobe - d * N1ave[k] * ABSprobe - scatter * d);
    }
    else
    {
        Gain[k] = exp(2* d * N3ave[k] * EMprobe - 2 * d * N1ave[k] * ABSprobe - 2 * scatter * d);
    }

    /* Losses from ground state absorption and Boltzman populated absorption */
    /* Gain with reflection losses normalized out */
    /* Calculate the fractional 900 transmission for each incident fluence from inside the crystal (i.e. no
reflectivity) */
    tmp1 = 0;
    tmp2 = 0;
    for(i=0;i<tpts;i++)
    {
```

```
            tmp1 = tmp1 + I900[i]*delt;
            tmp2 = tmp2 + I900_inc[i]*delt;
        }
        Trans[k] = tmp1/tmp2;

        /* Timer (for the impatient) */
        gotoxy(2,15);
        void clreol(void);
        printf("%-3d", Inpts-k);
        void clreol(void);
    } /* end of Intensity loop */

    /* End of main calculation */
    /* normalization and output */

    tmp1 = Gain[0];
    for(k=0;k < Inpts; k++) Gain[k] = Gain[k] / tmp1;  /* normalize gain to one at zero fluence. */
    gainprint();
    for(k=0;k < Inpts; k++) Fluor[k] = Fluor[k]/Fluor[Inpts -1]; /* normalize the fluorescence */
    if (fflu == 'y') fluprint();  /* Creates file of Trans, fluor, and N3ave versus fluence. */
    if (ppout == 'y') pumprint(); /* Creates file of pump output temporal profile for max intensity */
    if (nvst == 'y') n_vs_t(); /* Creates file of N1t and n3t versus time. */
    if (nvsz == 'y') n_vs_z(); /* Creates file of N3z vs. z. */
    if(ppar == 'y') par();  /* Creates file with all of the parameters used in this run */
}
/* end of main */
```

II: Pulsed gain saturation

The following code is written in Borland C^{++} and was run on a PC running Windows 95. The code typically runs in a few minutes. This program builds on the CW gain program in that it first calculates the 900 nm pump depleation and small signal gain (i.e. no change in excited state populations) from an arbitrary temporal pump pulse shape. It then calculates the saturated gain from a probe beam with either plane wave or elliptical gaussian spatial profile, and arbitrary temporal pulse shape. The following are user specifiable within the variable definitions at the beginning of the code: input and output filenames, pump and probe pulse shapes (both temporal and spatial), pump and probe polarizations, pump and probe passes through material, maximum pump fluence, maximum pump energy, pump and probe wavelengths, absorption and emission cross sections, dopant density, sample length, lifetime of upper laser level, as well as temporal and spatial step sizes.

```
/* Pulse Gain_Revision 2, Andy Bayramian, Copyright November, 1998 */

#include "stdio.h"
#include "math.h"
#include "stdlib.h"
#include "conio.h"

/* Defining Parameters */
FILE *infile, *outfile;
char fname[20];
char swap[20];
char run[20];
char ext[20] = ".dat";

char material[20] = "Sr5-FAP";          /* Material being tested */
char pumpext[20] = "900in.dat";         /* External input pump pulse (time, intensity) */
char pumpin[20] = "900in";              /*Input pump pulse shape file */
char absfile[20] = "abs056.dat";        /*Absorption cross section data file (lambda, p-pol, s-pol) */
char emfile[20] = "em056.dat";          /*Emmision cross section data file (lambda, p-pol, s-pol) */
char gaindata[20] = "gainall2.dat";     /*Experimental gain data file (gain, pump fluence, probe energy) */
char pumpout[20] = "900out_707_";       /*Output pump pulse shape file */
char amp[20] = "AmpShell";              /* Gaussian shell parameters */
char fluout[20] = "fluout_707_";        /*Output Transmission, fluorescence, and Nex files */
char gainfil[20] = "Energain_707_";     /*Output Gain vs probe energy and pump fluence */
char fgainfil[20] = "flugain_707_";     /*Output Gain vs probe and pump fluence */
char ssgainfil[20] = "ssgain_707_";     /*Small signal gain vs pump fluence */
char n3vst[20] = "N3vs-T_707_";         /*Populations versus time  (t, N1t,N3t) */
char n3vsz[20] = "N3vs-Z_707_";         /*N3 versus space (z, N3z_in) */
char param[20] = "parameter.dat";       /*A printout log of the parameters used in a particular calculation */
char optimize = 'y';                    /*Calculate gain from energy and fluence data (y/n) */
char tst1 = 'g';                        /*Pump pulse shape, g/s/e Gaussian, Square or External */
char tst2 = 'e';                        /* Probe pulse shape, g/s/e Gaussian, Square, or External */
char tst3 = 'g';                        /* Spatial probe pulse shape, g/s Gaussian, or Square */
char pumpsp = 'p';                      /* pump polarization (p/s) */
char probesp = 'p';                     /* probe polarization (p/s) */
char probepass = 's';                   /* Single or double pass gain (s/d) */
char pumppass = 's';                    /* Single or double pass pumping (s/d) */
char ppar = 'y';                        /* Print parameters? (y/n) */
char fflu = 'y';                        /* Print output trans, flour, and Nex files (y/n) */
char ppout = 'y';                       /* Print output temporal pump pulse? (y/n) */
char nvst = 'n';                        /* Print populations vs. time? (y/n) */
char nvsz = 'n';                        /* Print N3 vs space? (y/n) */
```

```
float Fpump_0 = 20.0;                /* Peak pump Fluence (J/cm2) */
float Emax = 0.04;                   /* Peak probe energy (J) */
float stepfactor_pump = 190;         /* The ratio: width/step factor gives pump time step */
float widthpump = 188e-6;            /*1/e Width of pump pulse (seconds) */
float widthprobe = 10.7e-9;          /* 1/e Width of probe pulse (seconds) */
float ABS_peak = 9.00e-20;           /* Peak pump absorption cross section (cm^2) */
float EM_peak = 6.2e-20;             /* Peak probe emission cross section (cm^2) */
float pumpwav = 900.4;               /* Pump wavelength used in calculation (nm) */
float probewav = 1047.60;            /* Probe wavelength used in calculation (nm) */
float N1_t0 = 2.17e19;               /* Dopant concentration (cm-3) */
float d = 3.37;                      /* Thickness of crystal (cm) */
float scatter = 0.01;                /* pump beam scatter loss cm-1 for poor TIR down rod */
float Rpump1 = 0.0567;               /* Pump Intensity Reflectivity of first surface (S1) */
float Rprobe1 = 0.0567;              /* Probe Intensity Reflectivity of first surface (S1) */
float hc = 1.9878e-16;               /* [h*c /(1e-9)]  using lambda (nm) gives hv (Joules) */
float tau = 1.14e-3;                 /* Experimental Fluorescent lifetime of the excited state (s) */
float probe_wa = 0.038;              /* elliptic 1/e2 waist radii in cm */
float probe_wb = 0.039;              /* elliptic 1/e2 waist radii in cm */
float radius_stepratio = 200;        /* Probe_wa/radius_stepratio = radial step increment in cm */
float abpeak_p = 9.054e-20;          /* Experimental absorption cross section peak p-pol. */
float empeak_p = 6.068e-20;          /* Experimental emission cross section peak p-pol. */
float abpeak_s = 3.87e-20;           /* Experimental absorption cross section peak s-pol. */
float empeak_s = 2.7e-20;            /* Experimental emission cross section peak s-pol. */
int time_pumppoints = 500;           /* Only used for internally generated pump pulse */
int zpts = 100;                      /*zpts = number of z slices in crystal */
int time_probepoints = 200;          /* Only used for internally generated probe pulse */
int Ipump_pts = 50;                  /* Pump Intensity points, max = 400 */
int Eprobe_pts = 50;                 /* Probe Energy points, max = 400 */
int radius_pts = 400;                /* Shell radius points (probe fluence points, max = 1000) */

int offset;                          /* Time offset for internally generated pulses */
int tpk;                             /*i = tpk + iwidth when N3 peaks */
int tpts;                            /*tpts = number of pump time points, max = 4000 */
int t2pts;                           /*t2pts = number of probe time points, max = 4000 */
int abpts;                           /*number of absorption data points, max = 4000 */
int empts;                           /*number of emmision data points, max = 4000 */
int i, j, k, l, m, n, pts, stop;

float shell_area[1002];              /* values for elliptical shell of an elliptical gaussian */
float shell_volume[1002];            /* values for elliptical shell of an elliptical gaussian */
float shell_energy[1002];            /* values for elliptical shell of an elliptical gaussian */
float shell_fluence[1002];           /* values for elliptical shell of an elliptical gaussian */
float shell_fraction[1002];          /* values for elliptical shell of an elliptical gaussian */
float t[4002];                       /* time for pump, slices = 4002 */
float t2[4002];                      /*time for probe, slices = 4002 */
float z[101];                        /* Distance into the sample in cm, spatial slices = 101 */
float N1[4002][101];                 /* N1 = the number density of ground state vs. time */
float N3[4002][101];                 /* N3 = the number density of excited state vs. time */
float N1t[4002];                     /* time dependent ground state density */
float N3t[4002];                     /* time dependent excited state density */
float Ipump[4002];                   /*pump output temporal profile */
float Ipump_inc[4002];               /*pump input incident profile */
float Ipump_tmp[4002];               /*temporary pump Intensity */
float Energy_probe[1002];            /* Input probe energy */
float N3z_in[101];                   /* Number density of Nex after pump vs. position at Fmax */
float N3z_out[101];                  /* Number density of Nex after probe vs. position at Fmax */
```

```
float N1z[101];                 /* Number density of Ngr vs. position at Fmax */
float N1old[101], N3old[101];   /*number density of states in the previous time slice */
float Flu_pump[1002];
float Flu_probe_out[1002];
float Trans[1002];              /* Transmission */
float Fluor[1002];              /*flourescence spectrum */
float N1ave_in[1002];           /* Average gound state density after pumping */
float N3ave_in[1002];           /* Average excited state density after pumping */
float Ntot[1002];               /*Total number density averaged over the crystal vs. Ipump */
float Gain[1002][1002];         /* Gain vs. probe energy and pump fluence */
float Flugain[1002][1002];      /* Gain vs. probe & pump fluence */
float Fluprobe[1002];           /* probe fluence */
float SSgain[1002];             /* Small signal gain at specified wavelength */
float Shellgain[1002];          /* Gain of elliptical shell at specified wavelength */
float totalvolume;              /* total volume of elliptical gaussian w/ max amplitude = 1 */
float amplitude[1002];          /* amplitude of gaussian function */
float ABSpump;                  /* pump absorption cross section (cm^2) used in calculation */
float EMpump;                   /* pump emission cross section (cm^2) used in calculation */
float ABSprobe;                 /* probe absorption cross section (cm^2) used in calculation */
float EMprobe;                  /* probe emission cross section (cm^2) used in calculation */
float delt;                     /* time slice (s) for pump */
float delt2;                    /* time slice (s) for probe */
float delz;                     /* thickness of crystal slice (cm) */
float Rpump2;                   /* pump intensity reflectivity for 2nd surface S2 */
float Rprobe2;                  /* probe intensity reflectivity for 2nd surface S2 */
float Ipump_0;                  /* peak pump Intensty in W/cm2 */
float Iprobe_0;                 /* peak probe Intensity in W/cm2 */

float G0N, T1N, gpts;
float Gaindat[1002], Flupumpdat[1002], Eprobedat[1002];
float x[4002], y[4002], zp[4002], x1[4002], yp[4002], ys[4002];
float tmp, tmp1, tmp2, tmp3, C1, C2, C3, C4, C5, C6;
float Fsat, SSgainnopump[1002], Gainnopump[1002], flugainnopump[1002];
float delta, Nmax, intarea, intarea2, ra[4002], rb[4002];
float Eout[1002], Etot[1002][1002], Energyavailable[1002], Energytotavail[1002][1002];
/********************** Printing, reading, writing and file creation routines **********************/

void errexit() /* This routine exits program when error occurs */
{
    printf("\n\n!!!!!!!ERROR!!!!!!\n\n");
    printf("Now exiting to system\n\n");
    exit(0);
}

int filecreation()
{
    stop = 0;
    for(i=0;i<20;i++)
    {
        if(swap[i] == NULL) break;
        fname[i] = swap[i];
    }
    stop = i;
    for(i=0;i<20;i++)
    {
        if(run[i] == NULL) break;
```

```
        fname[i + stop] = run[i];
    }
    stop = stop + i;
    for(i=0;i<20;i++)
    {
        if(ext[i] == NULL) break;
        fname[i + stop] = ext[i];
    }
    return(0);
}

int readxy() /* Routine to read a 2 column, space delimited file (max 4000 pts) w/ data in arrays x[i], y[i] */
{
    char buf[100];
    infile = fopen(fname, "r+") ;
    pts = 0 ;
    while(fgets(buf, 100, infile) != (NULL)) pts = pts + 1 ;
    pts = pts + 1;
    fclose(infile) ;
    if(pts < 1 || pts>4000)
    {
        printf("\n!!!! ERROR !!!!\n\nTHE DATA FILE DID NOT OPEN CORRECTLY\n");
        printf("\nOR THE NUMBER OF POINTS IS TOO LARGE\n");
        printf("\nPRESS RETURN TO CONTINUE\n");
        errexit();
    }
    infile = fopen(fname, "r+");
    for(i=0;i<pts;i++) fscanf(infile, "%G %G", &x[i], &y[i]);
    fclose(infile);
    delta = x[1] - x[0];
    return(0);
}

int normy() /* This routine normalizes input y[i] of (x,y) data */
{
    intarea = 0.0;
    for(i=0;i<pts;i++)  intarea = intarea + y[i] * (delta);
    for(i=0;i<pts;i++) y[i] = y[i] / intarea;
    return(0);
}

int readxyy() /* Routine reads a 3 column, space delimited file (max 4000 pts) in arrays x1[i], yp[i], ys[i] */

{
    char buf[100];
    infile = fopen(fname, "r+") ;
    pts = 0 ;
    while(fgets(buf, 100, infile) != (NULL)) pts = pts + 1 ;
    pts = pts + 1;
    fclose(infile) ;
    if(pts < 1 || pts>4000)
    {
        printf("\n!!!! ERROR !!!!\n\nTHE DATA FILE DID NOT OPEN CORRECTLY\n");
        printf("\nOR THE NUMBER OF POINTS IS TOO LARGE\n");
        printf("\nPRESS RETURN TO CONTINUE\n");
        errexit();
```

```
    }
    infile = fopen(fname, "r+");
    for(i=0;i<pts;i++) fscanf(infile, "%G %G %G", &x1[i], &yp[i], &ys[i]);
    fclose(infile);
    delta = x[1] - x[0];
    return(0);
}

int readxyz() /* Routine to read a 3 column, space delimited file (max 500 pts) w/ data in arrays x[i], y[i] */
{
    char buf[100];
    infile = fopen(fname, "r+") ;
    pts = 0 ;
    while(fgets(buf, 100, infile) != (NULL)) pts = pts + 1 ;
    fclose(infile) ;
    if(pts < 1 || pts>500)
    {
        printf("\n!!!! ERROR !!!!\n\nTHE DATA FILE DID NOT OPEN CORRECTLY\n");
        printf("\nOR THE NUMBER OF POINTS IS TOO LARGE\n");
        printf("\nPRESS RETURN TO CONTINUE\n");
        errexit();
    }
    infile = fopen(fname, "r+");
    for(i=0;i<pts;i++) fscanf(infile, "%G %G %G", &x[i], &y[i], &zp[i]);
    fclose(infile);
    return(0);
}

int shellamplitude()  /* Prints probe beam spatial shell parameters */
{
    for(i=0;i<20;i++) swap[i] = amp[i];
    filecreation();
    outfile = fopen(fname, "w+") ;
    for(m=1;m<radius_pts+1;m++)  fprintf(outfile, "%G %G %G %G %G %G \n", ra[m], rb[m],
shell_area[m], shell_volume[m], shell_fraction[m], totalvolume);
    fclose(outfile);
    return(0);
}

int ssgainprint()  /* Prints out gain vs. fluence file */
{
    for(i=0;i<20;i++) swap[i] = ssgainfil[i];
    filecreation();
    outfile = fopen(fname, "w+") ;
    for(k=0; k < Ipump_pts; k++)fprintf(outfile, "%G %G %G \n", Flu_pump[k], SSgain[k],
    SSgainnopump[k]);
    fclose(outfile);
    return(0);
}

int gainprint()  /* Prints out gain vs. fluence file */
{
    for(i=0;i<20;i++) swap[i] = gainfil[i];
    filecreation();
    outfile = fopen(fname, "w+") ;
    if (optimize == 'y')
```

```
    {
        for(k=0; k < Ipump_pts; k++) fprintf(outfile, "%G %G %G %G \n", Flu_pump[k],
Energy_probe[k], Gain[k][k], SSgain[k]);
    }
    else
    {
        for(k=0; k < Ipump_pts; k++)
        {
            for(l=1;l < Eprobe_pts+1; l++) fprintf(outfile, "%G %G %G %G %G %G \n", Flu_pump[k],
Energy_probe[l], Gain[k][l], Energyavailable[k], Etot[k][l], Energytotavail[k][l]);
        }
    }
    fclose(outfile);
    return(0);
}

int flugainprint()  /* Prints out gain vs. fluence file */
{
    for(i=0;i<20;i++) swap[i] = fgainfil[i];
    filecreation();
    outfile = fopen(fname, "w+") ;
    if(optimize == 'y')
    {
        for(k=0; k < Ipump_pts; k++) fprintf(outfile, "%G %G %G \n", Flu_pump[k], Fluprobe[k],
Flugain[k][k]);
    }
    else
    {
        for(k=0; k < Ipump_pts; k++)
        {
            for(l=1;l < Eprobe_pts+1; l++)  fprintf(outfile, "%G %G %G \n", Flu_pump[k], Fluprobe[l],
Flugain[k][l]);
        }
    }
    fclose(outfile);
    return(0);
}

int fluprint()  /* Prints out transmission, fluorescence, and Nex (Flu, T, Fluor, Nex) file */
{
    for(i=0;i<20;i++) swap[i] = fluout[i];
    filecreation();
    outfile = fopen(fname, "w+");
    for(k=0;k < Ipump_pts; k++) fprintf(outfile, "%G %G %G %G \n", Flu_pump[k], Trans[k], Fluor[k],
N3ave_in[k]);
    fclose(outfile);
    return(0);
}

int pumprint()  /* Prints pump output temporal profile (t, Ipump) file */
{
    for(i=0;i<20;i++) swap[i] = pumpout[i];
    filecreation();
    outfile = fopen(fname, "w+");
    for(i=0;i < tpts; i++) fprintf(outfile, "%G %G \n", t[i], Ipump[i]);
    fclose(outfile);
```

```
    return(0);
}

int n_vs_t() /* Prints a file of populations versus time (t, N1t, N3t) */
{
    for(i=0;i<20;i++) swap[i] = n3vst[i];
    filecreation();
    outfile = fopen(fname, "w+");
    for(i=0;i<tpts;i++)
    {
        N1t[i] = 0;
        N3t[i] = 0;
        for(j=0;j<zpts;j++)
        {
            N1t[i] = N1t[i] + N1[i][j]*delz ;
            N3t[i] = N3t[i] + N3[i][j]*delz ;
        }
        fprintf(outfile, "%G %G %G \n", t[i], N1t[i], N3t[i]);
    }
    fclose(outfile);
    return(0);
}

int n_vs_z() /* Prints a file of populations versus space (z, N3z) */
{
    for(i=0;i<20;i++) swap[i] = n3vsz[i];
    filecreation();
    outfile = fopen(fname, "w+");
    for(j=0;j<zpts;j++) fprintf(outfile, "%G %G \n", z[j], N3z_in[j]);
    fclose(outfile);
    return(0);
}

int par()  /* Prints the parameters of this calculation to a file */
{
    for(i=0;i<20;i++) fname[i] = param[i];
    outfile = fopen(fname, "a+") ;
    fprintf(outfile, "%s, %s, ", run, material);
    fprintf(outfile, "%c, %c, %c, %c, %c, %c, %c \n", tst1, tst2, tst3, pumppass, probepass, pumpsp,
probesp);
    fprintf(outfile, "%G, %G, %G, %G, %G, %G, %G \n", Fpump_0, Emax, stepfactor_pump, widthpump,
widthprobe, ABS_peak, EM_peak);
    fprintf(outfile, "%G, %G, %G, %G, %G, %G, %G, %G \n", pumpwav, probewav, N1_t0, d, scatter,
Rpump1, Rprobe1, tau);
    fprintf(outfile, "%G, %G, %G, %.3G, %.3G, %.3G, %.3G \n", probe_wa, probe_wb, radius_stepratio,
ABSpump, EMpump, ABSprobe, EMprobe);
    fprintf(outfile, "%d, %d, %d, %d, %d, %G \n", time_pumppoints, zpts, Ipump_pts, Eprobe_pts,
radius_pts, SSgainnopump[1]);
    fprintf(outfile, "\n \n \n");
    fprintf(outfile, "%G, %G, %G \n", Fsat, gpts, T1N);
    fclose(outfile);
    return(0);
}
```

```
/************************************ Main ******************************************/
main()
{
    if (optimize == 'y')
    {
        for(i=0;i<20;i++)fname[i] = gaindata[i];
        readxyz();
        Ipump_pts = pts;
        for(i=0;i<Ipump_pts;i++)
        {
            Gaindat[i] = x[i];
            Flupumpdat[i] = y[i];
            Eprobedat[i] = zp[i];
            /* printf("%G, %G, %G \n", Gaindat[i], Flupumpdat[i], Eprobedat[i]); */
        }
    }
    printf("This program calculates the fractional transmission for the pump wavelength \n");
    printf("for an arbitrary temporal profile with pump depletion due to ground state \n");
    printf("absorption, and pulsed extraction for an arbitrary probe spatial and temporal \n");
    printf("profile.  Output is automatically a Gain vs. Pump Fluence and Probe Energy \n");
    printf("(fluence) file, and and optional Transmission, Fluorescence, and N3 vs. \n");
    printf("fluence, transmitted pump intensity, N1, and N3 vs. time, N3 vs. z, and a \n");
    printf("parameter.dat file that lists all constants used.  All files are space \n");
    printf("delimited, with crystal and run number attached.  Units are in J, cm, and s.\n");
    printf("NO ASE or reabsorption is included.  Please input the run number:  ");
    scanf("%s", &run);
    getchar();
    printf("\n \n \n \n \n %d Total Pump Fluence Points", Ipump_pts);
    printf("\n %d Total Probe Energy Points", Eprobe_pts);
    printf("\n   Probe Energy Points Left");
    printf("\n   Pump Fluence Points Left");

    /*************** Define single or double pass pumping and reflectivities *****************/

    if(pumppass == 's') Rpump2 = Rpump1;/* single pass pumping */
    if(pumppass == 'd') Rpump2 = 0.95; /* double pass pumping */

    if(pumppass == 's') Rprobe2 = Rprobe1;/* single pass probe */
    if(pumppass == 'd') Rprobe2 = 0.95; /* double pass probe */

    /************************* Define the input pump pulse shape *************************/

    if(tst1 == 'e')
    {
        for(i=0;i<20;i++)fname[i] = pumpext[i];
        readxy();
        normy();
        tpts = pts;
        for(i=0;i<tpts;i++)
        {
            t[i] = x[i];
            Ipump[i] = y[i];
        }
        delt = delta;
    }
    else
```

```
{
    tpts = time_pumppoints;
    delt = 4*widthpump/tpts;
    offset = int(0.5*tpts);
    if(tpts>4000) errexit();
    if(tst1 == ‘g’) /* where width is 1/e */
    {
        for(i=0;i<tpts;i++)
        {
            t[i] = (i-offset) * delt;
            Ipump_0 = 1 / (0.886 * widthpump);
            Ipump[i] = Ipump_0 * exp(-4*(t[i]/widthpump) * (t[i]/widthpump));
        }
    }
    else  /* tst1 == “s”  */
    {
        for(i=0;i<tpts;i++)
        {
            t[i] = (i-offset) * delt;
            Ipump[i] = 0.0;
            Ipump_0 = 1 / widthpump;
            if((t[i] >= 0) && (t[i] <= widthpump)) Ipump[i] =  Ipump_0;
        }
    }
    /* Prints the internally generated input pulse to a file */
    for(i=0;i<20;i++) swap[i] = pumpin[i];
    filecreation();
    infile = fopen(fname, “w+”) ;
    for (i=1;i<tpts;i++) fprintf(infile, “\n %G %G”, t[i], Ipump[i]);
    fclose(infile);
}
for(i=0;i<tpts;i++)
{
    Ipump_inc[i] = Ipump[i];
    Ipump_tmp[i] = Ipump_inc[i];
}

/******* Break probe beam into concentric shells with constant amplitude (fluence) **********/
totalvolume = 0;
ra[0] = 0;
rb[0] = 0;
for(m=1;m<radius_pts+1;m++)
{
    ra[m] = m*probe_wa/radius_stepratio;
    rb[m] = m*probe_wb/radius_stepratio;
    if(tst3 == ‘g’)
    {
        amplitude[m] = exp(-(2*ra[m]*ra[m])/(probe_wa*probe_wa));
    }
    else /* (tst = ‘s’) */
    {
        amplitude[m] = 0;
        if(m <= radius_stepratio) amplitude[m] = 1;
    }
    shell_area[m] = M_PI*ra[m]*rb[m] - M_PI*ra[m-1]*rb[m-1];
    shell_volume[m] = shell_area[m]*amplitude[m];
```

```
    totalvolume = totalvolume + shell_volume[m];
}
for(m=1;m<radius_pts+1;m++)
{
    shell_fraction[m]=shell_volume[m]/totalvolume;
    /* shell_fraction[m] = amplitude[m]/shell_area[m];*/
}
shellamplitude();
/***************************** Define the spatial slicing *************************/

delz = d/(float)zpts;  /* thickness of z slice */
for(j = 0; j <zpts; j++) z[j] = (float)j * delz;

/********************** start of main calculation section ****************************/

/* Define cross sections and a few useful consants */

/* Reading absorption cross section file */
for(i=0;i<20;i++)fname[i] = absfile[i];
readxyy();
for(i=0;i<pts;i++) yp[i] = yp[i] / (abpeak_p);
for(i=0;i<pts;i++) ys[i] = ys[i] / (abpeak_s);
abpts = pts;

/* Now define the absorption cross sections at pump and probe wavelengths */
for(i=0;i<abpts;i++) if(x1[i]>pumpwav) break;
if(pumpsp== 'p') ABSpump = yp[i-1] + (pumpwav-x1[i-1])*(yp[i]-yp[i-1])/(x1[i]-x1[i-1]);
if(pumpsp== 's') ABSpump = ys[i-1] + (pumpwav-x1[i-1])*(ys[i]-ys[i-1])/(x1[i]-x1[i-1]);
for(i=0;i<abpts;i++) if(x1[i]>probewav) break;
if(probesp== 'p') ABSprobe = yp[i-1] + (probewav-x1[i-1])*(yp[i]-yp[i-1])/(x1[i]-x1[i-1]);
if(probesp== 's') ABSprobe = ys[i-1] + (probewav-x1[i-1])*(ys[i]-ys[i-1])/(x1[i]-x1[i-1]);
ABSpump = ABSpump*ABS_peak;
ABSprobe = ABSprobe*ABS_peak;

/* Reading emission cross section file */
for(i=0;i<20;i++)fname[i] = emfile[i];
readxyy();
for(i=0;i<pts;i++) yp[i] = yp[i] / (empeak_p);
for(i=0;i<pts;i++) ys[i] = ys[i] / (empeak_s);
empts = pts;

/* Now define the emission cross sections at pump and probe wavelengths */
for(i=0;i<empts;i++) if(x1[i]>pumpwav) break;
if(pumpsp== 'p') EMpump = yp[i-1] + (pumpwav-x1[i-1])*(yp[i]-yp[i-1])/(x1[i]-x1[i-1]);
if(pumpsp== 's') EMpump = ys[i-1] + (pumpwav-x1[i-1])*(ys[i]-ys[i-1])/(x1[i]-x1[i-1]);
for(i=0;i<empts;i++) if(x1[i]>probewav) break;
if(probesp== 'p') EMprobe = yp[i-1] + (probewav-x1[i-1])*(yp[i]-yp[i-1])/(x1[i]-x1[i-1]);
if(probesp== 's') EMprobe = ys[i-1] + (probewav-x1[i-1])*(ys[i]-ys[i-1])/(x1[i]-x1[i-1]);
EMpump = EMpump*EM_peak;
EMprobe = EMprobe*EM_peak;

C1 = ABSpump *  delt * pumpwav / hc;
C2 = EMpump * delt * pumpwav / hc;
C3 = delt / tau;

/* Now start main calculation */
```

```
/* Pump Intensity loop */
for(k=0;k < Ipump_pts; k++)
{
    /******* Timer (for the impatient) *********/
    gotoxy(2,19);
    void clreol(void);
    printf("%-3d", Ipump_pts - k);
    void clreol(void);
    /*****************************************/
    if(optimize == 'y')
    {
        for(i=0;i<tpts;i++) /* for a single pump intensity point */
        {
            Ipump_inc[i] = Flupumpdat[k]*Ipump_tmp[i];
            Ipump[i] = Ipump_inc[i];
            Flu_pump[k] = Flupumpdat[k];
        }

    }
    else
    {
        if(Ipump_pts != 1) for(i=0;i<tpts;i++)
        {
            Ipump_inc[i] = Fpump_0* Ipump_tmp[i] * (k + 0.00002) / (Ipump_pts-1);
            Ipump[i] = Ipump_inc[i];
        }
        else for(i=0;i<tpts;i++) /* for a single pump intensity point */
        {
            Ipump_inc[i] = Fpump_0*Ipump_tmp[i];
            Ipump[i] = Ipump_inc[i];
        }
        if(Ipump_pts != 1) Flu_pump[k] = Fpump_0 * (k+0.0001) /(Ipump_pts -1);
        if(Ipump_pts == 1) Flu_pump[k] = Fpump_0;
    }

    /* initialize the populations before the pulse hits the first spatial slice */

    N1ave_in[k] = 0.0;
    N3ave_in[k] = 0.0;
    Fluor[k] = 0.0;

    for(j = 0; j < zpts; j++)
    {
        N1old[j] = N1_t0;
        N3old[j]  = 0.0;
    }

    for(i = 0; i < tpts; i++)  /* time loop */
    {
        if(pumppass == 's')
        {
            for(j = 0; j < zpts; j++) /* first pass spatial loop */
            {
                /* restructure the temporal pulse shape for each spatial slice */
                Ipump[i] = Ipump[i] * exp(-(N1old[j] * ABSpump + scatter) * delz);
                N1[i][j] = N1old[j] * (1 - C1 * Ipump[i] ) + C3 * N3old[j] + N3old[j] *  C2 * Ipump[i];
```

```
                N3[i][j] = N3old[j] * (1 - C3 - C2 * Ipump[i] ) + N1old[j] * C1 * Ipump[i];
                N1old[j] = N1[i][j];
                N3old[j] = N3[i][j];
                Fluor[k] =  Fluor[k] + N3old[j] / zpts / tpts;
            }/* end of first pass spatial loop */
            Ipump[i] = Ipump[i]; /* reflection from surface S2 */

        }
        if(pumppass == 'd')
        {
            for(j = 0; j < zpts; j++) /* first pass spatial loop */
            {
                /* restructure the temporal pulse shape for each spatial slice */
                Ipump[i] = Ipump[i] * exp(-(N1old[j] * ABSpump + scatter) * delz);
                N1[i][j] = N1old[j] * (1 - C1 * Ipump[i] ) + C3 * N3old[j] / 2 + N3old[j] *  C2 *
Ipump[i];
                N3[i][j] = N3old [j]* (1 - C3 / 2 - C2 * Ipump[i] ) + N1old[j] * C1 * Ipump[i];
                N1old[j] = N1[i][j];
                N3old[j] = N3[i][j];
            }/* end of first pass spatial loop */
            Ipump[i] = Ipump[i] * Rpump2; /* reflect off the second surface once */
            for(j = zpts-1; j > -1; j--) /* second pass spatial loop */
            {
                /* restructure the temporal pulse shape for each spatial slice */
                Ipump[i] = Ipump[i] * exp(-(N1old[j] * ABSpump + scatter) * delz);
                N1[i][j] = N1old[j] * (1 - C1 * Ipump[i] ) + C3*N3old[j] / 2 +N3old[j] *  C2 * Ipump[i];
                N3[i][j] = N3old [j]* (1 - C3 / 2 - C2 * Ipump[i] ) + N1old[j] * C1 * Ipump[i];
                N1old[j] = N1[i][j];
                N3old[j] = N3[i][j];
                Fluor[k] =  Fluor[k] + N3old[j] / zpts / tpts;
            }/* end of second pass spatial loop */
            Ipump[i] = Ipump[i] * (1 - Rpump1); /* reflection upon exiting surface S1 */
        }
    }  /* end of time loop */

    tpk = 0;
    Nmax = 0.0;
    for(i=0;i<tpts-1;i++)
    {
        N3ave_in[k] = 0;
        for(j = 0; j < zpts; j++)
        {
            N3ave_in[k] = N3ave_in[k] + N3[i][j] / (zpts);
        }
        if(N3ave_in[k]>Nmax)
        {
            Nmax = N3ave_in[k];
            tpk = i;
        }
    }
    N3ave_in[k] = 0;
    N1ave_in[k] = 0;
    for(j = 0; j < zpts; j++)
    {
        N1ave_in[k] = N1ave_in[k] + N1[tpk][j] / (zpts);
        N3ave_in[k] = N3ave_in[k] + N3[tpk][j] / (zpts);
```

```
            N3z_in[j] = N3[tpk-20][j];
        }
        Ntot[k] = N1ave_in[k] + N3ave_in[k];
        SSgain[k] = exp(d * N3ave_in[k] * EMprobe - d * N1ave_in[k] * ABSprobe - scatter * d);
        SSgainnopump[k] = exp(- d * N1ave_in[k] * ABSprobe - scatter * d);
        if(Ipump_pts > 1) SSgain[k] = SSgain[k]/SSgainnopump[k]; /* this normalizes the gain for
experimental conditions i.e. gain is a measure of the change in a probe signal through a crystal with vs.
without pumping */
        Energyavailable[k] = N3ave_in[k]*d*M_PI*4*probe_wa*probe_wa*hc/probewav;

        /* Calculate the fractional 900 transmission for each incident fluence from inside the crystal (i.e. no
reflectivity) */

        tmp1 = 0;
        tmp2 = 0;
        for(i=0;i<tpts;i++)
        {
            tmp1 = tmp1 + Ipump[i]*delt;
            tmp2 = tmp2 + Ipump_inc[i]*delt;
        }
        Trans[k] = tmp1/tmp2;

        /********** Now start pulsed extraction calculation **********************/

        Fsat = hc/(EMprobe*probewav);  /* Note that the degeneracy factor K has been left out for Yb */
        gpts = int(log(SSgain[k])/log(1.3)) + 1; /* factor 1.3 is assures proper gain slicing for accurate
results */
        G0N = exp((log(SSgain[k]))/gpts);
        T1N = 1;
        /* Probe Energy loop */
        if(optimize == 'y')
        {
            Energy_probe[k] = Eprobedat[k];
            Energytotavail[k][k] = Energy_probe[k] + Energyavailable[k];
            /******* Timer (for the impatient) *********/
            gotoxy(2,18);
            void clreol(void);
            printf("%-3d", Eprobe_pts + 1 - l);
            void clreol(void);
            /*****************************************/
            for(m=1; m < radius_pts+1; m++)
            {
                shell_energy[m] = Energy_probe[k]*shell_fraction[m];
                shell_fluence[m] = shell_energy[m]/shell_area[m];
                Flu_probe_out[m] = shell_fluence[m];
                if(m==1) Fluprobe[k] = shell_fluence[m];
                for(n = 1; n < (gpts + 1); n++)
                {
                    Flu_probe_out[m] = T1N*Fsat*log(1+G0N*(exp(T1N*Flu_probe_out[m]/Fsat)-1));
                }
                if(m==1)Flugain[k][k] = Flu_probe_out[m]/shell_fluence[m];
                Eout[m] = Flu_probe_out[m]*shell_area[m];
            }
            Etot[k][k] = 0;
            for(m=1;m<radius_pts+1;m++) Etot[k][k] = Etot[k][k] + Eout[m];
            Gain[k][k] = Etot[k][k]/Energy_probe[k];
```

```
            /* Losses from ground state absorption and Boltzman populated absorption included */
            /* Gain with reflection losses normalized out */
        }
        else
        {
            for(l=1;l < Eprobe_pts+1; l++)
            {
                Energy_probe[l] = (Emax*l*l)/(Eprobe_pts*Eprobe_pts);
                Energytotavail[k][l] = Energy_probe[l] + Energyavailable[k];
                /******* Timer (for the impatient) *********/
                gotoxy(2,18);
                void clreol(void);
                printf("%-3d", Eprobe_pts + 1 - l);
                void clreol(void);
                /*****************************************/
                for(m=1; m < radius_pts+1; m++)
                {
                    shell_energy[m] = Energy_probe[l]*shell_fraction[m];
                    shell_fluence[m] = shell_energy[m]/shell_area[m];
                    Flu_probe_out[m] = shell_fluence[m];
                    if(m==1)Fluprobe[l] = shell_fluence[m];
                    for(n = 1; n < (gpts + 1); n++)
                    {
                        Flu_probe_out[m] = T1N*Fsat*log(1+G0N*(exp(T1N*Flu_probe_out[m]/Fsat)-1));
                    }
                    if(m==1)Flugain[k][l] = Flu_probe_out[m]/shell_fluence[m];
                    Eout[m] = Flu_probe_out[m]*shell_area[m];
                }
                Etot[k][l] = 0;
                for(m=1;m<radius_pts+1;m++) Etot[k][l] = Etot[k][l] + Eout[m];
                Gain[k][l] = Etot[k][l]/Energy_probe[l];
                if(k==0)
                {
                    Gainnopump[l] = Gain[k][l];
                    flugainnopump[l] = Flugain[k][l];
                }
                /* Losses from ground state absorption and Boltzman populated absorption included */
                /* Gain with reflection losses normalized out */
            } /* End of Probe Energy loop */
        }

    } /* end of Pump Intensity loop */
    /****************** End of main calculation ************************************/
    /* normalization and output */
    for(k=0;k < Ipump_pts; k++) Fluor[k] = Fluor[k] / Fluor[Ipump_pts-1] ; /* normalize the fluorescence
Intensity to one at the maximum fluence. */
    if(optimize == 'y')
    {
        ssgainprint();
        gainprint();
        flugainprint();
    }
    else
    {
        if(Ipump_pts == 1)
        {
```

```
            gainprint();
            flugainprint();
            ssgainprint();
        }
        else
        {
            for(k=0;k < Ipump_pts; k++)
            {
                for(l=1;l<Eprobe_pts+1;l++)
                {
                    Gain[k][l] = Gain[k][l]/Gainnopump[l];
                    /* for(l=1;l<Eprobe_pts+1;l++) Gain[k][l] = Gain[k][l]; */
                    Flugain[k][l] = Flugain[k][l]/flugainnopump[l];
                }
            }
            ssgainprint();
            gainprint();
            flugainprint();
        }
    }
    if (fflu == 'y') fluprint(); /*Creates file of Transmission, fluorescence, N3ave_in vs. fluence. */
    if (ppout == 'y') pumprint(); /*Creates file of pump output temporal profile at max intensity */
    if (nvst == 'y') n_vs_t(); /*Creates file of N1t and n3t versus time. */
    if (nvsz == 'y') n_vs_z(); /*Creates file of N3z_in vs. z. */
    if(ppar == 'y') par(); /* Creates file with all of the parameters used in this run */
}
/*end of main*/
```

IIa: Levenberg-Marquardt-Bard Reducer

The following code is written in Borland C++ and was run on a PC running Windows 95. The code typically runs in a few minutes. This program uses the Levenberg-Marquardt-Bard method to reduce the residual error when fitting gain saturation data taken with a gaussian extraction beam and involving a two ion model (inhomogeneous extraction). This Levenberg-Marquardt-Bard algorithm was patterned on a FORTRAN subroutine written by John Trenholme, and Ken Jancaitis: begun 11/4/90, last modified 11/22/90.

```
/*Gain Saturation LMB Reducer Revision 1, Andy Bayramian, November 15, 1998,*/

/********** Arguments **********

    np - number of parameters to be adjusted for the fit
    ny - number of residuals to be minimized
    resid(j, *p) - function to calculate the j'th residual value
    p[np] - vector of parameters to be adjusted for the fit (initial guess on input, best fit values on output
    sigma[np] - estimate for errors in the best fit values of p[np]
    gradient[np] - final gradient of the least-squares sum
    *ncall - number of evaluations of the residual vector used in fit

**********/

#include "stdio.h"
#include "math.h"
#include "stdlib.h"
#include "conio.h"
```

```
/* Defining Parameters */
FILE *infile, *outfile;
char fname[20];
char run[20];
char material[20] = "Sr5-FAP";          /* Material being tested */
char gaindata[20] = "gainallSS2a.dat"; /* Experimental gain data file (gain, pump fluence, probe energy) */
char gainfil[20] = "gainouta.dat";      /* Output fit gain data */
char param[20] = "parameter.dat";       /*A printout log of the parameters used in a particular calculation */
char tst3 = 'g';                        /* Spatial probe pulse shape, can be g/s Gaussian, or Square */
char pumpsp = 'p';                      /* pump polarization (p/s) */
float EMprobe = 6.2e-20;                /* peak probe emission cross section (cm^2) */
float probewav = 1047.6;                /* Probe wavelength used in calculation (nm) */
float hc = 1.9878e-16;                  /* [h*c /(1e-9)] dividing by lambda (nm) gives hv (Joules) */
float EM1frac = 1.05;                   /* Intensity multiplier for which modifying saturation fluence */
float Nfrac = 0.6;                      /* Intensity multiplier for which modifying saturation fluence */
float probe_wa = 0.038;                 /* elliptic 1/e2 waist radii in cm */
float probe_wb = 0.039;                 /* elliptic 1/e2 waist radii in cm */
float radius_stepratio = 200;           /* Probe_wa/radius_stepratio gives radial step increment in cm */
int radius_pts = 400;                   /* Shell radius points (also probe fluence points, max = 1000 */

float totalvolume;                      /* total volume of elliptical gaussian w/ max amplitude = 1 */
float Energy_probe[1002];               /* Input probe energy */
float Gain[1002];                       /* Gain vs. probe energy and pump fluence */
float SSgain[1002];                     /* Small signal gain at specified wavelength */
float amplitude[1002];                  /* amplitude of gaussian function */

float EM1, EM2, Fsat, Fsat1, Fsat2, G1, G2, G1N, G2N, T1N, gpts;
float shell_area[1002];
float shell_volume[1002];
float shell_energy[1002];
float shell_fluence[1002];
float shell_fraction[1002];
float Flu_probe_out[1002];
float Gaindat[1002];
float Flupumpdat[1002];
float Eprobedat[1002];
float ra[4002], rb[4002];
float w[4002], x[4002], y[4002], z[4002];
float Eout[1002], Etot[1002];
double resid[1002];
double rerel[1002];
double weight[1000];

/* Tolerance for the final change in the parameter values */

long i, j, k, l, m, n, nm, m1, np, ny, ncall, pts, datapts;
double sigma[1002];
double gradient[1002];
double p[1002];
double re, ss, ssqr, diagmax, s, h, b, t;
double *a, *c, *g, *v, *d, *diag;

double big = 10.0; /* Algorithm tuning parameters */
double dec = 0.4;
double eps = 0.001;
```

```
const double tol = 0.0000001;

/**********************Printing, reading, writing and file creation routines ************************/

void errexit() /*This routine exits program when error occurs*/
{
    printf("\n\n!!!!!!!ERROR!!!!!!\n\n");
    printf("Now exiting to system\n\n");
    exit(0);
}


int readwxyz() /*Routine to read a 4 column, space delimited (w x y z), file with a maximum of 500 points
and place data in arrays w[i], x[i], y[i], z[i]*/
{
    char buf[100];
    infile = fopen(fname, "r+") ;
    pts = 0 ;
    while(fgets(buf, 100, infile) != (NULL)) pts = pts + 1 ;
    fclose(infile) ;
    if(pts < 1 || pts>500)
    {
        printf("\n!!!! ERROR !!!!\n\nTHE DATA FILE DID NOT OPEN CORRECTLY\n");
        printf("\nOR THE NUMBER OF POINTS IS TOO LARGE\n");
        printf("\nPRESS RETURN TO CONTINUE\n");
        errexit();
    }
    infile = fopen(fname, "r+");
    for(i=0;i<pts;i++) fscanf(infile, "%G %G %G %G", &w[i], &x[i], &y[i], &z[i]);
    fclose(infile);
    return(0);
}

int Shell() /* Break probe beam into concentric shells with constant amplitude (fluence) */
{
    totalvolume = 0;
    ra[0] = 0;
    rb[0] = 0;
    for(m=1;m<radius_pts+1;m++)
    {
        ra[m] = m*probe_wa/radius_stepratio;
        rb[m] = m*probe_wb/radius_stepratio;
        if(tst3 == 'g')
        {
            amplitude[m] = exp(-(2*ra[m]*ra[m])/(probe_wa*probe_wa));
        }
        else /* (tst = 's') */
        {
            amplitude[m] = 0;
            if(m <= radius_stepratio) amplitude[m] = 1;
        }
        shell_area[m] = M_PI*ra[m]*rb[m] - M_PI*ra[m-1]*rb[m-1];
        shell_volume[m] = shell_area[m]*amplitude[m];
        totalvolume = totalvolume + shell_volume[m];
    }
    for(m=1;m<radius_pts+1;m++) shell_fraction[m]=shell_volume[m]/totalvolume;
```

```
    return(0);
}

int gainsat() /*** This is the function and residual being reduced (in this case gain saturation) ***/
{
    /******* Timer (for the impatient) *********/
    gotoxy(2,14);
    void clreol(void);
    printf("%-3d", datapts - j + 1);
    void clreol(void);
    /*****************************************/
    Fsat = hc/(EMprobe*probewav);
    EM1 = EMprobe*p[0];
    EM2= (EMprobe - p[1]*EM1)/(1-p[1]);
    G1 = exp(p[1]*log(SSgain[j]));
    G2 = exp((1-p[1])*log(SSgain[j]));
    Fsat1 = Fsat*EMprobe/EM1;
    Fsat2 = Fsat*EMprobe/EM2;
    gpts = int(log(SSgain[j])/log(1.3)) + 1;
    G1N=exp((log(G1))/gpts);
    G2N=exp((log(G2))/gpts);
    T1N=1;
    Energy_probe[j] = Eprobedat[j];
    for(m=1; m < radius_pts+1; m++)/* Fluence loop */
    {
        shell_energy[m] = Energy_probe[j]*shell_fraction[m];
            shell_fluence[m] = shell_energy[m]/shell_area[m];
        Flu_probe_out[m] = shell_fluence[m];
        for(n = 1; n < (gpts + 1); n++)
            {
            Flu_probe_out[m] = T1N*Fsat1*log(1+G1N*(exp(T1N*Flu_probe_out[m]/Fsat1)-1));
            Flu_probe_out[m] = T1N*Fsat2*log(1+G2N*(exp(T1N*Flu_probe_out[m]/Fsat2)-1));
        }
        Eout[m] = Flu_probe_out[m]*shell_area[m];
    }
    Etot[j] = 0;
    for(m=1;m<radius_pts+1;m++) Etot[j] = Etot[j] + Eout[m];
    Gain[j] = Etot[j]/Energy_probe[j];/*Gain with reflection and scatter losses normalized out*/
    weight[j] = 1;
    /*resid[j] = (Gain[j] - Gaindat[j])*weight[j];*/
    resid[j] = (Gaindat[j]/Gain[j] - 1)*weight[j];
    return(0);
}

int gainprint() /*   Prints out gain vs. fluence file */
{
    for(i=0;i<20;i++) fname[i] = gainfil[i];
    outfile = fopen(fname, "w+") ;
    for(k=0; k < datapts; k++) fprintf(outfile, "%G %G %G \n", Flupumpdat[k], Energy_probe[k],
Gain[k]);
    fclose(outfile);
    return(0);
}

int par()    /* Prints the parameters of this calculation to a file*/
{
```

```
    for(i=0;i<20;i++) fname[i] = param[i];
    outfile = fopen(fname, "a+") ;
    fprintf(outfile, "%s, %s, %c, %G \n", run, material, tst3, probewav);
    fprintf(outfile, "%G, %G, %G, %.3G \n", EM1frac, Nfrac, probe_wa, probe_wb, radius_stepratio,
EMprobe);
    fprintf(outfile, "%G, %G, %G, %G, %G, %G, %G, %G, %G, %G, %G \n", Fsat, EM1, EM2, G1, G2,
Fsat1, Fsat2, gpts, G1N, G2N, T1N);
    fprintf(outfile, "%G, %G, %G, %G \n", EM1frac, p[0], Nfrac, p[1]);
    fprintf(outfile, " \n \n");
    fclose(outfile);
    return(0);
}


/**********************************Main**********************************************/
main()
{
    for(i=0;i<20;i++)fname[i] = gaindata[i];
    readwxyz();
    datapts = pts;
    for(i=0;i<datapts;i++)
    {
        Flupumpdat[i] = w[i];
        Eprobedat[i] = x[i];
        Gaindat[i] = y[i];
        SSgain[i] = z[i];
    }

    printf("This program uses the Levenberg-Marquardt method to reduce the residual \n");
    printf("error in fitting gain saturation data taken with a gaussian extraction \n");
    printf("beam.  Saturation is modeled using a two ion model.  A parameter file, \n");
    printf("'parameter.dat' lists all constants used as well as fit results.    All \n");
    printf("files are space delimited, with crystal and run number attached. \n");
    printf("Units are in J, cm, and s. Please input the run number:");
    scanf("%s", &run);
    getchar();
    printf("\n \n \n \n \n %d Total Data Points", datapts);
    printf("\n       Data Points Left to be fit");
    printf("\n       Iteration number");

/*****************************************************************************************/
    Shell(); /* break gaussian into shells of constant intensity */

    ny = datapts;
    np = 2;
    p[0] = EM1frac;
    p[1] = Nfrac;
    nm = np * (np + 1) / 2;

/* Allocate temporary space for work arrays */
    a = (double *) malloc (nm * sizeof(double));
    c = (double *) malloc (nm * sizeof(double));
    g = (double *) malloc (np * sizeof(double));
    v = (double *) malloc (np * sizeof(double));
    d = (double *) malloc (np * sizeof(double));
    diag = (double *) malloc (np * sizeof(double));
```

```
    if (!a||!c||!g||!v||!d||!diag) { printf(" Error allocating work array space\n"); exit(0); }

    /* Initializations */

    for (j = 0; j < np; j++) diag[j] = 0.001;   /* Initial diagonal */
    ncall = 0;

    do /* Main loop starts here */
    {
        /******* Timer (for the impatient) *********/
        gotoxy(2,15);
        void clreol(void);
        printf("%-3d", ncall);
        void clreol(void);
        /*****************************************/
        ss = 0.0;
        for (j = 0; j < ny; j++)
        {
            gainsat();
            re = resid[j];
            ss = ss + re * re;   /* Get sum of squares */
        }
        (ncall)++;
        if (ncall == 1) ssqr = ss * 1.000001;
        if (ss < ssqr)
        {
            /* Try closer to gradient if no decrease in sum of squares decrease diagonal elements & get new
Jacobian */
            diagmax = 0.0;
            for (j = 0; j < np; j++)
            {
                diag[j] *= dec;
                if (diagmax < diag[j]) diagmax = diag[j];
            }
            /* Find JT*J and JT * f */
            for (j = 0; j < np; j++) { v[j] = 0.0; g[j] = 0.0; }
            for (j = 0; j < nm; j++) c[j] = 0.0;
            for (j = 0; j < ny; j++)
            {
                s = resid[j];
                for (k = 0; k < np; k++)
                {
                    h = eps * (abs(p[k]) + eps);
                    b = p[k];
                    p[k] += h;
                    gainsat();
                    re = resid[j];
                    d[k] = (re - s) / h;
                    g[k] += re * re;
                    p[k] = b;
                }
                for (k = 0; k < np; k++)
                {
                    t = d[k];
                    v[k] -= t * s;
                    m = k * (k + 1 ) / 2;
```

```
                for (l = 0; l <= k; l++) c[m + l] += t * d[l];
            }
        }
        (ncall) += np + 1;
        ssqr = ss;
        for (j = 0; j < np; j++) d[j] = p[j];
    }
    else
    {
        /* Increase diagonal elements and try to solve for step */
        diagmax = 0.0;
        for (j = 0; j < np; j++)
        {
            diag[j] *= big;
            if (diag[j] <= 0.0) diag[j] = 1.0e-10;
            if (diagmax < diag[j]) diagmax = diag[j];
        }
    }
    /* Invert matrix by Choleski decomposition maybe adjust lambda components */
    for (j = 0; j < nm; j++) a[j] = c[j];
    a[0] = a[0] * (1.0 + diag[0]) + diag[0];
    for (j = 0; j < np; j++)
    {
        n = j * (j + 3) / 2 - 1;
        if (j != 0)
        {
            for (k = j; k < np; k++)
            {
                m = k * (k + 1) / 2 - 1 + j; m1 = m + 1; s = 0.0;
                for (l = 0; l < j; l++) s += a[m - l] * a[n - l];
                t = a[m1];
                if (j >= k)
                {
                    t = a[m1] * (1.0 + diag[j]) + diag[j];
                    while (t <= s)
                    {
                        diag[j] = (s - a[m1]) / (1.0 + a[m1]) * big;
                        if (diag[j] < 1.0e-10) diag[j] = 1.0e-10;
                        t = a[m1] * (1.0 + diag[j]) + diag[j];
                    }
                }
                a[m1] = t - s;
            }
        }
        s = 1.0 / sqrt(a[n + 1]);
        for (k = j; k < np; k++){ m = k * (k + 1) / 2 + j; a[m] *=s; }
    }
    /* Forward and back substitute to solve equations for step */
    for (j = 0; j < np; j++) g[j] = v[j];
    g[0] /= a[0];
    if (np != 1)
    {
        n = 0;
        for (j = 1; j < np; j++)
        {
            for (k = 0; k < j; k++) { n++; g[j] -= a[n] * g[k]; }
```

```
                n++; g[j] /= a[n];
            }
        }
        g[np - 1] = g[np - 1] / a[nm - 1];
        if (np != 1)
        {
            for (j = np - 1; j > 0; j--)
            {
                n = j * (j + 1) / 2;
                for (k = 0; k < j; k++) g[k] -= g[j] * a[n + k];
                g[j-1] /= a[n - 1];
            }
        }
        /* Make the step and test for convergence */
        m = 0;
        for (j = 0; j < np; j++)
        {
            p[j] = d[j] + g[j];
            if (fabs(g[j] / p[j]) < tol) m++;
        }
    } while ((m < np) && (diagmax <= 1.0e+20));

    /* Converged to machine precision - finish up -- Bauer-Reinsch inversion of Jacobian */

    ss = ssqr / (ny - np);
    for (k = np - 1; k >= 0; k--)
    {
        m = 0;
        if (c[0] != 0.0) s = 1.0 / c[0]; else s = 1.0e+10;
        for (l = 1; l < np; l++)
        {
            n = m; m += l + 1; t = c[n + 1];
            if (l > k) g[l] = t * s; else g[l] = -t * s;
            for (j = n + 1; j < m; j++) c[j - l] = c[j + 1] + t * g[j - n];
        }
        c[m] = s;
        for (l = 1; l < np; l++) c[n + l] = g[l];
    }
    for ( j = 0; j < np; j++)
    {
        s = ss * c[j * (j + 3) / 2];
        if (s >= 0.0) sigma[j] = sqrt(s); else sigma[j] = 1000.0;
        gradient[j] = v[j];
    }
    free(a); free(c); free(g); free(v); free(d); free(diag);
    for(i = 1;i<100;i++) printf("Hello \n");
    gainprint();
    par();   /* Creates file with all of the parameters used in this run */
}
/*end of main*/
```

IIIa: SRS loss in Mercury

This is a Visualbasic code which is linked to a set of Excel spreadsheets and is run on a PC running Windows 95 and using Excel 97. This routine calculates the Mercury output energy versus pulse length such that the Stimulated Raman Scattering is at threshold (defined as 1% conversion of the laser energy). The spreadsheets used are named: SRS (which contains all of the input parameters), flu0.00x (where x = 1, 25, or 5 and contains the Mercury fluence levels for different reflectivities of the anti-reflection coatings on the S-FAP for a whole set of input fluences), and head (which contains the output of the code). Note that Mercury fluences are calculated using the code given in Appendix IIId, IIIe, and IIIf.

```
Sub SRSMercury()
'
'Main Macro
'Andy Bayramian 10/14/98
' Keyboard Shortcut: Ctrl+u

'**************SRS declarations and initializations******************
Const pts = 100 'number of data points
Const Tpts = 2000 'number of time pulse points
Const thresh = 0.01 'threshold SRS requirement = fraction of input pump energy

'pulse = 0.00000000195
frac = 0.000000000005

Dim Energyin(3001)
Dim SRSout(3001)
Dim pulseout(3001)
Dim Threshold(3001)
Dim SRSenergy(3001)

'*********SRS gain loop*****************************************
For g = 0 To 3 Step 1
    edge = Sqr(10 ^ g)
    Worksheets("SRS").Cells(59, 2).Value = edge
    Worksheets("SRS").Cells(60, 2).Value = edge
    Worksheets("head").Cells(2, (3 * g + 3)).Value = edge ^ 2
    Worksheets("SRS").Cells(63, 2).Value = 0.9975
    'SRSgaincoeff = 0.0012 + g * 0.0001
    'Worksheets("SRS").Cells(3, 2).Value = SRSgaincoeff
    'Worksheets("head").Cells(2, (3 * g + 3)).Value = SRSgaincoeff
    'Worksheets("SRS").Cells(63, 2).Value = 0.9975
    'If g = 0 Then ARreflect = 0.999
    'If g = 1 Then ARreflect = 0.9975
    'If g = 2 Then ARreflect = 0.995
    'Worksheets("SRS").Cells(3, 2).Value = 0.0013
    'Worksheets("SRS").Cells(63, 2).Value = ARreflect
    'Worksheets("head").Cells(2, (3 * g + 3)).Value = ARreflect

    pulse = 0.00000000005
    For p = 1 To pts Step 1
        For j = 0 To 840 Step 1
            'If g = 0 Then Worksheets("SRS").Cells(3 + j, 6).Value = Worksheets("flu0.001").Cells(3 + j, 2
+ p).Value
            'If g = 1 Then Worksheets("SRS").Cells(3 + j, 6).Value = Worksheets("flu0.0025").Cells(3 + j, 2
+ p).Value
```

```
            'If g = 2 Then Worksheets("SRS").Cells(3 + j, 6).Value = Worksheets("flu0.005").Cells(3 + j, 2
+ p).Value
            Worksheets("SRS").Cells(3 + j, 6).Value = Worksheets("flu0.0025").Cells(3 + j, 2 + p).Value
        Next j
        Energyin(p) = Worksheets("SRS").Cells(5, 2).Value
        Threshold(p) = thresh * Energyin(p)
        For t = 1 To Tpts Step 1
            pulse = pulse + frac
            Worksheets("SRS").Cells(2, 2).Value = pulse
            zero = 0#
            For r = 1 To 7 Step 1
                SRSenergy(r) = 0#
                SRS = 0#
                Worksheets("SRS").Cells(7, 2).Value = r
                pass = Worksheets("SRS").Cells(20, 2).Value
                If pass = 0 Then
                    If r < 7 Then GoTo 5
                End If
                totpass = Worksheets("SRS").Cells(19, 2).Value
                mult = 8 - r
                cellnum = (7 - r) * 15 + 738
                gIL = 0#
                For a = cellnum To 843 Step 1
                    gIL = gIL + Worksheets("SRS").Cells(a, 9).Value
                Next a
                Worksheets("SRS").Cells(10, 2).Value = gIL
                If pass > zero Then
                    q = 0
                    resid = totpass - pass
                    For n = 1 To pass Step 1
                        tempfrac = 1 + (1 - n) / (totpass)
                        q = q + 1
                        Worksheets("SRS").Cells(26, 2).Value = q
                        passE = tempfrac * Worksheets("SRS").Cells(28, 2).Value
                        SRS = SRS + passE
                    Next n
                    tempfrac = (resid) / (totpass)
                    SRSenergy(r) = mult * (SRS + tempfrac * Worksheets("SRS").Cells(24, 2).Value)
                Else
                    q = 0
                    SRS = mult * (Worksheets("SRS").Cells(15, 2).Value)
                    SRSenergy(r) = SRS
                End If
            5Next r
            SRStot = 0#
            For r = 1 To 7 Step 1
                SRStot = SRStot + SRSenergy(r)
            Next r
            If SRStot < Threshold(p) Then
                SRSout(p) = SRStot
                pulseout(p) = pulse
                Worksheets("head").Cells(p + 2, (3 * g + 1)).Value = pulseout(p)
                Worksheets("head").Cells(p + 2, (3 * g + 2)).Value = Energyin(p)
                Worksheets("head").Cells(p + 2, (3 * g + 3)).Value = SRSout(p)
                pulse = pulse - frac
                GoTo 10
```

```
            End If
        Next t
    10 Next p
Next g
End Sub 'SRSMercury
```

IIIa1 (Example spreadsheet associated with IIIa)

	A	B	C	D	E
1	1047 nm Beam Parameters			distance	distance
2	pulsewidth (s)	4.40E-09		normal (cm)	actual (cm)
3	g (cm/MW)	1.3000E-03		0.00	0.0000
4	delta L (cm) normal	0.0500		0.05	0.0500
5	1047 nm Output pulse energy (J)	99.3814		0.10	0.1000
6	Threshold for SRS	0.9938		0.15	0.1500
7	# slabs	7.0		0.20	0.2000
8	# gaps	6.0		0.25	0.2500
9	7.1857	738		0.30	0.3000
10	gIL (or slabs thereof last head)	7.185700		0.35	0.3500
11	fraction of total gIL	0.6579		0.40	0.4000
12	Length (cm)	9.0735		0.45	0.4500
13	# modes	3.2751E+10		0.50	0.5000
14	# photons after gain	4.0671E+13		0.55	0.5500
15	SRS energy (J) from all modes	6.9490E-06		0.60	0.6000
16				0.65	0.6500
17	reflection from surface	0.0025		0.70	0.7000
18	transmission of head	0.9405		0.75	0.7500
19	Length multiplier	14.5479		0.80	0.8000
20	number of reflections for pulse	14.0000		0.85	0.8500
21	Loss after all reflections	1.525760E-37		0.90	0.9000
22	# modes	2.8374E+08		0.95	0.9500
23	# photons after total reflections	1.0866E+17		1.00	1.0000
24	Energy in SRS after all reflections (J)	1.8565E-02		1.05	1.0500
25				1.10	1.1000
26	integer Number of passes	14.0000		1.15	1.1500
27	# photons after total reflections	9.1503E+17		1.20	1.2000
28	Energy in SRS after all reflections (J)	1.5634E-01		1.25	1.2500
29				1.30	1.3000
30	gIL (chain up to last head)	3.7792		1.35	1.3500
31	# modes	5.4469E+06		1.40	1.4000
32	# photons after gain	1.2961E+08		1.45	1.4500
33	SRS energy (J) from all modes with loss	2.2144E-11		1.50	1.5000
34				1.55	1.5500
35	gIL (last slice perp.)	9.7876		1.60	1.6000
36	Intensity (cm/MW)	1.5058E+03		1.65	1.6500
37	# modes	1.7746E+09		1.70	1.7000
38	# photons after gain	3.0824E+13		1.75	1.7500
39	SRS energy (J) from all modes with loss	5.2665E-06		1.80	1.8000
40				1.85	1.8500
41	gIL (whole chain)	10.9218		1.90	1.9000
42	T2 (Raman lifetime 1/pDn)	3.7900E-12		1.95	1.9500
43	Area of beam (cm^2)	15.0000		2.00	2.0000
44	Length (cm)	5.8500		2.05	2.0500
45	Pinhole radius (cm)	0.2		2.10	2.1000
46	focal length (cm)	50		2.15	2.1500
47	# modes	1.8848E+06		2.20	2.2000
48	# photons after gain	1.0436E+11		2.25	2.2500

	A	B	C	D	E
49	Transmission of chain	0.5099		2.30	2.3000
50	SRS energy (J) from all modes with loss	9.0910E-09		2.35	2.3500
51				2.40	2.4000
52	index of S-FAP	1.6140		2.45	2.4500
53	index of surroundings	1.0000		2.50	2.5000
54	angle of incidence (radians)	0.0000		2.55	2.5500
55	angle in S-FAP (radians)	0.0000		2.60	2.6000
56	delta L (cm) actual	0.0500		2.65	2.6500
57	slab thickness (cm)	0.75		2.70	2.7000
58	gap thickness (cm)	0.1		2.75	2.7500
59	Slab width (cm)	5		2.80	2.8000
60	Slab height (cm)	3		2.85	2.8500
61	Losses			2.90	2.9000
62	Bulk S-FAP loss	0.0050		2.95	2.9500
63	S-FAP surface transmission	0.9975		3.00	3.0000
64	Window transmission	0.9975		3.05	3.0500
65	Lens transmission	0.9975		3.10	3.1000
66	Mirror transmission	0.9950		3.15	3.1500
67				3.20	3.2000
68	c (m/s)	3.0000E+08		3.25	3.2500
69	h (J s)	6.6260E-34		3.30	3.3000
70	laser wavelength (m)	1.0476E-06		3.35	3.3500
71	stokes wavelength (m)	1.1634E-06		3.40	3.4000
72	anti-stokes wavelength (m)	9.5275E-07		3.45	3.4500
73	shift (cm-1)	950.3000		3.50	3.5000
74	laser wavenumber (cm-1)	9545.6281		3.55	3.5500
75	stokes wavenumber (cm-1)	8595.3281		3.60	3.6000
76	anti-stokes wavenumber (cm-1)	10495.9281		3.65	3.6500
77	laser photon energy (J)	1.8975E-19		3.70	3.7000
78	stokes photon energy (J)	1.7086E-19		3.75	3.7500
79	anti-stokes photon energy (J)	2.0864E-19		3.80	3.8000

Continued

	F	G	H	I	J
1	Fluence	inc intensity	bandwidth	g *I*dL	Total
2	(J/cm2)	(MW/cm2)	modifier		g*I*L
3	4.5E-05	1.0296E-02	1.00	0.0000E+00	0.0000E+00
4	4.6E-05	1.0508E-02	1.00	6.8302E-07	6.8302E-07
5	4.7E-05	1.0720E-02	1.00	6.9682E-07	1.3798E-06
6	4.8E-05	1.0933E-02	1.00	7.1062E-07	2.0905E-06
7	4.9E-05	1.1145E-02	1.00	7.2443E-07	2.8149E-06
8	5E-05	1.1357E-02	1.00	7.3823E-07	3.5531E-06
9	5.1E-05	1.1570E-02	1.00	7.5203E-07	4.3051E-06
10	5.2E-05	1.1782E-02	1.00	7.6584E-07	5.0710E-06
11	5.3E-05	1.1994E-02	1.00	7.7964E-07	5.8506E-06
12	5.4E-05	1.2207E-02	1.00	7.9344E-07	6.6441E-06
13	5.5E-05	1.2419E-02	1.00	8.0725E-07	7.4513E-06
14	5.6E-05	1.2632E-02	1.00	8.2105E-07	8.2724E-06
15	5.7E-05	1.2844E-02	1.00	8.3485E-07	9.1072E-06
16	5.7E-05	1.3056E-02	1.00	8.4865E-07	9.9559E-06
17	5.8E-05	1.3269E-02	1.00	8.6246E-07	1.0818E-05
18	5.9E-05	1.3481E-02	1.00	8.7626E-07	1.1695E-05
19	6E-05	1.3616E-02	1.00	8.8502E-07	1.2580E-05
20	6.1E-05	1.3885E-02	1.00	9.0252E-07	1.3482E-05
21	6.2E-05	1.4154E-02	1.00	9.2002E-07	1.4402E-05
22	6.3E-05	1.4423E-02	1.00	9.3752E-07	1.5340E-05
23	6.5E-05	1.4693E-02	1.00	9.5502E-07	1.6295E-05
24	6.6E-05	1.4962E-02	1.00	9.7251E-07	1.7267E-05
25	6.7E-05	1.5231E-02	1.00	9.9001E-07	1.8257E-05
26	6.8E-05	1.5500E-02	1.00	1.0075E-06	1.9265E-05
27	6.9E-05	1.5769E-02	1.00	1.0250E-06	2.0290E-05
28	7.1E-05	1.6039E-02	1.00	1.0425E-06	2.1332E-05
29	7.2E-05	1.6308E-02	1.00	1.0600E-06	2.2392E-05
30	7.3E-05	1.6577E-02	1.00	1.0775E-06	2.3470E-05
31	7.4E-05	1.6846E-02	1.00	1.0950E-06	2.4565E-05
32	7.5E-05	1.7115E-02	1.00	1.1125E-06	2.5677E-05
33	7.6E-05	1.7385E-02	1.00	1.1300E-06	2.6807E-05
34	7.7E-05	1.7540E-02	1.00	1.1401E-06	2.7947E-05
35	7.9E-05	1.7870E-02	1.00	1.1615E-06	2.9109E-05
36	8E-05	1.8199E-02	1.00	1.1829E-06	3.0292E-05
37	8.2E-05	1.8528E-02	1.00	1.2043E-06	3.1496E-05
38	8.3E-05	1.8857E-02	1.00	1.2257E-06	3.2722E-05
39	8.4E-05	1.9186E-02	1.00	1.2471E-06	3.3969E-05
40	8.6E-05	1.9515E-02	1.00	1.2685E-06	3.5237E-05
41	8.7E-05	1.9845E-02	1.00	1.2899E-06	3.6527E-05
42	8.9E-05	2.0174E-02	1.00	1.3113E-06	3.7839E-05
43	9E-05	2.0503E-02	1.00	1.3327E-06	3.9171E-05
44	9.2E-05	2.0832E-02	1.00	1.3541E-06	4.0525E-05
45	9.3E-05	2.1161E-02	1.00	1.3755E-06	4.1901E-05
46	9.5E-05	2.1490E-02	1.00	1.3969E-06	4.3298E-05
47	9.6E-05	2.1820E-02	1.00	1.4183E-06	4.4716E-05
48	9.7E-05	2.2149E-02	1.00	1.4397E-06	4.6156E-05

	F	G	H	I	J
49	9.8E-05	2.2308E-02	1.00	1.4500E-06	4.7606E-05
50	1E-04	2.2687E-02	1.00	1.4747E-06	4.9080E-05
51	0.0001	2.3067E-02	1.00	1.4993E-06	5.0580E-05
52	0.0001	2.3446E-02	1.00	1.5240E-06	5.2104E-05
53	0.0001	2.3826E-02	1.00	1.5487E-06	5.3652E-05
54	0.00011	2.4206E-02	1.00	1.5734E-06	5.5226E-05
55	0.00011	2.4585E-02	1.00	1.5980E-06	5.6824E-05
56	0.00011	2.4965E-02	1.00	1.6227E-06	5.8447E-05
57	0.00011	2.5344E-02	1.00	1.6474E-06	6.0094E-05
58	0.00011	2.5724E-02	1.00	1.6721E-06	6.1766E-05
59	0.00011	2.6104E-02	1.00	1.6967E-06	6.3463E-05
60	0.00012	2.6483E-02	1.00	1.7214E-06	6.5184E-05
61	0.00012	2.6863E-02	1.00	1.7461E-06	6.6930E-05
62	0.00012	2.7242E-02	1.00	1.7708E-06	6.8701E-05
63	0.00012	2.7622E-02	1.00	1.7954E-06	7.0496E-05
64	0.00012	2.7870E-02	1.00	1.8115E-06	7.2308E-05
65	0.00012	2.8393E-02	1.00	1.8455E-06	7.4154E-05
66	0.00013	2.8916E-02	1.00	1.8795E-06	7.6033E-05
67	0.00013	2.9439E-02	1.00	1.9135E-06	7.7947E-05
68	0.00013	2.9962E-02	1.00	1.9475E-06	7.9894E-05
69	0.00013	3.0485E-02	1.00	1.9815E-06	8.1876E-05
70	0.00014	3.1008E-02	1.00	2.0155E-06	8.3891E-05
71	0.00014	3.1531E-02	1.00	2.0495E-06	8.5941E-05
72	0.00014	3.2054E-02	1.00	2.0835E-06	8.8024E-05
73	0.00014	3.2577E-02	1.00	2.1175E-06	9.0142E-05
74	0.00015	3.3100E-02	1.00	2.1515E-06	9.2293E-05
75	0.00015	3.3623E-02	1.00	2.1855E-06	9.4479E-05
76	0.00015	3.4146E-02	1.00	2.2195E-06	9.6698E-05
77	0.00015	3.4669E-02	1.00	2.2535E-06	9.8952E-05
78	0.00015	3.5192E-02	1.00	2.2875E-06	1.0124E-04
79	0.00016	3.5544E-02	1.00	2.3103E-06	1.0355E-04

↓Continued↓

IIIb: SRS loss with bandwidth in Mercury

This is a Visualbasic code which is linked to a set of Excel spreadsheets and is run on a PC running Windows 95 and using Excel 97. This routine calculates the Mercury output energy versus pulse length such that the Stimulated Raman Scattering is at threshold (defined as 1% conversion of the laser energy) for a variety of input bandwidths. The spreadsheets used are named: SRS (which contains all of the input parameters), XGHz (where x = 4,60,200,300, or 684 and contain the Mercury fluence levels for different input bandwidths for Mercury for a whole set of input fluences), Raman Lorentzian (which contains bandwidth information about the Raman transition, and head (which contains the output of the code). Note that Mercury fluences are calculated using the code given in Appendix IIId, IIIe, and IIIf.

```
Sub SRSMercuryband()
'
'Main Macro
'Andy Bayramian 10/14/98
' Keyboard Shortcut: Ctrl+u
'
'This routine calculates the Mercury output energy versus pulse length such that the Stimulated
'Raman Scattering (SRS) is at threshold

'**************SRS declarations and initializations******************
Const pts = 100 'number of data points
Const Tpts = 2000 'number of time pulse points
Const thresh = 0.01 'threshold SRS requirement = fraction of input pump energy

frac = 0.000000000001

Dim Energyin(3001)
Dim SRSout(3001)
Dim pulseout(3001)
Dim Threshold(3001)
Dim SRSenergy(3001)

'*****************SRS gain loop*****************************************
Index = Worksheets("SRS").Cells(52, 2).Value
lorwidth = (2.8) * (30000000000#)
pulse = 0.000000000028
For b = 0 To 3 Step 1
    pulse = 0.000000000028
    If b = 0 Then bandsheet = "60GHz"
    If b = 1 Then bandsheet = "200GHz"
    If b = 2 Then bandsheet = "300GHz"
    If b = 3 Then bandsheet = "684GHz"
    Worksheets("head").Cells(2, 3 + 3 * b).Value = bandsheet
    For p = 1 To pts Step 1
        For j = 0 To 840 Step 1 '******Write fluences*******
            Worksheets("SRS").Cells(3 + j, 7).Value = Worksheets(bandsheet).Cells(3 + j, 2 + p).Value
        Next j
        For j = 0 To 4 Step 1 '*******Write bandwidth ratios******
            Worksheets("SRS").Cells(3 + j, 13).Value = Worksheets(bandsheet).Cells(845 + j, 2 + p).Value
        Next j
        bandwidth = Worksheets(bandsheet).Cells(854, 2 + p).Value
        Energyin(p) = Worksheets("SRS").Cells(5, 2).Value
        Threshold(p) = thresh * Energyin(p)
        For t = 1 To Tpts Step 1
```

```
            pulse = pulse + frac
            Worksheets("SRS").Cells(2, 2).Value = pulse
            zero = 0#
            For r = 1 To 7 Step 1
                SRSenergy(r) = 0#
                SRS = 0#
                Worksheets("SRS").Cells(7, 2).Value = r
                pass = Worksheets("SRS").Cells(20, 2).Value
                If pass = 0 Then
                    If r < 7 Then GoTo 5
                End If
                passtot = Worksheets("SRS").Cells(19, 2).Value
                mult = 8 - r
                cellnum = (7 - r) * 15 + 738
                gILf = 0#
                gILb = 0#
                '********gIL forward********
                For a = cellnum To 843 Step 1
                    gILf = gILf + Worksheets("SRS").Cells(a, 10).Value
                Next a
                Worksheets("SRS").Cells(10, 2).Value = gILf
                '**************************
                Ldb = (30000000000#) / (4 * Index * bandwidth)
                Ldt = 2 * Ldb
                L = (843 - celnum) * Worksheets("SRS").Cells(56, 2).Value
                pfactor = L / (gILf * Ldb)
                dfactor = lorwidth / bandwidth
                Ffactor = ((1 - (1 + dfactor) * pfactor) / 2) + Sqr(((1 - (1 + dfactor) * pfactor) / 2) ^ 2 +
dfactor * pfactor)
                Worksheets("SRS").Cells(7, 13).Value = Ffactor
                '********gIL backward*******
                For a = cellnum To 843 Step 1
                    gILb = gILb + Worksheets("SRS").Cells(a, 15).Value
                Next a
                Worksheets("SRS").Cells(10, 3).Value = gILb
                '**************************
                 If pass > zero Then
                    resid = passtot - pass
                    q = 0
                    Even = 0
                    For n = 1 To pass Step 1
                        If n / 2 = Int(n / 2) Then Even = 1
                        tempfrac = 1 + (1 - n) / (passtot)
                        If Even = 1 Then
                            gILfactor = (1 / 2) * gILb + (1 / 2) * gILf
                            Worksheets("SRS").Cells(26, 3).Value = gILfactor
                        Else '****Even = 0********
                            gILfactor = ((n - 1) / (2 * n)) * gILb + ((n + 1) / (2 * n)) * gILf
                            Worksheets("SRS").Cells(26, 3).Value = gILfactor
                        End If
                        q = q + 1
                        Worksheets("SRS").Cells(26, 2).Value = q
                        passE = tempfrac * Worksheets("SRS").Cells(28, 3).Value
                        SRS = SRS + passE
                        Even = 0
                    Next n
```

```
                    tempfrac = (resid) / (passtot)
                    If Even = 1 Then
                        gILfactor = (pass / (2 * passtot)) * gILb + (1 - pass / (2 * passtot)) * gILf
                        Worksheets("SRS").Cells(22, 3).Value = gILfactor
                    Else '****Even = 0********
                        gILfactor = (1 - (pass + 1) / (2 * passtot)) * gILb + ((pass + 1) / (2 * passtot)) * gILf
                        Worksheets("SRS").Cells(22, 3).Value = gILfactor
                    End If
                    SRSenergy(r) = mult * (SRS + tempfrac * Worksheets("SRS").Cells(24, 3).Value)
                Else
                    SRSenergy(r) = mult * (Worksheets("SRS").Cells(15, 2).Value)
                End If
            5Next r
            SRStot = 0#
            For r = 1 To 7 Step 1
                SRStot = SRStot + SRSenergy(r)
            Next r
            If SRStot < Threshold(p) Then
                SRSout(p) = SRStot
                pulseout(p) = pulse
                Worksheets("head").Cells(p + 2, 1 + 3 * b).Value = pulseout(p)
                Worksheets("head").Cells(p + 2, 2 + 3 * b).Value = Energyin(p)
                Worksheets("head").Cells(p + 2, 3 + 3 * b).Value = SRSout(p)
                pulse = pulse - frac
                GoTo 10
            End If
        Next t
    10 Next p
Next b
End Sub 'SRSMercuryband
```

IIIb1 (Example spreadsheet associated with IIIb with differences from IIIa1 shown)

	A	B	C	D
1	1047 nm Beam Parameters			
2	pulsewidth (s)	5.005E-09		
3	g (cm/MW)	0.0013		
4	delta L (cm) normal	0.05		
5	1047 nm Output pulse energy (J)	127.0226371		
6	Threshold for SRS	1.270226371		
7	# slabs	7	9.462104775	
8	# gaps	6	3.984080773	
9		738	Backward SRS	
10	gIL (or slabs thereof last head) forward	9.462104775	3.984080773	
11	fraction of total gIL	0.442114291		
12	Length (cm)	9.0735		
13	# modes	2.02935E+11		
14	# photons after gain	2.45498E+15		
15	SRS energy (J) from all modes	0.000419453		
16				
17	reflection from surface	0.0025		
18	transmission of head	0.940484916		
19	Length multiplier	16.54818978		
20	number of reflections for pulse	16		
21	Loss after all reflections	8.43454E-43	gIL factor	
22	# modes	1.74761E+11	6.797875189	
23	# photons after total reflections	1.4813E+37	1.05535E+18	
24	Energy in SRS after all reflections (J)	2.53092E+18	0.180315029	
25			gIL factor	
26	Number of passes	16	6.723092774	
27	# photons after total reflections	3.42464E+37	3.177E+18	
28	Energy in SRS after all reflections (J)	5.85126E+18	0.542814844	
29				
30	gIL (chain up to last head)	12.01353717		
31	# modes	1949082.112		
32	# photons after gain	1.74755E+11		
33	SRS energy (J) from all modes with loss	2.98583E-08		
34				
35	gIL (last slice perp.)	10.99763092		
36	Intensity (cm/MW)	1691.943218		
37	# modes	1796452247		
38	# photons after gain	1.04651E+14		
39	SRS energy (J) from all modes with loss	1.78804E-05		
40				
41	gIL (whole chain)	21.40194283		
42	T2 (Raman lifetime 1/pDn)	3.79E-12		
43	Area of beam (cm^2)	15		
44	Length (cm)	5.85		
45	Pinhole radius (cm)	0.2		
46	focal length (cm)	50		
47	# modes	1094076.86		
48	# photons after gain	2.15672E+15		

	A	B	C	D
49	Transmission of chain	0.509860349		
50	SRS energy (J) from all modes with loss	0.00018788		
51				
52	index of S-FAP	1.614		
53	index of surroundings	1		
54	angle of incidence (radians)	0		
55	angle in S-FAP (radians)	0		
56	delta L (cm) actual	0.05		
57	slab thickness (cm)	0.75		
58	gap thickness (cm)	0.1		
59	Slab width (cm)	5		
60	Slab height (cm)	3		
61	Losses			
62	Bulk S-FAP loss	0.005012542		
63	S-FAP surface transmission	0.9975		
64	Window transmission	0.9975		
65	Lens transmission	0.9975		
66	Mirror transmission	0.995		
67				
68	c (m/s)	300000000		
69	h (J s)	6.626E-34		
70	laser wavelength (m)	1.0476E-06		
71	stokes wavelength (m)	1.16342E-06		
72	anti-stokes wavelength (m)	9.5275E-07		
73	shift (cm-1)	950.3		
74	laser wavenumber (cm-1)	9545.628102		
75	stokes wavenumber (cm-1)	8595.328102		
76	anti-stokes wavenumber (cm-1)	10495.9281		
77	laser photon energy (J)	1.89748E-19		
78	stokes photon energy (J)	1.70858E-19		
79	anti-stokes photon energy (J)	2.08638E-19		

	J	K	L	M	N	O
1	g *I*dL	Total g*I*dL		Bandwidth	bandwidth	g*I*dL
2	Forward	Forward		Ratios	modifier	Backward
3	0	0	pass 0	0.10959236	0.2508067	0
4	2.51297E-05	2.51297E-05	pass 1	0.25080673	0.2508067	6.30269E-06
5	2.54949E-05	5.06246E-05	pass 2	0.37055367	0.2508067	6.39429E-06
6	2.58601E-05	7.64847E-05	pass 3	0.40291219	0.2508067	6.48589E-06
7	2.62253E-05	0.00010271	pass 4	0.42105651	0.2508067	6.57749E-06
8	2.65905E-05	0.000129301			0.2508067	6.66909E-06
9	2.69558E-05	0.000156256			0.2508067	6.76069E-06
10	2.7321E-05	0.000183577			0.2508067	6.85228E-06
11	2.76862E-05	0.000211263			0.2508067	6.94388E-06
12	2.80514E-05	0.000239315			0.2508067	7.03548E-06
13	2.84166E-05	0.000267731			0.2508067	7.12708E-06
14	2.87818E-05	0.000296513			0.2508067	7.21868E-06
15	2.91471E-05	0.00032566			0.2508067	7.31028E-06
16	2.95123E-05	0.000355173			0.2508067	7.40188E-06
17	2.98775E-05	0.00038505			0.2508067	7.49348E-06
18	3.02427E-05	0.000415293			0.2508067	7.58507E-06
19	3.03789E-05	0.000445672			0.2508067	7.61924E-06
20	3.08166E-05	0.000476488			0.2508067	7.72902E-06
21	3.12544E-05	0.000507743			0.2508067	7.8388E-06
22	3.16921E-05	0.000539435			0.2508067	7.94858E-06
23	3.21298E-05	0.000571565			0.2508067	8.05836E-06
24	3.25675E-05	0.000604132			0.2508067	8.16814E-06
25	3.30052E-05	0.000637137			0.2508067	8.27792E-06
26	3.34429E-05	0.00067058			0.2508067	8.3877E-06
27	3.38806E-05	0.000704461			0.2508067	8.49748E-06
28	3.43183E-05	0.000738779			0.2508067	8.60726E-06
29	3.4756E-05	0.000773535			0.2508067	8.71704E-06
30	3.51937E-05	0.000808729			0.2508067	8.82682E-06
31	3.56314E-05	0.00084436			0.2508067	8.9366E-06
32	3.60691E-05	0.000880429			0.2508067	9.04638E-06
33	3.65069E-05	0.000916936			0.2508067	9.15616E-06
34	3.66507E-05	0.000953587			0.2508067	9.19225E-06
35	3.71586E-05	0.000990746			0.2508067	9.31962E-06
36	3.76664E-05	0.001028412			0.2508067	9.44699E-06
37	3.81742E-05	0.001066586			0.2508067	9.57435E-06
38	3.8682E-05	0.001105268			0.2508067	9.70172E-06
39	3.91899E-05	0.001144458			0.2508067	9.82908E-06
40	3.96977E-05	0.001184156			0.2508067	9.95645E-06
41	4.02055E-05	0.001224361			0.2508067	1.00838E-05
42	4.07133E-05	0.001265075			0.2508067	1.02112E-05
43	4.12212E-05	0.001306296			0.2508067	1.03385E-05
44	4.1729E-05	0.001348025			0.2508067	1.04659E-05
45	4.22368E-05	0.001390262			0.2508067	1.05933E-05
46	4.27446E-05	0.001433006			0.2508067	1.07206E-05
47	4.32525E-05	0.001476259			0.2508067	1.0848E-05
48	4.37603E-05	0.001520019			0.2508067	1.09754E-05

Continued

IIIc: SRS loss with slab tilt in Mercury

This is a Visualbasic code which is linked to a set of Excel spreadsheets and is run on a PC running Windows 95 and using Excel 97. This routine calculates the Mercury output energy versus pulse length such that the Stimulated Raman Scattering is at threshold (defined as 1% conversion of the laser energy) for a variety of tilt angles between slab surfaces. The spreadsheets used are named: SRS (which contains all of the input parameters), flu0.0025 (contains the Mercury fluence levels for 0.25% reflectivity of the anti-reflection coatings on the S-FAP slabs for a whole set of input fluences), and angle (which contains the output of the code). Note that Mercury fluences are calculated using the code given in Appendix IIId, IIIe, and IIIf.

```
Sub SRSMercuryTilt()
'
'Main Macro
'01/14/99 by Andy Bayramian
' Keyboard Shortcut: Ctrl+a
'
'This routine calculates the Mercury output energy versus angle versus
'pulse length such that the Stimulated Raman Scattering (SRS) is at threshold

'**************SRS declarations and initializations******************
Const pts = 100 'number of data points
Const Tpts = 2000 'number of time pulse points
Const thresh = 0.01 'threshold SRS requirement = fraction of input pump energy

delta = 5
A0 = 5
frac = 0.000000000005
apmax = 2.9999999999999
apmin = -0.0000000000001

Dim Energyin(1001)
Dim SRSout(1001)
Dim pulseout(1001)
Dim Threshold(1001)
Dim SRSe(10)
Dim SRSg(10)

'*****************SRS gain loop*****************************************
For g = 0 To 3 Step 1
    Angle = g * delta + A0
    pulse = 0.00000000005
    Worksheets("angle").Cells(2, (3 * g + 3)).Value = Angle
    For p = 1 To pts Step 1
        For j = 0 To 840 Step 1
            Worksheets("SRS").Cells(3 + j, 6).Value = Worksheets("R0.0025").Cells(3 + j, 2 + p).Value
        Next j
        Energyin(p) = Worksheets("SRS").Cells(5, 2).Value
        Threshold(p) = thresh * Energyin(p)
        For t = 1 To Tpts Step 1
            pulse = pulse + frac
            Worksheets("SRS").Cells(2, 2).Value = pulse
            Worksheets("angle").Cells(2, 1).Value = pulse
            For r = 1 To 7 Step 1
                SRSenergyout = 0#
```

```
                SRSgenout = 0#
                subangle = r * Angle / 7
                Worksheets("SRS").Cells(5, 18).Value = subangle
                Worksheets("SRS").Cells(7, 2).Value = r
                pass = Worksheets("SRS").Cells(20, 2).Value
                passtot = Worksheets("SRS").Cells(19, 2).Value
                If pass = 0 Then
                    If r < 7 Then GoTo 5
                End If
                mult = 8 - r
                cellnum = (7 - r) * 15 + 738
                gIL = 0#
                For a = cellnum To 843 Step 1
                    gIL = gIL + Worksheets("SRS").Cells(a, 9).Value
                Next a
                Worksheets("SRS").Cells(10, 2).Value = gIL
                If pass > zero Then
                    resid = passtot - pass
                    For n = 1 To pass Step 1
                        tempfrac = 1 + (1 - n) / passtot
                        aperture = Worksheets("SRS").Cells(n + 2, 37).Value
                        If aperture > apmax Then GoTo 3
                        If aperture < apmin Then GoTo 3
                        passEgen = tempfrac * Worksheets("SRS").Cells(n + 2, 42).Value
                        SRSgenout = SRSgenout + passEgen
                        If n = pass Then
                            tempfrac = (resid) / (passtot)
                            passEgen = tempfrac *Worksheets("SRS").Cells(n + 2, 43).Value
                            SRSgenout = SRSgenout + passEgen
                        End If
                    Next n
                Else
                    SRSgenout = Worksheets("SRS").Cells(15, 2).Value
                End If
                3 SRSg(r) = mult * SRSgenout
            5Next r
            SRSgtot = 0#
            For r = 1 To 7 Step 1
                SRSgtot = SRSgtot + SRSg(r)
            Next r
            If SRSgtot < Threshold(p) Then
                SRSout(p) = SRSgtot
                pulseout(p) = pulse
                Worksheets("angle").Cells(p + 2, (3 * g + 1)).Value = pulseout(p)
                Worksheets("angle").Cells(p + 2, (3 * g + 2)).Value = Energyin(p)
                Worksheets("angle").Cells(p + 2, (3 * g + 3)).Value = SRSout(p)
                pulse = pulse - frac
                GoTo 10
            End If
        Next t
    10 Next p
Next g
End Sub 'SRSMercuryTilt
```

IIIc1 (Example spreadsheet associated with IIIc with differences from IIIa1 shown)

	Q	R	S	T	U	V
1	Modeling of angles and lengths travelled				Refracted Angles	
2	for arbitrary angle of incidence on			index	degrees	radians
3	amplifier slab			1	0.2478	0.0043
4	gil used	6.67431		2	0.4957	0.0087
5	Tilt angle of slab (degrees) (> 0.2)	0.2000		3	0.7435	0.0130
6	Tilt angle of slab (radians)	0.0035		4	0.9912	0.0173
7	n1 (index of surroundings)	1.0000		5	1.2390	0.0216
8	n2 (index of material)	1.6140		6	1.4867	0.0259
9	# of slabs	7.0000		7	1.7344	0.0303
10	# of gaps	6.0000		8	1.9820	0.0346
11	Slab Height (cm)	3.0000		9	2.2296	0.0389
12	Slab Depth (cm)	5.0000		10	2.4771	0.0432
13	Slab Width (cm)	0.7500		11	2.7245	0.0476
14	Gap Width (cm)	0.1000		12	2.9718	0.0519
15	L1	5.25		13	3.2191	0.0562
16	L2	0.6		14	3.4662	0.0605
17	OPL	9.0735		15	3.7133	0.0648
18	Critical angle in material (degrees)	38.2854		16	3.9602	0.0691
19	Critical angle in material (radians)	0.6682		17	4.2070	0.0734
20	Refractions possible	225				
21	gIL per centimeter	1.271297478				
22						
23	index of S-FAP	1.6140				
24	index of surroundings	1.0000				
25	angle of incidence (radians)	0.0000				
26	angle in S-FAP (radians)	0.0000				
27	delta L (cm) actual	0.0500				
28						
29	c (m/s)	3.0000E+08				
30	h (J s)	6.6260E-34				
31	laser wavelength (m)	1.0476E-06				
32	stokes wavelength (m)	1.1634E-06				
33	anti-stokes wavelength (m)	9.5275E-07				
34	shift (cm-1)	950.3000				
35	laser wavenumber (cm-1)	9545.6281				
36	stokes wavenumber (cm-1)	8595.3281				
37	anti-stokes wavenumber (cm-1)	10495.9281				
38	laser photon energy (J)	1.8975E-19				
39	stokes photon energy (J)	1.7086E-19				
40	anti-stokes photon energy (J)	2.0864E-19				

	W	X	Y	Z	AA	AB	AC
1	height change			height change			h
2	index	(cm)	Total in air (cm	index	(cm)	Total in material (cm	index
3	1	0.004189	0.004188858	2	0.02271	0.045417546	3
4	4	0.0084	0.012569605	5	0.04542	0.136252973	6
5	7	0.0126	0.025149615	8	0.06813	0.272506952	9
6	10	0.0168	0.041940609	11	0.09084	0.454180488	12
7	13	0.0210	0.062958664	14	0.11355	0.681274919	15
8	16	0.0253	0.088224219	17	0.13626	0.953791914	18
9	19	0.0295	0.117762093	20	0.15897	1.271733473	21
10	22	0.0338	0.151601491	23	0.18168	1.635101919	24
11	25	0.0382	0.18977603	26	0.2044	2.043899903	27
12	28	0.0425	0.232323753	29	0.22712	2.498130394	30
13	31	0.0470	0.279287153	32	0.24983	2.997796678	33
14	34	0.0514	0.330713199	35	0.27255	3.542902354	36
15	37	0.0559	0.386653363	38	0.29527	4.133451328	39
16	40	0.0605	0.447163651	41	0.318	4.769447809	42
17	43	0.0651	0.512304634	44	0.34072	5.450896302	45
18	46	0.0698	0.582141488	47	0.36345	6.177801606	48
19	49	0.0746	0.65674403	50	0.38618	6.950168802	51
20							
21							
22							
23							
24							
25							
26							
27							
28							
29							
30							
31							
32							
33							
34							
35							
36							
37							
38							
39							
40							

	AD	AE	AF	AG	AH	AI	AJ
1	eight change		Passes	length change	gIL adj.		Passes
2	(cm)	Total in air (cm)		(cm)			
3	0.0042	0.0042	1	0.0000	0.0000		1
4	0.0084	0.0126	2	0.0000	0.0001		2
5	0.0126	0.0252	3	0.0001	0.0001		3
6	0.0168	0.0420	4	0.0003	0.0004		4
7	0.0211	0.0630	5	0.0005	0.0006		5
8	0.0253	0.0883	6	0.0009	0.0012		6
9	0.0296	0.1179	7	0.0014	0.0017		7
10	0.0339	0.1519	8	0.0022	0.0027		8
11	0.0383	0.1902	9	0.0029	0.0037		9
12	0.0427	0.2328	10	0.0042	0.0053		10
13	0.0471	0.2800	11	0.0054	0.0069		11
14	0.0516	0.3316	12	0.0072	0.0091		12
15	0.0562	0.3877	13	0.0089	0.0114		13
16	0.0608	0.4485	14	0.0113	0.0144		14
17	0.0654	0.5139	15	0.0138	0.0175		15
18	0.0702	0.5841	16	0.0169	0.0215		16
19	0.0750	0.6591	17	0.0200	0.0255		17
20			18	0.0240	0.0305		18
21			19	0.0280	0.0356		19
22			20	0.0329	0.0418		20
23			21	0.0378	0.0481		21
24			22	0.0438	0.0556		22
25			23	0.0497	0.0632		23
26			24	0.0568	0.0722		24
27			25	0.0638	0.0812		25
28			26	0.0721	0.0917		26
29			27	0.0804	0.1022		27
30			28	0.0900	0.1145		28
31			29	0.0997	0.1267		29
32			30	0.1107	0.1408		30
33			31	0.1218	0.1548		31
34							32
35							33
36							34
37							35
38							36
39							37
40							38

↓Continued↓

	AK	AL	AM	AN	AO
1	Total Height	perture Reducti	# modes	# photons	Apertured SRS
2	Change (cm)	Factor (ARF)		after	(J)
3	0	1	4.9607E+11	3.6941E+14	6.3117E-05
4	0.0268976	0.99103412	4.4096E+11	6.0586E+14	1.0352E-04
5	0.0537966	0.98206781	4.3542E+11	1.1037E+15	1.8857E-04
6	0.107595	0.96413499	4.3408E+11	2.0109E+15	3.4358E-04
7	0.1613987	0.94620042	4.3360E+11	3.6700E+15	6.2706E-04
8	0.2421057	0.91929809	4.3338E+11	6.6350E+15	1.1336E-03
9	0.3228245	0.89239182	4.3328E+11	1.1988E+16	2.0482E-03
10	0.4304523	0.8565159	4.3322E+11	2.1417E+16	3.6593E-03
11	0.5381011	0.82063298	4.3318E+11	3.8199E+16	6.5266E-03
12	0.6726663	0.77577789	4.3316E+11	6.7224E+16	1.1486E-02
13	0.8072644	0.73091186	4.3314E+11	1.1791E+17	2.0146E-02
14	0.9687885	0.67707051	4.3313E+11	2.0334E+17	3.4742E-02
15	1.1303598	0.62321341	4.3312E+11	3.4843E+17	5.9532E-02
16	1.3188684	0.56037719	4.3312E+11	5.8326E+17	9.9655E-02
17	1.5074415	0.49751951	4.3311E+11	9.6405E+17	1.6472E-01
18	1.7229651	0.4256783	4.3311E+11	1.5356E+18	2.6237E-01
19	1.9385728	0.35380905	4.3311E+11	2.3761E+18	4.0598E-01
20	2.1811464	0.27295121	4.3310E+11	3.4126E+18	5.8308E-01
21	2.4238265	0.19205784	4.3310E+11	4.4704E+18	7.6380E-01
22	2.6934894	0.10217018	4.3310E+11	4.4274E+18	7.5645E-01
23	2.9632841	0.01223864	4.3310E+11	9.8733E+17	1.6869E-01
24	3.2600806	-0.08669354	4.3310E+11	-1.3020E+19	-2.2246E+00
25	3.5570367	-0.18567888	4.3310E+11	-5.1917E+19	-8.8704E+00
26	3.8810155	-0.29367185	4.3310E+11	-1.5287E+20	-2.6119E+01
27	4.2051844	-0.40172814	4.3310E+11	-3.8931E+20	-6.6516E+01
28	4.5563991	-0.51879969	4.3310E+11	-9.3598E+20	-1.5992E+02
29	4.9078369	-0.63594564	4.3310E+11	-2.1360E+21	-3.6495E+02
30	5.2863455	-0.76211515	4.3310E+11	-4.7655E+21	-8.1422E+02
31	5.6651132	-0.88837106	4.3310E+11	-1.0342E+22	-1.7669E+03
32	6.0709784	-1.02365947	4.3309E+11	-2.2185E+22	-3.7905E+03
33	6.4771415	-1.15904718	4.3309E+11	-4.6764E+22	-7.9900E+03
34	7.34406	-1.44802	4.3309E+11	-1.0877E+23	-1.8584E+04
35	8.266016	-1.75533868	4.3309E+11	-2.4546E+23	-4.1939E+04
36	8.266016	-1.75533868	4.3309E+11	-4.5698E+23	-7.8078E+04
37	8.266016	-1.75533868	4.3309E+11	-8.5075E+23	-1.4536E+05
38	8.266016	-1.75533868	4.3309E+11	-1.5838E+24	-2.7061E+05
39	8.266016	-1.75533868	4.3309E+11	-2.9486E+24	-5.0380E+05
40	8.266016	-1.75533868	4.3309E+11	-5.4895E+24	-9.3792E+05

↓Continued↓

	AP	AQ
1	Generated SRS	Total output
2	(J)	(J)
3	6.3117E-05	1.3696E+00
4	1.0306E-04	1.3573E+00
5	1.8773E-04	1.3450E+00
6	3.4051E-04	1.3204E+00
7	6.2134E-04	1.2959E+00
8	1.1180E-03	1.2590E+00
9	2.0191E-03	1.2222E+00
10	3.5889E-03	1.1730E+00
11	6.3959E-03	1.1239E+00
12	1.1190E-02	1.0625E+00
13	1.9599E-02	1.0010E+00
14	3.3564E-02	9.2729E-01
15	5.7369E-02	8.5353E-01
16	9.5195E-02	7.6747E-01
17	1.5664E-01	6.8138E-01
18	2.4662E-01	5.8299E-01
19	3.7867E-01	4.8456E-01
20	5.3619E-01	3.7382E-01
21	6.9829E-01	2.6303E-01
22	7.3517E-01	1.3993E-01
23	6.4000E-01	1.6761E-02
24	1.7028E+01	-1.1873E-01
25	-1.6634E+01	-2.5430E-01
26	-3.6507E+01	-4.0220E-01
27	-8.2045E+01	-5.5019E-01
28	-1.8848E+02	-7.1052E-01
29	-4.1374E+02	-8.7096E-01
30	-9.0836E+02	-1.0438E+00
31	-1.9341E+03	-1.2167E+00
32	-4.1172E+03	-1.4020E+00
33	-8.5801E+03	-1.5874E+00
34	-2.1362E+04	-1.9831E+00
35	-4.7169E+04	-2.4040E+00
36	-7.8078E+04	-2.4040E+00
37	-1.4536E+05	-2.4040E+00
38	-2.7061E+05	-2.4040E+00
39	-5.0380E+05	-2.4040E+00
40	-9.3792E+05	-2.4040E+00

↓Continued↓

IIId. Mercury excitation

This is a Visualbasic code which is linked to a set of Excel spreadsheets and is run on a PC running Windows 95 and using Excel 97. This routine is module 1 of a spreadsheet entitled "SI spectral pump and spectral extraction model with BeO BASIS and Yb:S-FAP ver 3.xls, " which calculates the absorption and resulting inversion from diode pumping in Mercury. The spreadsheets used are named: excitationextraction, ps_ext, thermal, fluence, extraction pulse, emission spectrum data, and slab spectral data.

```
Sub Excitation()

'For Yb:S-FAP
'
'3-Aug-98
'written by Raymond Beach, copyright 1999
'
' Main Macro
' Macro recorded 6/24/97 by Raymond J. Beach
'
' Keyboard Shortcut: Ctrl+p
'
'This routine calculates the pump excitation for the Hg laser system assuming there are
'two stacks of slabs and each stack is pumped from both ends

'Declarations
    Dim spec_abs_sig(201)              'spectroscopic absorption cros section (cm^2)
    Dim pow_spec_initial(201)          'power spectrum initial in (W/nm)
    Dim pow_spec_final(201)            'power spectrum final in (W/nm)
    Dim pow_spec_integrated_in(201)    'power spectrum integrated over pulse in (W/nm)
    Dim pow_spec_integrated_out(201)   'power spectrum integrated over pulse out (W/nm)
    Dim n0(14)                         'slab Nd number density (1/cm^3)
    Dim n2(14)                         'slab excited state density (1/cm^3)
    Dim gain_log(14)                   'gain-log of slabs (nepers)
    Dim tau_avg(14)                    'average storage lifetime in slabs (sec)
    Dim p_th(14)                       'thermal power generated in slab (W)
    Dim p_th_1(201)                    'slab 1 per pulse thermal power profile - time resolved
    Dim elapsed_time(201)              'elapsed time array to go with p_the_1
    Dim p_thppp(14)                    'thermal power density generated in slab (W/cm^3)
    Dim p_thpp(14)                     'thermal power intensity removed from slab face (W/cm^2)
    Dim slab_center_to_edge_temp(14)   '(degrees C)
    Dim slab_b(14)                     'fraction of fracture
    Dim spon_em_power(14)              'spontaneous emission power generated in each slab (W)
    Dim edge_clad_thermal(14)          'edge clad thermal loading (W)

    pi = 4 * Atn(1)                    'the ratio of a circle's circumference to its diameter

'Slab Parameter Initializations
    Worksheets("excitationextraction").Activate
    Range("nslabs").Select: nslabs = ActiveCell.Value
    Range("slab_height").Select: slab_height = ActiveCell.Value
    Range("slab_width").Select: slab_width = ActiveCell.Value
        slab_area = slab_width * slab_height
    Range("slab_thick").Select: slab_thick = ActiveCell.Value
        slab_vol = slab_area * slab_thick
    Range("slab1doping").Select:  n0(1) = ActiveCell.Value
```

```
    For i = 2 To nslabs
        n0(i) = ActiveCell.Offset(i - 1, 0).Value
    Next i
    Range("quenching_parameter").Select:  quenching_parameter = ActiveCell.Value
    Range("Rt").Select:  Rt = ActiveCell.Value
    Range("k_th").Select: k_th = ActiveCell.Value
    Range("ref_index").Select: ref_index = ActiveCell.Value
    Range("gamma_laser").Select: gamma_laser = ActiveCell.Value

'Yb spectroscopic parameters initializations
    Range("sigma_spec_laser").Select: sigma_spec_laser = ActiveCell.Value
    Range("fal").Select: fal = ActiveCell.Value
    Range("fbl").Select: fbl = ActiveCell.Value
    Range("fap").Select: fap = ActiveCell.Value
    Range("fbp").Select: fbp = ActiveCell.Value
    Range("lambda_l").Select: lambda_l = ActiveCell.Value
        hvl = 2E-16 / lambda_l
    Range("lambda_p").Select: lambda_p = ActiveCell.Value
        hvp = 2E-16 / lambda_p
    Range("beta_zero_line").Select: beta_zero_line = ActiveCell.Value
    Range("sigma_em_pol_ave").Select: sigma_em_pol_ave = ActiveCell.Value
    Range("sigma_zero_line").Select: sigma_zero_line = ActiveCell.Value

'Pump Parameter Initializations
    Range("p0").Select: p0 = ActiveCell.Value
    Range("prf").Select: prf = ActiveCell.Value
    Range("tau_pulse").Select: tau_pulse = ActiveCell.Value
    Range("lambda00").Select:  lambda00 = ActiveCell.Value
    Range("lambdaehw").Select: lambdaehw = ActiveCell.Value
    Range("alpha").Select: alpha = ActiveCell.Value
    Range("pdpdT").Select: pdpdT = ActiveCell.Value
    Range("dlambdadT").Select: dlambdadT = ActiveCell.Value
    Range("eta_geometric").Select: eta_geometric = ActiveCell.Value
    Range("eta_transport").Select: eta_transport = ActiveCell.Value
    Range("tau0").Select: tau0 = ActiveCell.Value

'Trapping and ASE length characteristic length paramater
    cos_theta_crit = Sqr(1 - 1 / ref_index ^ 2)
    l_trap = slab_thick * (1 - cos_theta_crit) + 0.5 * ((slab_height + slab_width) / 2) * cos_theta_crit
    Range("l_trap").Select: ActiveCell.Value = l_trap

'Pump delivery initializations
    eta_pump_delivery = eta_transport * eta_geometric
    Range("eta_pump_delivery").Select: ActiveCell.Value = eta_pump_delivery

'Generate integrated pump pulse power spectrum before slabs and output to slab spectral data
    del_time = tau_pulse / 100
    del_lambda = (925 - 875) / 200
    For i = 0 To 200
        lambda = 875 + i * del_lambda
        pow_spec_integrated_in(i) = 0
        pow_spec_integrated_out(i) = 0
        k = 1
        For t = 0 To tau_pulse Step del_time
            del_t = alpha * Sqr(t)
            p = p0 * (1 - pdpdT * del_t)
```

```
            lambda0 = lambda00 + dlambdadT * del_t
            pow_spec_integrated_in(i) = pow_spec_integrated_in(i) + p * Exp(-((lambda - lambda0) /
lambdaehw) ^ 2)
            k = k + 1
            Worksheets("slab spectral data").Cells(k, 11).Value = t
            Worksheets("slab spectral data").Cells(k, 12).Value = p
        Next t
        pow_spec_integrated_in(i) = pow_spec_integrated_in(i) * (del_time / (Sqr(pi) * lambdaehw))
    Next i
    'Output to slab spectral data with first cell at 2,6
    For i = 0 To 200
        Worksheets("slab spectral data").Cells(2 + i, 6).Value = pow_spec_integrated_in(i)
    Next i

'Generate initial instantaneous pump pulse power spectrum before slabs and output to slab spectral data
    For i = 0 To 200
        lambda = 875 + i * del_lambda
        t = 0
        del_t = alpha * Sqr(t)
        p = p0 * (1 - pdpdT * del_t)
        lambda0 = lambda00 + dlambdadT * del_t
        pow_spec_initial(i) = (p / (Sqr(pi) * lambdaehw)) * Exp(-((lambda - lambda0) / lambdaehw) ^ 2)
    Next i
    'Output to slab spectral data with first cell at 2,4
    For i = 0 To 200
        Worksheets("slab spectral data").Cells(2 + i, 4).Value = pow_spec_initial(i)
    Next i

'Generate final instantaneous pump pulse power spectrum before slabs and output to slab spectral data
    For i = 0 To 200
        lambda = 875 + i * del_lambda
        t = tau_pulse
        del_t = alpha * Sqr(t)
        p = p0 * (1 - pdpdT * del_t)
        lambda0 = lambda00 + dlambdadT * del_t
        pow_spec_final(i) = (p / (Sqr(pi) * lambdaehw)) * Exp(-((lambda - lambda0) / lambdaehw) ^ 2)
    Next i
    'Output to slab spectral data with first cell at 2,5
    For i = 0 To 200
        Worksheets("slab spectral data").Cells(2 + i, 5).Value = pow_spec_final(i)
    Next i

'Get the spectral absorption cross sections starting at cell 2,3
    For i = 0 To 200
        spec_abs_sig(i) = Worksheets("slab spectral data").Cells(2 + i, 3).Value * 1E-20
    Next i

'Initialize n2(i)
    For i = 1 To nslabs
        n2(i) = 0
    Next i

'Initialize spon_em_power(i)
    For i = 1 To nslabs
        spon_em_power(i) = 0
    Next i
```

```
'Propogate pump pulse through the stack of slabs (using double end pumping geometry)
    For j = 1 To nslabs
        tau_avg(j) = 0
        p_th(j) = 0
    Next j
    t_count = 0
    For t = 0 To tau_pulse Step del_time
        t_count = t_count + 1
        elapsed_time(t_count) = t
        p_th_1(t_count) = 0
        del_t = alpha * Sqr(t)  'delta in temperature
        p = p0 * (1 - pdpdT * del_t) * eta_pump_delivery
        lambda0 = lambda00 + dlambdadT * del_t
        For i = 0 To 200  'integrate over lambda
            lambda = 875 + i * del_lambda
            'First propogate a right going pulselet (slab 1 to slab 7)
            p_intensity = (p * del_lambda / (Sqr(pi) * lambdaehw)) * Exp(-((lambda - lambda0) /
lambdaehw) ^ 2) / slab_area
            For j = 1 To nslabs
                n2pint = ((fap + fbp) * n2(j) - fap * n0(j)) * slab_thick
                p_th(j) = p_th(j) + p_intensity * del_time * (1 - Exp(spec_abs_sig(i) * n2pint)) * slab_area *
(1 - hvl / hvp)
                If j = 1 Then
                    p_th_1(t_count) = p_th_1(t_count) + p_intensity * (1 - Exp(spec_abs_sig(i) * n2pint)) *
slab_area * (1 - hvl / hvp)
                End If
                n2int = n2(j) * slab_thick
                n2int = n2int + del_time * (p_intensity / hvp) * (1 - Exp(spec_abs_sig(i) * n2pint))
                p_intensity = p_intensity * Exp(spec_abs_sig(i) * n2pint)
                n2(j) = n2int / slab_thick
            Next j
            'update pow_spec_integrated_out
            pow_spec_integrated_out(i) = pow_spec_integrated_out(i) + (p_intensity / del_lambda) *
slab_area * del_time
            'Next propogate a left going pulselet (slab 7 to slab 1)
            p_intensity = (p * del_lambda / (Sqr(pi) * lambdaehw)) * Exp(-((lambda - lambda0) /
lambdaehw) ^ 2) / slab_area
            For j = nslabs To 1 Step -1
                n2pint = ((fap + fbp) * n2(j) - fap * n0(j)) * slab_thick
                p_th(j) = p_th(j) + p_intensity * del_time * (1 - Exp(spec_abs_sig(i) * n2pint)) * slab_area *
(1 - hvl / hvp)
                If j = 1 Then
                    p_th_1(t_count) = p_th_1(t_count) + p_intensity * (1 - Exp(spec_abs_sig(i) * n2pint)) *
slab_area * (1 - hvl / hvp)
                End If
                n2int = n2(j) * slab_thick
                n2int = n2int + del_time * (p_intensity / hvp) * (1 - Exp(spec_abs_sig(i) * n2pint))
                p_intensity = p_intensity * Exp(spec_abs_sig(i) * n2pint)
                n2(j) = n2int / slab_thick
            Next j
        Next i
        'Let population decay according to quenched, trapped and ase impacted lifetime
        For j = 1 To nslabs
            tau_quenched = tau0 / (1 + (n0(j) / quenching_parameter) ^ 2)
            'tau_trap = tau_quenched * 1.1667  'Steve Payne's Fudge factor for lifetime trapping in glass
```

```
            tau_trap = tau_quenched / (1 - beta_zero_line * (1 - Exp(-(n0(j) - n2(j)) * sigma_zero_line *
l_trap / 2)))
            Mase = Exp(n2(j) * sigma_em_pol_ave * l_trap + (n2(j) * sigma_em_pol_ave * l_trap) ^ 2 / 2)
            tau = tau_trap / Mase
            tau_avg(j) = tau_avg(j) + tau
            n2(j) = n2(j) * Exp(-del_time / tau)
            'Calculate the spontaneous emission power generated in each slab using the trapped and ase
impacted lifetime
            spon_em_power(j) = spon_em_power(j) + n2(j) * slab_vol * (del_time / tau) * hvl
        Next j
        'Take into account the heat generated due to the quenching
        For j = 1 To nslabs
            p_th(j) = p_th(j) + ((n0(j) / quenching_parameter) ^ 2 * (1 / tau0)) * (n2(j) * slab_height *
slab_width * slab_thick) * hvl * del_time
                If j = 1 Then
                    p_th_1(t_count) = p_th_1(t_count) + ((n0(j) / quenching_parameter) ^ 2 * (1 / tau0)) *
(n2(j) * slab_height * slab_width * slab_thick) * hvl
                End If
        Next j
    Next t
    For j = 1 To nslabs
        tau_avg(j) = tau_avg(j) / t_count
        p_th(j) = p_th(j) * prf
        p_thppp(j) = p_th(j) / (slab_area * slab_thick)
        p_thpp(j) = p_thppp(j) * slab_thick / 2
        slab_center_to_edge_temp(j) = (p_thppp(j) / (2 * k_th)) * (slab_thick / 2) ^ 2
        slab_b(j) = p_thppp(j) / (12 * Rt / slab_thick ^ 2)
        spon_em_power(j) = spon_em_power(j) * prf
    Next j
    For j = nslabs + 1 To 2 * nslabs
        tau_avg(j) = tau_avg(j - nslabs)
        p_th(j) = p_th(j - nslabs)
        p_thpp(j) = p_thpp(j - nslabs)
        p_thppp(j) = p_thppp(j - nslabs)
        slab_center_to_edge_temp(j) = slab_center_to_edge_temp(j - nslabs)
        slab_b(j) = slab_b(j - nslabs)
        n0(j) = n0(j - nslabs)
        n2(j) = n2(j - nslabs)
        spon_em_power(j) = spon_em_power(j - nslabs)
    Next j

'Output slab thermal data
    Worksheets("thermal").Activate
    Range("slab_thermal_home").Select
    For j = 1 To 2 * nslabs
        ActiveCell.Offset(j, 0).Value = j
        ActiveCell.Offset(j, 1).Value = p_th(j)
        ActiveCell.Offset(j, 2).Value = p_thpp(j)
        ActiveCell.Offset(j, 3).Value = p_thppp(j)
        ActiveCell.Offset(j, 4).Value = slab_center_to_edge_temp(j)
        ActiveCell.Offset(j, 5).Value = slab_b(j)
        ActiveCell.Offset(j, 6).Value = n2(j)
        ActiveCell.Offset(j, 7).Value = spon_em_power(j)
    Next j

'Calculate the edge cladding thermal load using a simple minded trapping argument
```

```
    For j = 1 To 2 * nslabs
        edge_clad_thermal(j) = Sqr(1 - 1 / ref_index ^ 2) * spon_em_power(j)
        ActiveCell.Offset(j, 8).Value = edge_clad_thermal(j)
    Next j

'Output integrated power spectrum after slabs to slab spectral data 2,7
    For i = 0 To 200
        Worksheets("slab spectral data").Cells(2 + i, 7).Value = pow_spec_integrated_out(i)
    Next i

'Transmission through the unbleached stack of slabs
    For i = 0 To 200
        lambda = 875 + i * del_lambda
        abs_alpha = 0
        For j = 1 To nslabs
            abs_alpha = abs_alpha + slab_thick * n0(j) * spec_abs_sig(i) * fap
        Next j
        transmission = Exp(-abs_alpha)
        Worksheets("slab spectral data").Cells(2 + i, 8).Value = transmission
        Worksheets("slab spectral data").Cells(2 + i, 9).Value = abs_alpha
    Next i

'Calculate pump energy generated by array and pump energy that leaks out of backside of stack
    E_out_of_array = 0
    E_out_of_stack = 0
    For i = 0 To 200
        E_out_of_array = E_out_of_array + pow_spec_integrated_in(i) * del_lambda
        E_out_of_stack = E_out_of_stack + pow_spec_integrated_out(i) * del_lambda
    Next i
    Worksheets("excitationextraction").Activate
    Range("E_out_of_array").Select:  ActiveCell.Value = E_out_of_array
    Range("E_out_of_stack").Select: ActiveCell.Value = E_out_of_stack
    'As a check, integrate p(t)
    E_out_of_array_check = 0
    For t = 0 To tau_pulse Step del_time
        del_t = alpha * Sqr(t)
        p = p0 * (1 - pdpdT * del_t)
        E_out_of_array_check = E_out_of_array_check + p * del_time
    Next t
    check = E_out_of_array_check / E_out_of_array  'This should equal 1

'Absorption in efficiencies
    Range("E_out_of_stack").Select:  ActiveCell.Value = E_out_of_stack
    crystal_absorption_efficiency = (E_out_of_array * eta_pump_delivery - E_out_of_stack) /
(E_out_of_array * eta_pump_delivery)
    Range("crystal_absorption_efficiency").Select: ActiveCell.Value = crystal_absorption_efficiency
    eta_pabsnet = (E_out_of_array * eta_pump_delivery - E_out_of_stack) / E_out_of_array
    Range("eta_pabsnet").Select: ActiveCell.Value = eta_pabsnet

'Output slab data to table
    Range("slab_data_home").Select
    For j = 1 To nslabs
        gain_log(j) = ((fal + fbl) * n2(j) - fal * n0(j)) * sigma_spec_laser * slab_thick
        ActiveCell.Offset(j, 0).Value = j
        ActiveCell.Offset(j, 1).Value = gain_log(j)
        ActiveCell.Offset(j, 2).Value = tau_avg(j)
```

```
        ActiveCell.Offset(j, 3).Value = n2(j) / n0(j)
    Next j
    For j = nslabs + 1 To 2 * nslabs
        gain_log(j) = gain_log(j - nslabs)
        tau_avg(j) = tau_avg(j - nslabs)
        n2(j) = n2(j - nslabs)
        ActiveCell.Offset(j, 0).Value = j
        ActiveCell.Offset(j, 1).Value = gain_log(j)
        ActiveCell.Offset(j, 2).Value = tau_avg(j)
        ActiveCell.Offset(j, 3).Value = n2(j) / n0(j)
    Next j

'Calculate the initial gain-log of the entire chain
    g0 = 0
    For j = 1 To 2 * nslabs
        g0 = g0 + gain_log(j)
    Next j
    Worksheets("excitationextraction").Activate
    Range("g0").Select:  ActiveCell.Value = g0

'More outputs
    P_th_max = 12 * Rt / slab_thick ^ 2
    Range("P_th_max").Select:  ActiveCell.Value = P_th_max
    F_sat = (2E-16 / ((fal + fbl) * lambda_l * sigma_spec_laser)) 'saturation fluence (J/cm^2)
    Range("F_sat").Select:  ActiveCell.Value = F_sat

'Calculate the total stored and extractable energy and then output
    slab_area = slab_width * slab_height
    e_extractable = slab_area * F_sat * g0
    e_for_transparency = 0
    For j = 1 To 2 * nslabs
        e_for_transparency = e_for_transparency + n0(j)
    Next j
    e_for_transparency = e_for_transparency * (fal / (fal + fbl)) * hvl * slab_area * slab_thick
    e_total_stored = e_extractable + e_for_transparency
    Range("e_for_transparency").Select:  ActiveCell.Value = e_for_transparency
    Range("e_extractable").Select:  ActiveCell.Value = e_extractable
    Range("e_total_stored").Select:  ActiveCell.Value = e_total_stored

'Output the time resolved thermal power deposition profile for slab 1
    Worksheets("thermal").Activate
    Range("slab_1_thermal_home").Select
    i = 0
    For t = 0 To tau_pulse Step del_time
        i = i + 1
        ActiveCell.Offset(i, 0).Value = elapsed_time(i)
        ActiveCell.Offset(i, 1).Value = p_th_1(i)
    Next t

End Sub
```

IIIe. Mercury Extraction

This is a Visualbasic code which is linked to a set of Excel spreadsheets and is run on a PC running Windows 95 and using Excel 97. This routine is module 2 of a spreadsheet entitled "SI spectral pump and spectral extraction model with BeO BASIS and Yb:S-FAP ver 3.xls, " which calculates the gain, extraction, and output fluence from the excitation data in module 1for Mercury. The spreadsheets used are named: excitationextraction, ps_ext, thermal, fluence, extraction pulse, emission spectrum data, and slab spectral data.

```
Sub Extraction()
'
' Extraction Macro
'Written by Raymond Beach, copyright 1999
'
' Keyboard Shortcut: Ctrl+l
'
'Declarations
    Dim ps_ext(100, 100)          'extraction power spectrum pulse (time, lambda) distribution
    Dim wav(200)                  'wavelength from emission cross section data
    Dim sig(200)                 'emission cross section data
    Dim lambda(200)               'wavelength of extraction pulse
    Dim sigma(200)                'cross section appropriate for the array lambda(j)
    Dim n0(14)                    'doping of individual slabs (1/cm^3)
    Dim n2(14)                    'excited state slab population (1/cm^3)
    Dim gain_log(14)             'gain log of individual slabs (nepers)
    Dim p_th(14)                 'thermal power (W)
    Dim p_thpp(14)                'thermal power per unit area off slab surfaces (W/cm^2)
    Dim p_thppp(14)               'thermal power per unit volume (W/cm^3)
    Dim slab_center_to_edge_temp(14)     '(degrees C)
    Dim p_th_1(201)                    'slab 1 per pulse thermal power profile - time resolved
    Dim elapsed_time(201)               'elapsed time array to go with p_the_1
    Dim slab_b(14)                'fraction of fracture
    Dim spon_em_power(14)          'total power that goes into spontaneous emission (W)
    Dim edge_clad_thermal(14) 'edge clad thermal loading
    Dim B(100)                    'B-integral value time resolved through the pulse
    Dim fluence_path_res(60, 2)  'Fluence just before (1) and after (2) every slab for the amplifier chain
(J/cm^2)

'Initializations
    pi = 4 * Atn(1)

'Optics Chain initializations
    Worksheets("excitationextraction").Activate
    Range("mirror_loss").Select:  mirror_loss = ActiveCell.Value
    Range("lens_surface_loss").Select:  lens_surface_loss = ActiveCell.Value
    Range("window_surface_loss").Select:  window_surface_loss = ActiveCell.Value
    Range("slab_surface_loss").Select: slab_surface_loss = ActiveCell.Value
    Range("slab_bulk_loss").Select:  slab_bulk_loss = ActiveCell.Value
    Range("eta_modefill").Select:  eta_modefill = ActiveCell.Value
    Range("w_thick").Select: w_thick = ActiveCell.Value
    Range("slab_thick").Select: slab_thick = ActiveCell.Value
    Range("slab_width").Select: slab_width = ActiveCell.Value
    Range("slab_height").Select: slab_height = ActiveCell.Value
        slab_area = slab_height * slab_width
        slab_vol = slab_area * slab_thick
```

```
    Range("nslabs").Select: nslabs = ActiveCell.Value
    Range("k_th").Select: k_th = ActiveCell.Value
    Range("Rt").Select: Rt = ActiveCell.Value
    Range("tau_pulse").Select: tau_pulse = ActiveCell.Value
    Range("ref_index").Select: ref_index = ActiveCell.Value 'slab refractive index

'Yb spectroscopic initializations
    Range("beta_zero_line").Select: beta_zero_line = ActiveCell.Value
    Range("sigma_em_pol_ave").Select: sigma_em_pol_ave = ActiveCell.Value
    Range("sigma_zero_line").Select: sigma_zero_line = ActiveCell.Value

'Lens thickness and window thickness initializations (all in cm)
    Range("l1_thick").Select: l1_thick = ActiveCell.Value
    Range("l2_thick").Select: l2_thick = ActiveCell.Value
    Range("l3_thick").Select: l3_thick = ActiveCell.Value
    Range("l4_thick").Select: l4_thick = ActiveCell.Value
    Range("l5_thick").Select: l5_thick = ActiveCell.Value
    Range("l6_thick").Select: l6_thick = ActiveCell.Value
    Range("l7_thick").Select: l7_thick = ActiveCell.Value
    Range("l8_thick").Select: l8_thick = ActiveCell.Value

'Beam areal magnification factors at lenses relative to slab aperture
    Range("m_1").Select: m_1 = ActiveCell.Value
    Range("m_2").Select: m_2 = ActiveCell.Value
    Range("m_3").Select: m_3 = ActiveCell.Value
    Range("m_4").Select: m_4 = ActiveCell.Value
    Range("m_5").Select: m_5 = ActiveCell.Value
    Range("m_6").Select: m_6 = ActiveCell.Value
    Range("m_7").Select: m_7 = ActiveCell.Value
    Range("m_8").Select: m_8 = ActiveCell.Value

'Nonlinear indices of refraction
    Range("gamma_laser").Select: gamma_laser = ActiveCell.Value
    Range("gamma_fused_silica").Select: gamma_fused_silica = ActiveCell.Value

'Front end inializations using a square in time and Gaussian in frequency spectrum pulse
    Range("prf").Select: prf = ActiveCell.Value
    Range("e_in").Select: E_in = ActiveCell.Value
    Range("tau_ext").Select: tau_ext = ActiveCell.Value
        tau_ext = tau_ext * 0.000000001
    Range("n_time_bins").Select: n_time_bins = ActiveCell.Value
    Range("n_frequency_bins").Select: n_frequency_bins = ActiveCell.Value
    Range("lambda_0").Select: lambda_0 = ActiveCell.Value
    Range("lambda_e").Select: lambda_e = ActiveCell.Value
    del_t = tau_ext / n_time_bins

    '*********************************************************************************
    'Track the frequency spectrum out to two e-foldings on either side of the peak
    del_lambda = Worksheets("emission spectrum data").Cells(3, 1).Value - Worksheets("emission
spectrum data").Cells(2, 1).Value

     i = -1
    For t = 0 To tau_ext Step del_t
        i = i + 1
        For j = 0 To n_frequency_bins - 1 Step 1
            ps_ext(i, j) = (E_in / tau_ext) * Worksheets("emission spectrum data").Cells(j + 2, 8).Value
```

```
            'ps_extinp(i, j) = ps_ext(i, j)
            lambda(j) = Worksheets("emission spectrum data").Cells(j + 2, 1).Value
            sigma(j) = (1E-20) * (Worksheets("emission spectrum data").Cells(j + 2, 2).Value)
             j_lambda_max = j
        Next j
    Next t

    i_t_max = i

    'Check
    check = 0
    For i = 0 To i_t_max
    For j = 0 To j_lambda_max
        check = check + ps_ext(i, j)
    Next j
    Next i
    check = check * del_t * del_lambda

'Output initial ps_ext(i,j)
    Worksheets("ps_ext").Activate
    Range("ps_initial_home").Select
    For i = 0 To i_t_max
        For j = 0 To j_lambda_max
            ActiveCell.Offset(i + 1, j).Value = ps_ext(i, j)
        Next j
    Next i

'*****************************************************************************************

'Output temporal and spectral extraction pulse data
    Worksheets("extraction pulse").Activate
    Range("extraction_spectral_home").Select
    For j = 1 To j_lambda_max
        ActiveCell.Offset(j, 0).Value = lambda(j)
        dEdlambda = 0
        For i = 0 To i_t_max
            dEdlambda = dEdlambda + ps_ext(i, j)
        Next i
        dEdlambda = dEdlambda * del_t
        ActiveCell.Offset(j, 1).Value = dEdlambda
        ActiveCell.Offset(j, 2).Value = sigma(j)
    Next j
    Range("extraction_time_home").Select
    For i = 0 To i_t_max
        ActiveCell.Offset(i + 1, 0).Value = i * del_t
        dEdt = 0
        For j = 0 To j_lambda_max
            dEdt = dEdt + ps_ext(i, j)
        Next j
        dEdt = dEdt * del_lambda
        ActiveCell.Offset(i + 1, 1).Value = dEdt
    Next i

'Active ion initializations on laser transition
    Worksheets("excitationextraction").Activate
    Range("sigma_spec_laser").Select: sigma_spec_laser = ActiveCell.Value
```

```
    Range("fal").Select: fal = ActiveCell.Value
    Range("fbl").Select: fbl = ActiveCell.Value
    Range("fap").Select: fap = ActiveCell.Value
    Range("fbp").Select: fbp = ActiveCell.Value
    Range("lambda_l").Select: lambda_l = ActiveCell.Value
    Range("lambda_p").Select: lambda_p = ActiveCell.Value

    hvl = 2E-16 / 1047                  'laser photon energy in J
    F_sat = (2E-16 / ((fal + fbl) * lambda_l * 10000000# * sigma_spec_laser)) 'saturation fluence (J/cm^2)
    Range("f_sat").Select:  ActiveCell.Value = F_sat

'Nd lifetime initializations
    Range("quenching_parameter").Select:  quenching_parameter = ActiveCell.Value
    Range("tau0").Select:  tau0 = ActiveCell.Value

'Pump wavelength
    Range("lambda_p").Select:  lambda_p = ActiveCell.Value

'Import Slab doping density
    Worksheets("excitationextraction").Activate
    Range("slab1doping").Select: n0(1) = ActiveCell.Value
    For i = 2 To nslabs
        n0(i) = ActiveCell.Offset(i - 1, 0).Value
    Next i
    For i = nslabs + 1 To 2 * nslabs
        n0(i) = n0(i - nslabs)
    Next i

'Import excited state number density and thermal data valid at the end of the pump pulse
    Worksheets("thermal").Activate
    Range("slab_thermal_home").Select
    For j = 1 To 2 * nslabs
        p_th(j) = ActiveCell.Offset(j, 1).Value
        p_thpp(j) = ActiveCell.Offset(j, 2).Value
        p_thppp(j) = ActiveCell.Offset(j, 3).Value
        slab_center_to_edge_temp(j) = ActiveCell.Offset(j, 4).Value
        slab_b(j) = ActiveCell.Offset(j, 5).Value
        n2(j) = ActiveCell.Offset(j, 6).Value
        spon_em_power(j) = ActiveCell.Offset(j, 7).Value
    Next j

'Extract through the total set of two stacks of slabs (1 to 14 to 1 to 14 to 1 and out)
    For i = 0 To i_t_max
        B(i) = 0            'B integral
    Next i
    T_1way_optics = 1  '1-way transmission due to optics alone (sans LG-750 bulk and surface losses)

    'Setup pass table with slab gains and fluence
    Worksheets("excitationextraction").Activate
    Range("pass_table_home").Select
    ActiveCell.Offset(0, 1).Value = "pass 0"
    ActiveCell.Offset(0, 2).Value = "pass 1"
    ActiveCell.Offset(0, 3).Value = "pass 2"
    ActiveCell.Offset(0, 4).Value = "pass 3"
    ActiveCell.Offset(0, 5).Value = "pass 4"
    ActiveCell.Offset(0, 6).Value = "pass 5"
```

```
    ActiveCell.Offset(0, 7).Value = "pass 6"
    ActiveCell.Offset(0, 8).Value = "pass 7"
    ActiveCell.Offset(0, 9).Value = "pass 8"
    ActiveCell.Offset(1, 0).Value = "fluence (J/cm^2)"
    ActiveCell.Offset(2, 0).Value = "B-integral"
    For i = 1 To 2 * nslabs
        ActiveCell.Offset(2 + i, -1).Value = "gain of slab "
        ActiveCell.Offset(2 + i, 0).Value = i
    Next i

'Update pass 0
    slab_counter = 0        'increment after passing through each slab
    pass = 0
    Call fluence_calc(slab_area, del_t, i_t_max, j_lambda_max, del_lambda, fluence, ps_ext)
    'Initialize n2
    Worksheets("thermal").Activate
    Range("slab_thermal_home").Select
    For j = 1 To 2 * nslabs
        n2(j) = ActiveCell.Offset(j, 6).Value
    Next j
    'calculate the gain in the various slabs
    Call gain_calc(slab_thick, nslabs, fal, fbl, n0, n2, sigma_spec_laser, gain_log)

    'Update the 0-pass gain-log values
    Call pass_update(ps_ext, del_lambda, j_lambda_max, del_t, i_t_max, nslabs, pass, gain_log, B, fluence,
lambda, dEdlambda)

    'hit reverser mirror (M8,9,10)
    Call mirror_calc(i_t_max, j_lambda_max, mirror_loss, T_1way_optics, ps_ext)

    'go through lens L5
    Call lens_calc(slab_area, pi, del_lambda, i_t_max, j_lambda_max, m_5, l5_thick, gamma_fused_silica,
lens_surface_loss, B, lambda, ps_ext, T_1way_optics)

    'hit mirror M5
    Call mirror_calc(i_t_max, j_lambda_max, mirror_loss, T_1way_optics, ps_ext)

    'go through window
    Call wind_calc(slab_area, pi, del_lambda, i_t_max, j_lambda_max, w_thick, gamma_fused_silica,
window_surface_loss, B, lambda, ps_ext, T_1way_optics)

    'Go through slabs (1 to nslabs)
    first_slab = 1
    last_slab = nslabs
    Call slab_calc(slab_counter, fluence_path_res, slab_bulk_loss, slab_area, first_slab, last_slab, pi, del_t,
del_lambda, i_t_max, j_lambda_max, slab_thick, gamma_laser, slab_surface_loss, B, lambda, sigma, fal,
fbl, n2, n0, ps_ext, T_1way_optics)

    'Go through window
    Call wind_calc(slab_area, pi, del_lambda, i_t_max, j_lambda_max, w_thick, gamma_fused_silica,
window_surface_loss, B, lambda, ps_ext, T_1way_optics)

    'hit mirror M4
    Call mirror_calc(i_t_max, j_lambda_max, mirror_loss, T_1way_optics, ps_ext)

    'go through lens L4
```

```
    Call lens_calc(slab_area, pi, del_lambda, i_t_max, j_lambda_max, m_4, l4_thick, gamma_fused_silica,
lens_surface_loss, B, lambda, ps_ext, T_1way_optics)

    'go through lens L3
    Call lens_calc(slab_area, pi, del_lambda, i_t_max, j_lambda_max, m_3, l3_thick, gamma_fused_silica,
lens_surface_loss, B, lambda, ps_ext, T_1way_optics)

    'hit mirror M3
    Call mirror_calc(i_t_max, j_lambda_max, mirror_loss, T_1way_optics, ps_ext)

    'Go through window
    Call wind_calc(slab_area, pi, del_lambda, i_t_max, j_lambda_max, w_thick, gamma_fused_silica,
window_surface_loss, B, lambda, ps_ext, T_1way_optics)

    'Go through slabs (nslabs+1 to 2*nslabs)
    first_slab = nslabs + 1
    last_slab = 2 * nslabs
    Call slab_calc(slab_counter, fluence_path_res, slab_bulk_loss, slab_area, first_slab, last_slab, pi, del_t,
del_lambda, i_t_max, j_lambda_max, slab_thick, gamma_laser, slab_surface_loss, B, lambda, sigma, fal,
fbl, n2, n0, ps_ext, T_1way_optics)

    'Go through window
    Call wind_calc(slab_area, pi, del_lambda, i_t_max, j_lambda_max, w_thick, gamma_fused_silica,
window_surface_loss, B, lambda, ps_ext, T_1way_optics)

    'hit mirror M2
    Call mirror_calc(i_t_max, j_lambda_max, mirror_loss, T_1way_optics, ps_ext)

    'go through lens L2
    Call lens_calc(slab_area, pi, del_lambda, i_t_max, j_lambda_max, m_2, l2_thick, gamma_fused_silica,
lens_surface_loss, B, lambda, ps_ext, T_1way_optics)

    'go through lens L1
    Call lens_calc(slab_area, pi, del_lambda, i_t_max, j_lambda_max, m_1, l1_thick, gamma_fused_silica,
lens_surface_loss, B, lambda, ps_ext, T_1way_optics)

    'hit mirror M1
    Call mirror_calc(i_t_max, j_lambda_max, mirror_loss, T_1way_optics, ps_ext)

    'update pass 1
    pass = 1
    Call fluence_calc(slab_area, del_t, i_t_max, j_lambda_max, del_lambda, fluence, ps_ext)
    Call gain_calc(slab_thick, nslabs, fal, fbl, n0, n2, sigma_spec_laser, gain_log)
    Call pass_update(ps_ext, del_lambda, j_lambda_max, del_t, i_t_max, nslabs, pass, gain_log, B, fluence,
lambda, dEdlambda)

    'go through lens L1
    Call lens_calc(slab_area, pi, del_lambda, i_t_max, j_lambda_max, m_1, l1_thick, gamma_fused_silica,
lens_surface_loss, B, lambda, ps_ext, T_1way_optics)

    'go through lens L2
    Call lens_calc(slab_area, pi, del_lambda, i_t_max, j_lambda_max, m_2, l2_thick, gamma_fused_silica,
lens_surface_loss, B, lambda, ps_ext, T_1way_optics)

    'hit mirror M2
    Call mirror_calc(i_t_max, j_lambda_max, mirror_loss, T_1way_optics, ps_ext)
```

```
'Go through window
Call wind_calc(slab_area, pi, del_lambda, i_t_max, j_lambda_max, w_thick, gamma_fused_silica,
window_surface_loss, B, lambda, ps_ext, T_1way_optics)

'Go through slabs (2*nslabs to nslabs+1)
first_slab = 2 * nslabs
last_slab = nslabs + 1
Call slab_calc(slab_counter, fluence_path_res, slab_bulk_loss, slab_area, first_slab, last_slab, pi, del_t,
del_lambda, i_t_max, j_lambda_max, slab_thick, gamma_laser, slab_surface_loss, B, lambda, sigma, fal,
fbl, n2, n0, ps_ext, T_1way_optics)

'Go through window
Call wind_calc(slab_area, pi, del_lambda, i_t_max, j_lambda_max, w_thick, gamma_fused_silica,
window_surface_loss, B, lambda, ps_ext, T_1way_optics)

'hit mirror M3
Call mirror_calc(i_t_max, j_lambda_max, mirror_loss, T_1way_optics, ps_ext)

'go through lens L3
Call lens_calc(slab_area, pi, del_lambda, i_t_max, j_lambda_max, m_3, l3_thick, gamma_fused_silica,
lens_surface_loss, B, lambda, ps_ext, T_1way_optics)

'go through lens L4
Call lens_calc(slab_area, pi, del_lambda, i_t_max, j_lambda_max, m_4, l4_thick, gamma_fused_silica,
lens_surface_loss, B, lambda, ps_ext, T_1way_optics)

'hit mirror M4
Call mirror_calc(i_t_max, j_lambda_max, mirror_loss, T_1way_optics, ps_ext)

'Go through window
Call wind_calc(slab_area, pi, del_lambda, i_t_max, j_lambda_max, w_thick, gamma_fused_silica,
window_surface_loss, B, lambda, ps_ext, T_1way_optics)

'Go through slabs (nslabs to 1)
first_slab = nslabs
last_slab = 1
Call slab_calc(slab_counter, fluence_path_res, slab_bulk_loss, slab_area, first_slab, last_slab, pi, del_t,
del_lambda, i_t_max, j_lambda_max, slab_thick, gamma_laser, slab_surface_loss, B, lambda, sigma, fal,
fbl, n2, n0, ps_ext, T_1way_optics)

'Go through window
Call wind_calc(slab_area, pi, del_lambda, i_t_max, j_lambda_max, w_thick, gamma_fused_silica,
window_surface_loss, B, lambda, ps_ext, T_1way_optics)

'hit mirror M5
Call mirror_calc(i_t_max, j_lambda_max, mirror_loss, T_1way_optics, ps_ext)

'go through lens L5
Call lens_calc(slab_area, pi, del_lambda, i_t_max, j_lambda_max, m_5, l5_thick, gamma_fused_silica,
lens_surface_loss, B, lambda, ps_ext, T_1way_optics)

'hit reversor mirror (M8,9,10)
Call mirror_calc(i_t_max, j_lambda_max, mirror_loss, T_1way_optics, ps_ext)

'go through lens L6
```

```
    Call lens_calc(slab_area, pi, del_lambda, i_t_max, j_lambda_max, m_6, l6_thick, gamma_fused_silica,
lens_surface_loss, B, lambda, ps_ext, T_1way_optics)

    'hit mirror (M6,7)
    Call mirror_calc(i_t_max, j_lambda_max, mirror_loss, T_1way_optics, ps_ext)

    'update pass 2
    pass = 2
    Call fluence_calc(slab_area, del_t, i_t_max, j_lambda_max, del_lambda, fluence, ps_ext)
    Call gain_calc(slab_thick, nslabs, fal, fbl, n0, n2, sigma_spec_laser, gain_log)
    Call pass_update(ps_ext, del_lambda, j_lambda_max, del_t, i_t_max, nslabs, pass, gain_log, B, fluence,
lambda, dEdlambda)

    'go through lens L6
    Call lens_calc(slab_area, pi, del_lambda, i_t_max, j_lambda_max, m_6, l6_thick, gamma_fused_silica,
lens_surface_loss, B, lambda, ps_ext, T_1way_optics)

    'hit reversor mirror (M8,9,10)
    Call mirror_calc(i_t_max, j_lambda_max, mirror_loss, T_1way_optics, ps_ext)

    'go through lens L5
    Call lens_calc(slab_area, pi, del_lambda, i_t_max, j_lambda_max, m_5, l5_thick, gamma_fused_silica,
lens_surface_loss, B, lambda, ps_ext, T_1way_optics)

    'hit mirror M5
    Call mirror_calc(i_t_max, j_lambda_max, mirror_loss, T_1way_optics, ps_ext)

    'Go through window
    Call wind_calc(slab_area, pi, del_lambda, i_t_max, j_lambda_max, w_thick, gamma_fused_silica,
window_surface_loss, B, lambda, ps_ext, T_1way_optics)

    'Go through slabs (1 to nslabs)
    first_slab = 1
    last_slab = nslabs
    Call slab_calc(slab_counter, fluence_path_res, slab_bulk_loss, slab_area, first_slab, last_slab, pi, del_t,
del_lambda, i_t_max, j_lambda_max, slab_thick, gamma_laser, slab_surface_loss, B, lambda, sigma, fal,
fbl, n2, n0, ps_ext, T_1way_optics)

    'Go through window
    Call wind_calc(slab_area, pi, del_lambda, i_t_max, j_lambda_max, w_thick, gamma_fused_silica,
window_surface_loss, B, lambda, ps_ext, T_1way_optics)

    'hit mirror M4
    Call mirror_calc(i_t_max, j_lambda_max, mirror_loss, T_1way_optics, ps_ext)

    'go through lens L4
    Call lens_calc(slab_area, pi, del_lambda, i_t_max, j_lambda_max, m_4, l4_thick, gamma_fused_silica,
lens_surface_loss, B, lambda, ps_ext, T_1way_optics)

    'go through lens L3
    Call lens_calc(slab_area, pi, del_lambda, i_t_max, j_lambda_max, m_3, l3_thick, gamma_fused_silica,
lens_surface_loss, B, lambda, ps_ext, T_1way_optics)

    'hit mirror M3
    Call mirror_calc(i_t_max, j_lambda_max, mirror_loss, T_1way_optics, ps_ext)
```

```
    'Go through window
    Call wind_calc(slab_area, pi, del_lambda, i_t_max, j_lambda_max, w_thick, gamma_fused_silica,
window_surface_loss, B, lambda, ps_ext, T_1way_optics)

'Go through slabs (nslabs+1 to 2*nslabs)
    first_slab = nslabs + 1
    last_slab = 2 * nslabs
    Call slab_calc(slab_counter, fluence_path_res, slab_bulk_loss, slab_area, first_slab, last_slab, pi, del_t,
del_lambda, i_t_max, j_lambda_max, slab_thick, gamma_laser, slab_surface_loss, B, lambda, sigma, fal,
fbl, n2, n0, ps_ext, T_1way_optics)

    'Go through window
    Call wind_calc(slab_area, pi, del_lambda, i_t_max, j_lambda_max, w_thick, gamma_fused_silica,
window_surface_loss, B, lambda, ps_ext, T_1way_optics)

    'hit mirror M2
    Call mirror_calc(i_t_max, j_lambda_max, mirror_loss, T_1way_optics, ps_ext)

    'go through lens L2
    Call lens_calc(slab_area, pi, del_lambda, i_t_max, j_lambda_max, m_2, l2_thick, gamma_fused_silica,
lens_surface_loss, B, lambda, ps_ext, T_1way_optics)

    'go through lens L1
    Call lens_calc(slab_area, pi, del_lambda, i_t_max, j_lambda_max, m_1, l1_thick, gamma_fused_silica,
lens_surface_loss, B, lambda, ps_ext, T_1way_optics)

    'hit mirror M1
    Call mirror_calc(i_t_max, j_lambda_max, mirror_loss, T_1way_optics, ps_ext)

    'update pass 3
    pass = 3
    Call fluence_calc(slab_area, del_t, i_t_max, j_lambda_max, del_lambda, fluence, ps_ext)
    Call gain_calc(slab_thick, nslabs, fal, fbl, n0, n2, sigma_spec_laser, gain_log)
    Call pass_update(ps_ext, del_lambda, j_lambda_max, del_t, i_t_max, nslabs, pass, gain_log, B, fluence,
lambda, dEdlambda)

    'go through lens L1
    Call lens_calc(slab_area, pi, del_lambda, i_t_max, j_lambda_max, m_1, l1_thick, gamma_fused_silica,
lens_surface_loss, B, lambda, ps_ext, T_1way_optics)

    'go through lens L2
    Call lens_calc(slab_area, pi, del_lambda, i_t_max, j_lambda_max, m_2, l2_thick, gamma_fused_silica,
lens_surface_loss, B, lambda, ps_ext, T_1way_optics)

    'hit mirror M2
    Call mirror_calc(i_t_max, j_lambda_max, mirror_loss, T_1way_optics, ps_ext)

    'Go through window
    Call wind_calc(slab_area, pi, del_lambda, i_t_max, j_lambda_max, w_thick, gamma_fused_silica,
window_surface_loss, B, lambda, ps_ext, T_1way_optics)

    'Go through slabs (2*nslabs to nslabs+1)
    first_slab = 2 * nslabs
    last_slab = nslabs + 1
```

```
    Call slab_calc(slab_counter, fluence_path_res, slab_bulk_loss, slab_area, first_slab, last_slab, pi, del_t,
del_lambda, i_t_max, j_lambda_max, slab_thick, gamma_laser, slab_surface_loss, B, lambda, sigma, fal,
fbl, n2, n0, ps_ext, T_1way_optics)

    'Go through window
    Call wind_calc(slab_area, pi, del_lambda, i_t_max, j_lambda_max, w_thick, gamma_fused_silica,
window_surface_loss, B, lambda, ps_ext, T_1way_optics)

    'hit mirror M3
    Call mirror_calc(i_t_max, j_lambda_max, mirror_loss, T_1way_optics, ps_ext)

    'go through lens L3
    Call lens_calc(slab_area, pi, del_lambda, i_t_max, j_lambda_max, m_3, l3_thick, gamma_fused_silica,
lens_surface_loss, B, lambda, ps_ext, T_1way_optics)

    'go through lens L4
    Call lens_calc(slab_area, pi, del_lambda, i_t_max, j_lambda_max, m_4, l4_thick, gamma_fused_silica,
lens_surface_loss, B, lambda, ps_ext, T_1way_optics)

    'hit mirror M4
    Call mirror_calc(i_t_max, j_lambda_max, mirror_loss, T_1way_optics, ps_ext)

    'Go through window
    Call wind_calc(slab_area, pi, del_lambda, i_t_max, j_lambda_max, w_thick, gamma_fused_silica,
window_surface_loss, B, lambda, ps_ext, T_1way_optics)

    'Go through slabs (nslabs to 1)
    first_slab = nslabs
    last_slab = 1
    Call slab_calc(slab_counter, fluence_path_res, slab_bulk_loss, slab_area, first_slab, last_slab, pi, del_t,
del_lambda, i_t_max, j_lambda_max, slab_thick, gamma_laser, slab_surface_loss, B, lambda, sigma, fal,
fbl, n2, n0, ps_ext, T_1way_optics)

    'Go through window
    Call wind_calc(slab_area, pi, del_lambda, i_t_max, j_lambda_max, w_thick, gamma_fused_silica,
window_surface_loss, B, lambda, ps_ext, T_1way_optics)

    'hit mirror M5
    Call mirror_calc(i_t_max, j_lambda_max, mirror_loss, T_1way_optics, ps_ext)

    'go through lens L5
    Call lens_calc(slab_area, pi, del_lambda, i_t_max, j_lambda_max, m_5, l5_thick, gamma_fused_silica,
lens_surface_loss, B, lambda, ps_ext, T_1way_optics)

    'go through lens L8
    Call lens_calc(slab_area, pi, del_lambda, i_t_max, j_lambda_max, m_6, l6_thick, gamma_fused_silica,
lens_surface_loss, B, lambda, ps_ext, T_1way_optics)

    'update pass 4
    pass = 4
    Call fluence_calc(slab_area, del_t, i_t_max, j_lambda_max, del_lambda, fluence, ps_ext)
    Call gain_calc(slab_thick, nslabs, fal, fbl, n0, n2, sigma_spec_laser, gain_log)
    Call pass_update(ps_ext, del_lambda, j_lambda_max, del_t, i_t_max, nslabs, pass, gain_log, B, fluence,
lambda, dEdlambda)

'Ouput gain-log in slabs after extraction
```

```
    Worksheets("excitationextraction").Activate
    Range("slab_data_home").Select
    For j = 1 To 2 * nslabs
        ActiveCell.Offset(j, 5).Value = gain_log(j)
        ActiveCell.Offset(j, 6).Value = n2(j) / n0(j)
    Next j

'Output pulse energy and efficiency
    e_out = eta_modefill * fluence * slab_area
    Range("e_out").Select: ActiveCell.Value = e_out
    Range("E_out_of_array").Select: E_out_of_array = ActiveCell.Value
    opt_to_opt_eff = e_out / (4 * E_out_of_array)
    Range("opt_to_opt_eff").Select: ActiveCell.Value = opt_to_opt_eff

'Output 1-way cavity transmission (sans LG-750 bulk and surface loss) and f_sat and other stuff
    T_1way_optics = T_1way_optics ^ (1 / 8)
    Range("T_1way_optics").Select: ActiveCell.Value = T_1way_optics

'Input the time resolved thermal energy deposition profile for slab 1 up until the end of the pump pulse
    Worksheets("thermal").Activate
    Range("slab_1_thermal_home").Select
    del_time = ActiveCell.Offset(2, 0).Value - ActiveCell.Offset(1, 0).Value
    i = 0
    For t = 0 To tau_pulse Step del_time
        i = i + 1
        elapsed_time(i) = ActiveCell.Offset(i, 0).Value
        p_th_1(i) = ActiveCell.Offset(i, 1).Value
    Next t
    t_count = i

'Let the rest of the population decay away and generate heat
    'Input thermal history prior to extraction
    Worksheets("thermal").Activate
    Range("slab_thermal_home").Select
    For j = 1 To 2 * nslabs
        p_th(j) = ActiveCell.Offset(j, 1).Value
        spon_em_power(j) = ActiveCell.Offset(j, 7).Value
    Next j
    dell_time = tau0 / 10
    i = 0
    For t = 0 To 3 * tau0 Step dell_time
        i = i + 1
        For j = 1 To 2 * nslabs
            tau_quenched = tau0 / (1 + (n0(j) / quenching_parameter) ^ 2)
            'tau_trap = tau_quenched * 1.1667  'Steve Payne's Fudge factor for lifetime trapping in glass
            tau_trap = tau_quenched / (1 - beta_zero_line * (1 - Exp(-(n0(j) - n2(j)) * sigma_zero_line *
l_trap / 2)))
            Mase = Exp(n2(j) * sigma_em_pol_ave * l_trap + (n2(j) * sigma_em_pol_ave * l_trap) ^ 2 / 2)
            tau = tau_trap / Mase
            n2(j) = n2(j) * Exp(-dell_time / tau)
            p_th(j) = p_th(j) + ((n0(j) / quenching_parameter) ^ 2 * (1 / tau0)) * (n2(j) * slab_height *
slab_width * slab_thick) * hvl * dell_time * prf
                If j = 1 Then
                    p_th_1(t_count + i) = (((n0(j) / quenching_parameter) ^ 2 * (1 / tau0)) * (n2(j) *
slab_height * slab_width * slab_thick) * hvl)
                    elapsed_time(t_count + i) = elapsed_time(t_count) + t
```

```
                End If
        'Calculate the spontaneous emission power generated in each slab using the trapped and ase
impacted lifetime
            spon_em_power(j) = spon_em_power(j) + n2(j) * slab_vol * (dell_time / tau) * hvl * prf
        Next j
    Next t
    t_count = t_count + i
    For j = 1 To 2 * nslabs
        p_thppp(j) = p_th(j) / (slab_area * slab_thick)
        p_thpp(j) = p_thppp(j) * slab_thick / 2
        slab_center_to_edge_temp(j) = (p_thppp(j) / (2 * k_th)) * (slab_thick / 2) ^ 2
        slab_b(j) = p_thppp(j) / (12 * Rt / slab_thick ^ 2)
    Next j
    Worksheets("thermal").Activate
    Range("slab_thermal_home_2").Select
    For j = 1 To 2 * nslabs
        ActiveCell.Offset(j, 0).Value = j
        ActiveCell.Offset(j, 1).Value = p_th(j)
        ActiveCell.Offset(j, 2).Value = p_thpp(j)
        ActiveCell.Offset(j, 3).Value = p_thppp(j)
        ActiveCell.Offset(j, 4).Value = slab_center_to_edge_temp(j)
        ActiveCell.Offset(j, 5).Value = slab_b(j)
        ActiveCell.Offset(j, 6).Value = n2(j)
        ActiveCell.Offset(j, 7).Value = spon_em_power(j)
    Next j

'Calculate the edge cladding thermal load using a simple minded trapping argument
    For j = 1 To 2 * nslabs
        edge_clad_thermal(j) = Sqr(1 - 1 / ref_index ^ 2) * spon_em_power(j)
        ActiveCell.Offset(j, 8).Value = edge_clad_thermal(j)
    Next j

'Output ps_ext(i,j)
    Worksheets("ps_ext").Activate
    Range("del_t").Select:  ActiveCell.Value = del_t
    Range("del_lambda").Select:  ActiveCell.Value = del_lambda
    Range("i_t_max").Select:  ActiveCell.Value = i_t_max
    Range("j_lambda_max").Select:  ActiveCell.Value = j_lambda_max
    Range("ps_time").Select
    For i = 0 To i_t_max
        ActiveCell.Offset(i + 1, 0).Value = i * del_t
    Next i
    Range("ps_lambda").Select
    For j = 0 To j_lambda_max
        ActiveCell.Offset(j + 1, 0).Value = lambda(j)
    Next j
    Range("ps_home").Select
    For i = 0 To i_t_max
        For j = 0 To j_lambda_max
            ActiveCell.Offset(i + 1, j).Value = ps_ext(i, j)
        Next j
    Next i

'Output temporal and spectral extraction output pulse data
    Worksheets("extraction pulse").Activate
    'Range("extraction_output_spectral_home").Select
```

```
    'For j = 0 To j_lambda_max
    '     ActiveCell.Offset(j, 0).Value = lambda(j)
    '      dEdlambda = 0
    '      For i = 0 To i_t_max
    '           dEdlambda = dEdlambda + ps_ext(i, j)
    '      Next i
    '      dEdlambda = dEdlambda * del_t
    '      ActiveCell.Offset(j, 1).Value = dEdlambda
    '      ActiveCell.Offset(j, 2).Value = sigma(j)
    ' Next j
    Range("extraction_output_time_home").Select
    For i = 0 To i_t_max
        ActiveCell.Offset(i + 1, 0).Value = i * del_t
        dEdt = 0
        For j = 0 To j_lambda_max
            dEdt = dEdt + ps_ext(i, j)
        Next j
        dEdt = dEdt * del_lambda
        ActiveCell.Offset(i + 1, 1).Value = dEdt
    Next i

'Output the time resolved thermal power deposition profile for slab 1
    Worksheets("thermal").Activate
    Range("slab_1_thermal_home_b").Select
    For i = 1 To t_count
        ActiveCell.Offset(i, 0).Value = elapsed_time(i)
        ActiveCell.Offset(i, 1).Value = p_th_1(i)
    Next i

'Output the fluence before and after each slab as the extracting pulse winds its way through the amplifier
chain
    Worksheets("fluence").Activate
    Range("fluence_home").Select
    For i = 1 To slab_counter
        ActiveCell.Offset(i, 0).Value = i
        ActiveCell.Offset(i, 1).Value = fluence_path_res(i, 1)
        ActiveCell.Offset(i, 2).Value = fluence_path_res(i, 2)
    Next i

'Go home and quit
    Worksheets("excitationextraction").Activate

End Sub

Sub fluence_calc(slab_area, del_t, i_t_max, j_lambda_max, del_lambda, fluence, ps_ext)
'Calculate the local Fluence
    fluence = 0
    For i = 0 To i_t_max
    For j = 0 To j_lambda_max
        fluence = fluence + ps_ext(i, j)
    Next j
    Next i
    fluence = fluence * del_t * del_lambda / slab_area
End Sub

Sub gain_calc(slab_thick, nslabs, fal, fbl, n0, n2, sigma_spec_laser, gain_log)
```

```
'Calculate the gain in the slabs
    For j = 1 To 2 * nslabs
        gain_log(j) = ((fal + fbl) * n2(j) - fal * n0(j)) * sigma_spec_laser * slab_thick
    Next j
End Sub

Sub pass_update(ps_ext, del_lambda, j_lambda_max, del_t, i_t_max, nslabs, pass, gain_log, B, fluence,
lambda, dEdlambda)
'Output gain values to excitationextraction sheet
    Worksheets("excitationextraction").Activate
    Range("pass_table_home").Select
    ActiveCell.Offset(1, 1 + pass).Value = fluence
    'Find the maximum B-integral
    B_max = 0
    For i = 0 To i_t_max
        If B(i) > B_max Then B_max = B(i)
    Next i
    ActiveCell.Offset(2, 1 + pass).Value = B_max
    For i = 1 To 2 * nslabs
        ActiveCell.Offset(2 + i, 1 + pass).Value = gain_log(i)
    Next i

    Worksheets("extraction pulse").Activate
    Range("pass_time_home").Select
    For i = 0 To i_t_max
        If pass = 0 Then
            ActiveCell.Offset(i + 1, 0).Value = i * del_t
        End If
        dEdt = 0
        For j = 0 To j_lambda_max
            dEdt = dEdt + ps_ext(i, j)
        Next j
        dEdt = dEdt * del_lambda
        ActiveCell.Offset(i + 1, pass + 1).Value = dEdt
    Next i
    '**********************************
    Range("pass_wav_home").Select
    For j = 0 To j_lambda_max
        If pass = 0 Then ActiveCell.Offset(j + 1, 0).Value = lambda(j)
        dEdlambda = 0
        For i = 0 To i_t_max
            dEdlambda = dEdlambda + ps_ext(i, j)
        Next i
        dEdlambda = dEdlambda * del_t
        ActiveCell.Offset(j + 1, pass + 1).Value = dEdlambda
    Next j
    '**********************************
End Sub

Sub mirror_calc(i_t_max, j_lambda_max, mirror_loss, T_1way_optics, ps_ext)
'Update fluence for mirror loss
    For i = 0 To i_t_max
    For j = 0 To j_lambda_max
        ps_ext(i, j) = ps_ext(i, j) * (1 - mirror_loss)
    Next j
    Next i
```

```
    T_1way_optics = T_1way_optics * (1 - mirror_loss)
End Sub

Sub lens_calc(A, pi, del_lambda, i_t_max, j_lambda_max, magnification, thickness, gamma,
lens_surface_loss, B, lambda, ps_ext, T_1way_optics)
'Update fluence and B-integral after transmission through lens
    For i = 0 To i_t_max
    For j = 0 To j_lambda_max
        ps_ext(i, j) = ps_ext(i, j) * (1 - lens_surface_loss)
    Next j
    Next i
    T_1way_optics = T_1way_optics * (1 - lens_surface_loss)
    For i = 0 To i_t_max
    For j = 0 To j_lambda_max
        B(i) = B(i) + (2 * pi / lambda(j)) * (ps_ext(i, j) * del_lambda / (A * magnification)) * gamma *
thickness * 10000000#
    Next j
    Next i
    For i = 0 To i_t_max
    For j = 0 To j_lambda_max
        ps_ext(i, j) = ps_ext(i, j) * (1 - lens_surface_loss)
    Next j
    Next i
    T_1way_optics = T_1way_optics * (1 - lens_surface_loss)
End Sub

Sub wind_calc(A, pi, del_lambda, i_t_max, j_lambda_max, thickness, gamma, window_surface_loss, B,
lambda, ps_ext, T_1way_optics)
    For i = 0 To i_t_max
    For j = 0 To j_lambda_max
        ps_ext(i, j) = ps_ext(i, j) * (1 - window_surface_loss)
    Next j
    Next i
    T_1way_optics = T_1way_optics * (1 - window_surface_loss)
    For i = 0 To i_t_max
    For j = 0 To j_lambda_max
            B(i) = B(i) + (2 * pi / lambda(j)) * (ps_ext(i, j) * del_lambda / A) * gamma * thickness *
10000000#
    Next j
    Next i
    For i = 0 To i_t_max
    For j = 0 To j_lambda_max
        ps_ext(i, j) = ps_ext(i, j) * (1 - window_surface_loss)
    Next j
    Next i
    T_1way_optics = T_1way_optics * (1 - window_surface_loss)
End Sub

Sub slab_calc(slab_counter, fluence_path_res, slab_bulk_loss, A, first_slab, last_slab, pi, del_t,
del_lambda, i_t_max, j_lambda_max, thickness, gamma, slab_surface_loss, B, lambda, sigma, fal, fbl, n2,
n0, ps_ext, T_1way_optics)
If first_slab > last_slab Then
    del_slab = -1
Else
    del_slab = 1
End If
```

```
For k = first_slab To last_slab Step del_slab
    For i = 0 To i_t_max
    For j = 0 To j_lambda_max
        ps_ext(i, j) = ps_ext(i, j) * (1 - slab_surface_loss)
    Next j
    Next i
    T_1way_optics = T_1way_optics * (1 - slab_surface_loss)
        'fluence just prior to going through the salb
        slab_counter = slab_counter + 1
        Call fluence_calc(A, del_t, i_t_max, j_lambda_max, del_lambda, fluence_path_res(slab_counter, 1),
ps_ext)
    For i = 0 To i_t_max
    For j = 0 To j_lambda_max
            hvl = 2E-16 / lambda(j)
            del_ps_ext = ps_ext(i, j) * (Exp(((fal + fbl) * n2(k) - fal * n0(k)) * thickness * sigma(j)) - 1)
            B(i) = B(i) + (2 * pi / lambda(j)) * ((ps_ext(i, j) + del_ps_ext / 2) * del_lambda / A) * gamma *
thickness * 10000000#
            ps_ext(i, j) = ps_ext(i, j) + del_ps_ext
            n2(k) = n2(k) - del_ps_ext * del_lambda * del_t / (hvl * A * thickness)
    Next j
    Next i
        'fluence just subsequent to going through the slab
        Call fluence_calc(A, del_t, i_t_max, j_lambda_max, del_lambda, fluence_path_res(slab_counter, 2),
ps_ext)
    For i = 0 To i_t_max
    For j = 0 To j_lambda_max
        ps_ext(i, j) = ps_ext(i, j) * (1 - slab_bulk_loss) * (1 - slab_surface_loss)
    Next j
    Next i
    T_1way_optics = T_1way_optics * (1 - slab_surface_loss)
Next k
End Sub
```

IIIf. Mercury Fluences

This is a Visualbasic code which is linked to a set of Excel spreadsheets and is run on a PC running Windows 95 and using Excel 97. This routine is module 2 of a spreadsheet entitled “SI spectral pump and spectral extraction model with BeO BASIS and Yb:S-FAP ver 3.xls, ” which calculates the fluence as a function of distance through the amplifier slabs using the data from module 2 for Mercury. The spreadsheets used are named: excitationextraction, ps_ext, thermal, fluence, extraction pulse, emission spectrum data, and slab spectral data.

```
Sub SRSfluence()
'
'Written by Andy Bayramian 08/03/98
'
'incremental fluence calculation declarations and initializations
    'inputenergy = 0.00002       'Joules
    inputenergy = 0.00015       'Joules
    Eslice = 0.00001 'Joules
    step = 0.05
    bandwidthcheck = 1

'Mercury Energy loop
    Worksheets("excitationextraction").Activate
```

```
    Range("energypoints").Select:  energypoints = ActiveCell.Value
    Range("slab_thick").Select:  slab_thick = ActiveCell.Value
    Range("nslabs").Select:  nslabs = ActiveCell.Value
    Range("n_frequency_bins").Select:  freqpts = ActiveCell.Value

For p = 1 To energypoints Step 1
    Worksheets("excitationextraction").Cells(51, 1).Value = inputenergy
    Worksheets("fluence").Cells(2, 2).Value = p
    'inputenergy = inputenergy + Eslice
    inputenergy = inputenergy * 10
    Eslice = Eslice + 0.000005  'this scales the energy step s.t. as amps saturate step gets bigger
    Call Extraction
    slab_counter = nslabs * 2 * 4
    If p = 1 Then
        totpts = Int(slab_counter * slab_thick / step)
        slabpts = Int(slab_thick / step)
        For i = 0 To totpts Step 1
            Worksheets("fluence").Cells(3 + i, 5).Value = i * step
        Next i
    End If
    For i = 1 To slab_counter Step 1
        Slope = (Worksheets("fluence").Cells(i + 4, 3).Value - Worksheets("fluence").Cells(i + 4, 2).Value)
/ (slab_thick)
        If i = 1 Then Worksheets("fluence").Cells(3, p + 5).Value = Worksheets("fluence").Cells(5,
2).Value
        For j = 1 To slabpts Step 1
            Worksheets("fluence").Cells((i - 1) * slabpts + j + 3, p + 5).Value = Slope * step * j +
Worksheets("fluence").Cells(i + 4, 2).Value
        Next j
    Next i

    If bandwidthcheck = 1 Then
    '****************bandwidth adjustment*******************************'
    Worksheets("extraction pulse").Activate
    Range("pass_wav_home").Select

    band0 = Worksheets("extraction pulse").Cells(2, 28).Value
    widthdef = 0.5
    Lorwidth = 84.1 * 1000000000#
    lambda0 = ActiveCell.Offset(band0, 0).Value
    For z = 0 To 4 Step 1
        emm1 = ActiveCell.Offset(band0, z + 1).Value
        oldemm1 = emm1
        widthemm = widthdef * emm1
        For y = 1 To 1000 Step 1
            emm1 = ActiveCell.Offset(band0 + y, z + 1).Value
            If emm1 < widthemm Then
                percent = (oldemm1 - widthemm) / (oldemm1 - emm1)
                lambda1 = ActiveCell.Offset(band0 + y - 1, 0).Value + percent * (ActiveCell.Offset(band0 +
y, 0).Value - ActiveCell.Offset(band0 + y - 1, 0).Value)
                Widthneg = 3E+17 * ((1 / lambda0) - (1 / lambda1))
                GoTo 1
            End If
            oldemm1 = emm1
        Next y
1     emm2 = ActiveCell.Offset(band0, z + 1).Value
```

```
        oldemm2 = emm2
        For y = 1 To 1000 Step 1
            emm2 = ActiveCell.Offset(band0 - y, z + 1).Value
            If emm2 < widthemm Then
                percent = (oldemm2 - widthemm) / (oldemm2 - emm2)
                lambda2 = ActiveCell.Offset(band0 - y + 1, 0).Value - percent * (ActiveCell.Offset(band0 -
y + 1, 0).Value - ActiveCell.Offset(band0 - y, 0).Value)
                Widthpos = 3E+17 * ((1 / lambda2) - (1 / lambda0))
                GoTo 2
            End If
            oldemm2 = emm2
        Next y
2     Totwidth = Widthneg + Widthpos
        Bandratio = Lorwidth / (Lorwidth + Totwidth)
        lineout = 845
        Worksheets("fluence").Cells(lineout + z, p + 5).Value = Bandratio
        Worksheets("fluence").Cells(lineout + z + 5, p + 5).Value = Totwidth
    Next z
    '************************************************************'

    End If

Next p

End Sub
```

IIIf1 (Example spreadsheet associated with IIId, IIIe, IIIf)

	A	B	C	D	E	F	G
1	**Si spectral pump and spectral extraction model**						
2	**Diode parameters are for BeO BASIS**						
3	**Amplifer slabs are Yb:S-FAP**						
4							
5	Type control-p to update						
6	**Slab Data Input Parameters:**						
7	7		number of slabs in stack				
8	3		height of slab (cm)				
9	5		width of slab (cm)				
10	0.75		thickness of slab (cm)				
11	1.40E+19		Yb doping density (cm^-3)				
12	1.70E+19		Yb doping density (cm^-3)				
13	2.00E+19		Yb doping density (cm^-3)				
14	2.00E+19		Yb doping density (cm^-3)				
15	2.00E+19		Yb doping density (cm^-3)				
16	1.70E+19		Yb doping density (cm^-3)				
17	1.40E+19		Yb doping density (cm^-3)				
18	1.2		slab Rt value (W/cm)				
19	0.02		slab termal conductivity (W/cm-C)				
20	1.6252		refractive index of slabs				
21	4.10E-16		slab nonlinear index parameter (cm^2/W)				
22							
23	**Yb Spectroscopic Input Parameters:**						
24	6.00E-20		spectroscopic peak laser emission cross section (cm^2)				
25	0.05		lower laser level Boltzmann occupation factor, fal				
26	0.99		upper laser level Boltzmann occupation factor, fbl				
27	0.81		lower pump level Boltzmann occupation factor, fap				
28	0.01		upper pump level Boltzmann occupation factor, fbp				
29	1.00E+50		q, the quenching parameter (1/cm^3)				
30	0.0011		lifetime w/o quenching, trapping or ASE (sec)				
31	1047.00		laser wavelength (nm)				
32	900.00		pump wavelength (nm)				
33	3.30E-01		zero-line branching ratio				
34	2.93E-20		polarization averaged emission cross section (cm^2)				
35	8.00E-20		zero-line absorption cross section (cm^2)				
36							
37	**Pump Characteristics Input Parameters:**						
38	160000		initial pump power at each end of stack (W)				
39	10		laser PRF (Hz)				
40	0.00075		pump pulse duration (sec)				
41	895.5		initial center wavelength of pump pulse (nm)				
42	4.8		instantaneous pump spectral 1/e halfwidth (nm)				
43	632		alpha (deg-C/sqrt(sec))				

	A	B	C	D	E	F	G
44	0.00385		fractional pump power degradation rate (1/deg-C)				
45	0.3		wavelength chirp with temperature (nm/deg-C)				
46	0.95		pump overlap with extracted area				
47	0.85		pump transport efficiency to slabs				
48							
49							
50	**Extracting Beam Input Parameters:**						
51	0.025265		front end energy delivered to amplifier (J)				
52	3		number of input front end energy points				
53	10		extraction pulse width (nsec)				
54	25		number of time bins over the pulse				
55	77		number of frequency bins over the pulse				
56	1047.75		central wavelength of input pulse (nm)				
57	1		1/e-half width of initial extraction pulse spectrum (nm)				
58							
59	**Optics Chain Input parameters:**						
60	0.005		loss per mirror surface				
61	0.0025		loss per lens surface				
62	0.0025		loss per window surface				
63	0.0025		loss per slab surface				
64	0.005		bulk slab loss (1/cm)				
65	0.87		modefill efficiency				
66	1		window thickness (cm)				
67	2.85E-16		fused silica nonlinear index parameter (cm^2/W)				
68							
69	**Lens Characteristics Input Parameters:**						
70	Lens	thickness	areal magnification of beam relative to size in slabs				
71		(cm)					
72	1	2.4	9				
73	2	0.8	1				
74	3	0.8	1				
75	4	0.8	1				
76	5	0.8	1				
77	6	0.4	0.16				
78	7	0.4	0.16				
79	8	0.8	1				
80							
81	**Output Parameters for the Pump Sequence:**						
82	1.7353576		trapping length in slabs (cm)				
83	0.8075		net pump transport efficiency to slabs				
84	114.71074		total pump energy from each array at end of stack (J)				
85	14.539839		total pump energy that leaks out end of stack (J)				
86	0.8430313		crystal absorption efficiency				
87	0.6807478		fraction of total pump absorbed in crystals				
88	3.5653829		initial gain-log of entire chain (nepers)				
89	3.075E-07		Nd:LG-750 laser transition saturation fluence (J/cm^2)				
90	25.6		thermal power density at fracture (W/cm^3)				

	A	B	C	D	E	F	G
91	187.7228		total stored energy (J)				
92	23.293427		stored energy needed to reach transparency (J)				
93	164.42937		extractable stored energy (J)				
94							
95							
96							
97	**Output Parameters for the Extraction Sequence:**						
98	0.2369169		900 nm to 1053 nm efficiency				
99	108.70765		pulse energy out of amplifier(J)				
100	0.9293835		Passive 1-way cavity transmissio				
101							
102	**Slab Data Prior to Extraction**					**Slab Data Subsequent**	
103	slab	gain_log	tau_avg	ex_frac		gain-log	ex_frac
104	1	0.266515	0.001059	0.452959		0.006891	0.05498579
105	2	0.261339	0.001114	0.37433		0.007961	0.05447261
106	3	0.249373	0.001164	0.312005		0.008566	0.05361439
107	4	0.228244	0.001187	0.289334		0.008481	0.05352329
108	5	0.249371	0.001164	0.312003		0.009719	0.05485189
109	6	0.261337	0.001114	0.374328		0.010385	0.0575325
110	7	0.266513	0.001059	0.452957		0.010436	0.0604196
111	8	0.266515	0.001059	0.452959		0.009511	0.0590023
112	9	0.261339	0.001114	0.37433		0.008641	0.05533178
113	10	0.249373	0.001164	0.312005		0.007434	0.05239984
114	11	0.228244	0.001187	0.289334		0.006026	0.05088855
115	12	0.249371	0.001164	0.312003		0.005708	0.05054746
116	13	0.261337	0.001114	0.374328		0.005029	0.05077085
117	14	0.266513	0.001059	0.452957		0.004194	0.05085231
118							
119							
120							
121							
122							
123							
124							
125							
126							
127							
128							
129							
130							
131							
132							
133							
134							
135							
136							

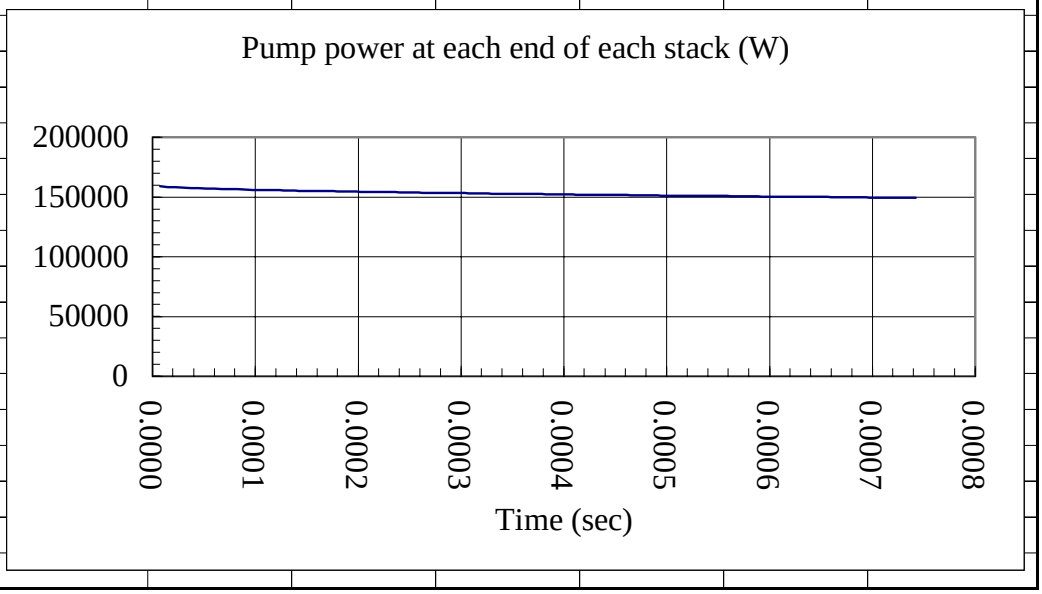

Pump Excitation Equations

$$\frac{\partial^2 E}{\partial t \, \partial \lambda} = \frac{P(t)}{\sqrt{\pi}\,\lambda_{1/eHW}} e^{-\left(\frac{\lambda - \lambda_0(t)}{\lambda_{1/eHW}}\right)^2}$$

where:

$$\lambda_0(t) = \lambda_{00} + \frac{d\lambda}{dT}\Delta T$$

$$P(t) = P_0\left(1 - \left(\frac{1}{P}\frac{dP}{dT}\right)\Delta T\right)$$

$$\Delta T = \alpha\sqrt{t}$$

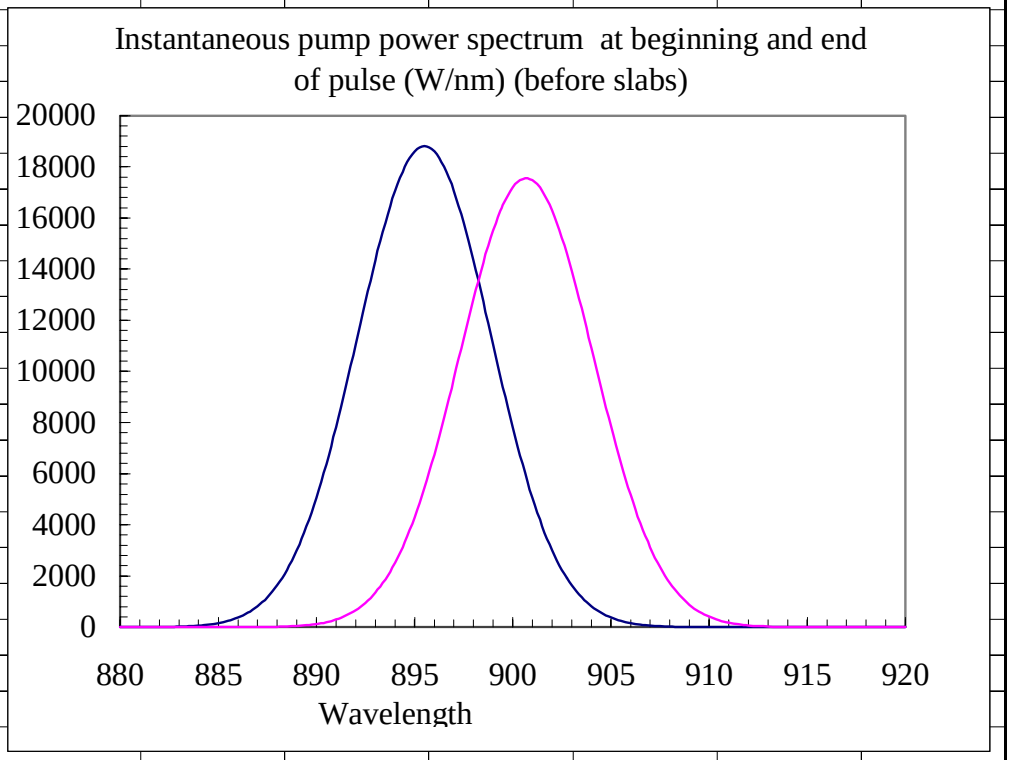

	H	I	J	K	L	M	N
48							
49		**Slab Data as a Function of Pass Number:**					
50			pass 0	pass 1	pass 2	pass 3	pass 4
51		fluence (J/	0.001684	0.044783	1.011995	6.284861	8.330088
52		B-integral	0	0.000566	0.02039	0.314641	1.793061
53	gain of slal	1	0.266515	0.266355	0.196561	0.139001	0.006891
54	gain of slal	2	0.261339	0.261138	0.204628	0.136422	0.007961
55	gain of slal	3	0.249373	0.249129	0.204774	0.1275	0.008566
56	gain of slal	4	0.228244	0.227965	0.194393	0.11231	0.008481
57	gain of slal	5	0.249371	0.248989	0.218836	0.115933	0.009719
58	gain of slal	6	0.261337	0.260827	0.235372	0.112066	0.010385
59	gain of slal	7	0.266513	0.265846	0.245206	0.102933	0.010436
60	gain of slal	8	0.266515	0.265683	0.2489	0.093249	0.009511
61	gain of slal	9	0.261339	0.260292	0.24731	0.079403	0.008641
62	gain of slal	10	0.249373	0.248103	0.23828	0.064999	0.007434
63	gain of slal	11	0.228244	0.226791	0.219564	0.050872	0.006026
64	gain of slal	12	0.249371	0.247384	0.241042	0.046955	0.005708
65	gain of slal	13	0.261337	0.258689	0.253443	0.040517	0.005029
66	gain of slal	14	0.266513	0.263054	0.258871	0.033321	0.004194
67							
68							
69				Laser Extraction Equations			
70							
71	$\Delta ps\_ext(i,j) = ps\_ext(i,j)\left[\left(f_{al} + f_{bl}\right)n_2 - f_{al}n_0\right]l_s\sigma(j)$						
72							
73	$\Delta n_2 = -\frac{\Delta ps\_ext(i,j)\,dt\,d\lambda}{h\upsilon_l A l_s}$						
74							
75							
76	$where,$						
77							
78	$ps\_ext \equiv \frac{\partial^2 E}{\partial t\,\partial \lambda}$						
79							
80							
81	ps_ext(i,j) is the power spectrum of the extracting pulse (t,lambda)						
82							

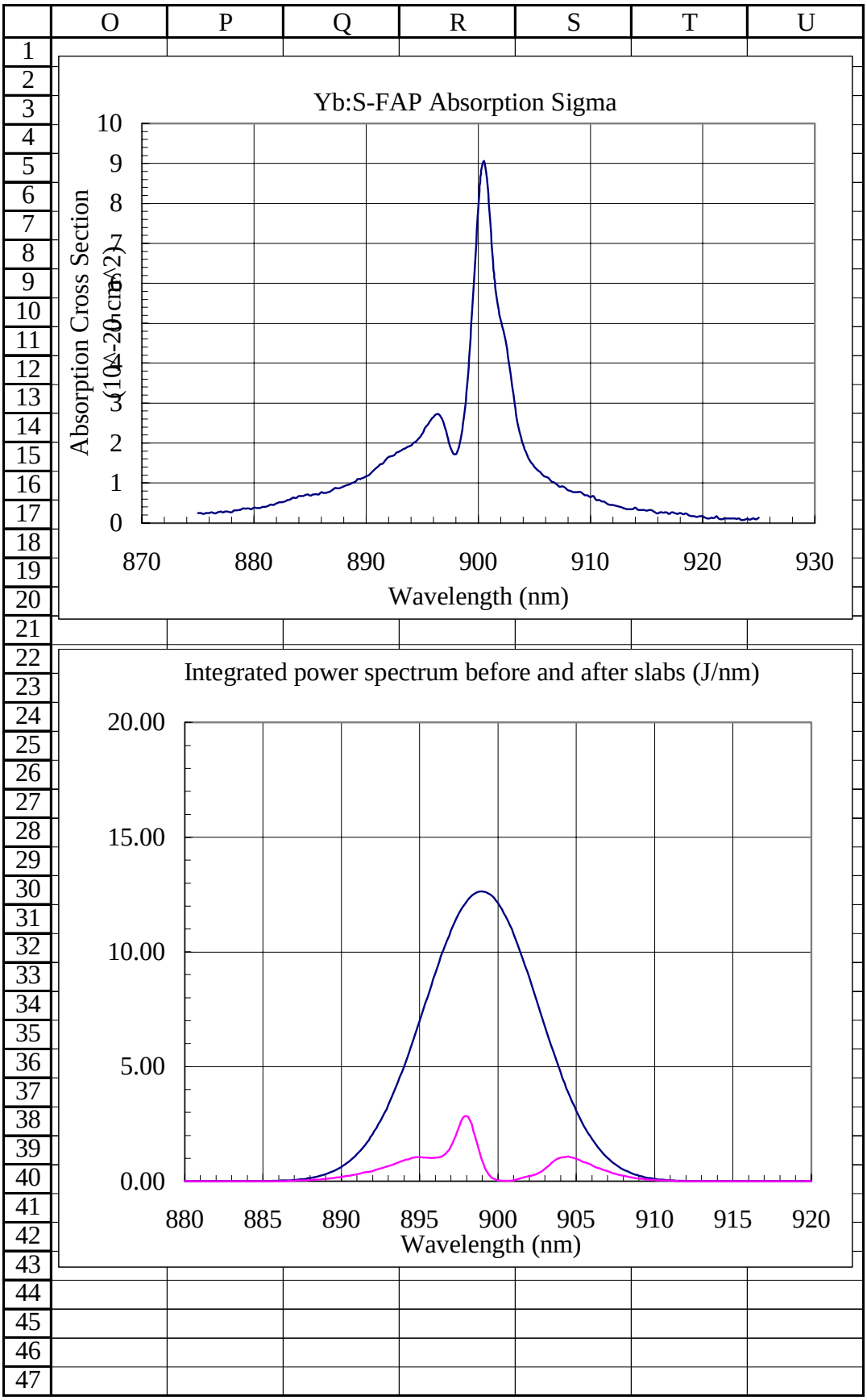
Yb:S-FAP Absorption Sigma
Absorption Cross Section (10^-20 cm^2)
0
1
2
3
4
5
6
7
8
9
10
870
880
890
900
910
920
930
Wavelength (nm)
Integrated power spectrum before and after slabs (J/nm)
0.00
5.00
10.00
15.00
20.00
880
885
890
895
900
905
910
915
920
Wavelength (nm)

	O	P	Q	R	S	T	U
48							
49							
50	pass 5	pass 6	pass 7	pass 8			
51	0.560997	1.213789	2.210083	3.225539			
52	0.022446	0.05769	0.127162	0.246869			
53	0.097469	0.079499	0.064377	0.036587			
54	0.077976	0.064356	0.051434	0.029756			
55	0.067291	0.056073	0.044323	0.02602			
56	0.063847	0.053667	0.042005	0.024995			
57	0.067132	0.056923	0.044122	0.026625			
58	0.07759	0.06643	0.05094	0.031241			
59	0.096681	0.083725	0.063358	0.039644			
60	0.096455	0.084075	0.063054	0.039669			
61	0.076894	0.067567	0.049752	0.031766			
62	0.06616	0.058516	0.042436	0.027422			
63	0.062606	0.055699	0.03985	0.026033			
64	0.065651	0.058753	0.041481	0.027404			
65	0.075653	0.068145	0.047418	0.03173			
66	0.09393	0.085254	0.058282	0.039615			
67							
68							

IVa. Q-Switch output for arbitrary mode size and pump fluence

This is a Visualbasic code which is linked to a set of Excel spreadsheets and is run on a PC running Windows 95 and using Excel 97. This routine calculates pump depletion for an arbitrary temporal pump pulse in Yb:S-FAP, and the resulting Q-switched output energy versus mode area or input fluence. The spreadsheets used are named: Param (which contains all of the input parameters), abs&emm (which contain absorption and emission cross sections versus wavelength), pump (which contains the pump temporal profile), and Output (which contains the output of the code).

```
Sub Qswitch()
'
'Main Macro
'Andy Bayramian 07/21/99
' Keyboard Shortcut: Ctrl+u
'
'This routine calculates the peak Q-switched output energy versus mode spot size and absorbed pump energy
'in an end-pumped, pulsed laser system with a single Q-switch pulse for every pump pulse

'**********declarations and initializations**********
zpts = 100
Step = 100000000000000#
Dim time(400)
Dim tpulse(400)
Dim z(400)
Dim intensity0(2000)
Dim intensity(400)
Dim N1(2000, 400)
Dim N2(2000, 400)
Dim N1old(400)
Dim N2old(400)
Dim N1ave(400)
Dim N2ave(400)
Dim N2t(400)
Dim Ntot(400)
Dim fluence(400)
Dim fluor(400)
Dim gain(400)

'**********read in data**********
apts = Worksheets("Param").Cells(19, 4).Value '# of area points
astart = Worksheets("Param").Cells(20, 4).Value 'Starting area fraction
acnt = 1
For a = 1 To apts Step 1
afrac = acnt / apts
rp = astart + 0.2 * afrac 'Pump mode radius
rc = astart + 0.2 * afrac 'Cavity mode radius
Worksheets("Param").Cells(21, 2).Value = rp
Worksheets("Param").Cells(22, 2).Value = rc
Ap = Worksheets("Param").Cells(23, 2).Value 'Pump mode area
Ac = Worksheets("Param").Cells(24, 2).Value 'Cavity mode area
flupts = Worksheets("Param").Cells(21, 4).Value '# of fluence points
fracstart = Worksheets("Param").Cells(22, 4).Value 'Starting fluence fraction
h = Worksheets("Param").Cells(1, 2).Value 'Planck's constant
clight = Worksheets("Param").Cells(2, 2).Value 'Speed of light
```

```
lem = Worksheets("Param").Cells(3, 2).Value 'Emission wavelength
sem = Worksheets("Param").Cells(5, 2).Value 'Peak emission cross section
lpump = Worksheets("Param").Cells(6, 2).Value 'Pump wavelength
polem = Worksheets("Param").Cells(4, 2).Value 'Emission polarization
polpump = Worksheets("Param").Cells(7, 2).Value 'Pump polarization
tem = Worksheets("Param").Cells(9, 2).Value 'Emission lifetime
N0 = Worksheets("Param").Cells(10, 2).Value 'Dopant number density
fa = Worksheets("Param").Cells(12, 2).Value 'Boltzmann fraction in the bottom lower state
fb = Worksheets("Param").Cells(13, 2).Value 'Boltzmann fraction in the bottom upper state
RM2 = Worksheets("Param").Cells(15, 2).Value 'Reflectivity of the output coupler
loss = Worksheets("Param").Cells(16, 2).Value 'Scatter loss in gain medium
Trans1way = Worksheets("Param").Cells(18, 2).Value '1 way cavity transmission
Length = Worksheets("Param").Cells(19, 2).Value 'Length of gain medium
tpump = Worksheets("Param").Cells(20, 2).Value 'Pump pulsewidth
maxE = Worksheets("Param").Cells(25, 2).Value 'Maximum pump energy
flumax = Worksheets("Param").Cells(28, 2).Value 'Maximum pump fluence
dt = Worksheets("Param").Cells(31, 2).Value 'Pump time step
'*****************find absorption and emission cross sections at required
wavelengths*********************
If polem = 1 Then
    cole = 6
    colne = 7
Else
    cole = 7
    colne = 6
End If
If polpump = 1 Then
    colp = 2
    colnp = 3
Else
    colp = 3
    colnp = 2
End If

For i = 0 To 3400 Step 1
    wav = Worksheets("abs&emm").Cells(3 + i, 5).Value
    If wav > lem Then
        If wavold < lem Then
            frac = (lem - wavold) / (wav - wavold)
            EMprobe = (1 - frac) * Worksheets("abs&emm").Cells(2 + i, cole).Value + frac *
Worksheets("abs&emm").Cells(3 + i, cole).Value
            GoTo 5
        Else
            EMprobe = Worksheets("abs&emm").Cells(2 + i, cole).Value
            GoTo 5
        End If
    End If
    wavold = wav
Next i
5 Worksheets("Param").Cells(5, 2).Value = EMprobe  'Emission cross section at the probe wavelength

For i = 0 To 3400 Step 1
    wav = Worksheets("abs&emm").Cells(3 + i, 5).Value
    If wav > lpump Then
        If wavold < lpump Then
            frac = (lpump - wavold) / (wav - wavold)
```

```
            EMpump = (1 - frac) * Worksheets("abs&emm").Cells(2 + i, colne).Value + frac *
Worksheets("abs&emm").Cells(3 + i, colne).Value
            GoTo 7
        Else
            EMpump = Worksheets("abs&emm").Cells(2 + i, colne).Value
            GoTo 7
        End If
    End If
    wavold = wav
Next i
7 Worksheets("Param").Cells(26, 2).Value = EMpump  'Emission cross section at the pump wavelength

For i = 0 To 3400 Step 1
    wav = Worksheets("abs&emm").Cells(3 + i, 1).Value
    If wav > lpump Then
        If wavold < lpump Then
            frac = (lpump - wavold) / (wav - wavold)
            ABSpump = (1 - frac) * Worksheets("abs&emm").Cells(2 + i, colp).Value + frac *
Worksheets("abs&emm").Cells(3 + i, colp).Value
            GoTo 10
        Else
            ABSpump = Worksheets("abs&emm").Cells(2 + i, colp).Value
            GoTo 10
        End If
    End If
    wavold = wav
Next i
10 Worksheets("Param").Cells(8, 2).Value = ABSpump  'Absorption cross section at the pump wavelength

 For i = 0 To 3400 Step 1
    wav = Worksheets("abs&emm").Cells(3 + i, 1).Value
    If wav > lem Then
        If wavold < lem Then
            frac = (lem - wavold) / (wav - wavold)
            ABSprobe = (1 - frac) * Worksheets("abs&emm").Cells(2 + i, colnp).Value + frac *
Worksheets("abs&emm").Cells(3 + i, colnp).Value
            GoTo 13
        Else
            ABSprobe = Worksheets("abs&emm").Cells(2 + i, colnp).Value
            GoTo 13
        End If
    End If
    wavold = wav
Next i
13 Worksheets("Param").Cells(27, 2).Value = ABSprobe  'Absorption cross section at the probe
wavelength
'*****************Initialize and define constants*************************************
For j = 1 To 2000 Step 1
    time(j) = Worksheets("pump").Cells(2 + j, 4).Value
    If time(j) = 99999 Then GoTo 20
Next j
20 Tpts = j - 1

For k = 1 To zpts Step 1
    z(k) = k * Length / zpts
Next k
```

```
delz = Length / zpts

C1 = ABSpump * dt * lpump / (h * clight)
C2 = EMpump * dt * lpump / (h * clight)
C3 = dt / tem
DNthresh = (-Log(RM2 * (Trans1way) ^ 2)) / (2 * EMprobe * Length) 'Threshold inversion density
Worksheets("Param").Cells(32, 2).Value = DNthresh
cnt = 1

'*****************Pump absorption and Gain loop*****************************************
For i = 1 To flupts + 1 Step 1
    frac = fracstart + (1 - fracstart) * ((cnt - 1) / flupts) ^ 2

    fluence(i) = flumax * frac
    fluor(i) = 0#

    For j = 1 To Tpts Step 1
        intensity(j) = Worksheets("pump").Cells(2 + j, 6).Value * frac
    Next j

    For k = 1 To zpts Step 1
        N1old(k) = N0
        N2old(k) = 0#
    Next k

    For j = 1 To Tpts Step 1
        For k = 1 To zpts Step 1
        'restructure the temporal pulse shape for each spatial slice
                intensity(j) = intensity(j) * Exp(-(N1old(k) * ABSpump + loss) * delz)
                N1(j, k) = N1old(k) * (1 - C1 * intensity(j)) + C3 * N2old(k) + N2old(k) * C2 * intensity(j)
                N2(j, k) = N2old(k) * (1 - C3 - C2 * intensity(j)) + N1old(k) * C1 * intensity(j)
                N2old(k) = N2(j, k)
                N1old(k) = N1(j, k)
                fluor(i) = fluor(i) + N2old(k) / (zpts * Tpts)
        Next k
    Next j

    tpk = 0#
    Nmax = 0#
    For j = 1 To Tpts Step 1
        N2ave(i) = 0#
        For k = 1 To zpts Step 1
                N2ave(i) = N2ave(i) + N2(j, k) / zpts
                 'If cnt = flupts + 1 Then Worksheets("N2").Cells(j, k).Value = N2(j, k)
        Next k
        If N2ave(i) > Nmax Then
            Nmax = N2ave(i)
            tpk = j
        End If
    Next j
    'Worksheets("output").Cells(20, 13).Value = tpk
    tpk = 229
    N2ave(i) = 0#
    N1ave(i) = 0#
    For k = 1 To zpts Step 1
        N1ave(i) = N1ave(i) + N1(tpk, k) / (zpts)
```

```
        N2ave(i) = N2ave(i) + N2(tpk, k) / (zpts)
    Next k

    Ntot(i) = N1ave(i) + N2ave(i)
    gain(i) = Exp(Length * N2ave(i) * EMprobe - Length * N1ave(i) * ABSprobe - Length * loss)

    fluout = 0
    For j = 1 To Tpts Step 1
        fluout = fluout + intensity(j) * dt
    Next j
    '*****************Q-switched extraction section***********************************
    trans = fluout / fluence(i)
    Einc = frac * maxE
    Eabs = (1 - trans) * Einc
    DNi = (fb * N2ave(i) - fa * N1ave(i)) 'Initial inverison after pumping

    If DNi < DNthresh Then
        DNf = DNi
        Eout = 0#
        GoTo 100
    End If
    DNf = DNi * Exp((-(DNi)) / (DNthresh)) 'Final inversion after extraction
    gamma = 2E+17
    While gamma < DNf
        gamma = gamma + Step
        'If gamma / 1E+17 = Int(gamma / 1E+17) Then Worksheets("output").Cells(25, 13).Value = gamma
        DNf = DNi * Exp((gamma - DNi) / (DNthresh))
    Wend
    Eout = ((DNi - DNf) / (fa + fb)) * ((Ap + Ac) / 2) * Length * h * (clight / lem) * (Log(RM2) /
Log(RM2 * (Trans1way) ^ 2))
    gammaold = gamma
100  Efficiency = Eout / Einc
    Worksheets("output").Cells(2 + i, 1).Value = Einc
    Worksheets("output").Cells(2 + i, 2).Value = fluence(i)
    Worksheets("output").Cells(2 + i, 3).Value = N2ave(i)
    Worksheets("output").Cells(2 + i, 4).Value = N1ave(i)
    Worksheets("output").Cells(2 + i, 5).Value = fluor(i)
    Worksheets("output").Cells(2 + i, 6).Value = gain(i)
    Worksheets("output").Cells(2 + i, 7).Value = DNi
    Worksheets("output").Cells(2 + i, 8).Value = DNf
    Worksheets("output").Cells(2 + i, 9).Value = Eabs
    Worksheets("output").Cells(2 + i, 10).Value = Eout
    Worksheets("output").Cells(2 + i, 11).Value = trans

    cnt = cnt + 1
150 Next i

    Worksheets("output").Cells(2 + m, 32).Value = rp
    Worksheets("output").Cells(2 + m, 33).Value = Eabs
    Worksheets("output").Cells(2 + m, 34).Value = Eout
    Worksheets("output").Cells(2 + m, 35).Value = Einc
    Worksheets("output").Cells(2 + m, 36).Value = fluence(i)
    Worksheets("output").Cells(2 + m, 37).Value = N2ave(i)
    Worksheets("output").Cells(2 + m, 38).Value = N1ave(i)
    Worksheets("output").Cells(2 + m, 39).Value = DNi
    Worksheets("output").Cells(2 + m, 40).Value = DNf
```

```
    Worksheets("output").Cells(2 + m, 41).Value = Efficiency

    acnt = acnt + 1
Next a 'mode spot size loop

For j = 1 To Tpts Step 1
    N2t(j) = 0#
    For k = 1 To zpts
        N2t(j) = N2t(j) + N2(j, k) / (zpts)
    Next k
    Worksheets("output").Cells(2 + j, 12).Value = time(j)
    Worksheets("output").Cells(2 + j, 13).Value = N2t(j)
    Worksheets("output").Cells(2 + j, 14).Value = intensity(j)
    Worksheets("output").Cells(2 + j, 15).Value = intensity0(j)
Next j

End Sub 'Qswitch
```

IVa1 (Example spreadsheet associated with IVa)

	A	B	C	D
1	h (J s) (h)	6.626E-34		
2	c (cm/s)	30000000000	photon energy	2.0174E-19
3	emission wavelength (cm)	0.000098535		
4	emission polarization (1 = p, 0 = s)	0		
5	probe emission cross section (cm^2)	7.00003E-20		
6	pump wavelength (cm)	0.00009004		
7	pump polarization (1 = p, 0 = s)	1		
8	pump absorption cross section (cm^2	8.01734E-20		
9	emission lifetime (s)	0.00113		
10	Yb concentration (cm-3)	1.87E+19		
11	pump quantum efficiency	0.99		
12	fraction in lower level	0.808866939		
13	fraction in upper level with pumping	0.989452008		
14	Mirror Reflectivity (#1)	1		
15	Mirror Reflectivity (#2)	0.845	0.84	
16	Loss coefficient (cm-1)	0	0.017	
17	Single pass loss	0		
18	One way cavity transmission	0.85		
19	Crystal Length(cm)	0.82		
20	pump pulsewidth (s)	0.00018	0.032	
21	pump beam radius (cm)	0.005		
22	cavity beam radius (cm)	0.005		
23	pump beam area (cm^2)	7.85398E-05	Volume (cm3	6.4403E-05
24	cavity beam area (cm^2)	7.85398E-05	# in Vol.	1.2043E+15
25	Input Energy (J)	0.36	Max Ener (J)	0.00024296
26	pump emission cross section (cm2)	7.244E-22		
27	probe absorption cross section (cm2)	7.74237E-20	7.74237E-20	
28	Input Fluence (J/cm2)	4583.662361		
29	Single pass Polarizer loss	0.15		
30	Single pass Q-switch loss	0		
31	pump time step	2E-06		
32	DNthreshold (cm-3)	4.29839E+18	4.29839E+18	
33	Cavity Length (cm)	21	23.12	
34	Q-switch time step (s)	7E-10		
35				
36	Yb Energy levels (cm-1)	E (Joules)	DE (Joules)	thermal
37	0	0	0	1
38	362	7.19584E-21	7.19584E-21	0.1760049
39	597	1.18672E-20	1.18672E-20	0.05698245
40	1190	2.36548E-20	2.36548E-20	0.00330993
41	10150	2.01762E-19	0	1
42	11110	2.20845E-19	1.90829E-20	0.00998118
43	11670	2.31976E-19	3.02146E-20	0.00067926
44	Temperature(K) (Temp)	300		
45	Boltzman constant (kb)	1.3807E-23		

	E
36	Boltz fraction
37	0.808866939
38	0.142364547
39	0.04609122
40	0.002677294
41	0.989452008
42	0.009875894
43	0.000672098

IVb. Temporal pulse compression

This is a Visualbasic code which is linked to a set of Excel spreadsheets and is run on a PC running Windows 95 and using Excel 97. This routine calculates temporal pulse compression with increasing gain in Q-switched pulses in Yb:S-FAP. The spreadsheets used are named: Param (which contains all of the input parameters), abs&emm (which contain absorption and emission cross sections versus wavelength), pump (which contains the pump temporal profile), and Output (which contains the output of the code).

```
Sub Qswitchtemporal()
'
'Main Macro
'Andy Bayramian 07/21/99
' Keyboard Shortcut: Ctrl+u
'
'This routine calculates the Q-switched pulsewidth versus pump fluence for an end-pumped, pulsed laser system

'**************declarations and initializations******************
    Tpts = 4000
    PumpIntensity = 103

    Dim time(10000)
    Dim F(10000)
    Dim DN(10000)

'*****************read in data****************************************
h = Worksheets("Param").Cells(1, 2).Value 'Planck's constant
clight = Worksheets("Param").Cells(2, 2).Value 'speed of light
lem = Worksheets("Param").Cells(3, 2).Value 'emission wavelength
EMprobe = Worksheets("Param").Cells(5, 2).Value 'emission cross section at emission wavelength
fa = Worksheets("Param").Cells(12, 2).Value 'Boltzmann fraction in lower level
fb = Worksheets("Param").Cells(13, 2).Value 'Boltzmann fraction in upper level
RM2 = Worksheets("Param").Cells(15, 2).Value 'Reflectivity of output coupler
Trans1way = Worksheets("Param").Cells(18, 2).Value '1 way cavity transmission
Length = Worksheets("Param").Cells(19, 2).Value 'length of gain medium
Ac = Worksheets("Param").Cells(24, 2).Value 'Area of cavity mode
'DNthresh = Worksheets("Param").Cells(32, 2).Value 'Threshold inversion
Cavlength = Worksheets("Param").Cells(33, 2).Value 'Cavity length
DNthresh = 3E+18

PumpIntensity = 26
'maxpts = 103 - PumpIntensity
maxpts = 79
For k = 1 To maxpts Step 1
    DNi = Worksheets("Output").Cells(PumpIntensity, 7).Value 'Initial inversion after pumping
    DNf = Worksheets("Output").Cells(PumpIntensity, 8).Value 'Final inversion after extraction
    Qtstep = Worksheets("Param").Cells(34, 2).Value 'Q-switch time step
    C1 = (clight * EMprobe * Length * Qtstep) / (Cavlength)
    C2 = (clight * EMprobe * (fa + fb) * Qtstep)

    time(1) = Qtstep
    DN(1) = DNi
    F(1) = 1000000000000#
    Worksheets("output").Cells(3, 43).Value = time(1)
    Worksheets("output").Cells(3, 44).Value = F(1)
    Worksheets("output").Cells(3, 45).Value = DN(1)
```

```
    j = 1
    cnt = 1
    Fold = 1000000000000#
    DNold = DN(1)
    Ftot = Fold
    Fmax = 10
'*****************extract the pulse*****************************************
    Do
        time(j) = cnt * Qtstep
        DN(j) = DNold - C2 * Fold * DNold
        F(j) = (Fold + Trans1way * C1 * (DNold - DNthresh) * Fold)
        Fold = F(j)
        If Fold > Fmax Then
            Fmax = Fold
            jmax = cnt
        End If
        DNold = DN(j)
        Worksheets("output").Cells(2 + j, 43).Value = time(j)
        Worksheets("output").Cells(2 + j, 44).Value = F(j)
        Worksheets("output").Cells(2 + j, 45).Value = DN(j)
        Ftot = Ftot + Fold
        cnt = cnt + 1
        j = j + 1
    'Next j
    Loop While Fold > 0.5
'***************************Now find 1/2 way points ************************
    jfinal = j
    For j = 2 To jmax Step 1
        If F(j) > (0.5 * Fmax) Then
            t1 = time(j - 1) + Qtstep * ((0.5 * Fmax) - F(j - 1)) / (F(j) - F(j - 1))
            GoTo 10
        End If
    Next j
10  For j = jmax To jfinal Step 1
         If F(j) < (0.5 * Fmax) Then
             t2 = time(j - 1) + Qtstep * (F(j - 1) - (0.5 * Fmax)) / (F(j - 1) - F(j))
             GoTo 20
         End If
    Next j

20  fluence = Worksheets("output").Cells(PumpIntensity, 2).Value
    Worksheets("output").Cells(2 + k, 47).Value = fluence
    Worksheets("output").Cells(2 + k, 48).Value = t2 - t1 'temporal pulsewidth

    PumpIntensity = PumpIntensity + 1
30 Next k

End Sub 'Qswitchtemporal
```

V. Nonlinear Frequency conversion for Gaussian spatial and arbitrary temporal pump profile

This is a Visualbasic code which is linked to a set of Excel spreadsheets and is run on a PC running Windows 95 and using Excel 97. This routine calculates temporal pulse compression with increasing gain in Q-switched pulses in Yb:S-FAP. The spreadsheets used are named: input data (which contains all of the input parameters and output), Temporal profile (which contains the pump temporal profile), and Spatial Profile (which contains information about the spatial profile of the pump laser beam).

```
Sub Harmonic_conversion()
'
'Main Macro
'Andy Bayramian 02/20/00
' Keyboard Shortcut: Ctrl+u
'
'This routine calculates the 2nd harmonic conversion from a user specified crystal, temporal pulseshape and
M2 gaussian spatial profile

'**************declarations and initializations******************
Dim E2w(1000)
Dim E1w(1000)
Dim eff(1000)
'*****************read in data****************************************
epts = Worksheets("input data").Cells(12, 2).Value 'Energy points
Emax = Worksheets("input data").Cells(13, 2).Value 'Maximum Energy
tpts = Worksheets("input data").Cells(27, 2).Value 'Time points
zpts = Worksheets("input data").Cells(18, 2).Value 'length points
zstep = Worksheets("input data").Cells(19, 2).Value 'length step
rpts = Worksheets("input data").Cells(35, 2).Value 'radial points
tstep = Worksheets("input data").Cells(28, 2).Value 'time step
'*****************find absorption and emission cross sections at required
wavelengths********************
j = 1
tamp = 0#
For t = 1 To tpts Step 1
       amp = Worksheets("Temporal Profile").Cells(j + 1, 3).Value
       If amp > tamp Then
          tamp = amp
          imax = j
       End If
      j = j + 1
Next t

i = 1
For E = 1 To epts Step 1
   E1w(E) = i * Emax / epts
   Worksheets("input data").Cells(14, 2).Value = E1w(E)
   j = 1
   E2w(E) = 0#
   For t = 1 To tpts Step 1
      Worksheets("input data").Cells(29, 2).Value = Worksheets("Temporal Profile").Cells(j + 1, 1).Value
      Worksheets("input data").Cells(30, 2).Value = Worksheets("Temporal Profile").Cells(j + 1, 3).Value
      E2w_slice = Worksheets("Spatial Profile").Cells(2, 11).Value
      E2w(E) = E2w(E) + E2w_slice
```

```
        Worksheets("input data").Cells(2, 6).Value = E2w(E)
        j = j + 1
    Next t
    eff(E) = E2w(E) / E1w(E)
    Worksheets("input data").Cells(i + 1, 7).Value = E1w(E)
    Worksheets("input data").Cells(i + 1, 8).Value = E2w(E)
    Worksheets("input data").Cells(i + 1, 9).Value = eff(E)
    i = i + 1
Next E
End Sub 'Harmonic_conversion()
```

Va (Example spreadsheet associated with V)

	A	B	C	D
1	Crystal	YCOB		
2	Phase match type	2		
3	lambda1(nm)	985	w1	1.91366E+15
4	lambda2 (nm)	985	w2	1.91366E+15
5	lambda3 (nm)	492.5	w3 = w1 + w2	3.82732E+15
6	lambda3 (nm)	#DIV/0!	w3 = |w1 - w2|	0
7		CGS	MKS	
8	cl (cm/s)	3E+10	300000000	
9	h (J s)	6.626E-34		
10	e0 (A/V cm)	8.85E-14	8.85E-12	
11	lambda1(cm)	0.0000985	0.000000985	
12	energy points	50		
13	Energy maximum (J)	0.0075		
14	input energy, E (J)	0.0075		
15	lambda2 (cm)	0.00004925	4.925E-07	
16	Longitudinal parameters			
17	Length of crystal (cm) (2.63 orig)	2.66	0.088666667	
18	length pts (< 200)	30	100	
19	length step (cm)	0.08866667	0.000886667	
20	waist position, z0 (cm)	1.33		
21	position, z (cm)	1.73	-0.088666667	
22				
23				
24	Temporal parameters			
25	Area under curve (not normed)	8.9415E-09		
26	Area under curve (normed)	1		
27	time points	84	82	184
28	time step (s)	4E-10		
29	Time (s)	3.32E-08		
30	normed output	1000.05332		
31	energy slice	3.0002E-09		
32	instantaneous power	7.50039988		
33				
34	Radial parameters			
35	radial pts	500		
36	radial step wa (cm)	2.586E-05		
37	radial step wb (cm)	3.1719E-05		
38	total volume	8.0099E-05		
39	Mx2	1.32088551	2.267	
40	gaussian waist, W0x (cm)	0.0058		
41	gaussian waist, Wx (cm)	0.00646511	0.011672801	
42	optimum Wx for gaussian beam	0.0174633		
43	My2	1.8025222	3.09362	
44	gaussian waist, W0y (cm)	0.0073		
45	gaussian waist, Wy (cm)	0.00792968	0.013187806	
46	optimum Wy for gaussian beam	0.02197967		
47				
48	deff (cm/V)	1.14E-10	1.14E-12	
49	walkoff angle (raidans)	0.0202871	0.0202871	0.011523719

	A	B	C	D
50	acceptance angle (mrad cm)	1.3		
51	n1	1.71627289		
52	n2	1.71627289		
53	theta (degrees)	0.16406399		
54	Dk	0		E1w
55	sinc(Dkl/2)	1		0.00015
56	La (cm) = sqrt(p)*w0/p	0.80930321		0.0003
57		CGS	MKS	0.00045
58	intensity (W/cm2)	301429816	3.0143E+12	0.0006
59	Intensity 2w (depleted) (W/cm2)	1402770.08	14027700785	0.00075
60	Intensity 2w (undepleted) (W/cm2	1407137.73		0.0009
61	flat top temporal pulse (s)	8.8E-09		0.00105
62	flat top spatial radius (cm)	0.03		0.0012
63				0.00135
64				0.0015
65				0.00165
66				0.0018
67				0.00195
68				0.0021
69				0.00225

	E	F	G	H	I	J
50			0.00735	0.0071532	0.97322448	
51			0.0075	0.0073028	0.97370675	
52						
53						
54	I1w (W/cm2	I2w (W/cm	E2w	Eff	E2w (undep)	Eff
55	6028596.3	449028.1	1.12E-05	0.074483	1.1761E+13	7.8406E+16
56	12057193	1709297	4.25E-05	0.1417657	4.7044E+13	1.5681E+17
57	18085789	3666189	9.12E-05	0.202711	1.0585E+14	2.3522E+17
58	24114385	6222922	0.000155	0.2580585	1.8818E+14	3.1363E+17
59	30142982	9297448	0.000231	0.3084449	2.9402E+14	3.9203E+17
60	36171578	12819947	0.000319	0.3544205	4.2339E+14	4.7044E+17
61	42200174	16730802	0.000416	0.3964629	5.7629E+14	5.4885E+17
62	48228771	20978935	0.000522	0.434988	7.527E+14	6.2725E+17
63	54257367	25520454	0.000635	0.4703593	9.5264E+14	7.0566E+17
64	60285963	30317534	0.000754	0.5028954	1.1761E+15	7.8406E+17
65	66314560	35337486	0.000879	0.5328767	1.4231E+15	8.6247E+17
66	72343156	40551994	0.001009	0.5605505	1.6936E+15	9.4088E+17
67	78371752	45936467	0.001143	0.5861355	1.9876E+15	1.0193E+18
68	84400349	51469505	0.001281	0.6098257	2.3052E+15	1.0977E+18
69	90428945	57132446	0.001422	0.6317938	2.6462E+15	1.1761E+18

University of California
Lawrence Livermore National Laboratory
Technical Information Department
Livermore, CA 94551